

Improving Public Safety Through Spatial Synthesis, Mapping, Modeling, and Performance Analysis of Emergency Evacuation Routes in California Localities

December
2024

A Research Report from the National Center
for Sustainable Transportation

Miguel Jaller, University of California, Davis

James H. Thorne, University of California, Davis

Daniel Rivera-Royero, University of California, Davis

Jason Whitney, University of California, Davis

Alexander Kenichi Hu, University of California, Davis

Ayush Saha, University of California, Davis



National Center
for Sustainable
Transportation
A USDOT University Transportation Center



UC DAVIS
Institute of Transportation Studies

TECHNICAL REPORT DOCUMENTATION PAGE

1. Report No. NCST-UCD-RR-24-42	2. Government Accession No. N/A	3. Recipient's Catalog No. N/A	
4. Title and Subtitle Improving Public Safety through Spatial Synthesis, Mapping, Modeling, and Performance Analysis of Emergency Evacuation Routes in California Localities		5. Report Date December 2024	
		6. Performing Organization Code N/A	
7. Author(s) Miguel Jaller, Ph.D., https://orcid.org/0000-0003-4053-750X James H. Thorne, Ph.D., https://orcid.org/0000-0002-9130-9921 Daniel Rivera-Royero, https://orcid.org/0000-0003-2137-5664 Jason Whitney, https://orcid.org/0000-0003-0934-2675 Alexander Kenichi Hu, https://orcid.org/0009-0000-0914-8827 Ayush Saha, https://orcid.org/0000-0001-9480-1332		8. Performing Organization Report No. UCD-ITS-RR-24-82	
12. Sponsoring Agency Name and Address U.S. Department of Transportation Office of the Assistant Secretary for Research and Technology 1200 New Jersey Avenue, SE, Washington, DC 20590 California Department of Transportation Division of Research, Innovation and System Information, MS-83 1727 30th Street, Sacramento, CA 95816		10. Work Unit No. N/A	
		11. Contract or Grant No. Caltrans 65A0686 Task Order 076 USDOT Grant 69A3551747114	
15. Supplementary Notes DOI: https://doi.org/10.7922/G27D2SG5 Dataset DOI: https://doi.org/10.5061/dryad.w9ghx3g0j Supplemental information: https://doi.org/10.5281/zenodo.14232538		13. Type of Report and Period Covered Final Research Report (May 2023 – September 2024)	
		14. Sponsoring Agency Code USDOT OST-R Caltrans DRISI	
16. Abstract This project examines multi-hazard risks and the performance of emergency evacuation routes in California using spatial synthesis, mapping, modeling, and performance analysis techniques. It enhances evacuation planning by analyzing road networks under natural hazard scenarios. Key tasks included: 1. Collecting and organizing evacuation route data for 190 cities, revealing that only 23 had comprehensive GIS maps, highlighting gaps in current planning. 2. Assessing road network performance under various hazards for 450 cities, identifying high-risk areas, and classifying cities based on risk levels and concentration. 3. Analyzing evacuation routes during the 2018 Camp and Thomas fires, using mathematical modeling and Omniscape to assess bottlenecks and evacuation efficiency. 4. Evaluating evacuation route performance for different population segments and proposing improvements, including using public transit for future wildfire evacuations. The findings provide actionable insights for improving emergency evacuation strategies in the state.			
17. Key Words Risk, resilience, wildfire, multi-hazard, evacuation, California, spatial index		18. Distribution Statement No restrictions.	
19. Security Classif. (of this report) Unclassified	20. Security Classif. (of this page) Unclassified	21. No. of Pages 146	22. Price N/A

Form DOT F 1700.7 (8-72)

Reproduction of completed page authorized

About the National Center for Sustainable Transportation

The National Center for Sustainable Transportation is a consortium of leading universities committed to advancing an environmentally sustainable transportation system through cutting-edge research, direct policy engagement, and education of our future leaders. Consortium members include: the University of California, Davis; California State University, Long Beach; Georgia Institute of Technology; Texas Southern University; the University of California, Riverside; the University of Southern California; and the University of Vermont. More information can be found at: ncst.ucdavis.edu.

Disclaimer

The contents of this report reflect the views of the authors, who are responsible for the facts and the accuracy of the information presented herein. This document is disseminated in the interest of information exchange. The report is partially or entirely funded by a grant from the U.S. Department of Transportation's University Transportation Centers Program and partially or entirely, by a grant from the State of California. However, the U.S. Government and the State of California assume no liability for the contents or use thereof. Nor does the content necessarily reflect the official views or policies of the U.S. Government or the State of California. This report does not constitute a standard, specification, or regulation. This report does not constitute an endorsement by the California Department of Transportation of any product described herein.

The U.S. Department of Transportation and the State of California require that all University Transportation Center reports be published publicly. To fulfill this requirement, the National Center for Sustainable Transportation publishes reports on the University of California open access publication repository, eScholarship. The authors may copyright any books, publications, or other copyrightable materials developed in the course of, or under, or as a result of the funding grant; however, the U.S. Department of Transportation reserves a royalty-free, nonexclusive and irrevocable license to reproduce, publish, or otherwise use and to authorize others to use the work for government purposes.

Acknowledgments

This study was funded, partially or entirely, by a grant from the National Center for Sustainable Transportation (NCST), supported by the U.S. Department of Transportation (USDOT) and the California Department of Transportation (Caltrans) through the University Transportation Centers program. The authors would like to thank the NCST, the USDOT, and Caltrans for their support of university-based research in transportation and especially for the funding provided in support of this project.

Improving Public Safety Through Spatial Synthesis, Mapping, Modeling, and Performance Analysis of Emergency Evacuation Routes in California Localities

A National Center for Sustainable Transportation Research Report

December 2024

Miguel Jaller, Professor, Department of Civil and Environmental Engineering, University of California, Davis

James H. Thorne, Professional Researcher, Department of Environmental Science and Policy, University of California, Davis

Daniel Rivera-Royero, Transportation, Technology and Policy Program, Institute of Transportation Studies, University of California, Davis

Jason Whitney, Geography Graduate Group, University of California, Davis

Alexander Kenichi Hu, University of California, Davis

Ayush Saha, University of California, Davis

[page intentionally left blank]

TABLE OF CONTENTS

EXECUTIVE SUMMARY	viii
Introduction	1
Literature Review.....	3
Road Network Performance	4
Evacuation Performance.....	7
Bottleneck Analysis with Omniscape	10
Methodology.....	13
Task 1: Evacuation Routes Data Collection and Database Construction.....	13
Task 2: Assessing the Performance of the Road Network.....	14
Task 3: Assessing the Map of Evacuation Routes Using the Other Data Collected to Determine the Equity of Access to Evacuations	18
Task 4: Assessing the Performance of the Evacuation Routes to Serve Different Segments of the Population.....	27
Empirical Results	30
Task 1: Evacuation Routes Data Collection and Database Construction.....	30
Task 2: Assessing the Performance of the Road Network.....	32
Task 3: Assessing the Map of Evacuation Routes Using the Other Data Collected to Determine the Equity of Access to Evacuations	45
Task 4: Assessing the Performance of the Evacuation Routes to Serve Different Segments of the Population.....	57
Discussion.....	73
Road network performance Risk	74
Evacuation Performance.....	76
Limitations and Assumptions.....	77
Conclusion and Key Takeaways	80
References	82
Data Summary.....	92
Appendix A. Summary of RNP Metrics and Models	93
Appendix B. SSRI and NRI for Multiple Hazards.....	101
Appendix C. Thomas Fire Case Study.....	110
Data Management	110

Evacuation Plan Risk Assessment	121
Appendix D. Sociodemographic Characteristics of Paradise and Magalia	127

List of Tables

Table 1. Taxonomy evacuation management (LP: Linear Programming, IP: Integer Programming, NLP: No linear programming, MIP: Mixed Integer Programming, ABS: Agent-Based Simulation, MCS: Montecarlo Simulation, TS: Traffic Simulation.)	11
Table 2. Theme and variables used for the Social Vulnerability Index from American Community Survey.....	45
Table 3. Clearance Time, Total Evacuation Time, and Average Evacuation Time when closing each exit node.....	64
Table 4. Estimation of the probability of each grade and direction of the road network	66
Table 5. Estimates the expected clearance time, total evacuation time, and average evacuation time.	67
Table A.1. Overview of Mathematical formulation for the 11 RNPs (connectivity, redundancy, accessibility, reliability, resilience, robustness, flexibility, and vulnerability)	93
Table C.1. Theme and variables used for the Social Vulnerability Index from American Community Survey.....	110
Table C.2. Summary of the population percentage with each of the characteristics required to estimate the Social Vulnerability Index at the census block group in Ventura, Santa Paula, and Ojai.	111
Table C.3. Spatial distribution of the variables required to estimate Theme 1: Socio-economic status: poverty, unemployment, house burdened, high school diploma, and health insurance (Thomas Fire Cities).....	114
Table C.4. Spatial distribution of the variables required to estimate Theme 2: Household characteristics: Age 65 or older, age 17 and younger, civilian with a disability, single-parent households, English language proficiency (Thomas Fire Cities).	114
Table C.5. Spatial distribution of the variables required to estimate Theme 3: Racial & Ethnic: Minority status: belongs to a minority group (Thomas Fire Cities).....	115
Table C.6. Spatial distribution of the variables required to estimate Theme 4: Housing type and Transportation: Multi-unit structure, mobile home, crowding, no vehicle, group quarter (Thomas Fire Cities).	115
Table C.7. Spatial distribution of the four themes and the Social Vulnerability index at the census block level.	116
Table C.8. Spatial distribution of each Social Vulnerability index, Community Resilience, Expected Annual Loss, and the National Risk Index (NRI) at the census block level.....	117
Table C.9. Clearance Time, Total Evacuation Time, and Average Evacuation Time when closing each exit node.....	123
Table C.10. Estimation of the probability of each grade and direction of the road network	124

Table C.11. Estimation of the expected clearance time, total evacuation time, and average evacuation time.	125
Table D.1. Spatial distribution of the variables required to estimate Theme 1: Socio-economic status: poverty, unemployment, house burdened, high school diploma, and health insurance.....	127
Table D.2. Spatial distribution of the variables required to estimate Theme 2 Household characteristics	128
Table D.3. Spatial distribution of the variables required to estimate Theme 3: Racial & Ethnic	128
Table D.4. Spatial distribution of the variables required to estimate Theme 4: Housing type and Transportation: Multi-unit structure, mobile home, crowding, no vehicle, group quarter.	129
Table D.5. Spatial distribution of the four themes and the Social Vulnerability index at the census block level.	130
Table D.6. Spatial distribution of each Social Vulnerability index, Community Resilience, Expected Annual Loss, and the National Risk Index (NRI) at the census block level.....	131
Table D.7. Summary of the population percentage with each characteristic required for the SOVI at the census block group.	132

List of Figures

Figure 1. Road Network performance classification. From Rivera-Royero, et.al. [10].....	5
Figure 2. Methodology classification on the literature review, including Mathematical Programming and Simulation	10
Figure 3. RNPrisk methodology steps.....	15
Figure 4. General methodology	19
Figure 5. Traffic flow and evacuation choke points derived by Omniscape for Davis, CA.	26
Figure 6. Database characteristics	31
Figure 7. Number of localities with each safety element	32
Figure 8. California evacuation hazards dashboard.....	32
Figure 9. Percentage viz vs θiz , BCi and Ai with original and normalized values.....	35
Figure 10. Road network and histogram of the risk ψrzviz vs ψrzθiz , ψrzAi , ψrzBCi in San Francisco	37
Figure 11. Road network and histogram of the risk (ψrz (viz) vs ψrz (θiz) , ψrz (Ai) , ψrz BCi)) in Los Angeles	38
Figure 12. Correlation of SSRIzψrzθiz , SSRIzψrzAi and SSRIzψrzBCi on SSRIzψrzviz	39
Figure 13. Contribution of SSRIzψrzθiz , SSRIzψrzAi and SSRIzψrzBCi on SSRIzψrzviz	40
Figure 14. P-value of GAM model between SSRIzψrzviz and a set of RNP measurements. ..	40
Figure 15. ALL hazards: Cluster and California region classification: a) Cluster classification, b) cluster distribution among California cities, c) Region distribution, d) Spatial distribution of cluster classification on California Regions.....	43
Figure 16. WIFIR hazard: Cluster and California region classification: a) Cluster classification, b) cluster distribution among California cities, c) Region distribution, d) Spatial distribution of cluster classification on California Regions.....	44
Figure 17. Paradise Map with the labels of the source and sink nodes demand and sink capacity	47
Figure 18. Density distribution of the arcs of the road network, including length, capacity, speed, and travel time	48
Figure 19. Evacuation percentage with time in minutes	49
Figure 20. Exit nodes evacuation, evacuation rate, and cumulative percentage of vehicles evacuated under the ENP and EPWP models	50
Figure 21. Departure (top) /Arrival (bottom) time comparison between paths	51

Figure 22. Evolution of the total evacuation on the Paradise-Magalia Case (minutes)	52
Figure 23. Traffic flow and evacuation choke points (City of Paradise)	54
Figure 24. Traffic flow and evacuation choke points (City of Magalia)	55
Figure 25. Traffic flow and evacuation points (City of Magalia and Paradise)	56
Figure 26. Correlation analysis Travel time OD, demand, and SOVI versus departure and arrival time (Y= Q (Departure/Arrival time) (min, Q1, Q2, Q3, Max))	58
Figure 27. Density probability factors of the ν_j parameter (units) (min, max, mean)	59
Figure 28. Risk, risk and time, clearance time of EPWP models with different pools of paths....	61
Figure 29. a) distribution of evacuation by exit nodes, b) evacuation flow, and c) cumulative flow of the four models ENP, EPWP (time), EPWP (risk), and EPWP (time & risk)	62
Figure 30. Corridor importance of different EPWP objectives	63
Figure 31. Clearance Time and Average Evacuation Time when closing each exit node	64
Figure 32. Comparison Evacuation Routes with the routes based on the different models	68
Figure 33. Recommendation Improvement compared with importance measurement of case analysis.....	69
Figure 34. Prioritized risk and time with transit stop and CI Score.	70
Figure 35. Prioritized risk and time with transit stop and NRI.	71
Figure 36. Prioritized risk and time with transit stop and (left) Transit Stops/1000 residents; and (right) Combined Vulnerability Index.	72
Figure B.1. Winter Weather (WNTW)	101
Figure B.2. Earthquake (ERQK).....	101
Figure B.3. Drought (DRGT).....	102
Figure B.4. Cold Wave (CWAV)	102
Figure B.5. Coastal Flooding (CFLD)	103
Figure B.6. Avalanche (AVLN)	103
Figure B.7. Hail (HAIL)	104
Figure B.8. Hot Wave (HWAV)	104
Figure B.9. Hurricane (HRCN).....	105
Figure B.10. Landslide (LNDS)	105
Figure B.11. Lighting (LTNG)	106
Figure B.12. Strong Wind (SWND)	106
Figure B.13. Rapid Flood (RFLD).....	107

Figure B.14. Tornado (TRND)	107
Figure B.15. Tsunami (TSUN)	108
Figure B.16. Volcano (VLCN)	108
Figure B.17. Wildfire (WFIR)	109
Figure B.18. All hazards (ALL).....	109
Figure C.1. Ventura, Ojai, Santa Paula with the labels of the source and sink nodes demand and sink capacity.....	118
Figure C.2. Density distribution of the arcs of the road network, including length, capacity, speed, and travel time Thomas Fire	119
Figure C.3. Evacuation percentage with time in minutes in 2018 Thomas Fire Cites	120
Figure C.4. Density probability factors of the v_j parameter (units) (min, max, mean) in Thomas Fire Cities.....	122
Figure C.5. Clearance Time and Average Evacuation Time when closing each exit node	126

Improving Public Safety Through Spatial Synthesis, Mapping, Modeling, and Performance Analysis of Emergency Evacuation Routes in California Localities

EXECUTIVE SUMMARY

This project uses spatial synthesis, mapping, modeling, and performance analysis techniques to analyze multi-hazard risks and network topology potential impacts for emergency evacuation routes in various California localities.

This project aims to enhance the understanding of road network performance under natural hazards and to help support evacuation planning. The report begins with a comprehensive literature review on road network performance measurements and evacuation performance analysis. The methodology consists of applying various methods to address four key tasks. These methods include risk performance measurement and evacuation performance analysis. The evacuation performance analysis involves mathematical programming models and Omniscape as an alternative congestion and bottleneck analysis method. Risk assessment and mathematical programming models are used to create disaster scenarios and sensitivities to identify the most important corridors within the road network in various case studies. The key findings and implications are organized into four key tasks:

Task 1: Evacuation routes data collection and database construction

Evacuation route data was collected from 190 cities in California, revealing that only 23 had online GIS maps, while the rest relied on less accessible PDF plans. This highlights a critical gap in evacuation planning and the need for improved methodologies to support localities lacking detailed plans.

Task 2: Assessing the performance of the road network

A novel methodology evaluated road network risks across three levels: local (node-specific risks), regional (directional risks), and system-wide (risk concentration). Analysis of 450 cities categorized them into four priority groups, offering tailored insights for decision-makers. Key findings include identifying high-risk areas and factors driving road network performance risk, enabling targeted mitigation efforts.

Task 3: Assessing the map of evacuation routes using the other data collected to determine the equity of access to evacuations

Case studies of the 2018 Camp Fire in Paradise and Magalia and the Thomas Fire in Ojai, Ventura, and other localities were analyzed using mathematical programming models and Omniscape models to evaluate evacuation performance.

- The mathematical programming models obtained comparable clearance times (~1 hour, 50 minutes) between the two case studies despite area and vehicle demand differences. This was attributed to variations in exit routes and road network capacity. The Thomas Fire area has more exit routes than the Camp Fire area. Additionally, the road network capacity in the Thomas Fire area is greater than that of the Camp Fire area, providing insights into the reasons for this difference in performance.
- Omniscape analysis identified congestion "choke points" at local and regional levels, aligning with mathematical modeling results and providing insights into traffic bottlenecks during evacuations.

Task 4: Assessing the performance of the evacuation routes to serve different segments of the population.

Evacuation routes were evaluated under various scenarios, revealing critical corridors for reducing clearance times and highlighting common strategies between model predictions and current local plans. Public transit networks were identified as a valuable but underutilized resource for enhancing wildfire evacuation strategies.

Introduction

Evacuation is a disaster management strategy where people at risk need to relocate to safer places at minimal risk [1]. This process usually relies on the road network, and one of its main characteristics is that heavy congestion on roads can quickly saturate the limited exit routes due to the high influx of vehicles [2]. Evacuation planning is crucial in areas prone to geophysical events and extreme weather, which pose risks to human safety, critical infrastructure, property, and homeland security [3].

This is one of many reasons why public safety is a major concern for policymakers, as it impacts individuals' quality of life and assets. In this project, we analyzed public safety, specifically during evacuation events, through mapping, modeling, and analyzing the performance of the road network that supports emergency evacuation processes in California localities and the expected evacuation performance.

The characteristics of the evacuation process vary depending on the type of natural hazard. For example, evacuations during hurricanes are larger than during wildfires, regarding land affected, population affected, and distance between the affected area to safe destinations. Early evacuation is the preferred disaster management strategy during wildfires in the US [4]. However, the complexity of evacuations during wildfires becomes critical when anticipated evacuations are impossible because information about the wildfire is only available at short or no notice.

2018 was California's year with the highest cost on property damage, business interruptions, and agricultural losses due to wildfires, with \$30bn, followed by 2017 and 2020, with \$23bn and \$20bn, respectively [5]. Between 2017 and 2019, eleven large-scale wildfires caused the evacuation of at least ten thousand individuals each [6] in California. The 2018 Camp Fire was the deadliest and most destructive wildfire in the last 90 years of wildfire records in California, with 85 fatalities and 18,804 structures destroyed [7]. One of the reasons for such devastating consequences is that it was a fast-moving wildfire, where many vehicles attempted to escape on a restricted road network with short notice.

Wildland-urban interface areas (WUI) are those areas where people live surrounded by wildfire-driven fuels [8], and those are the places with a major concern for wildfires—considering that a significant share of people live in WUI areas. The impact and negative consequences of climate-driven wildfires are expected to increase. Different agencies have invested in developing preparedness, mitigation, and adaptation plans, but evacuation is critical for short- or no-notice fast-moving wildfire events.

Moreover, it is important to note that the transportation infrastructure is one of the most affected assets by natural disasters and carries many costs [9]. Therefore, it is extremely important to identify adequate evacuation routes and assess the road network performance on which those evacuation routes rely. Additionally, it is important to consider the various assumptions about transportation accessibility (e.g., vehicle availability, mobility constraints) for different population segments to use such routes.

California has recognized the need to strengthen disaster response through AB747 (https://leginfo.ca.gov/faces/billNavClient.xhtml?bill_id=201920200AB747), which requires cities and counties to adopt a comprehensive long-term general plan that includes safety elements for the community from unreasonable risks associated with various hazards. AB 747 requires local jurisdictions to identify evacuation routes and their capacity, safety, and viability under various emergency scenarios. Many agencies are important in these safety elements, maintaining and strengthening evacuation routes and ensuring public access. These routes must be identified in advance and maintained to provide transportation during evacuations.

This project had four main objectives or named tasks:

- First, to *collect evacuation route plans from different jurisdictions within the state and create a centralized database.*
- The second objective is to perform a *road network analysis based on the team's experience with road network performance, access restoration, and critical infrastructure modeling* for case studies [10, 11, 12]. Such quantitative analyses of the networks use several performance measures as described in [10].
- The third objective was to assess how well these evacuation routes align with the State Highway, bus, and rail System *and how well they compare with actual evacuation events* in case studies using data or findings from previous evacuations in California.
- Finally, the fourth objective involved *analyzing different metrics about the evacuation routes' performance for different population segments.*

Overall, this project helps consolidate and assess evacuation routes and their impact on the population's evacuation ability. It will also inform infrastructure investment priority decisions by identifying the road segments with the largest impact on the evacuation route/network performance and which cities have the highest priority among the California cities.

Literature Review

The review focused on four main topics: road network performance, road network performance risk, spatial analysis, evacuation performance, and an evaluation of bottlenecks using *Omniscape*.

The first part of our literature review focused on **road network performance (RNP)**. The RNP literature has focused on defining, analyzing, and formulating different measurements to assess the strengths and weaknesses of road networks. RNP measurements can be classified as global, regional, or local RNP measurements. Global RNPs are a single value that represents the entire road network, regional RNPs are a set of values that group the characteristic of a set of nodes or arcs into subgroups and regions in the road network, and local RNP measurements are a set of local values that represent the RNP characteristics of each node or arc of the road network.

Local RNP measurements provide spatial data of the nodes and arcs within the road network. However, nodes have an advantage over arcs because it is possible to identify a single and precise coordinate in the network. Each road network has different shapes, sizes, geometries, areas, and population densities, so using the local RNP measurements directly to compare two or more road networks is a challenge. One option to compare road networks is to use sums or averages and estimate the variance of such local RNP measurements. This approach does not allow us to maintain their spatial information. Additionally, using clusters or regions to group the local RNP measurements described by Derrible and Kennedy [13] or Jenelius [14] might not be sufficient because such subgroups are not standard and do not allow fair comparison between road networks. There is also a lack of methods focusing on risk, spatial analysis, and practical application through case studies or implementation scalability.

The papers that assess RNP risk use centrality measurements as part of the risk and involve simulation data for natural hazard events, mostly for hydro-meteorological natural hazards. Still, natural risk measurements that consider the historical data, the population's socioeconomic characteristics, and the road network's topological characteristics are lacking. In the literature, most authors analyzed hypothetical or real-life road networks using a single or small sample of road networks. This hampers generalizations and benchmarking assessments of the applicability of different measurements across real road networks, considering each location's inherent natural hazard risks.

Based on the analysis of the available literature, current RNP measurements do not offer an effective way of comparing road network performance while considering a variety of specific natural hazard risks inherent to each location. Despite the analysis of natural hazard risks on road networks by various authors, there remains a lack of understanding of the trends and patterns of these risks. This gap includes understanding how the risk of each natural hazard is distributed or spread within the road network of a particular location and whether there are specific directions within the road network where such risks are most concentrated and require priority. Moreover, measuring network patterns such as orientation (North-South-West-East) and geometry can help researchers and planners evaluate a transportation system [15]. Understanding these trends can help prioritize operational management strategies effectively.

Consequently, this project provides a method to identify the areas with the highest concentration of risk and their effect within road networks. This approach prioritizes mitigation, preparedness, and disaster response planning by evaluating the risk posed by natural hazards on road networks, their spatial patterns, and their implications for community risk and resilience. Concerning the RNP, this project makes three primary contributions to literature.

1. First, it introduces a method that addresses an underexplored aspect of RNP risk measurement by combining historical data on past natural hazards and the socioeconomic characteristics of the population, such as community vulnerability and resilience, with the topological characteristics of the road network, like centrality and accessibility measurements, to provide a Road Network Performance Risk measurement.
2. Second, it adapts Boeing's orientation methodology [15] to standardize the natural hazard risk in road networks spatially and compare a wide variety of locations and natural hazards in a standardized way, which would help planners in their prioritization decision-making process.
3. Third, the proposed method is applied in a case study involving many locations in California. The study analyzes the 18 natural hazards included in the National Risk Index (NRI), e.g., avalanche, coastal flooding, cold wave, drought, earthquake, hail, heat wave, hurricane, ice storm, landslide, lightning, riverine flooding, strong wind, tornado, tsunami, volcanic activity, wildfire, and winter weather, and collectively assessing all these hazards in conjunction.

Regarding **Evacuation performance**, the literature review highlights the need to develop a generalizable method to design evacuation plans based on risks. This method should incorporate general information from each location, such as historical wildfire data, socioeconomic characteristics of the population, and road network topology. One of the objectives of developing evacuation plans is identifying the most critical corridors within a road network and examining various scenarios, including simulated real-life wildfires. Additionally, identify corridors' performance regarding time, risk, and resource minimization to enhance their resilience for vulnerable populations in future evacuations. Table 1 shows the lack of consideration of expected risk perceived by the evacuees during the evacuation process and an analysis of the sociodemographic information and its influence on the evacuation. This project provides a decision-makers tool to identify the main corridors to be prioritized in a location to increase their resilience to vulnerable populations based on the population's socioeconomic characteristics and the risk assessment [4].

Road Network Performance

One of the main objectives of this project is to evaluate the strengths and weaknesses of the road network by focusing a literature review on the analysis of the RNP measurements [16]. Literature provides various concepts, definitions, and methods to measure them, which could lead to confusion between concepts. Rivera-Royero et al. [10] provide a classification scheme to distinguish and identify relationships between a set of eleven RNPs: i) *connectivity*, ii) *redundancy*, iii) *accessibility*, iv) *reliability*, v) *connectivity reliability (CR)*, vi) *travel time*

reliability (TTR), vii) capacity reliability (AR), viii) robustness, ix) flexibility, x) resilience, and xi) vulnerability. Additionally, they classify RNP concepts into three sets: I) *Topology-based (T)* for those that rely on the network infrastructure/topology, and decision-makers use them when they have the objective of designing or redesigning road networks, e.g., *connectivity*, *redundancy*, *accessibility*, *reliability*, and *vulnerability*. II) *Threshold-based (H)* for those that depend on a threshold defined by users, which generally involves the traffic speed, flow, and density, e.g., *accessibility*, *reliability*, *TTR*, *AR*, and *CR*. Finally, III) *Event-based (E)* for those considered when analyzing the impact of disturbing events on the road network, e.g., *robustness*, *resilience*, *flexibility*, *reliability (TTR, AR)*, and *vulnerability* [10] (See Figure 1).

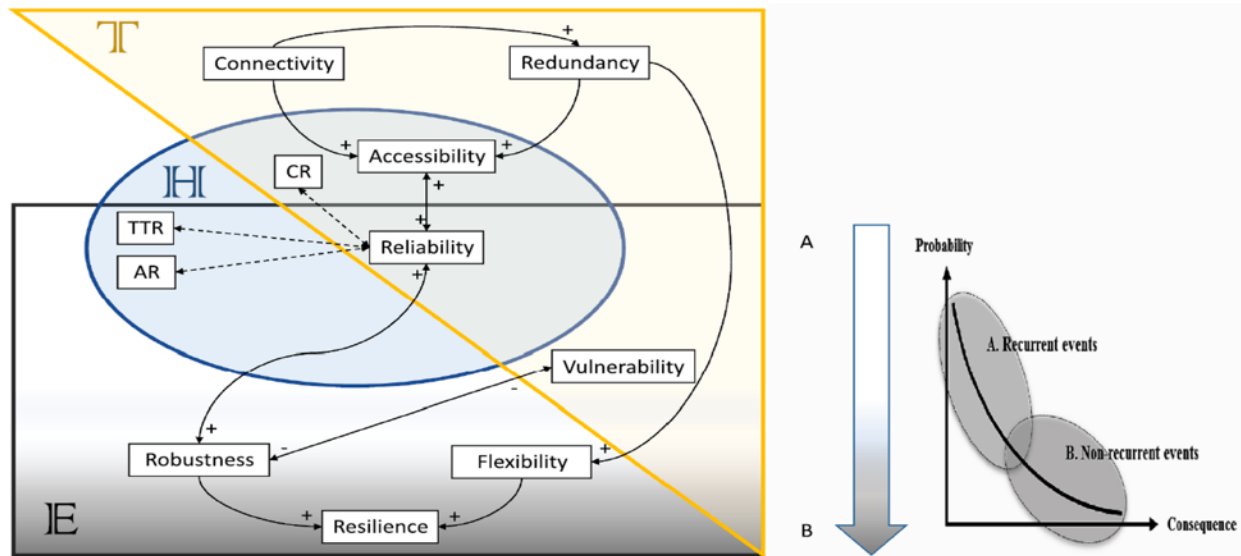


Figure 1. Road Network performance classification. From Rivera-Royero, et.al. [10]

Appendix A offers an expanded overview of the eighty-seven RNP measurements from Rivera-Royero et al. [10], including the mathematical formulas and their key characteristics. None of the RNP measurements in Appendix A enables the identification of high-risk areas within a road network as they solely rely on road network characteristics without considering natural hazard risks. Nevertheless, some of these measurements provide insight into identifying nodes or arcs of relatively high importance within the road network. To identify the areas and directions with the highest risk concentration within a road network, we can construct upon the knowledge behind those 87 RNP measurements.

The 87 RNP measurements indicate the strengths and weaknesses of the road network. These measurements can be categorized into global, regional, and local. *Global* RNP measurements consist of a single value representing the entire road network, *regional* RNP measurements consider a set of values for subgroups of elements (arcs or nodes) within the road network, and *local* RNP measurements provide values for each node or arc of the road network. Furthermore, the RNP measurements may or may not require information regarding traffic flow data for their computation. The authors can identify the network's characteristics by eliminating the impact of traffic behavior within the population and by analyzing those RNP

measurements that do not require traffic data. The RNP measurements that do not require traffic data can be classified as topology-based measurements and are supported by a well-developed network science framework [17, 18].

Local RNP measurements that do not require traffic data possess a mathematical formula that allows a relatively straightforward and quick estimation, facilitating comparison across a wide range of road networks. Furthermore, local RNP measurements provide spatial information on road network characteristics, as the precise location of each node is determined in the Coordinate Reference System (CRS). Therefore, *local* RNP node-based measures allow for identifying nodes of significant importance and their location. If combined with natural hazard risk data, it would be possible to identify high-risk areas within a road network. In this sense, eight of the 87 RNP measurements shown in Appendix A are *local* RNP measurements that do not require traffic data. These RNP measurements include i) 'degree node' and 'number of paths' [19] for *connectivity*, ii) '*Hansen integral accessibility index*' [20], '*betweenness centrality*,' '*normalized betweenness centrality*,' '*normalized closeness centrality*' [21], and '*average Shimbel index*' [22] for *accessibility*. Additionally, *resilience* has a '*node resilience index*' [23].

Road Network Performance Risk

'Risk' is an RNP measurement not discussed in Rivera-Royero et al. [14] and is extended in this section. In addition to the previous RNP measurements, we identified measurements combining risk and the topological structure of the road network. For example, Casali and Heinimann [24], Zhang and Alipour [25], and Nelson et al. [18] addressed the risk of natural hazards on the road network using centrality measurements as indicators of the road network risk, e.g., *betweenness centrality* and *closeness centrality*, among others. Casali and Heinimann [24] examined flood impacts on road network topological characteristics in Zurich, Switzerland. The authors used centrality metrics such as node and edge betweenness and closeness centrality. They utilized GIS layers to visualize the centrality results on the map. One of the limitations of Casali and Heinimann [24] is that it was only performed in one city, and it does not allow for comparison with other locations or other natural hazards. Furthermore, each measurement was analyzed independently and did not include a measurement of the natural hazard risk. Likewise, Zhang and Alipour [25] linked connectivity measures with the topological risk analysis, and they proposed a framework for assessing the risk for Iowa's primary road network system in the event of flooding. They used the average node degree, cluster coefficients, and shortest path as the connectivity measures at the topologic network-level risk assessment.

Despite identifying data scarcity in most disaster-prone cities, Nelson et al. [18] found that connectivity and centrality measurements could assess vulnerabilities and risks on the road network of Freetown, Sierra Leona. They identified high-centrality interceptions and high-hazard areas with mainstream environmental GIS data. They measured the risk through the interaction of topological centrality and multi-hazard layers, where risk is the likelihood of occurrence of natural hazards times the consequences of the disruption given by the *betweenness centrality*. Finally, they provided a risk matrix for the city, where they classify the

road network nodes into nine clusters, given by the combination of low, moderate, or high hazard risk and low, moderate, or high *betweenness centrality*, e.g., cluster 1: low hazard risk and low *betweenness centrality*, cluster 2: low hazard risk and moderate *betweenness centrality*, etc. However, their limited data sources and specific methodology applied to a single location do not allow comparative analysis between different locations. In addition, most papers have only considered hydrological natural hazards for analyzing road network risk, excluding other types of natural hazards such as wildfires.

Road Network Performance Risk: Spatial Analysis

Appendix A shows three RNP measurements that group nodes into subgroups or regions: i) *clustering* (connectivity) [13], ii) *total exposure* (vulnerability), and iii) *regional importance* (vulnerability) [14]. However, those subgroups are not standard for all road networks and do not allow comparative analyses between two or more locations. Recalling that one of the main objectives of this project is to identify the areas and directions with the highest risk concentration within a road network and to provide a method that allows the comparison of risk between a set of locations and different natural hazards for prioritization purposes. One alternative is to provide a standard method that allows such comparison. This study uses a spatial method derived from the transportation system's urban landscape literature [15]. Boeing compared the orientation of the network patterns of around one hundred cities worldwide, independently of their geometry and shapes. Boeing [15] analyzed this diverse set of road networks by subgrouping the arcs using counterclock angle orientation, e.g., (90°) North, (270°) South, (180°) West, and (0°) East. Boeing divided the city into thirty-six equal-sized bins, each representing 10°, and assigned an entropy value representing each angle. Finally, the method provided one entropy metric that identifies if a city stands on an idealized grid (North-South-East-West) ($\phi = 0$), or if the city is in complete disorder ($\phi = 1$). It is important to note that Boeing's orientation analysis does not include an assessment of the road network capabilities or risk against natural hazards in each location.

Evacuation Performance

Disaster Operation Management (DOM) strategies include the actions taken before, during, and after a natural or anthropogenic disaster [26]. DOM differs from commercial management operations because disasters are rare. This means that operations during a disaster have many uncertainties that increase complexity, e.g., unknown demand and supply, information systems disrupted, shorter response times, and social objectives are commonly used [27]. DOM strategies include mitigation, preparedness, response, and recovery [28]. Commonly, DOM relies on operations research and management science (OR/MS) [29]. Other examples of DOM are prepositioning supplies [30] and distributing relief items [31, 32]. Evacuations are one of the DOMs, and they play an important role in saving lives before and during natural hazards such as hurricanes, wildfires, and tsunamis.

In the literature, researchers study evacuation by examining behavioral and engineering perspectives. From the initial perspective, researchers attempt to distinguish the factors that influence the decisions of the evacuees. Including behavioral elements in the transportation

models allows a more realistic estimation of the evacuation time [33, 34]. Studies examine the behaviors from surveys of the affected population after specific disasters by stated preference surveys evaluating hypothetical scenarios or by using walking evacuation simulation [35].

From the engineering perspective, researchers focus on time performance estimation and traffic flow modeling, among others [33]. The strategies to deal with evacuations from an engineering perspective can be based on the demand and supply of the transportation network. Strategies for the traffic supply include transit operations, special signal timings, shoulder lane use, crossing elimination, and contraflow operations [36, 37, 38]. The demand involves evacuation staging, departure time, route assignment, and reducing shadow or background traffic [37, 36].

This project analyzes the performance of evacuation plans through optimization models, considering expected wildfire risk, evacuation time, vehicle demand, and road network capacities. One objective was to determine how the current state of the road network may impact evacuation performance and develop a generalized methodology for various locations. This scope limits the direct consideration of behavioral elements; however, the study considers the population's socioeconomic characteristics in the evacuation risk analysis estimation. Table 1 summarizes papers that estimated the evacuation performance using the 'evacuation scheduling problem' and 'evacuation network clearance time.' All these papers involve traffic routing or traffic assignments in their modeling. Eighteen of the 47 papers focus on the staggered evacuation of the demand side, and just three papers combine the staggered evacuation with supply-side strategies, such as contraflow [38, 39] or traffic signal [40]. Thirteen papers provide shelter information in the modeling as part of the destination. Around 20 papers used city level in their evacuation process, and the analyzed events are wildfire, hurricanes, floods, nuclear plants, and terrorist attack evacuation scenarios. The solution methods used in the modeling included mathematical programming (32), simulation (26), and algorithms (4). Twelve papers combined simulation and mathematical programming in the solution method, while 25 of the 30 papers used heuristics to solve the mathematical programming models. The papers have a variety of objective functions, but in general, the most widely used objectives are minimizing evacuation time and minimizing clearance time [41, 38]. Clearing time refers to when the last member of the population exits the area, and the total evacuation time refers to the total time spent by all the individuals exiting the area. Most papers assume safe collection points in the area and that it is possible to exit the town by vehicle. Among the constraints employed in literature, models usually include mass flow balance and capacities in the links and nodes.

Additionally, the authors include behavioral elements in the transportation models; this allows a more realistic estimation of the evacuation time [33, 34]. In the literature, researchers obtain the simulation parameters from surveys of the affected population after the disaster or by stated preference survey when the interviewer provides hypothetical scenarios; however, such a methodology is beyond this project's scope. Another way to include the behavioral aspects in estimating the evacuation time is to use the parameters described in the literature [38].

Moreover, Figure 2 summarizes relevant evacuation studies from the perspective of the evaluation approaches: mathematical programming (MP) and simulation (S), with MP&S being the sub-set with the largest share. However, [42, 43, 44] also considers the application of models such as machine learning, deep learning, and others that are beyond this project's scope due to the significant amount of data required from evacuation settings. As a source of such data, researchers have identified the Internet of Emergency Services (IoES) as an implementation of the Internet of Things (IoT) in emergency settings [45].

Among the papers belonging to MP, only [46], [47], and [48] analyze the evacuation without including *shelters* as an option. On the one hand, [46] uses a time-expanded model to optimize the evacuation plan, and [47] models the capacity-constrained evacuation scheduling problem over discrete time as an integer optimization model. These approaches suffer from high computational costs and do not scale to large transportation networks. On the other hand, [48] provides a method to obtain the optimal egress time and path generation for large evacuation networks when all the population is requested to evacuate with no predetermined priorities, obtaining a set of mathematical models able to handle large-size networks with low computation time. Among papers on the MP set, only [49] include a risk analysis based on the time you are exposed to a particular hazard.

In the simulation set (S), [50] used a household survey to model the risk perception of wildfire in a traffic simulation model. This survey method works well for evacuees' behavior in the specific case of Mati, Greece; however, such results cannot be generalized to other cases in different places. [51] discuss another type of risk assessment based on priorities determined by the time the natural hazard is expected to affect a given node, allowing only a limited time for the population in those nodes to evacuate. They implement the method in a hurricane setting with path projections made in advance. In the event of a short- or no-notice wildfire, such projections are not feasible, as the information is usually unavailable, and the evacuation should be carried out quickly. Therefore, it is essential to use a methodology that is adaptable to different settings and does not depend on a priory projection but instead provides a robust plan for various situations, such as short- or no-time wildfire events.

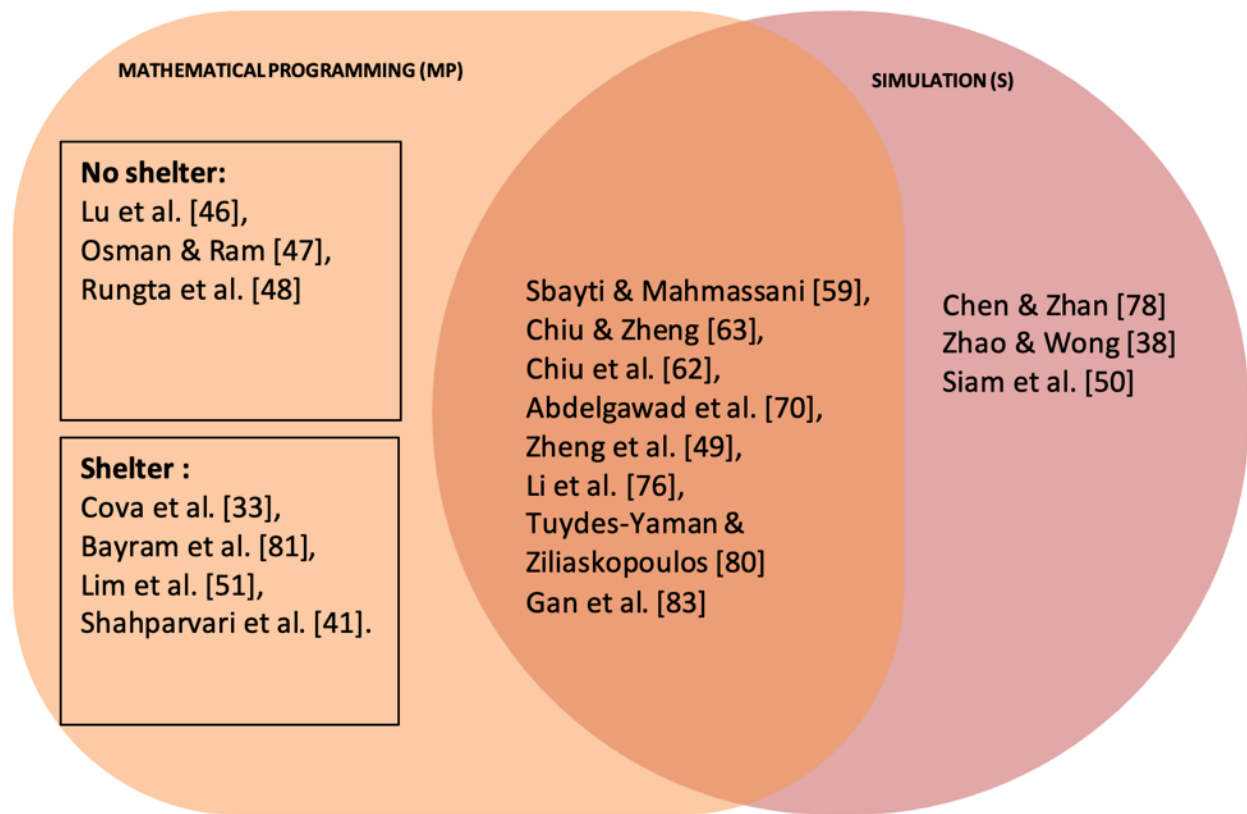


Figure 2. Methodology classification on the literature review, including Mathematical Programming and Simulation

Bottleneck Analysis with Omniscape

Omniscape [89] is a raster-based model based on circuit theory [90] that uses a GIS to analyze flow or blockage levels across all landscape elements. It has been widely used in conservation assessments to simulate the connectivity of habitats or potential movement patterns of species [91]. The model is also used where current climates in some areas may be found, based on climate change projections [92, 93, 94]. More recently, team member Thorne applied it to model open space connectivity in Seoul, a city with 10 million inhabitants [95]. In this case, we restricted the “landscape” of the modeling to the transportation network of our test cities. We conducted a sensitivity analysis to determine whether the tool could be used to identify areas with a high potential for traffic bottlenecks during an evacuation.

Table 1. Taxonomy evacuation management (LP: Linear Programming, IP: Integer Programming, NLP: No linear programming, MIP: Mixed Integer Programming, ABS: Agent-Based Simulation, MCS: Montecarlo Simulation, TS: Traffic Simulation.)

Author	Evacuation						Geographical level						Natural or Manmade disaster						Modeling			Mathematical Modeling						Solution method																																																																																																																																																																																																																																																																																																																																																																																																																																																																																																																																																																																																																																																																															
	Demand		Supply			Disaster																																																																																																																																																																																																																																																																																																																																																																																																																																																																																																																																																																																																																																																																																																					

Author	Evacuation						Geographical level							Natural or Manmade disaster						Modeling			Mathematical Modeling						Solution method					
	Demand		Supply		Behavioral	Shelter	Federal	State	Regional	County	City	Town	Neighbor	Hurricane	Wildfire	Flood	Terrorist Attack	Nuclear Plant	Not specified	MP	Simulation	Algorithm	LP	IP	NLP	MIP	Stochastic	Dynamic	Exact	Heuristic	Simulation			
	Staggered	Traffic Routing	Contraflow	traffic signal																											ABS	MCS	TS	
Ozbay et al [75]		1												1					1														1	
Rungta et al. [48]	1	1						1												1					1	1		1						
Li et al. [76]	1	1				1		1						1						1	1					1	1			1				
Coutinho et.al [77]		1				1				1					1					1			1			1				1				
Nassir et.al. [40]		1		1						1									1	1														
Chen & Zhan [78]	1	1			1							1	1	1							1						1							
Lim et al. [79]		1								1				1						1	1			1	1		1	1	1	1			1	
Tuydes-Yaman et.al [80]	1	1						1						1						1	1			1	1		1		1	1			1	
Bayram el al. [81]	1	1				1				1										1					1				1					
Shahparvari et.al [82]	1					1				1					1					1				1	1					1				
Gan et al. [83]	1	1								1					1					1	1			1				1	1	1			1	
Beloglazov et. Al [84]		1			1			1							1						1				1			1	1	1				1
Steer et al. [85]		1			1	1		1							1													1			1			
Shahabi el al. [86]		1				1				1					1					1		1				1		1		1				
Shahparvari el al. [87]		1				1				1					1					1			1							1				
Zhao et al. [38]	1	1	1		1																													
Siam el al. [50]	1	1			1	1																										1		
Grajdura el al. [88]		1			1					1					1						1										1			
This study	1	1								1				1	1	1	1	1		1				1			1		1	1				

Methodology

The author analyzed a sample of municipalities in California, for which the team had collected their evacuation plans and analyzed the natural hazard risk on their road networks. Based on the road network risk analysis results, the team selected a case study of a locality with a high risk of wildfire and conducted an in-depth analysis of evacuation that could be replicated in other localities. The project involves four tasks described as follows:

Task 1: Evacuation Routes Data Collection and Database Construction

California's 58 counties and its many incorporated municipalities have obligations under Assembly Bill 747 to consider safety elements in their general plans, including identifying evacuation routes. However, these plans have not been compiled into a comprehensive database. This project addressed Caltrans' data need to compile the evacuation routes developed by California municipalities into a single database to support other agencies in planning, maintaining, and providing access to routes that use state transportation highways under evacuation settings. This stage of the project did not involve the collection of original data. We conducted a search of different cities and counties to identify: 1) which jurisdictions have already identified their evacuation routes under AB 747; 2) which are in the process of doing so as part of their updates to their local hazard mitigation plans; 3) which have planned for the process; 4) which have evacuation routes, but not specific to wildfire, and 5) which have no available information. The search used publicly available spatial data from highways, buses, rail, and vulnerable communities. The team looked for data from previous evacuation events, as compiled by agencies such as Caltrans or CAL FIRE.

This task aimed to create and maintain a database with the road network and evacuation routes. Among the data collected for each County or City were the Safety Elements, Local Hazard Mitigation Plan (LHMP), Emergency Operations Plan (EOP), Evacuation Map, Evacuation Analysis, GIS Map, Multimodal Evacuation Accessibility, and Shelter Map. Additionally, the contact information of the office responsible for the safety information for each locality in California at a county/MPO/city level was collected, depending on the public availability of the information. Local agencies usually provide such information following AB 747. The evacuation route collection was managed in an open architecture database that contains information on GIS maps for the localities that had such information, as well as the plans developed by the different localities. We analyzed the data from the cities according to the different formats they were in interactive maps, map pdfs, or evacuation routes for multiple hazards (e.g., tsunamis, floods, fires). For those evacuation routes not in GIS format, the team compiled the data in other formats and constructed (digitized) the routes for the two case study wildfire events.

Additionally, the team collected information about the State Highway System and passenger rail and intercity bus routes and compared them with the current evacuation routes for our case study events. Most of this information is publicly available in the California State Geoportal [96] and is usually updated with information about its conditions. We also collected a range of other data for the analyses conducted in this study. Those data include sources such as California Department of Fish and Wildlife Regions, National Risk Index Census Tracts, Highway

Performance Monitoring System Layer, Fire Hazard Severity Zones Layer, National Land Cover Database Land Cover, CalEnviroScreen 4.0 Results, Wildland Urban Interface, and State Highway System data on passenger rail and intercity bus routes; US Census data [97].

Task 2: Assessing the Performance of the Road Network

The team performed a quantitative assessment of the road networks for a representative selection of more than 450 cities in California based on historical information on different natural hazard risks, including wildfires, hurricanes, tsunamis, and earthquakes, among other risks. The proposed metrics were standardized or used network topography measures (e.g., connectivity, accessibility, degree). This task provides a quantitative analysis using the latest literature regarding performance metrics as described in [10].

The team determined each selected location's Road Network Performance Risk using multiple descriptive statistics, graph theory algorithms, and spatial pattern analysis. This methodology incorporates natural hazard risk, socio-demographic vulnerability, and community resilience with Road Network Performance accessibility ($RNP_{accessibility}$) indexes, which represent the importance of the road network nodes. These $RNP_{accessibility}$ measurements can either reduce or exacerbate the natural hazard risk for the population in each location. If a natural hazard affects crucial road network nodes vital for accessibility and mobility, the overall natural hazard risk for the population can increase. Figure 3 depicts the methodology followed to analyze each road network and the description of each measurement estimated in each step of the RNP_{risk} methodology is given as follows.

The methodology provides measurements at three levels of the road network: local at node level, regional level, and global or system-wide level. These different levels help, for example, to identify the geographic area of the most vulnerable nodes, sections, or directions of the road network against different types of natural hazards; to compare the RNP_{risk} of multiple locations or to identify the most vulnerable cities among a large set of locations, among other purposes. The main steps of the methodology include:

1. Determining the Road Network for Each Location

For this step, the authors used the 'graph_from_place' function from OpenStreetMapNX (OSMnx) [98, 99]. Based on the authors' experience, the road networks obtained directly from this function for each city do not reflect entirely the characteristics of the city boundaries; for this reason, the authors added a buffer between 1 and 2 miles depending on the diameter of the city.

Natural hazard, Socio-Geographical & Road Network Risk

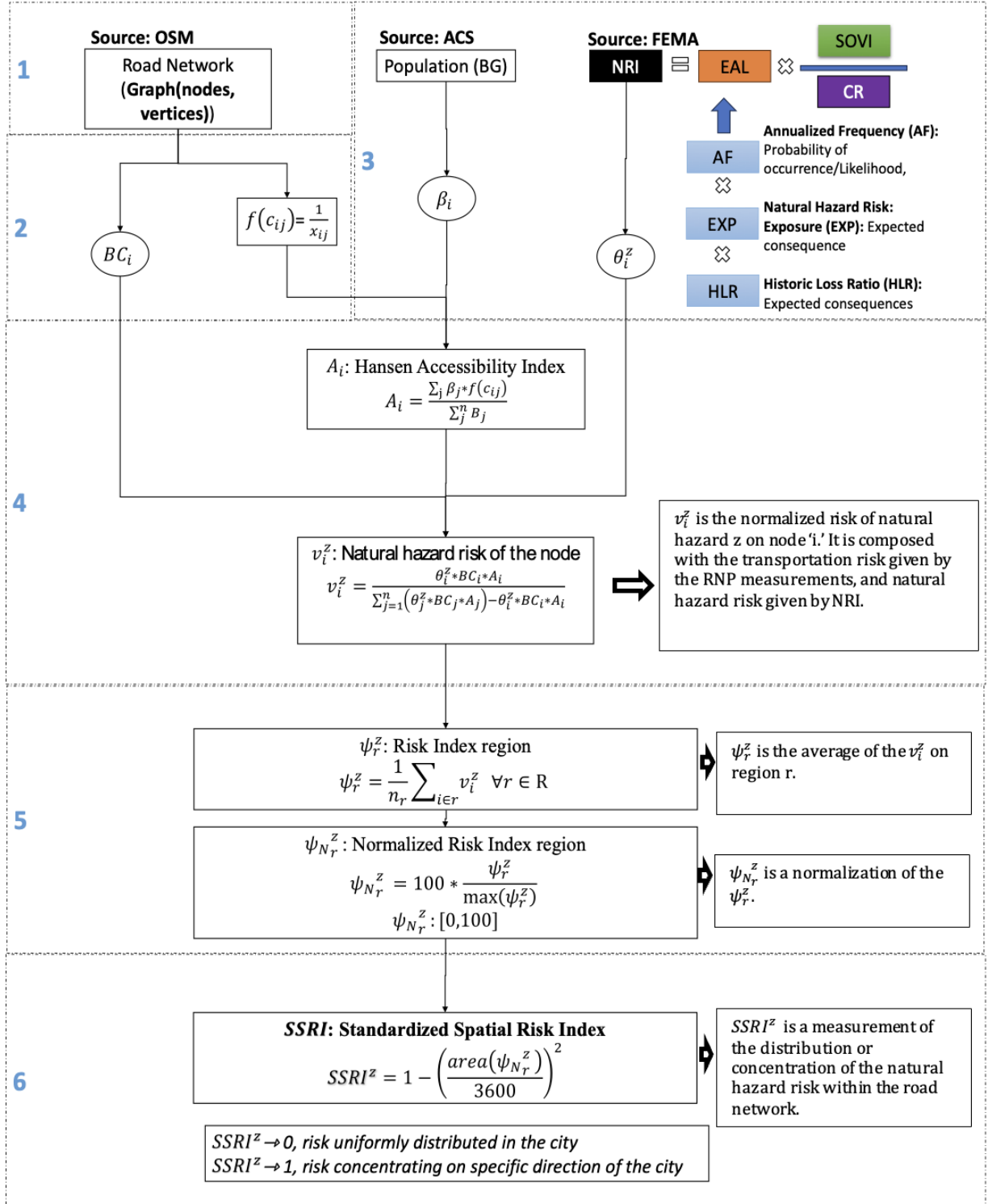


Figure 3. RNP_{risk} methodology steps.

2. Estimating the Natural Risk (θ_i^z) and Population (β_i) at the Node Level

According to Bründl [100], natural hazard risk depends on the probability of natural hazards and their consequences. To obtain the natural hazard risk of each node of each locality for each natural hazard θ_i^z , the authors adapted the method used by FEMA in the construction of the National Risk Index (NRI) [101, 97]. NRI considers eighteen different types of natural hazards and provides individual and generalized risks considering All hazards (All-HZ). The data allows comparison and prioritization of strategies that depend on the type of natural hazard. NRI's formulation is as follows:

$$NRI^z = Expected Annual Loss^z * Community Risk Factor \quad Eq.1$$

$$Expected Annual Loss^z = Annual Frequency^z * Exposure^z * Historic Loss Ratio^z \quad Eq.2$$

$$Community Risk Factor = f\left(\frac{Social Vulnerability}{Community Resilience}\right) \quad Eq.3$$

The NRI calculates natural risk as the expected annual loss (EAL). This is determined by estimating the likelihood of the natural hazard through its annual frequency (AF) and assessing the consequences based on exposure (EXP) and the historical loss ratio (HLR). The NRI also utilizes a community risk factor influenced by two main elements: the Social Vulnerability Index (SOVI) and Community Resilience (CR). These community risk factors can increase or mitigate the natural hazard risk based on the community's socioeconomic characteristics. According to FEMA [101], the risk of a location increases with higher EAL and SOVI and decreases with higher CR. SOVI and CR are independent of the type of natural hazard (z). The EAL is distributed in dollars, while the other elements are represented as indexes. However, all are normalized between 0 and 100 using their maximum and minimum values. The NRI is also normalized according to the geographical area. FEMA provides the NRI to the county and census tract levels; in this project, the authors estimate the NRI at the census block group level and then at the local level using the road network nodes.

Estimating the NRI at the *census block group* requires estimating or downscaling its components (e.g., SOVI, CR) at this geographical level. First, the SOVI considers sixteen variables obtained from the American Community Survey (ACS) [102]. The variables used to estimate the SOVI include the percentage of unemployed, the percentage of people living below 150% poverty, and the percentage of the population with a high school diploma, among others (see more details in [103]). It is important to highlight that not all the variables had values at the *census block group*; thus, the study utilized the census tract values for those cases since the variables are mostly percentage-based and independent of the geographical area. In the original method, the CDC grouped the 16 variables into four *themes* [103]: *socioeconomic status*, *household characteristics*, *racial & ethnic minority status*, and *housing type & transportation*. Estimating the SOVI requires selecting each variable and then adding the ranks grouped by each theme of variables. Afterward, it requires adding the ranks of all the themes and ranking them to acquire the SOVI for each census block group. The authors estimated the EAL at the census block group level as a proportion of the population of each census block relative to the census tract. In conclusion, as the CR is initially located at the county level and

then downscaled at the census tract in the NRI, this methodology employed the same assumption to downscale at the census block group level.

The next step was to use Eq.1 to estimate the NRI at the node level (θ_i^z), estimated as a proportion of the population assigned to each node relative to the population of the *census block group* to which the node belongs. Note that the population of each *census block group* is composed of the ACS and is assigned evenly proportional to the number of nodes in each census block group (β_i).

3. **Normalized Betweenness Centrality (BC_i), Shortest Path Distance (x_{ij}), and Hansen Accessibility Index (A_i)**

From each road network, the method estimates the shortest path distance x_{ij} between each pair of nodes (i, j) in the graph, and the normalized betweenness centrality for each node (BC_i). Based on Casali and Heinemann [21], BC_i is the proportion of times that node i is in the shortest path of all the pairs of nodes (excluding pairs where i is the origin or destination node) in the road network. To obtain x_{ij} and BC_i efficiently, the authors modified the 'floyd_warshall' function given by python's packages 'NetworkX' [104]. x_{ij} is the input of impedance function $f(x_{ij}) = \frac{1}{x_{ij}}$, which is an indicator of the easiness of reaching all the other nodes from node i [105]. The smaller the shortest path distance (x_{ij}) between a pair the nodes, the larger the value of $f(x_{ij})$. Meaning easier reachability or higher accessibility between them, in comparison with other pairs of nodes. Then, the methods estimate the Hansen Accessibility Index (A_i) for each node i that includes the population (β_i) on node i and the $f(x_{ij})$ impedance function. A_i is a measurement indicating how far away or how easily vehicles can travel from node i to the rest of the nodes of the road network based on the population assigned to each node. Note that BC_i and A_i are independent of the natural hazard risk.

4. **RNP_{risk} at the Node Level: v_i^z**

v_i^z represents the normalized risk of natural hazard z on node i , including the transportation risk represented by the RNP accessibility measurements. v_i^z associates the risk θ_i^z of natural hazards z enhanced or reduced by the socio-geographical characteristics of the population, and the road network performance accessibility measurements given by BC_i and A_i . BC_i and A_i act as measurements of how important the node is relative to the others. Therefore, the natural hazard risk is enhanced by the node's importance and the potential damage to its functionality due to a natural hazard.

$$v_i^z(\theta_i^z, BC_i, A_i) = \frac{\theta_i^z * BC_i * A_i}{\sum_{j=1}^n (\theta_j^z * BC_j * A_j) - \theta_i^z * BC_i * A_i} \quad \text{Eq.4}$$

5. **RNP_{risk} at the Regional Level: ψ_r^z and $\psi_{N_r}^z$**

To spatially standardize the risk of natural hazards on different types of road networks, the author used the 36-bin classification mentioned by Boeing in his orientation index estimation

[15]. Still, instead of estimating the entropy, the authors estimated a natural hazard risk at a regional level:

$$\psi_r^z(v_i^z) = \frac{1}{n_r} \sum_{i \in r} v_i^z \quad \forall r \in R \quad \text{Eq.5}$$

$$\psi_{N_r}^z(\psi_r^z) = 100 * \frac{\psi_r^z}{\max(\psi_r^z)} \quad \forall r \in R \quad \text{Eq.6}$$

ψ_r^z is the average of the v_i^z on n_r , while $\psi_{N_r}^z$ is a normalization of the ψ_r^z , based on the maximum value of ψ_r^z in all the regions. n_r is the number of nodes in region r (bin), and the regions are $R = \{0^\circ, 10^\circ, \dots, 90^\circ, \dots, 180^\circ, \dots, 350^\circ, 0^\circ\}$. Note that $\psi_{N_r}^z$ can take values between 0 and 100. When $\psi_{N_r}^z$ is closer to one hundred means that the natural hazard risk, enhanced by the transportation risk at such a region (direction), is highly concentrated.

6. RNP_{risk} at the global level: Standardized Spatial Risk Index ($SSRI^z$)

Finally, the authors propose the Standardized Spatial Risk Index as a measure of the concentration of the natural hazard risk within the city.

$$SSRI^z(\psi_{N_r}^z) = 1 - \left(\frac{\text{area}(\psi_{N_r}^z)}{3600} \right)^2 \quad \text{Eq.6}$$

In this case, if $SSRI^z \rightarrow 0$, it means that the risk is distributed uniformly within the city; otherwise, if $SSRI^z \rightarrow 1$ means that the risk concentrates in a specific(s) direction(s) of the city. Knowing such characteristics is essential to identify insights about prioritizing attention in a set of cities depending on the natural hazard considered.

Task 3: Assessing the Map of Evacuation Routes Using the Other Data Collected to Determine the Equity of Access to Evacuations

This task aimed to develop evacuation performance metrics and compare the evacuation routes against best practices. The team reviewed the previous evacuation events, examining data availability and historical consequences of these events. The team also assessed the accuracy of the evacuation routes relative to actual evacuation travel in the case study. We evaluated which sections of the state highway system and local streets are most important to maintain for evacuations based on local views of evacuation priorities and the level of evacuation routes served by bus and rail. Overall, these issues were addressed by conducting two independent modeling analyses: 1) *Assessing evacuation time with mathematical programming modeling*, where we modeled evacuation times on two urban areas that were affected by previous evacuation wildfire events, the 2018 Camp Fire that affected Paradise and Magalia, and the 2018 Thomas Fire that affected Ventura, Santa Paula, Ojai and other cities; and 2) *Assessing bottleneck with Omniscape*: where we employed a connectivity modeling tool to assess where bottlenecks were likely to occur. This section first details the evacuation time modeling with mathematical programming and then the bottleneck analysis with **Omniscape**.

Assessing Evacuation Time with Mathematical Programming Modeling

We used a four-step modeling framework to design evacuation plans with a wildfire risk assessment depicted in Figure 4.

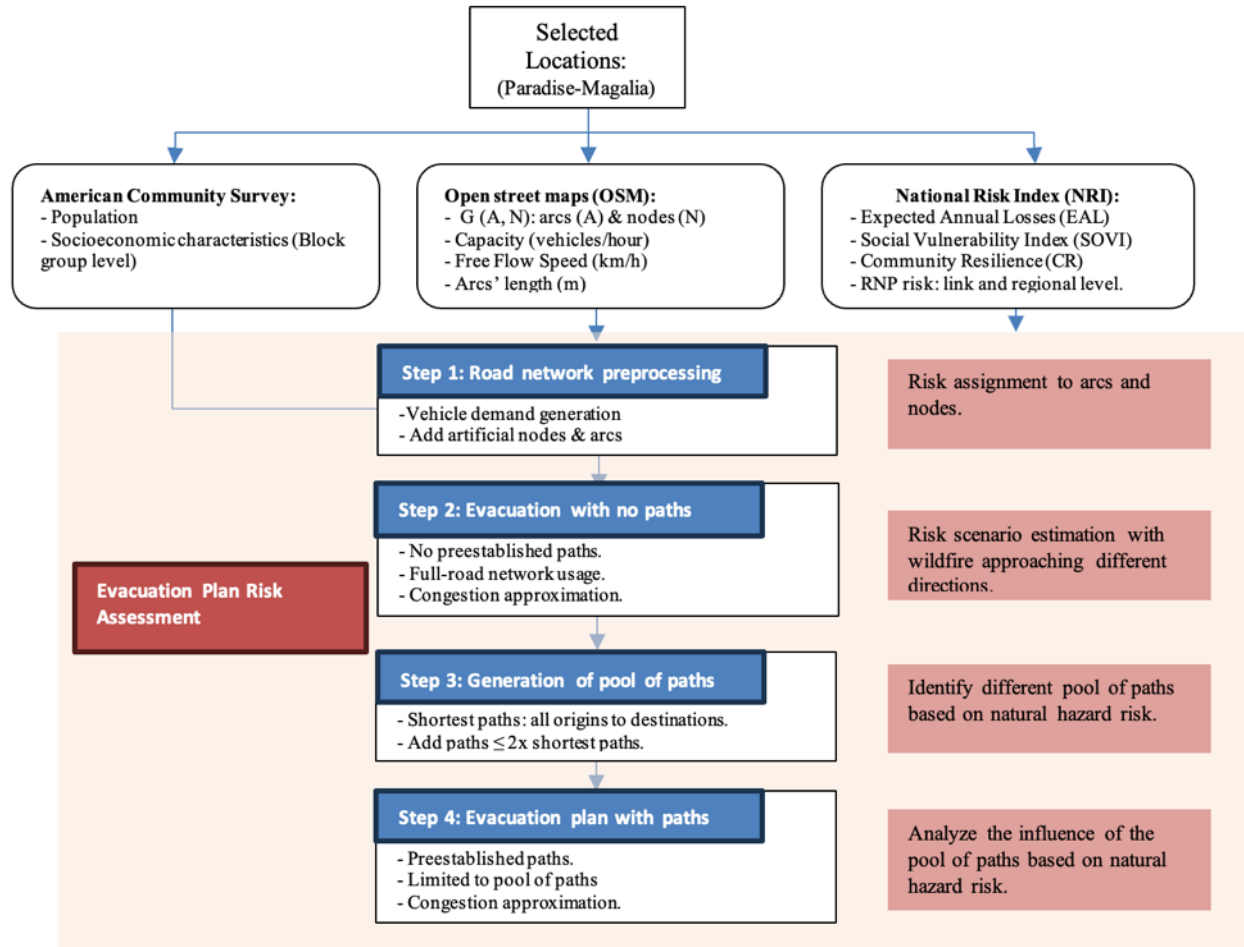


Figure 4. General methodology

Step 1: Road network preprocessing

The team used Open Street Maps (OSM) to obtain the road network $G = (N, A)$, where A is the set of arcs (or streets) and N nodes (or intersections) [98]. Complex intersections in road networks could be simplified to reduce the complexity of mathematical models. The nodes N can be classified as sink (N_s) or intermediate (N_i) nodes. N_s are the nodes connected to external nodes that lead to safe locations outside the road network. Additionally, the arcs obtained from OSM contain information about the highway type and length and partial information about the maximum speed and number of lanes. The mathematical models consider the arc's travel time (tt) and capacity (μ). The authors use the arc's length (l) and speed (v) to calculate the tt ($tt = l/v$). Additionally, the authors use the information described in [106] that depends on the highway type to obtain the μ , number of lanes, and the speed for

those arcs with not information available in OSM. Two types of artificial nodes are created to model the traffic demand: source nodes (N_a) and a super-node (SN).

- **Super-Node (SN):** This artificial node is connected to the all the N_s . SN has enough capacity to attract the total vehicle demand, simplifying the problem into a multiple origin and single destination problem. Let us remark that this model evacuates the population to external areas outside the network, and no internal safe locations were considered.
- **Source Nodes (N_a):** These are origin nodes, with one N_a corresponding to each census block group (CBG) in the location. The vehicle demand assigned to each N_a can be obtained from the American Community Survey (ACS) by using the average household size and vehicle availability per CBG [102]. N_a are connected to the road network via the two closest nodes using artificial arcs.

The artificial arcs connecting N_s to SN , and N_a to the road network have zero travel time and high capacity, ensuring smooth flow. This study builds on the methodologies discussed in [48] to develop the models in Stages 2, 3, and 4. The differences between our models in this project and the models in [48] are described as follows:

Step 2: Evacuation with no paths (ENP)

The problem setting in this stage is to evacuate all vehicle demand from N_a to a safe location outside the road network, the SN . There is no pre-established path; vehicles can use the entire road network and leave it as soon as possible without exceeding arcs' capacity. The mathematical formulation of the ENP model is described as follows:

Sets:

T : Set of time periods, indexed by t .
 N_a : Set of source nodes, i .
 N_s : Set of sink nodes, i
 N_i : Set of intermediate nodes, i
 N : Set of nodes in the road network, indexed by i . ($N_a \cup N_s \cup N_i$)
 SN : Super node
 A : Set of arcs in the road network, indexed by (i,j) .
 $A(i)$: Set of arcs going out of node i , indexed by (i,j) .
 $A^{-1}(i)$: Set of arcs going into node i , indexed by (i,j) .

Parameters:

ξ_i : Initial number of vehicles in node i
 ς_i : Capacity of node i
 μ_{ij} : Maximum capacity of arc from node i to node j

Variables:

y_{ij}^t : Flow of vehicles from node i to node j at time t
 x_i^t : Number of vehicles present at node i at time t

Objective Function

$$Z_{max} \sum_{t \in T} t * x_{i \in SN}^t \quad \text{Eq.8}$$

Constraints

1. Initializing vehicle demand in source nodes N

$$x_i^0 + \sum_{(i,j) \in A(i)} y_{ij}^0 = \xi_i \quad \forall i \in N \quad \text{Eq.9}$$

2. Updating vehicle flow in nodes N

$$x_i^t - x_i^{t-1} + \sum_{(i,j) \in A(i)} y_{ij}^t - \sum_{(j,i) \in A^{-1}(i)} y_{ji}^{t-1} = 0 \quad \forall t \in T \setminus \{0\}, \forall i \in N \quad \text{Eq.10}$$

3. Updating vehicle flow in nodes SN .

$$x_i^t - x_i^{t-1} - \sum_{(j,i) \in A^{-1}(i)} y_{ji}^t = 0 \quad \forall t \in T \setminus \{0\}, i = SN \quad \text{Eq.11}$$

4. No vehicles at the end of the planning horizon.

$$x_i^{|T|-1} = 0 \quad \forall i \in N \quad \text{Eq.12}$$

5. Bounds of the vehicle inventory variable

$$0 \leq x_i^t \leq \varsigma_i \quad \forall i \in N, \forall t \in T \quad \text{Eq.13}$$

6. Limitation flow to Super Node

$$\sum_{(j,i) \in A^{-1}(SN)} \sum_{t \in T} y_{ji}^t = \sum_{i \in N} \xi_i \quad \text{Eq.14}$$

7. Limitation flow for each node.

$$\sum_{t \in T \setminus \{0\}} \sum_{(j,i) \in A^{-1}(i)} y_{ji}^{t-1} \leq \varsigma_i \quad \forall i \in N_s \quad \text{Eq.15}$$

8. Limitation flow for each arc.

$$0 \leq y_{ij}^t \leq \mu_{ij} \quad \forall t \in T, \forall (i,j) \in A \quad \text{Eq.16}$$

9. Nature of the variables

$$y_{ij}^t, x_i^t \in \mathbb{Z}^+ \quad \text{Eq.17}$$

One of the main differences between the ENP and the Minimum Egress Time (MET) model described in [48] is in the objective function. The objective function of the ENP is to maximize the cumulative number of vehicles evacuated to the SN weighted by time ($Z_{max} \sum_{t \in T} t * x_{i \in SN}^t$) (see Eq.8), while the objective of the MET is to minimize the flow of vehicles to the N_s for each time-unit (TU) in the planning horizon ($Z_{min} \sum_{t \in T} \sum_{(i,j) \in A(N_s)} t * y_{(i,j)}^t$). In both cases, the objective is to minimize the time when all vehicles evacuate the location; however, Eq.8 avoids possible delays in the flow from N_s to the SN, as may occur in MET. The ENP model is designed for road networks with arcs with 1 TU travel time. Initially, travel times could be in seconds; therefore, converting those travel times into TUs is necessary. One TU is the value of the minimum travel time within all the arcs ($\min(tt_a)$), and the travel time for each arc in TU is obtained as $TU_a = \lceil tt_a / \min(tt_a) \rceil$. After determining the travel time in TU units, it is necessary to add as many artificial nodes and arcs as required between each pair of nodes with travel times greater than one TU. For example, if the minimum travel time in free flow in the road

network is 10 seconds, and the travel time for a random arc in free flow speed is 60 seconds, then it requires 6 TUs to cross the arc. Therefore, it is necessary to add 5 artificial nodes between these two nodes, connected by 6 arcs with one TU each and capacity transformed to the number of vehicles per $\min(tt_a)$. This process results with a road network with a larger size, $G_{mod} = (N_{mod}, A_{mod})$. From, Eq.9 initializes the demand for vehicles for each N_a . Eq.10 is a flow balance constraint to each node. Eq.11 updates the number of vehicles reaching the SN by adding the flow entering the SN from all the N_s . Eq.12 establishes that at the end of the planning horizon, the road network is empty, while Eq.13 and Eq.16 provide the bounds and the integer nature of each decision variable. Note that in Eq.13, the ζ_i for intermediate nodes N_i , must be zero, while for Eq.16, the arc's flow value is constrained by the arc's maximum capacity during each time. Eq.14 establishes that all the demand at the beginning of the planning horizon reaches the SN, and the time 't' when the total demand is evacuated is when Eq.14 is activated. Finally, Eq.15 restricts the flow entering the N_s to their capacities.

Step 3: Generation of a pool of paths

The GPP model uses the original road network described in Stage 1, and the mathematical formulation is described as follows:

Sets:

N_a : Set of source nodes, i .

N_s : Set of sink nodes, i

N_i : Set of intermediate nodes, i

N : Set of nodes in the road network, indexed by i . ($N_a \cup N_s \cup N_i$)

A : Set of arcs in the road network, indexed by (i,j) .

$A(i)$: Set of arcs going out of node i , indexed by (i,j) .

$A^{-1}(i)$: Set of arcs going into node i , indexed by (i,j) .

Parameters:

t_{ij} : Travel time of arc from node i to node j

Variables:

y_{ij} : 1 if arc (i,j) is present in the shortest path, 0 otherwise

Objective Function

$$Z_{min} \sum_{(i,j) \in A} t_{ij} * y_{ij} \quad \text{Eq.18}$$

Constraints

1. Initializing vehicle flow in the source node N_a

$$\sum_{j|(i,j) \in A(i)} y_{ij} - \sum_{j|(j,i) \in A^{-1}(i)} y_{ji} = 1 \quad i = N_a(o) \quad \text{Eq.19}$$

2. Vehicle flow in intermediate nodes N

$$\sum_{j|(i,j) \in A(i)} y_{ij} - \sum_{j|(j,i) \in A^{-1}(i)} y_{ji} = 0 \quad \forall i \in N \setminus \{N_a(o) \cup N_s(d)\} \quad \text{Eq.20}$$

3. Initializing vehicle flow in the source node N_s

$$\sum_{j|(i,j) \in A(i)} y_{ij} - \sum_{j|(j,i) \in A^{-1}(i)} y_{ji} = -1 \quad i = N_s(d) \quad \text{Eq.21}$$

4. Initializing vehicle flow in the source node N_s

$$\sum_{j|(i,j) \in A(i)} y_{ij} \leq 1 \quad \forall i \in N \quad \text{Eq.22}$$

5. Initializing vehicle flow in the source node N_s

$$\sum_{j|(j,i) \in A^{-1}(i)} y_{ji} \leq 1 \quad \forall i \in N \quad \text{Eq.23}$$

6. Nature of the variables

$$y_{ij} \in B^+\{0,1\} \quad \text{Eq.24}$$

The difference between the GPP and PG models, described in [26], is in the problem setting. The GPP model estimates the shortest path between each pair of nodes (N_a, N_s) , instead of obtaining the shortest paths between each origin node N_a to the SN. The advantage of this assumption is that it creates a more diverse set of paths compared to the method implemented in [48]. The pool of feasible paths includes those with an objective function that can be, at most, double the optimal shortest path time for each Origin-Destination pair. In Eq.18, the authors seek to minimize the total travel time in the network for one origin and destination pair (N_a, N_s) . Eq.19 indicates that from the selected origin node, only one arc exiting this node can have a non-zero value. Eq.20 indicates that the sum of the arcs selected to enter each node must equal those that exit (clear the system). Eq.21 indicates that only one arc must be selected to enter the sink node. Eq.22 and 23 provide the bounds of the decision variable, and Eq. 24 provides the nature of the decision variable.

Step 4: Evacuation plan with paths

The mathematical formulation of the EPWP model is described in this stage. The pool of paths obtained from Stage 3 is an input to the EPWP model, and the initial value of T is the clearance time (CT) obtained in Stage 2. Note it is possible that no feasible solution could be found when solving the EPWP with the initial CT and the pool of paths. Therefore, the EPWP is resolved iteratively, increasing the value of T by one unit for each iteration until the optimal solution is found.

Sets:

T : Set of time periods, indexed by t .

P : Set of paths, indexed by p .

N_a : Set of source nodes, indexed by i .

N_s : Set of sink nodes, indexed by i

N : Set of nodes in the road network, indexed by i . ($N_a \cup N_s \cup N_i$)

SN : Super node

A : Set of arcs in the road network, indexed by a .

δ_a : Set of paths that use arc a , indexed by a

β_p : Set of arcs used in path p , indexed by p

Parameters:

ξ_i : Initial number of vehicles in node i

ς_i : Capacity of node i

θ_{pa} : time to reach arc a from the origin node of path p

μ_a : Maximum capacity of arc a

O_p : Origin node of path p

D_p : Destination node of path p

$\alpha_p: \min(\mu_a) \forall a \in \beta_p$

Variables:

f_p^t : Flow of vehicles on path ' p ' at time t

y_p : 1 if path p is selected, 0 otherwise.

Objective Function

$$Z_{min} \sum_{p \in P} y_p \quad \text{Eq.25}$$

Constraints

1. Arc capacity restrictions from all paths.

$$\sum_{p \in \delta_a} f_p^{(t-\theta_{pa})} \leq \mu_a \quad \forall a \in A, \forall t | \{t - \theta_{pa} \geq 0\} \quad \text{Eq.26}$$

2. Active flow on selected paths.

$$\sum_{t \in T} f_p^t \leq \xi_{[O_p]} * y_p \quad \forall p \in P \quad \text{Eq.27}$$

3. Flow from the origin nodes for each path.

$$\sum_{p | O_p = i} \sum_{t \in T} f_p^t = \xi_i \quad \forall i \in N_a \quad \text{Eq.28}$$

4. Updating vehicles flow in nodes SN .

$$\sum_{p | D_p = i} \sum_{t \in T} f_p^t \leq \zeta_i \quad \forall i \in N_s \quad \text{Eq.29}$$

5. Active flow on selected paths.

$$f_p^t \leq \alpha_p \quad \forall p \in P, \forall t \in T \quad \text{Eq.30}$$

6. Nature of the variables

$$y_p \in B^+ \{0,1\}, f_p^t \in Z^+ \quad \text{Eq.31}$$

Eq.25 seeks to minimize the number of selected paths for evacuation. Eq.26 ensures that the incoming flow from all the paths reaching the arc a at time $t - \theta_{pa}$ to be lower or equal to the maximum capacity of the arc. Eq.27 indicates that the total flow departing from path p if selected, should be lower or equal to the initial demand at the N_a . Eq.28 establishes that the total flow leaving each N_a must be equal to the initial vehicle demand. Eq.29 establishes that the total flow entering N_s cannot exceed its capacity. The main difference between the EPWP model and the PSFG described in [48] is the addition of Eq.30, where the flow departing from each path at any time during the planning horizon cannot exceed the maximum capacity of the arc with the minimum capacity belonging to each path. This constraint avoids possible overlapping flow in all the arcs. Finally, Eq.31 provides the nature of the decision variables.

Assessing Bottlenecks with Omniscape

We used Omniscape [89], a raster-based model based on circuit theory [90] that has been widely used in regional conservation efforts to simulate the connectivity of habitats or potential movement patterns of species [91]. In this case, we modified the application to assess the strength of the road network connections. We calibrated the model using the road network in Davis, CA, because this is a city we know well. The model uses two scores, which must be assigned to every grid cell: source and resistance. Source is an index for the suitability of a grid cell; resistance is the relative ease or difficulty of transitioning that cell. We used population numbers derived from the UC Census as an index of Source, with the idea that this would show the demand for a given cell in the network from the people living there. Resistance was determined based on road attributes such as type, number of lanes, and max speed in which any grid cell occurred. We also tested putting a strong attractor around the edge of the city to simulate the flow of traffic to the outside of the urban area during an evacuation. The model uses a moving window and tests the connectivity of every cell in the network relative to the radius of cells around it. In Figure 5, we tested radii of 50, 100, 200, and 400 pixels using a 30m raster of the road network in Davis buffered by 20m from the linear version of the roads. The dark outlines represent a model version with a strong exterior attraction to the city. Higher normalized demand indicates greater traffic congestion relative to the travel capacity of those roads. PEB (Population Edge Buffer) is the maximum population density value per pixel.

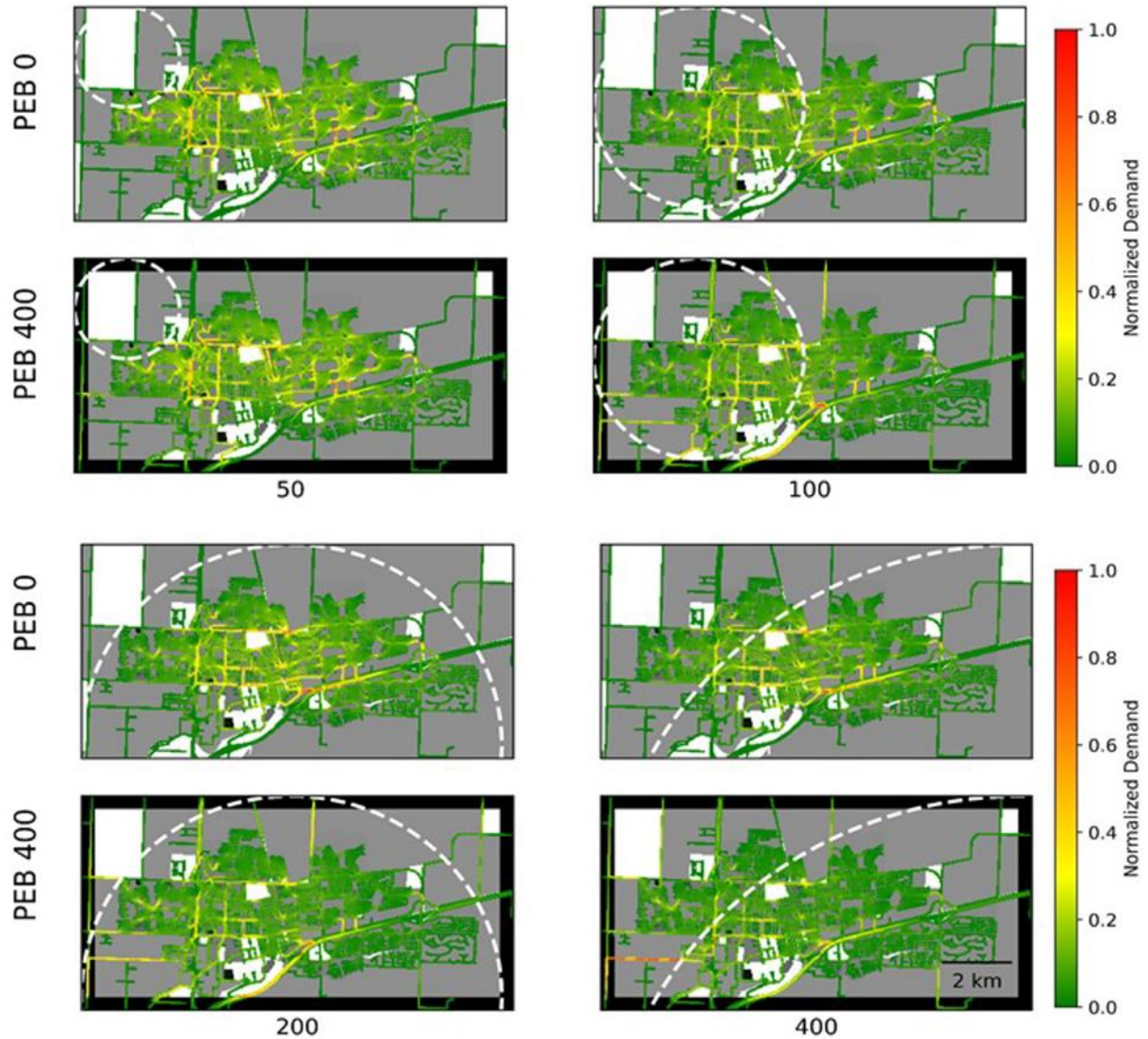


Figure 5. Traffic flow and evacuation choke points derived by Omniscape for Davis, CA.

We found that those provided similar outputs but that the variable range helped to identify local traffic congestion within neighborhoods from 50-200 pixels, while the 200–400-pixel radius moving windows helped to identify potential slowdown areas around the major exits of the city. The model produces a view of the relative strength of connectivity, which stands for demand. It was particularly effective at identifying choke points (bottlenecks) within the road network modeled.

Task 4: Assessing the Performance of the Evacuation Routes to Serve Different Segments of the Population

Here, we examined how the evacuation models would affect people with limited mobility. We also incorporated the local public transportation network and assessed the access to and vulnerability of that network under our simulated evacuation. First, we present methods for the performance evaluation and then for the public transportation network.

Evacuation Route Performance for Different Segments of the Population

For this analysis, the team conducted a detailed analysis of the case study cities to estimate performance metrics concerning the ability of the routes to serve different segments of the population. In doing so, the team analyzed the socio-demographic distribution of the population and its ability to evacuate the location into consideration. The team collected disaggregated information from the Census block groups to identify the socioeconomic characteristics of different regional populations corresponding to the social vulnerability index. For the entire population, we analyzed statistically how the population's socioeconomic characteristics affect the evacuees' perceived risk and evacuation time to establish whether the identified routes provide equitable evacuation opportunities.

Evacuation Plan Risk Assessment

To analyze the evacuation plan risk assessment, it was required to estimate the Road Network Risk (RNP_{risk}^z) for wildfires. For this, the authors followed the methodology developed in [107]. This methodology assesses the RNP_{risk} for different natural hazards (z) at three different levels of the road network: i) node level (v_i^z), ii) regional level (ψ_r^z), and iii) global level (Standardized Spatial Risk Index ($SSRI^z$)). In this project, the authors use the risk at the node level (v_i^z), and at the regional level (ψ_r^z), but not the $SSRI^z$, specifically for wildfires.

v_i^z depends on the road network's topology given by the Betweenness Centrality (BC_i) and the Hansen Accessibility Index (A_i) of each node. Additionally, v_i^z depends on the National Risk Index (NRI) (θ_i^z) defined at the node level [101]. NRI depends on the expected annual losses (EAL) from historical data of a set of different natural hazards, and its consequences increase when the Social Vulnerability index (SOVI) is high but are reduced when the Community Resilience (CR) is high. The SOVI and CR are two indexes that depend on the socioeconomic characteristics of the population living in the area. v_i^z formulation is given in Eq.32:

$$v_i^z = \frac{\theta_i^z * BC_i * A_i}{\sum_{j=1}^n (\theta_j^z * BC_j * A_j) - \theta_i^z * BC_i * A_i} \quad \text{Eq.32}$$

The function of ψ_r^z is to group the v_i^z based on the directions or regions R from the center of the road network and to obtain its average, as described in Eq.33. Note that R is the set of regions, ranging from 0 to 360 degrees in increments of 10 degrees, e.g., $r = \{0, 10, 20, \dots, 350\}$, and n_r is the number of nodes that belong to each region r.

$$\psi_r^z = \frac{1}{n_r} \sum_{i \in r} v_i^z \quad \forall r \in R \quad \text{Eq.33}$$

ψ_r^z is used to estimate the likelihood of a wildfire in specific directions of the network and analyze the sensitivity of the evacuation process if different exit routes are closed due to wildfire.

The risk assessment consisted of three main tasks:

- First, we modified the original objective function of the GPP model given in Eq.10 is travel time minimization from the origin node N_a to destination node N_s . The authors modified the GPP model's objective function to analyze how the evacuation pattern changes to obtain different paths for input to the EPWP model. The two alternative objective functions are:

$$Z_{min} = \sum_{(i,j) \in A} r_{ij} * y_{ij} \quad \text{Eq.34}$$

$$Z_{min} = \sum_{(i,j) \in A} t_{ij} * r_{ij} * y_{ij} \quad \text{Eq.35}$$

Where Eq.34 minimizes the risk of the selected path, and Eq.35 minimizes the risk and time for each origin N_a to destination N_s . r_{ij} is the risk associated with the link (i, j), and it is obtained as the average of the v_i between each pair of nodes (See Eq.36).

$$r_{ij} = \frac{v_i + v_j}{2} \quad \text{Eq.36}$$

Then, using different paths, the team identified the most important corridors among different scenarios. These analyses' results allow for identifying *investment priorities to maintain and support specific infrastructure*.

- Second, the team generated network disruption scenarios for the study cases by using ψ_r^z , as an estimation of the likelihood of a wildfire in specific directions. In this case, we analyzed evacuation risk as a measurement involving the road network's inherent characteristics. In this sense, the influence of road network characteristics on the performance of the evacuation process is expected to be identified. Such criticality assessment of the road network under disruptions and evacuation routes requires evaluating their effectiveness under a scenario or evacuation setting. As mentioned, the metrics indicate potential throughput in vehicles or people evacuated per unit of time, travel distance, or the impact of network disruptions on such metrics. Considering the findings and methodology developed by the PI in [12].
- Finally, we analyzed how our evacuation assessment aligned with the safety elements of emerging plans to previous evacuations by comparing our results with the ones observed in the documents disclosed by the cities affected by the fire in our case study. The case studies analysis is essentially a sensitivity analysis that examines how well local planning does in anticipating actual evacuations, which has been simulated. If travel data from actual events is like the evacuation plans, then the plans could be considered relatively robust. At the same time, disagreement would lead to further opportunities to refine and improve the plans.

Evaluation of the Public Transit Network During Evacuations

We collected data on various characteristics of the transit routes in California to create a vulnerability index, a composite metric designed to evaluate transit accessibility and vulnerability across census tracts in California. It integrates three key factors:

- Transit stops per 1,000 residents
- Community resilience (CIScore)
- Hazard risk (FEMA risk score)

These components are weighed to reflect their differing impacts on the overall vulnerability of a community. Each component metric (stops_per_1000_residents, CScore, risk_score) is normalized to a 0-1 range for comparability. The following weights are assigned to each metric:

- 1/3 for stops_per_1000_residents_norm (negative factor)
- 1/3 for ciscore_norm (positive factor)
- 1/3 for risk_score_norm (positive factor)

The Combined Vulnerability Index is calculated using the following formula:

$$\begin{aligned} \text{combined_vulnerability_index} = & (-1/3 * \text{stops_per_1000_residents_norm}) \\ & + (1/3 * \text{risk_score_norm}) + (1/3 * \text{ciscore_norm}) \end{aligned} \quad \text{Eq.37}$$

This formula supposes equal positive contributions of the CalEnviroScreen CIScore and FEMA NRI Risk Score and the equal negative contribution of the number of stops per 1,000 residents.

Empirical Results

The results of this project are based on the 4-task described in the methodology section.

Task 1: Evacuation Routes Data Collection and Database Construction

In this part of the project, the team created a database of cities and counties with available evacuation routes resulting from efforts as part of AB 747 requirements. The team gathered publicly available information for the routes.

Figure 6 shows screenshots of the appearance of the database; when clicking on Search Database, a second window appears, where users can provide information such as the county or city name, and then the link of the safety elements obtained from each location appears. The database contains the safety elements of county and city general plans. It digitizes and compiles the evacuation routes into a centralized geographic information system (GIS) database with an architecture permitting subsequent additions and editing. Currently, the database contains information from more than 190 Localities, and the information collected includes the Safety Element, Local Hazard Mitigation Plan (LHMP), Emergency Operations Plan (EOP), Evacuation Map, Evacuation Analysis, GIS Map, Multimodal Evacuation Accessibility, Shelter Map and Contact person. Figure 7 shows the localities with public information about the above safety elements. Note that in this sample, there is a lack of localities that have public information about evacuation maps and their GIS maps.

Additionally, the team created a centralized GIS portal that connects the database's information to the local jurisdiction evacuation plans and collects GIS of the State Highway System, bus and rail routes, CalEnviroScreen4, and other spatial data. The team developed an open architecture that will permit the addition of other evacuation routes and provide more details as plans develop, as well as metadata for all data fields and plans that are added to the database. It also provides information about the Road Network Performance measurements, including the RNP risk obtained in this project. The team categorized and processed the layers and created a database of evacuation routes in the state. The team conducted a descriptive analysis of the information in the basic database.

Additionally, the team developed a dashboard that provides information for each locality and compiles the models' results, such as the risk at the node level of the road network and its directionality, displayed in the polar histogram. Figure 8 shows a dashboard sample where the user can interact with various map elements, such as selecting the city to analyze, the hazard type, and the different measurements defined for each road network node. Switching between data layers, such as the National Risk Index at the census tract level, the Fire Hazard Severity Zones layer, and others, is possible.

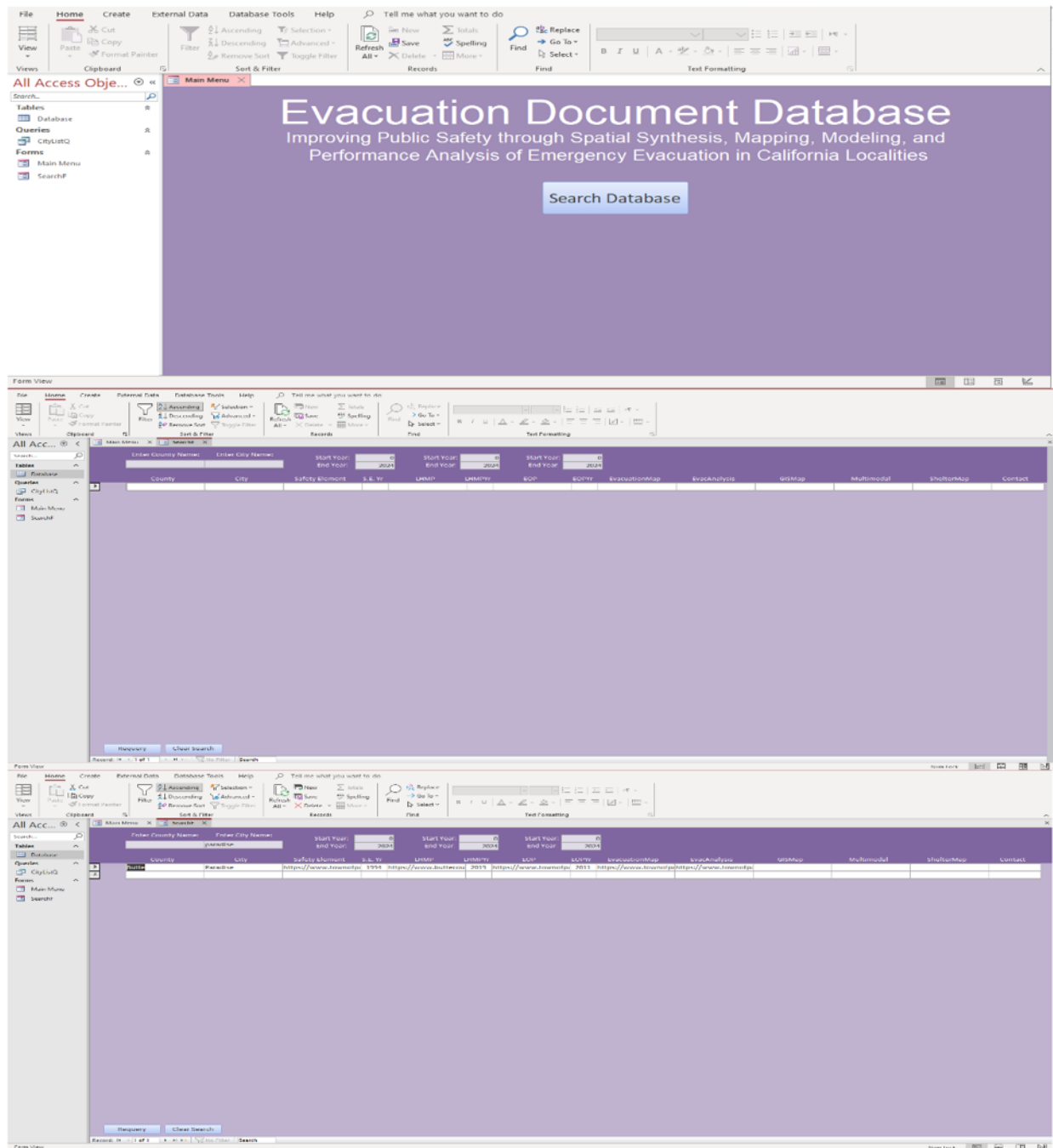


Figure 6. Database characteristics

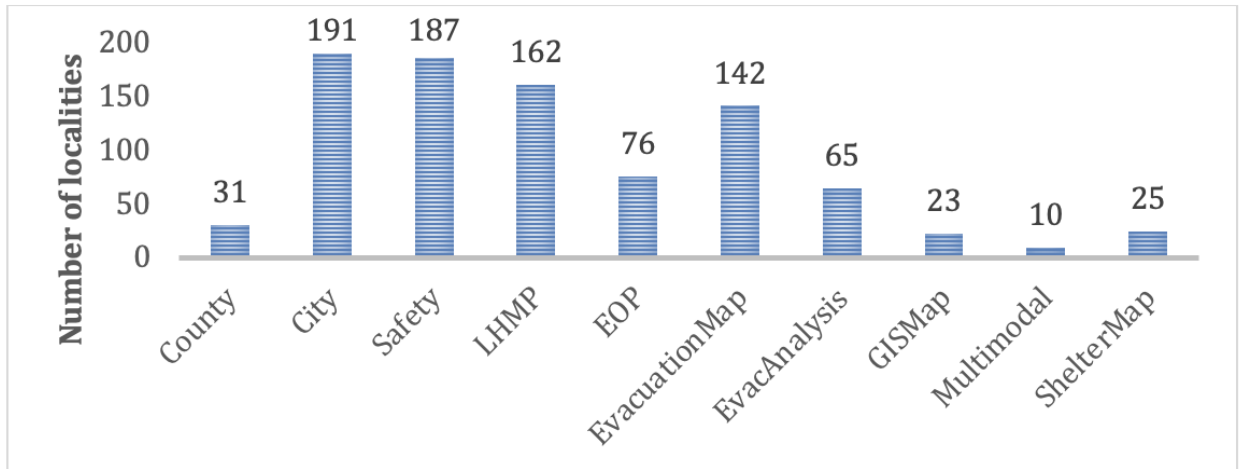


Figure 7. Number of localities with each safety element

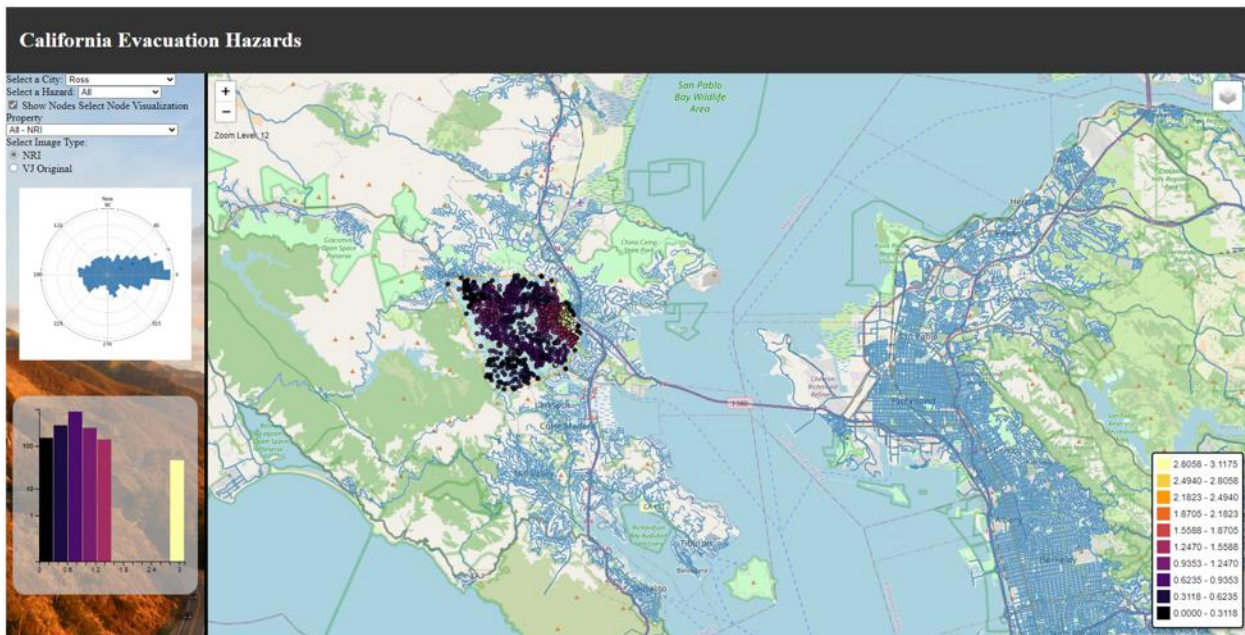


Figure 8. California evacuation hazards dashboard

Task 2: Assessing the Performance of the Road Network

For this task, the team used a sample of 475 of the more than 500 cities with Municipal codes in California, United States [108, 109]. One of the main interests of the authors is to provide evidence of the importance and utility of this RNP Risk methodology. For this, the authors analyze the influence of the main factors of the methodology: i) Hansen Accessibility Index (A_i), ii) normalized betweenness (BC_i) and iii) the NRI (θ_i^Z), on the proposed metrics at each road network level. The first analysis identifies two values for such factors: i) the original values and ii) the min-max normalized values.

1. RNP_{risk} at the Node Level: Influence of θ_i^z , BC_i and A_i on v_i^z

The team analyzes the proportional impact of both the original values and the max-min normalized values of θ_i^z , BC_i and A_i on the numerator of the RNP_{risk} at the node level v_i^z (See Eq.4). This analysis is conducted across 475 cities in California, considering the eighteen natural hazards. Figure 9 shows evidence that the percentage influence of each factor fluctuates across different natural hazards. Figure 9's x-axis is organized in ascending order based on the number of municipalities affected by the natural hazard risk in California: 1) cold wave (CWAV), 2) volcanic activity (VLCN), 3) avalanche (AVLN), 4) hurricane (HRCN), 5) tsunami (TSUN), 6) coastal flooding (CFLD), 7) winter weather (WNTW), 8) drought (DRGT), 9) landslide (LNDS), 10) riverine flood (RFLD), 11) wildfires (WFIR), 12) heat wave (HWAV), 13) earthquake (ERQK), 14) hail (HAIL), 15) lightning (LTNG), 16) tornado (TRND), 17) strong wind (SWND), and 18) All hazards (ALL). Ice storms (ISTM) are part of the NRI dataset, but not a single municipality in our sample in California has significant data on this natural hazard risk. Figure 9 shows the number of municipalities affected by each natural hazard based on the pointed line with the yellow dots. Additionally, the colors of the bars represent the influence of each factor θ_i^z (natural hazard risk), BC_i (Betweenness Centrality) and for A_i (Hansen Accessibility Index) on the numerator of v_i^z (local RNP_{risk}^z) denoted by its percentage in the y-axis. Note on Figure 9 that less than 470 of the 475 municipalities in California (<99%) are at risk for the following natural hazards: CWAV, VLCN, AVLN, HRCN, TSUN, CFLD, WNTW, DRGT, LNDS, RFLD, and WFIR. The influence of the three factors on the v_i^z are around 52% for θ_i^z , 33% for BC_i and 15% for A_i , and the influence of their normalized values are around 30%, 12%, and 58% for θ_i^z , BC_i and A_i , respectively. In contrast, for other natural hazards like HWAV, SWND, ERQK, HAIL, TRND, LTNG, ALL, where more than 470 cities in California are in high risk (>99%), a noticeable imbalance emerges between the contribution of the original values and the contribution of normalized values to the numerator of v_i^z . Specifically, the influence of θ_i^z , BC_i and A_i with the original values is 91%, 5% and 4%, respectively. Yet, these influences shift to 50%, 8% and 42% upon using normalized values. This disparity arises due to the different scales of each factor; for instance, A_i is in the thousandth range, BC_i in the millionth/thousandth range, and θ_i^z ranges from 0 to 100. It is important to note that the normalization brings balance to the expected influence of each factor on the v_i^z across most of the natural hazards. Consequently, the remaining analysis uses the normalized values of θ_i^z , BC_i and A_i .

2. RNP_{risk} at the Regional Level: Influence of $\psi_r^z(\theta_i^z)$, $\psi_r^z(A_i)$ and $\psi_r^z(BC_i)$ on $\psi_r^z(v_i^z)$

It is important to identify how the RNP_{risk} at the regional level ψ_r^z (or $\psi_{N_r}^z$) is affected by θ_i^z , BC_i and A_i . For this, the authors obtained the ψ_r^z as a function of v_i^z , θ_i^z , BC_i and A_i , individually. The team used a polar histogram based on the values of the regions given by Eq.5 and Eq.6 to better understand how the risk spreads inside the cities. Each polar histogram has thirty-six regions, each with an angle of ten° (0° to 360°), and each bar of the polar histogram is the $\psi_{N_r}^z(v_i^z)$. The length of each bar represents the relative risk of such direction compared to the other directions of the same city. This includes the natural hazard risk θ_i^z enhanced or reduced by A_i and BC_i . Figure 10 and Figure 11 show the use of the polar histogram that standardizes the road networks in San Francisco and Los Angeles and three natural hazards categories: i) all hazards (ALL), ii) wildfires (WFIR), and iii) earthquakes in SF and tsunamis

(TSUN) in LA. In both figures, the authors superpose the patterns of the RNP_{risk} at the regional level $\psi_r^z(v_i^z)$ (blue) on top of the patterns of each factor at the regional level $\psi_r^z(\theta_i^z)$ (Orange), $\psi_r^z(A_i)$ (Green) and $\psi_r^z(BC_i)$ (Gray), for comparison purposes. For the estimation of $\psi_r^z(\theta_i^z)$, $\psi_r^z(A_i)$ and $\psi_r^z(BC_i)$, the authors used Eq.5 and Eq.6., but instead of using the v_i^z , the team used the values of θ_i^z , BC_i and A_i .

It is interesting to see how the pattern of the $\psi_r^z(\theta_i^z)$ plays an important role in the pattern of $\psi_r^z(v_i^z)$, and how the behavior of $\psi_r^z(A_i)$ and $\psi_r^z(BC_i)$, may enhance or reduce the risk of some regions (directions) relative to others. For example, Figure 10 depicts that when analyzing wildfires (WFIR) in San Francisco, specifically the natural hazard risk given by θ_i^z on the direction of 130° is greater than the risk on 120° ($\psi_{N(r=130^\circ)}^z(\theta_i^z) > \psi_{N(r=120^\circ)}^z(\theta_i^z)$), however when analyzing the RNP risk that includes the RNP accessibility indexes A_i and BC_i , can be noted that RNP risk at 120° is higher than the RNP risk at 130° ($\psi_{N(r=130^\circ)}^z(v_i^z) < \psi_{N(r=120^\circ)}^z(v_i^z)$).

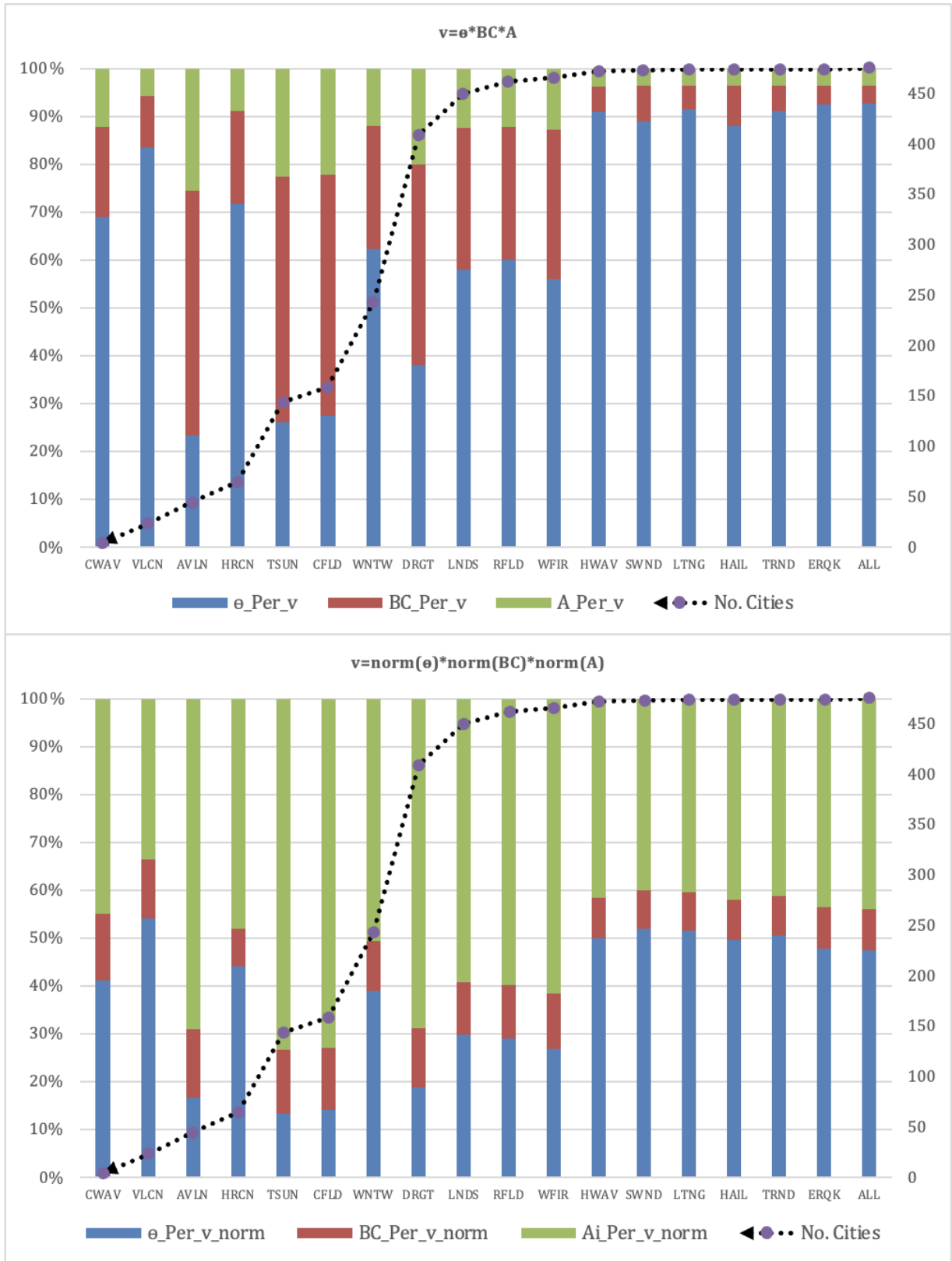


Figure 9. Percentage v_i^z vs θ_i^z , BC_i and A_i with original and normalized values.

This is because, despite there being a high risk of natural hazards at 130°, the relatively low importance of the nodes at 130° in comparison to the high importance of the nodes at 120°, makes the risk higher at 120°. The RNP risk leads to different conclusions when different factors are used as input in regional measurement. Situations like those described before can be found in different cities and different natural hazards, making clear the importance of including the $RNP_{accessibility}$ measurements on the natural hazard risk to reduce and enhance the consequences of the natural hazard risks on the performance of the transportation network.

3. RNP_{risk} at the Global Level: Influence of $SSRI^z(\psi_r^z(\theta_i^z))$, $SRI^z(\psi_r^z(A_i))$ and $SSRI^z(\psi_r^z(BC_i))$ on $SSRI^z(\psi_r^z(v_i^z))$

The authors identified how each factor's spatial distribution affects the spatial distribution of the risk on the network given by the standardized spatial risk index ($SSRI^z$) at the global level. The authors estimate the relationship between the $SSRI^z$ as a function of $\psi_r^z(v_i^z)$, against $SSRI^z$ as a function of $\psi_r^z(\theta_i^z)$, $\psi_r^z(A_i)$ and $\psi_r^z(BC_i)$, by using Eq.7.

Figure 12 shows that there is a relatively high and positive relationship between the $SSRI^z(\psi_r^z(v_i^z))$, against $SSRI^z(\psi_r^z(\theta_i^z))$, $SSRI^z(\psi_r^z(A_i))$ and $SSRI^z(\psi_r^z(BC_i))$. This means that all positively affect the shape of the distribution of the risk, but neither of them has total control over the shape of the risk distribution. Statistically, the authors found a correlation between $SSRI^z(\psi_r^z(A_i))$ and $SSRI^z(\psi_r^z(BC_i))$. Such a situation is expected because, despite A_i and BC_i having different interpretations, both measurements depend on the shortest paths between each pair of nodes. Given such a multicollinearity issue, Ordinary Least Square (OLS) regression models are not recommended; therefore, the authors implemented the Ridge, Lasso, and Generalized Additive Model (GAM) to identify the influence of $SSRI^z(\psi_r^z(\theta_i^z))$, $SSRI^z(\psi_r^z(A_i))$ and $SSRI^z(\psi_r^z(BC_i))$, on $SSRI^z(\psi_r^z(v_i^z))$. Those regression methods allow us to address the collinearity and overfitting problem frequently arising in multiple linear regression [110, 111, 112]. Figure 13 depicts that all the factors have a positive contribution given by the values within each stacked bar. Additionally, the y-axis of Figure 13 provides information about each factor's contribution percentage based on the regression models used. Note a consistent behavior in the percentage influence among the three factors on the different regression models, with around 15% influence of $SSRI^z(\psi_r^z(A_i))$, between 50 and 65% of the influence of $SSRI^z(\psi_r^z(BC_i))$ and between 20% and 40% of the influence of $SSRI^z(\psi_r^z(A_i))$.

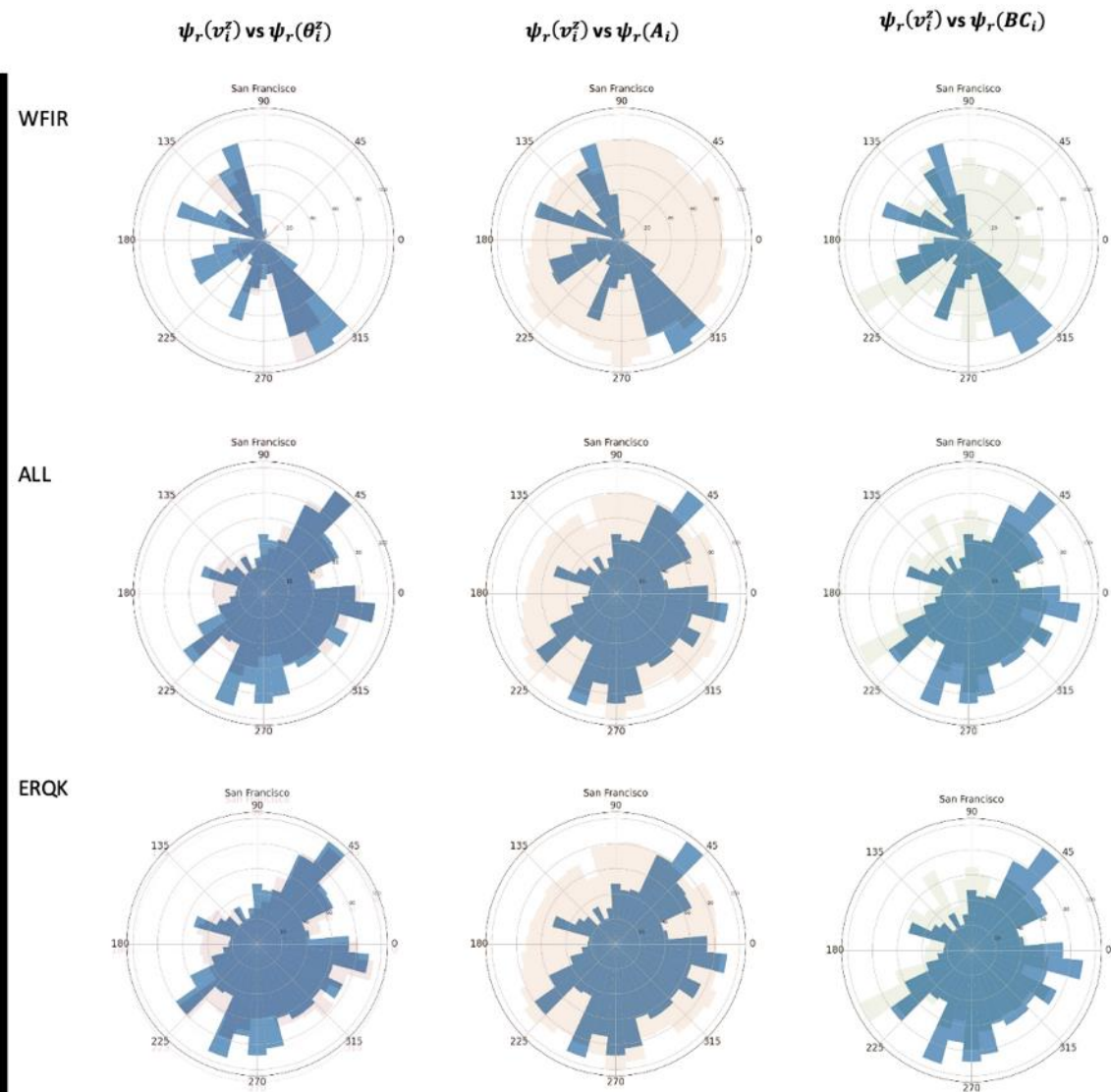


Figure 10. Road network and histogram of the risk ($\psi_r^z(v_i^z)$ vs $\psi_r^z(\theta_i^z), \psi_r^z(A_i), \psi_r^z(BC_i)$) in San Francisco

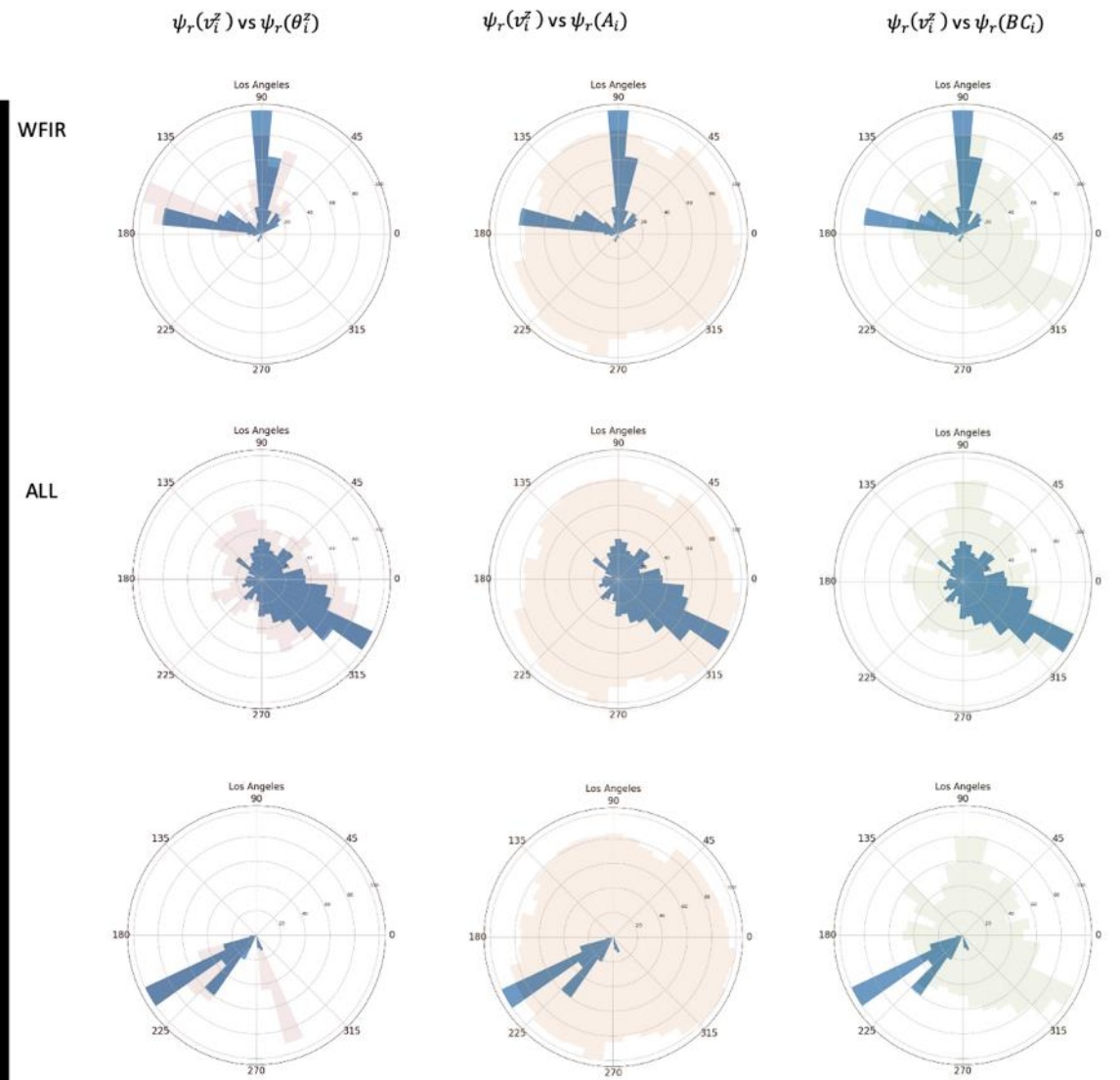
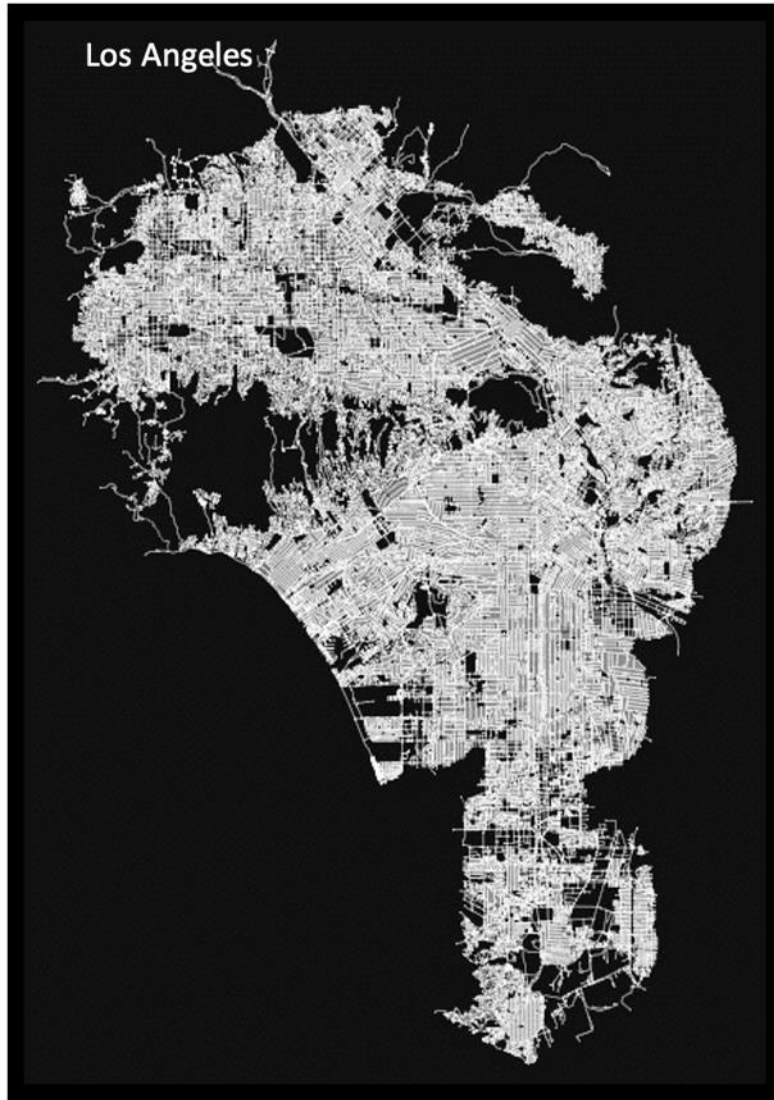


Figure 11. Road network and histogram of the risk ($\psi_r^z(v_i^z) \text{ vs } \psi_r^z(\theta_i^z), \psi_r^z(A_i), \psi_r^z(BC_i)$) in Los Angeles

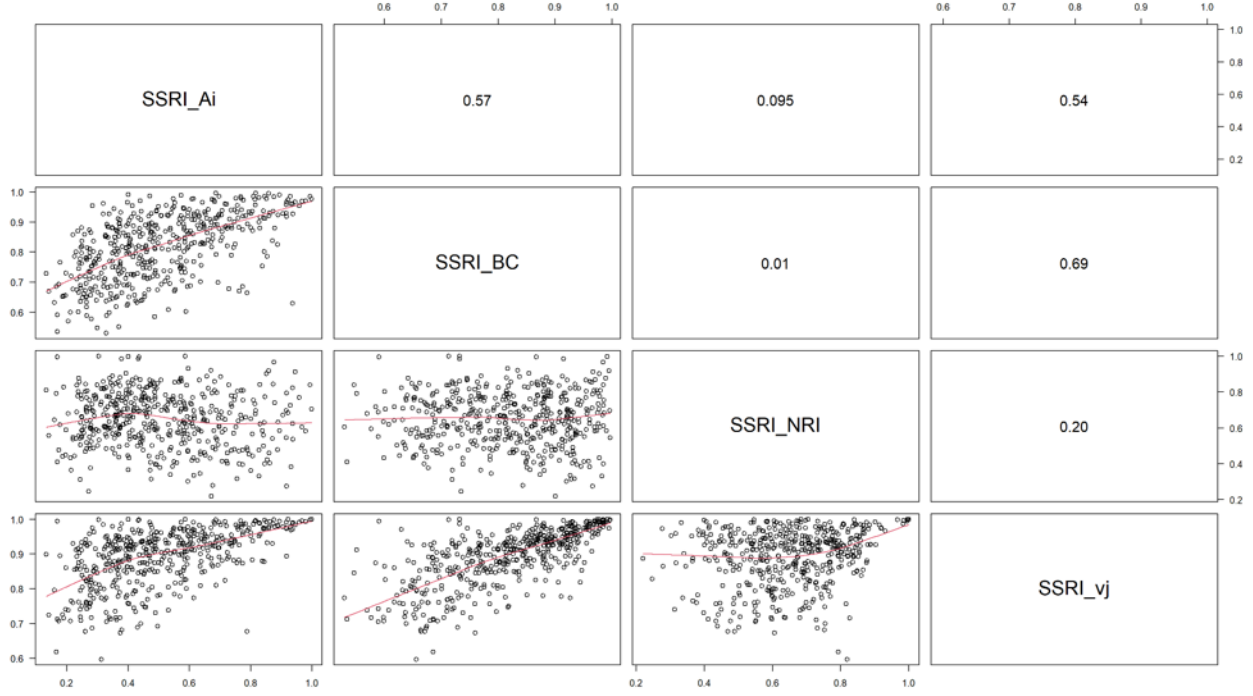


Figure 12. Correlation of $SSRI^z(\psi_r^z(\theta_i^z))$, $SSRI^z(\psi_r^z(A_i))$ and $SSRI^z(\psi_r^z(BC_i))$ on $SSRI^z(\psi_r^z(v_i^z))$

On the other hand, recall that $(SSRI^z(\psi_r^z(v_i^z)))$ provides a single value that represents the global network; therefore, the authors statistically compare the $(SSRI^z(\psi_r^z(v_i^z)))$ with the other RNP measurements that do not require traffic data obtained in Appendix A and provide a global value representing the road network using a GAM regression function. Among the RNP measurements to compare are: n (number of nodes), m (number of edges), \bar{k} (average degree), μ (cyclomatic number) [113, 19, 13, 114, 22], β (beta index) [19, 13, 114, 22, 14, 21], α (alpha index) [19, 13], γ (gamma index, planar and no planar) [19, 13], μ_{max} (maximum network circuit, planar and no planar) [19, 13], e_{max} (Maximum number of edges, planar and no planar) [19, 13], η (Eta or Average Edge Length), NS (Network density), and ζ (circuitry). Note that most of the selected RNP are considered as connectivity RNP measurements based on the classification given in Appendix A. The findings in Figure 14 indicate that Eta and circuitry average exhibit correlations with the $SSRI^z(\psi_r^z(v_i^z))$, collectively explaining around 27% of $SSRI^z(\psi_r^z(v_i^z))$, variability. Circuitry average and Eta are calculated differently: circuitry average is the sum of edge lengths divided by the sum of straight-line distances between edge endpoints. Eta is the average edge length, obtained as the sum of edge lengths divided by the number of edges. This suggests that larger road networks may correspond to higher $SSRI^z(\psi_r^z(v_i^z))$ values. However, this relationship is not conclusive, as these variables only explain 27% of the variations of $SSRI^z(\psi_r^z(v_i^z))$. In essence, none of the RNP measurements adequately capture the distribution of risk within a city, as they do not incorporate historical data on natural hazard risks, and their effectiveness is based solely on the characteristics of the roadway.

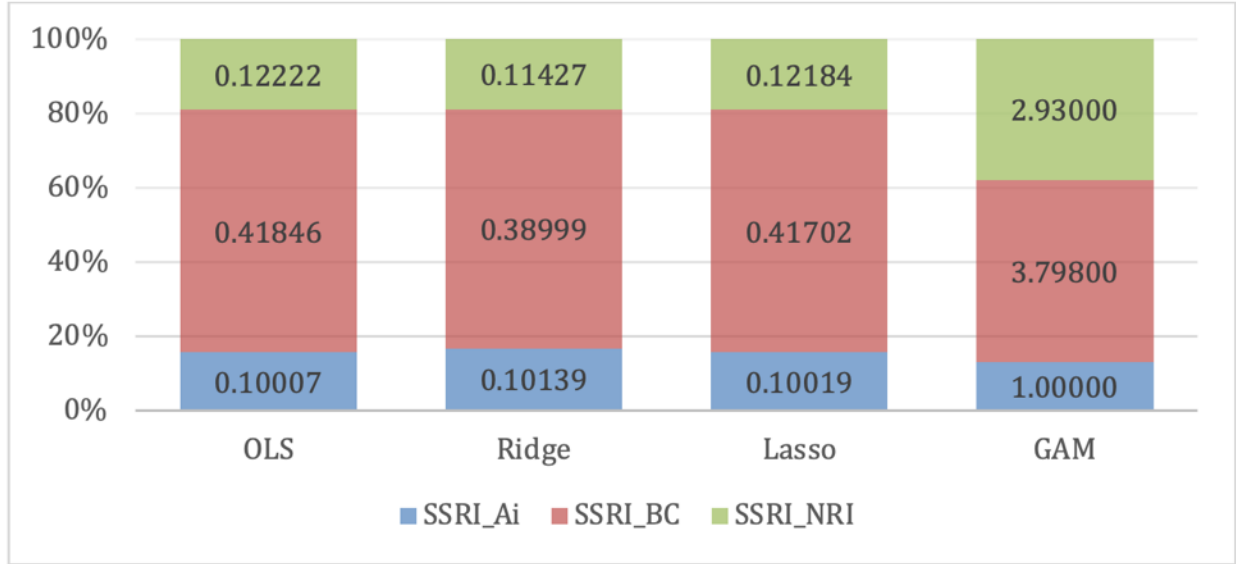


Figure 13. Contribution of $SSRI^z(\psi_r^z(\theta_i^z))$, $SSRI^z(\psi_r^z(A_i))$ and $SSRI^z(\psi_r^z(BC_i))$ on $SSRI^z(\psi_r^z(v_i^z))$

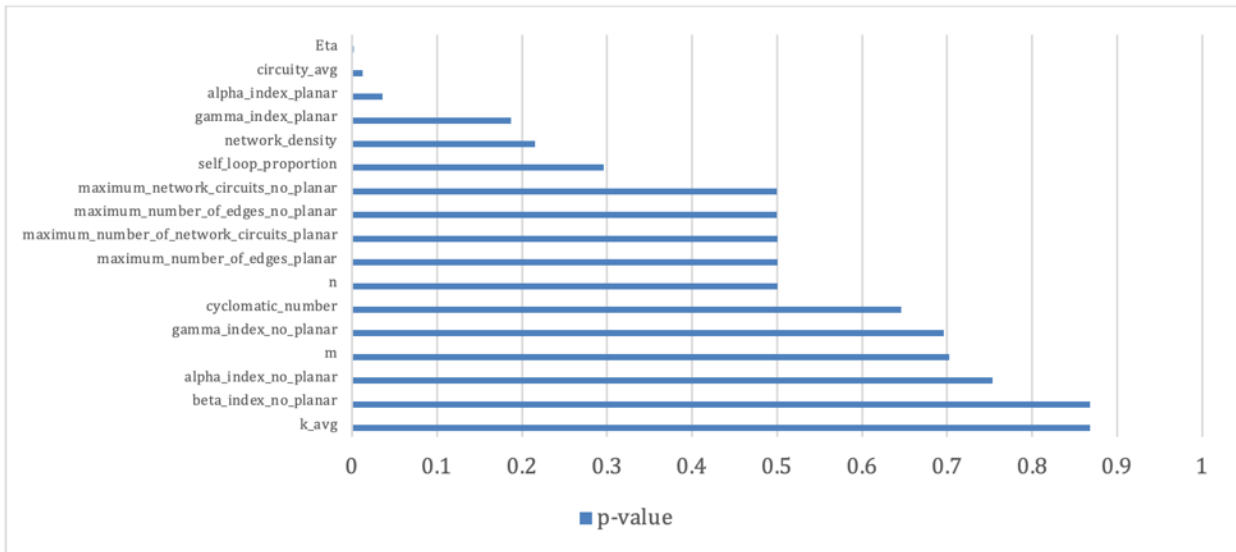


Figure 14. P-value of GAM model between $SSRI^z(\psi_r^z(v_i^z))$ and a set of RNP measurements.

4. Clustering Analysis Using the $SSRI^z$

As previously mentioned, the orientation of natural hazard risks differs depending on the specific type of natural hazard, the socio-demographic characteristics of the city, and its road network performance. Being familiar with these patterns, their directions, and the intensity of associated risks presents an opportunity to categorize and prioritize cities effectively. This awareness is essential in directing focused attention to planning and implementing disaster response operations adapted to the distinct needs of each city and the nature of the potential

hazards they face. Figure 15.a. and Figure 16.a. provide a clustering classification scheme of the cities for prioritization purposes for all hazards (ALL) and wildfire (WFIR) scenarios (See Appendix B to see the clustering classification of the 18 natural hazards). Where the y-axis indicates the average NRI ($\bar{\theta}^z$) of each city as a measurement of how risky each city is, and the x-axis is the $SSRI^z$, that allows us to identify how the natural hazards will affect the road network of the city or the risk concentration. The size of the bubbles is a relationship between each city's population and network density. The color of the bubbles is derived from the region of California: *Bay Area, Inland Desert, Northern, North Central, Central Region, and South Coast*. The clustering classification scheme represented in Figure 15.a and Figure 16.a divides the scatter plot into four clusters depending on the median of each axis $\bar{\theta}^z$ and $SSRI^z$. Cluster 1: Moderate Risk ($\bar{\theta}^z \leq \bar{\theta}^z$) and Low-Risk concentration ($SSRI^z \leq SSRI^z$), Cluster 2: Moderate Risk ($\bar{\theta}^z \leq \bar{\theta}^z$) and High-Risk concentration ($SSRI^z > SSRI^z$), Cluster 3: High Risk ($\bar{\theta}^z > \bar{\theta}^z$) and Low-Risk concentration ($SSRI^z \leq SSRI^z$), and Cluster 4: High Risk ($\bar{\theta}^z > \bar{\theta}^z$) with High-Risk concentration ($SSRI^z > SSRI^z$). Figure 15.d and Figure 16.d provide the spatial distribution of each city on the map of California regions, where each city is represented depending on its cluster. This classification provides significant insights. In addition, the cities with the highest priority of attention are those with high risk, Cluster 3, and Cluster 4. However, the planning implications differ between the two cities. This is because, in Cluster 4, the risk is mainly in one or a few directions of the road network, while for cities in Cluster 3, the entire city is in danger. Prioritization also depends on the size of bubbles representing the population size concerning the network density. It is important to note that the priority ranking of risk depends on the considered natural hazard (these figures use ALL and WFIR hazards as examples).

Additionally, based on Figure 15.c, the *Inland Desert, Northern, and South Coast* regions have the largest proportion of cities with a high risk of natural hazards, with 80%, 70%, and 55% of their cities in Cluster 3 or 4, respectively. Furthermore, cities in the Bay Area, Central Region, and Northern Central are relatively less risky than those mentioned before when analyzing ALL hazards. Figure 15.b shows that many cities in Cluster 3 belong to the *South Coast region*, meaning that such cities are at high risk of all natural hazards, which can affect the entire city. In contrast, the proportion of cities that belong to Cluster 4 is generally distributed among the six regions. On the other hand, when focusing on Wildfires, Figure 16.c depicts that all the *Northern* cities are at high risk of wildfire, followed by around 80% of the cities in *Inland Deserts* and around 65% in *North Central*. This shows that wildfire greatly affects the northern section of California. Figure 16.b shows that although only 40% of the cities that belong to the *South Coast* are at high risk of wildfire, they represent more than 30% of all the cities in Cluster 4, which is the largest proportion of all the cities that belong to Cluster 4 based on wildfire risk. However, the proportion of cities on the *South Coast* that belong to Cluster 3 is relatively small. The largest proportion of the cities in Cluster 3, where the entire city or a large area of the city is at risk of being affected by wildfires, is in the *Inland Desert* region. Finally, observe that the risk's behavior and distribution vary among natural hazards. However, compared to the rest, it is important to observe the vulnerability of cities in the *Inland Desert, Northern, and South*

Coast areas. The results highlight how *South Coast* and *Inland Desert* cities are closer to each other, which appears to share its clustering classification, with their geographical location being a key factor in their risk classification.

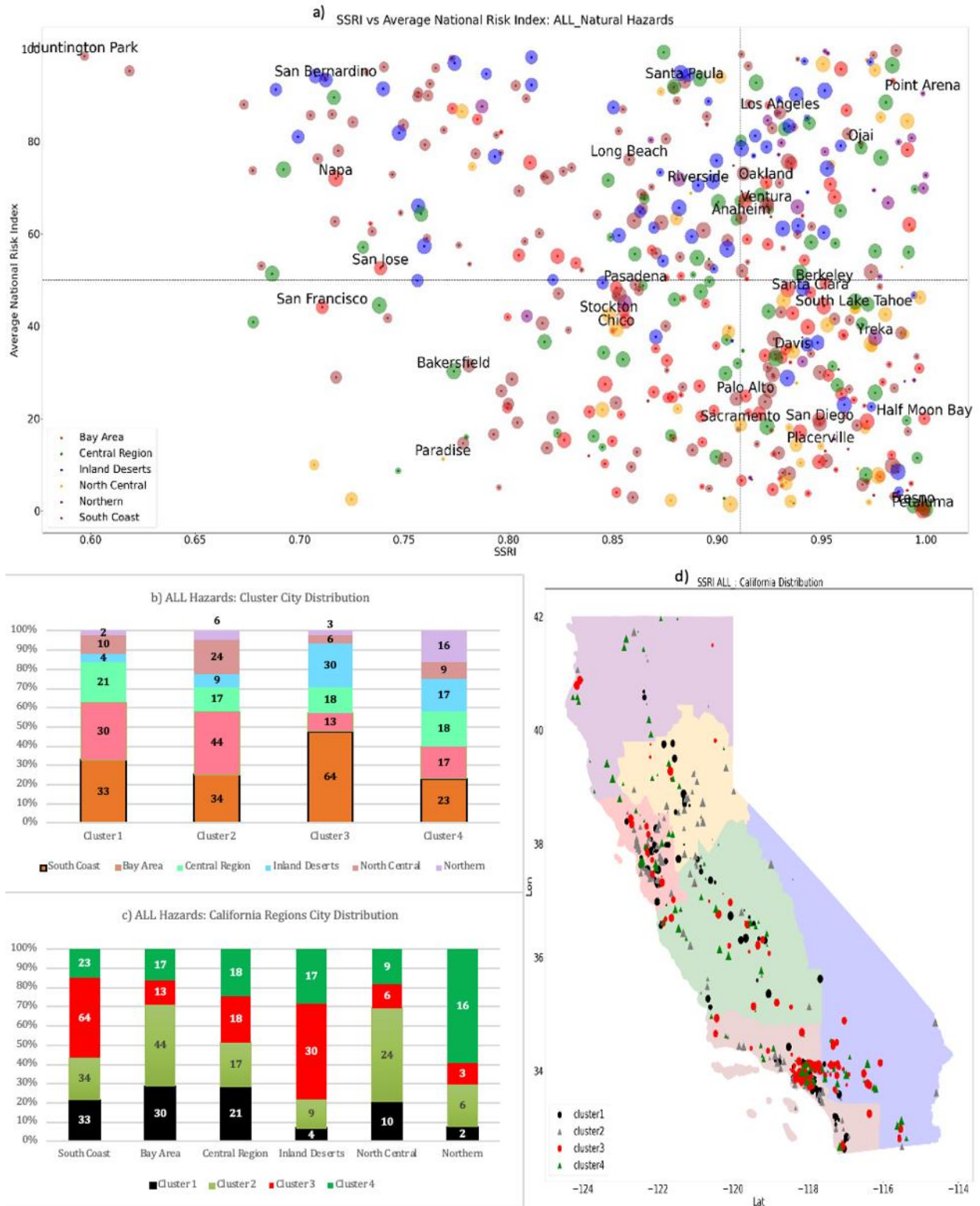


Figure 15. ALL hazards: Cluster and California region classification: a) Cluster classification, b) cluster distribution among California cities, c) Region distribution, d) Spatial distribution of cluster classification on California Regions

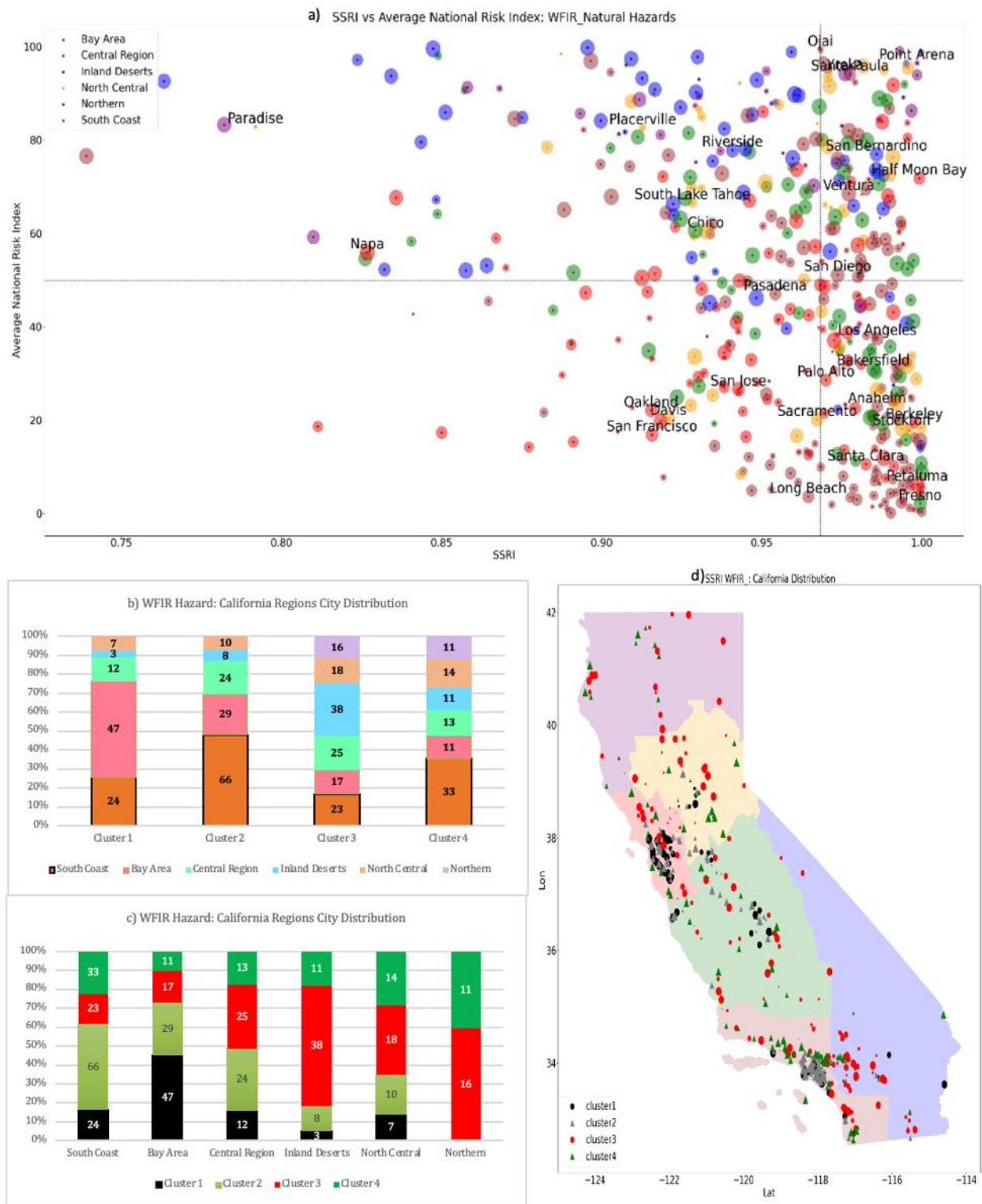


Figure 16. WFIR hazard: Cluster and California region classification: a) Cluster classification, b) cluster distribution among California cities, c) Region distribution, d) Spatial distribution of cluster classification on California Regions

Task 3: Assessing the Map of Evacuation Routes Using the Other Data Collected to Determine the Equity of Access to Evacuations

Based on the results obtained in Task 2, the team identified a set of previous evacuation events. It sought reports and data to identify them as case studies. Potential examples could be from numerous wildfires. In our case study, the team used two locations with a high risk of wildfires in California i) Paradise and Magalia, where the Camp Fire occurred in 2018. The team also analyzed the Thomas Fire in 2018, affecting many cities, including Ventura, Ojai, and Santa Paula. The analysis of the Thomas Fire case is described in Appendix C.

The team utilized their data or reports regarding the previous evacuations to assess how well aligned the safety elements of the emerging plans are relative to previous evacuation routes used. In this task, the team conducts the modeling and quantitative evaluation of the performance based on two methods: 1) Mathematical Programming and 2) bottleneck analysis by using Omniscape.

Assessing Evacuation Time with Mathematical Modeling

Data Management

Generally, this project uses data from three main sources. For Steps 1 to 4, the team requires data from open street maps (OSM) and the American Community Survey (ACS). The team used data from the National Risk Index (NRI) from FEMA for the Evacuation Plan Risk Assessment. To estimate the social Vulnerability Index (SOVI), the team collected the following variables from the American Community Survey [103]. See Appendix D. Sociodemographic Characteristics of Paradise and Magalia, for summaries of the variables in the study area.

Table 2. Theme and variables used for the Social Vulnerability Index from American Community Survey.

Theme	Variable
Theme 1: Socioeconomic Status	POV150: Proportion of population under 150% poverty level.
	UNEMP: Proportion of population unemployed.
	HBURD: Proportion of population cost-burdened.
	NOHSDP: Proportion of the population with no high school diploma.
	UNINSUR: Proportion of the population with no insurance.
Theme 2: Household characteristics	AGE65: Proportion of the population with 65 or more years.
	AGE17: Proportion of population with 17 or less years.
	DISABL: Proportion of population with disability.
	SNGPNT: Proportion of the population is single parents.
	LIMENG: Proportion of population with English limitations.
Theme 3: Minority	MINRTY: Proportion of the population considered to be minority.
Theme 4: housing type & transportation	MUNIT: Proportion of structures with 10 or more units.
	MOBILE: Proportion of the population living in mobile homes.
	CROWD: Proportion of structures with more inhabitants than rooms.
	NOVEH: Proportion of the population with no vehicle.
	GROUPQ: Proportion of population living in group quarters.

Step 1: Road network preprocessing

Figure 17 shows the map of Paradise and Magalia, highlighting the sink (X) and origin (O) nodes. Each origin node has been assigned a vehicle demand from the American Community Survey at the Census Block group level. Additionally, Figure 18 describes the most important parameters from the 1860 arcs of the road network of Paradise and Magalia. The arc's length is 101 to 2722 meters, and most arcs are shorter than 1 km (1000 m). Furthermore, the arc's capacity ranges from 600 to 4000 vehicles/hour, and most arcs possess a capacity of 1200 vehicles/hour or less. The speed information not available in OSM was completed with the information given by [106], resulting in speeds ranging from 30 to 88.5 km/h. In this study, the authors used a congestion factor obtained from [106] to reduce the speed as an approximation of congestion speed in each arc of the road network. In this case, the minimum travel time is 15 seconds, while the maximum is 389 seconds, based on the speed, arc lengths, and congestion factors. The minimum travel time is crucial in the ENP model because it is the basis for transforming (expanding) the road network for mathematical modeling.

Step 2: Evacuation with no paths (ENP)

The ENP model requires the expansion of the road network, resulting in a time-expanded network with 6,673 nodes and 7,834 arcs. The authors initiated the modeling with many T, specifically 1,000 time-units (TUs), where each TU represents 15 seconds. The ENP model aims to maximize the number of vehicles reaching the SN at the minimum time. When constructing the ENP model in our case study, the last time window where all vehicles reached the SN (assumed safe destination) was 411 TU (6165 seconds, 102.75 minutes, or 1 hour and 42 minutes). Figure 19 shows the evacuation rate and % of evacuated vehicles by time in minutes during the planning period of 411 UT (102 minutes).

Step 3: Generation of a pool of paths

The Paradise-Magalia case has 36 source nodes and nine sink nodes (See Figure 17), meaning at least 333 ($36 \times 9 = 333$) paths exist. However, the authors included 43 additional feasible paths with a travel time at most double the shortest path of each OD pair, making 376 different paths.

Step 4: Evacuation plan with paths

To solve the EPWP model, the authors start solving the model with a $T = CT$ obtained in the ENP model (411 TU). However, after increasing the value of T by one unit, the first feasible solution is obtained when T is equal to 450 TU (equivalent to 6750 seconds, 112.5 minutes, or one hour and 52.5 minutes). This indicates that with the chosen set of paths, it is possible to evacuate the city in only ten minutes more than the ENP, where all vehicles use any potential arc in the road network without any pre-existing path set.

Figure 20.a indicates that the number of vehicles evacuating on each exit node is similar in both models, EPWP and ENP. Figure 20.b shows a decrease in the evacuation rate between both models: 30-40 for the EPWP model and 40-45 for the ENP model. Additionally, Figure 20.c shows the slope differences between both models.

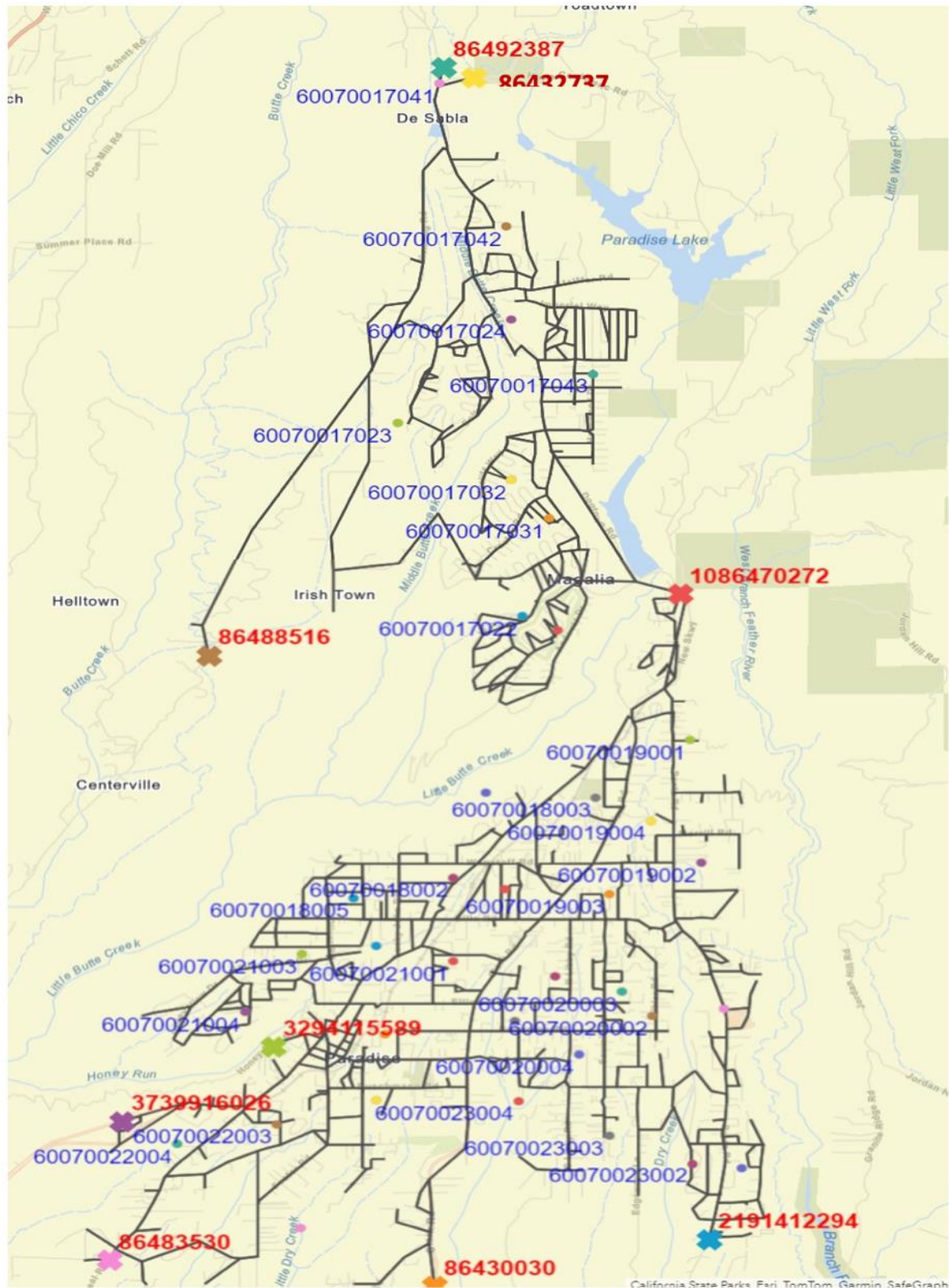
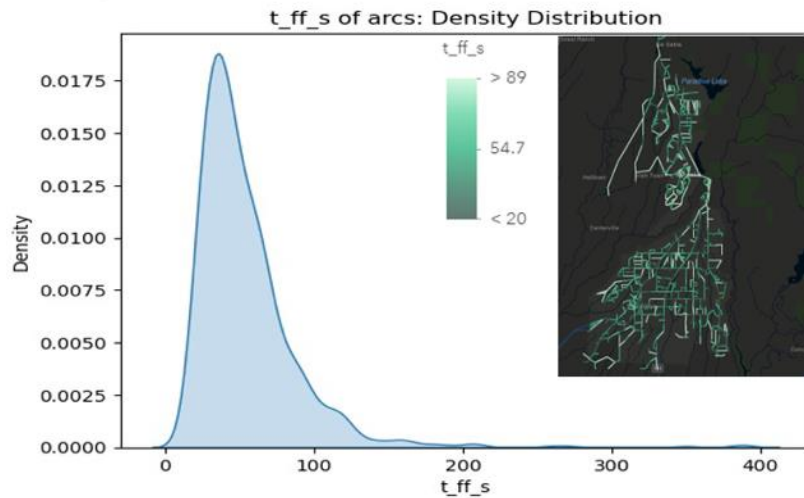


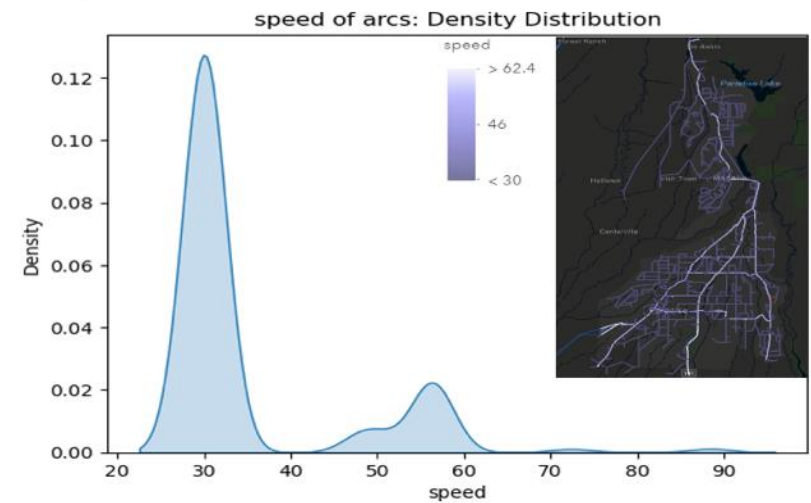
Figure 17. Paradise Map with the labels of the source and sink nodes demand and sink capacity

Parameter (units) (min, max, mean)

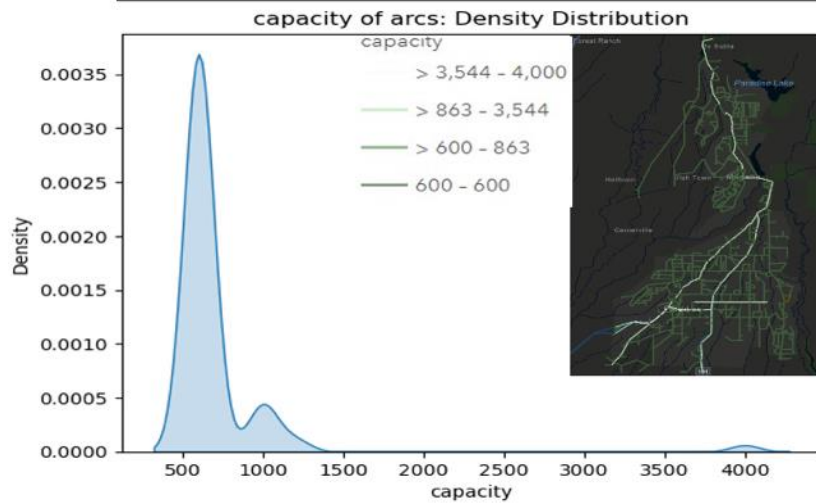
Travel time (s) (15, 389, 54.5)



Speed (km/h) (30, 88.5, 35.4)



Capacity (veh/h) (600, 4000, 702)



Length (m) (101.2, 2722.3, 292.9)

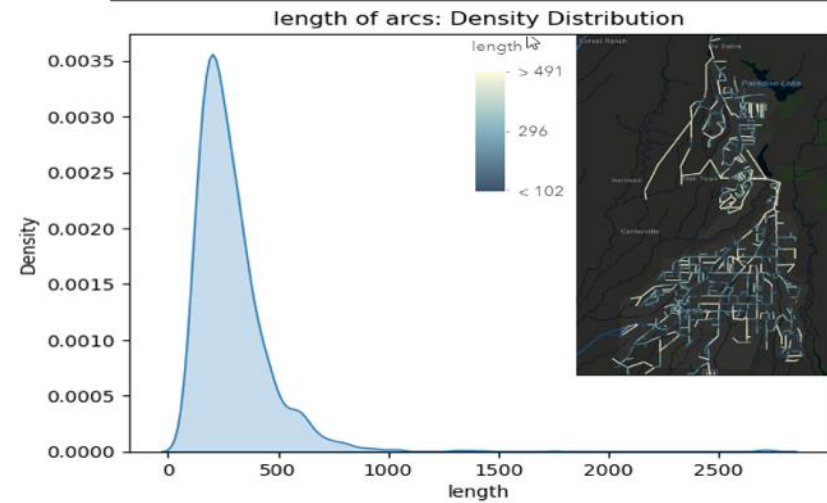


Figure 18. Density distribution of the arcs of the road network, including length, capacity, speed, and travel time

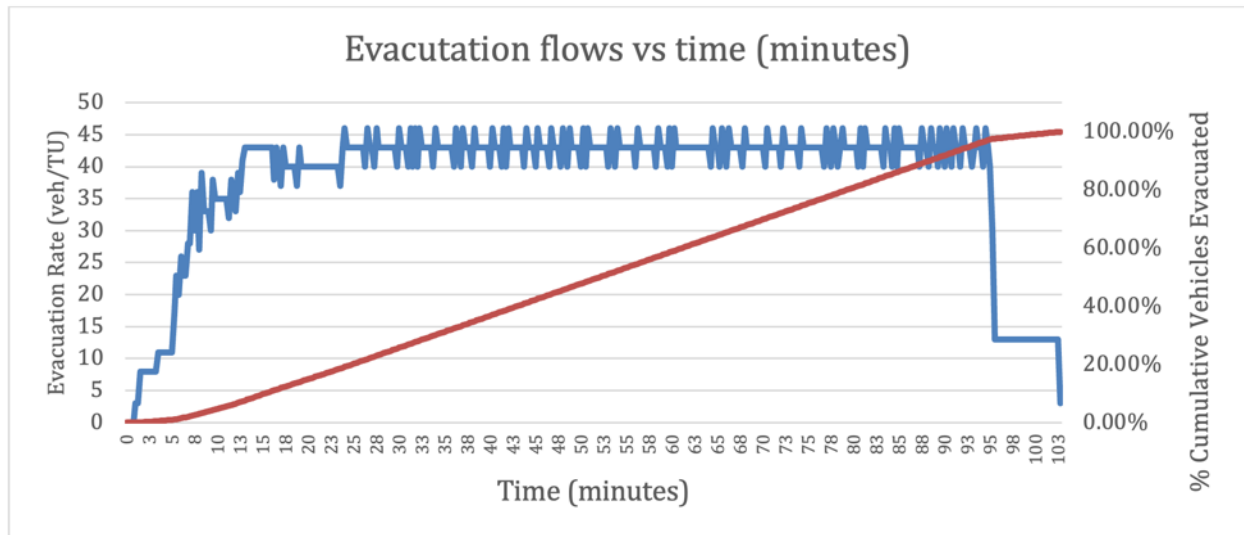


Figure 19. Evacuation percentage with time in minutes

The box plot in Figure 21 depicts the departure and arrival times distribution for vehicles across different paths originating from each census block group (CBG). Figure 21.a shows that most paths have at least one vehicle departing at time zero, while Figure 21.b shows that most paths have at least one vehicle reaching the safe node at time 450. However, the distribution of vehicles throughout the planning horizon differs significantly across different regions.

Figure 22 provides a snapshot of the evolution of Paradise-Magalia evacuation based on the EPWP model for around 110 minutes, highlighting the minimum number of corridors expected to be used during the evacuation process.

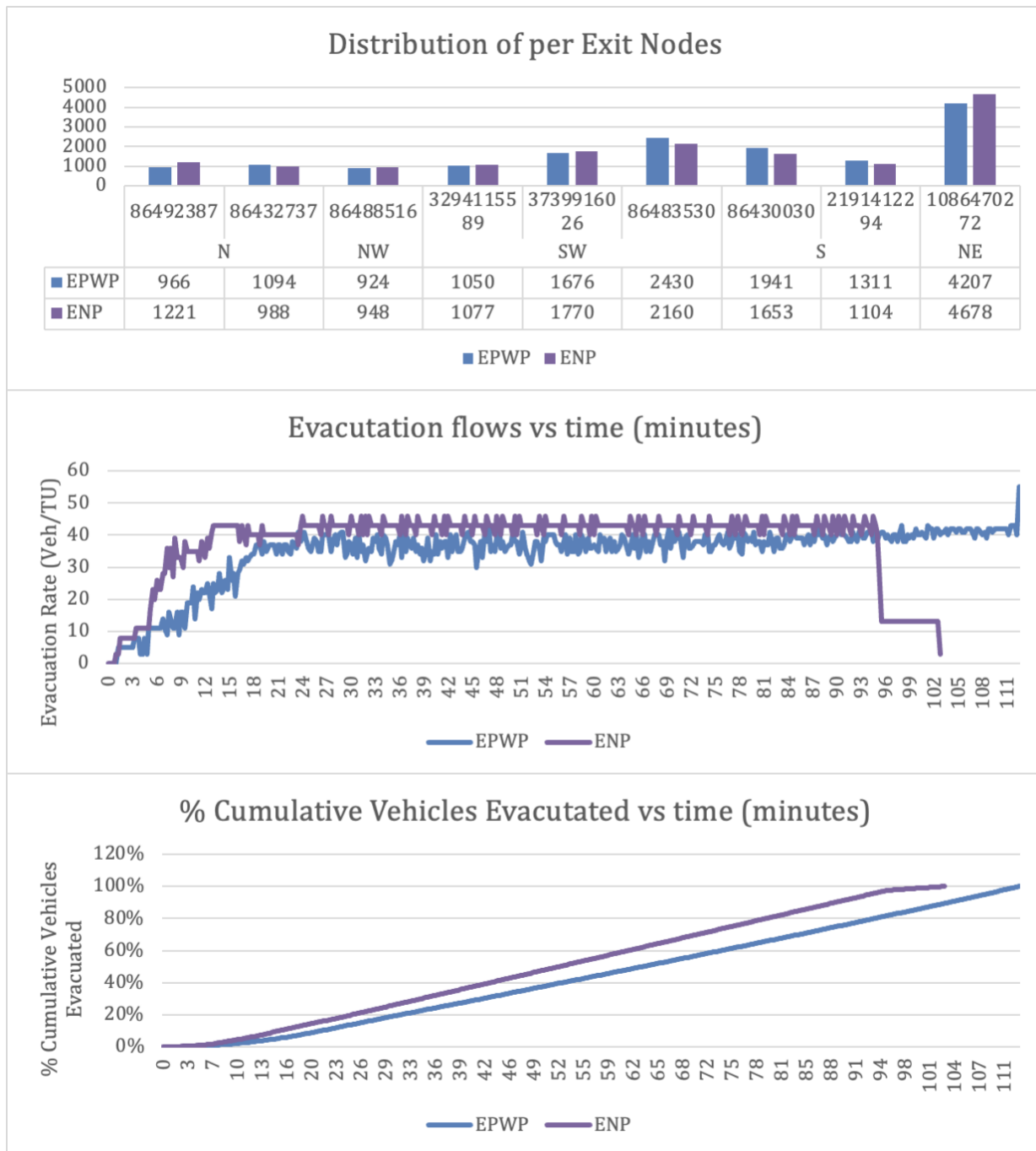


Figure 20. Exit nodes evacuation, evacuation rate, and cumulative percentage of vehicles evacuated under the ENP and EPWP models



Figure 21. Departure (top) /Arrival (bottom) time comparison between paths

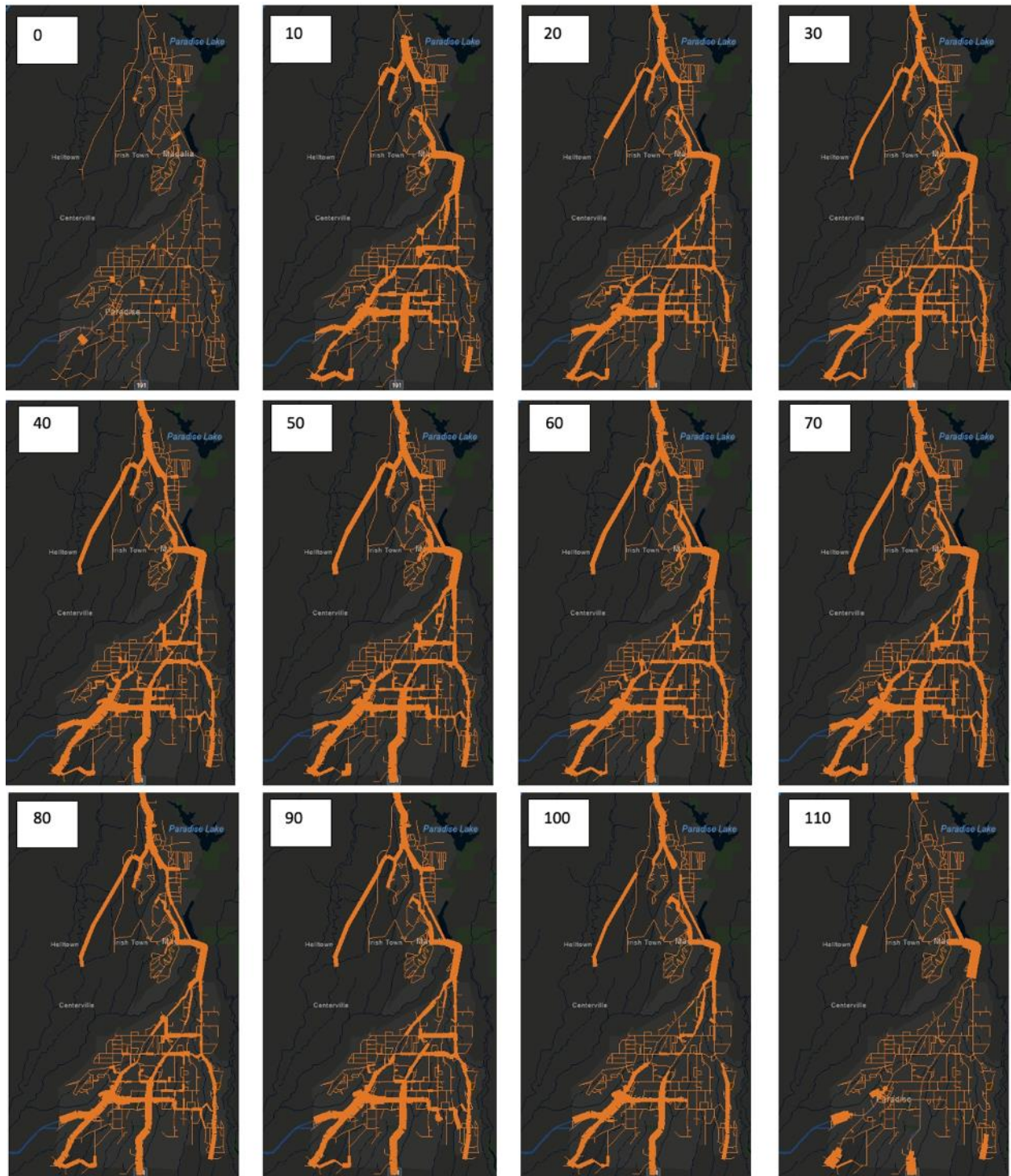


Figure 22. Evolution of the total evacuation on the Paradise-Magalia Case (minutes)

Assessing Bottlenecks with Omniscape

Here, we present the Omniscape outputs for Paradise, Magalia, and the combined metro region. The plots show the output for the cumulative current flow within the road network as the resistance layer connects source (population) pixels.

The Paradise transportation network is shown without and with an external attractor, PEB (Population Edge Buffer). The population edge buffer is part of the source layer and extends 400 meters from the outer edge of the raster plot. It has a value equal to the maximum population density per pixel from the interior of the source layer. This visualization shows how localized congestion gradually shifts towards more arterial roads as the search radius increases, and the edge buffer's effect connects more source pixels to the edge buffer. This view is of 4 moving window scales (25-400 pixel moving window). These visualizations were chosen from an extensive set to illustrate the local and regional effects of the model. When the population edge buffer is zero, the road network connects population clusters in a neighborhood. As the radius increases, the neighborhoods become connected. The central sectors show potential bottlenecks at 25 and 50, while the 100 and 200 models with an edge buffer show the bottlenecks emerging on the major north-south exit routes. These differences correspond roughly to the sequence of evacuations, with local neighborhoods first experiencing local slowdowns, followed by larger traffic delays on the major internal evacuation routes. With a strong external attraction (boxes with black outlines), some internal congestion appears in the 100-pixel model. Still, the congestion on the major exit routes to the south comes into focus in the 200-radius version (Figure 23).

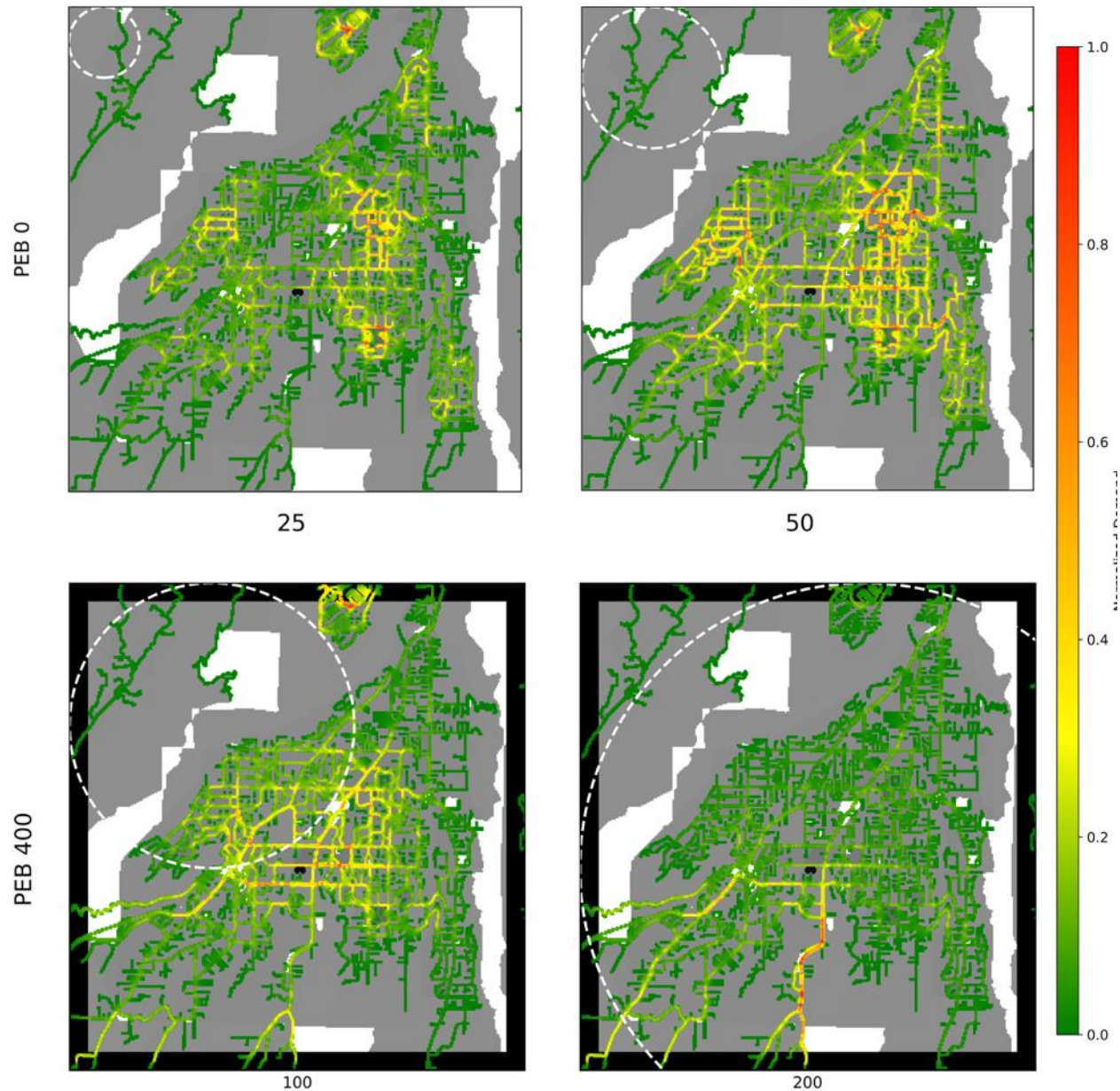


Figure 23. Traffic flow and evacuation choke points (City of Paradise)

For Magalia, the results are much the same. The model PEB 0 shows the internal traffic choke points and the southern connection to Paradise. The PEB 400, with an external attractor, shows the subsequent slowdowns on the major evacuation routes, with all four cardinal directions showing some about of slowdown (Figure 24).

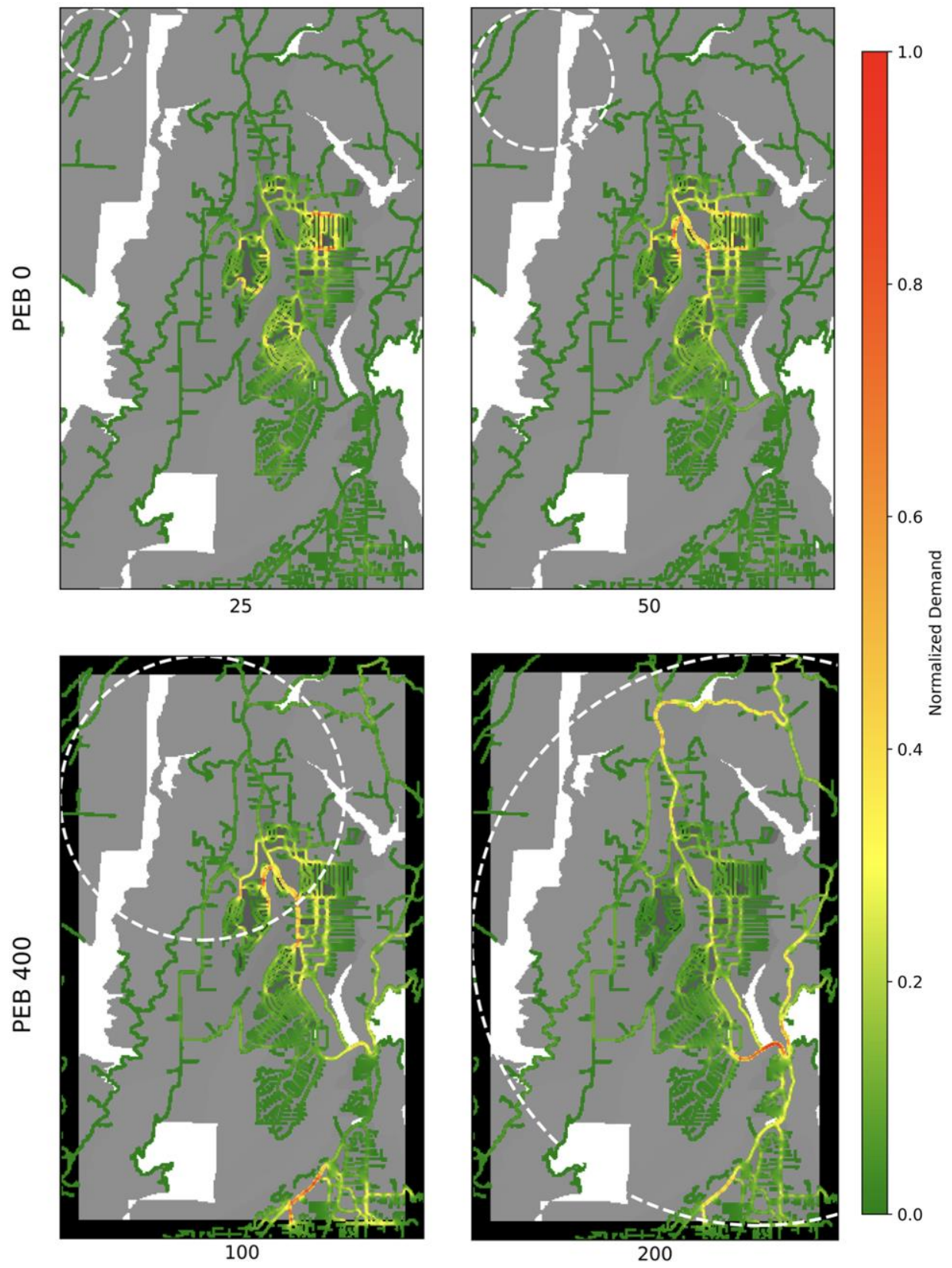


Figure 24. Traffic flow and evacuation choke points (City of Magalia)

The combined metro region of Paradise-Magalia emphasizes the radius's impact, showing as much of the internal congestion as possible. However, it illustrates that the connector route between the two cities is a major choke point, and the 200 and 400 radii versions suggest that the northern evacuation route will experience the most slow-down, assuming the flow is not otherwise directed (Figure 25).

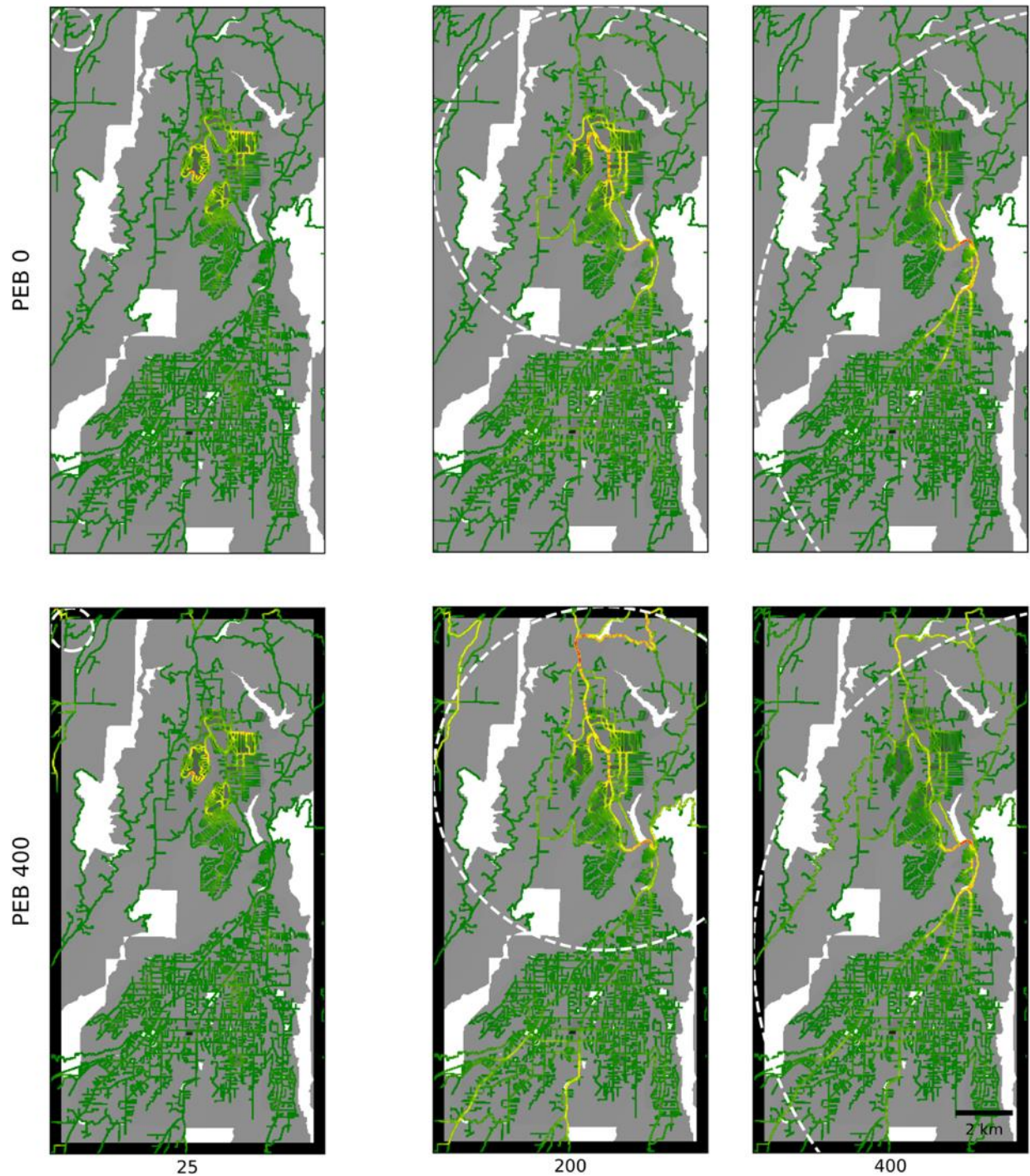


Figure 25. Traffic flow and evacuation points (City of Magalia and Paradise)

Task 4: Assessing the Performance of the Evacuation Routes to Serve Different Segments of the Population

Evacuation Route Performance for Different Segments of the Population

In this Task, the team analyzed using the Social Vulnerability Index, National Risk Index, and the American Community Survey to identify different population segments and conduct performance assessments specific to their characteristics and transport requirements.

To understand the behavior of arrival and departure times, we analyzed their correlation against the travel time of paths originating from each CBG, the population of the CBG, and the Social Vulnerability Index (SVI) of each CBG, which depends on socioeconomic characteristics.

- In this analysis, Figure 26 demonstrates that travel time is the most significant factor in the decision-making process.
- For those vehicles that depart 50-75% later than the rest of the vehicles, longer travel times tend to result in earlier departures than the rest.
- Travel times are primarily impacted by the arrival times of vehicles that reach the safe node early. However, this does not significantly alter the arrival times of the remaining vehicles.
- The population and Social Vulnerability Index were considered in the analysis but did not significantly impact the scheduling of departure and arrival times compared to travel time.
- It is possible to indicate that travel time is the primary factor guiding the scheduling of vehicle departures and arrivals.
- Larger travel times necessitate earlier departures to ensure timely arrivals at safe nodes, highlighting the importance of accounting for travel time in evacuation planning.

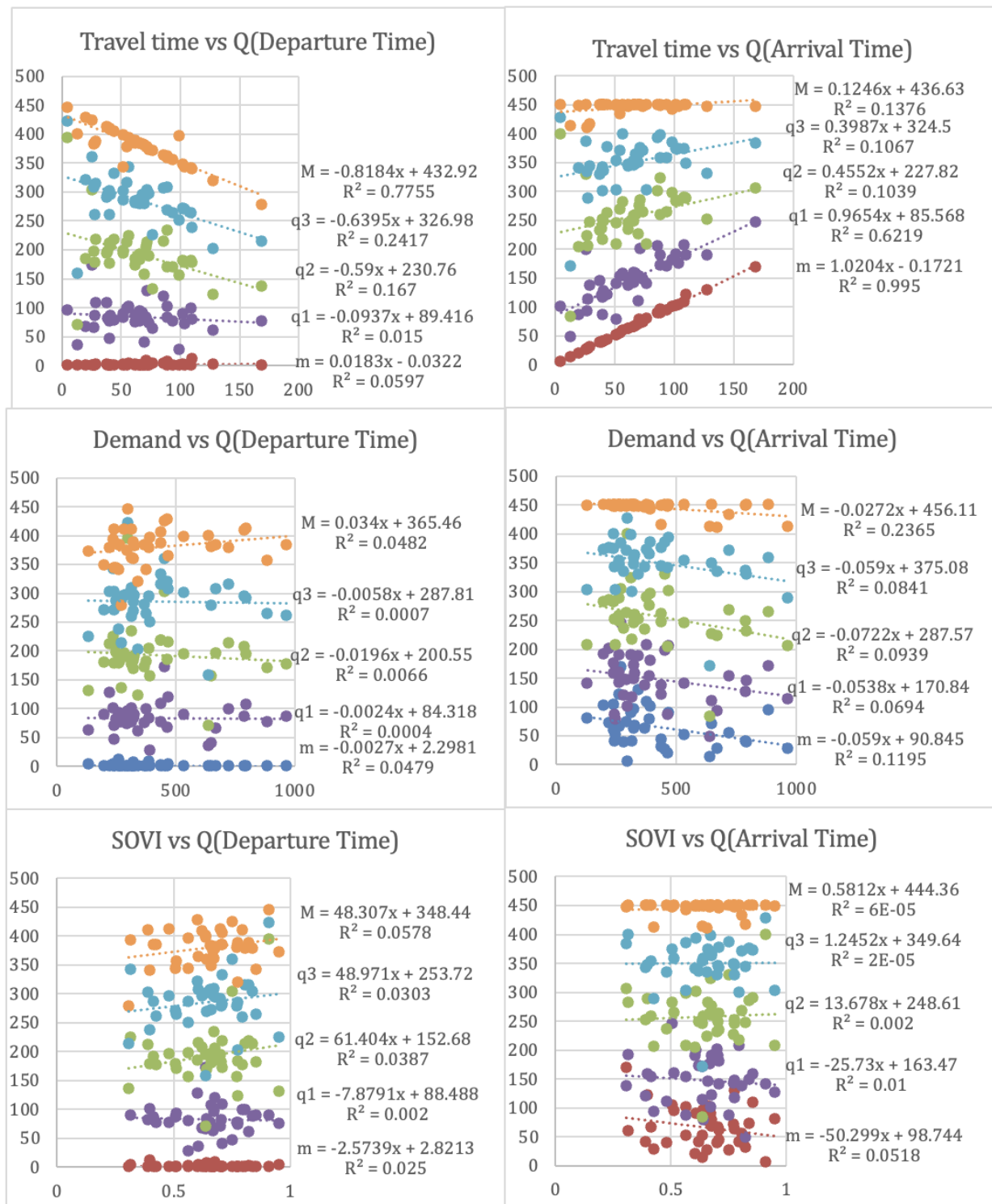


Figure 26. Correlation analysis Travel time OD, demand, and SOVI versus departure and arrival time (Y= Q (Departure/Arrival time) (min, Q1, Q2, Q3, Max))

Evacuation Plan Risk Assessment

The authors followed the methodology in [107], described in Task 2, to obtain the values of the natural hazard risk at the node level v_j for each node of the road network. Figure 27 summarizes the density distribution of the factors affecting the RNP risk at the local level, particularly for all the road network nodes.

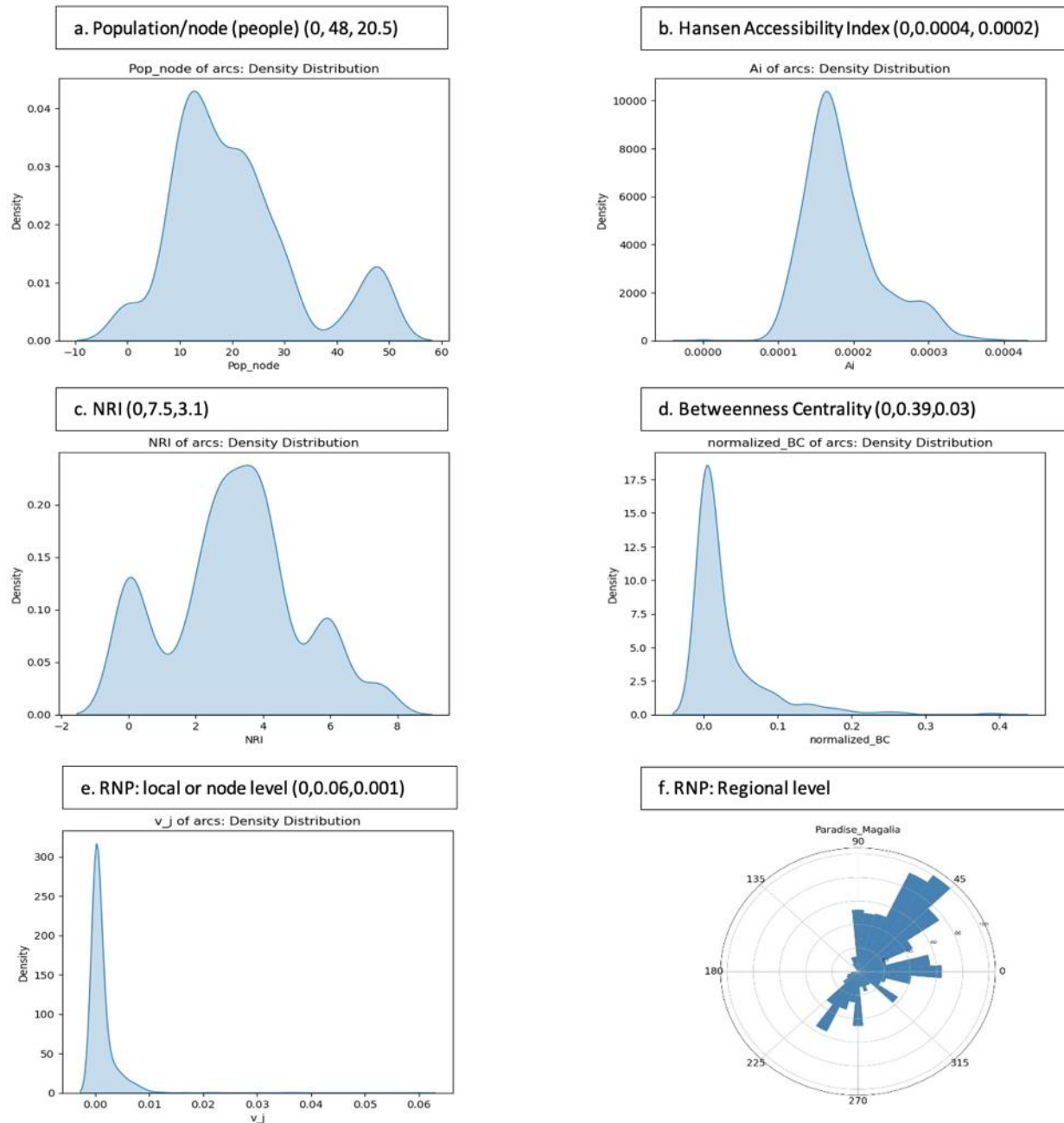


Figure 27. Density probability factors of the v_j parameter (units) (min, max, mean)

The Hansen Accessibility Index (b) displays an almost symmetric distribution, while the Betweenness Centrality (d) among the nodes is skewed to the right. The NRI (c) displays a distribution with three modes. When analyzing the RNP at the local or node level v_j , it has a right-skewed distribution, indicating that some nodes have higher RNP risk than others. The RNP risk at the regional level indicates that the RNP risk is higher in the northeastern direction; however, there are some smaller risks in the north, east, and southwest of Paradise and Magalia. This stage analyzed three different scenarios.

First, we modify the pool of paths by using two other objective functions in the GPP model. Secondly, we determine the anticipated risk of a wildfire on the evacuation by affecting the exit routes in different directions of the road network, such as N, S, W, E, NE, NW, SE, and SW. The RNP risk at the regional level allows for the identification of the likelihood of wildfire and the estimation of the anticipated evacuation time under risk conditions. Thirdly, we determine how aligned our modeling results are with the current analysis conducted by authorities in our case study.

Modifying paths pool: based on different objective functions in the GPP model

First, the authors obtain the pool of paths using two other objectives of the GPP model (see Eq.25 and Eq. 26). The pool size minimizing time, risk, and time is 362, 356, and 407, respectively. Recalling that the risk for each arc is based on Eq.38, where v_j is the RNP at the node level.

$$r_{ij} = \frac{v_i + v_j}{2} \quad \text{Eq.38}$$

Figure 28 shows that the result of the EPWP model is consistent with their objective. The model EPWP (r) has the lowest expected evacuation risk perceived by the evacuees, while the model EPWP (r*t) has the lowest expected evacuation risk combined with time. The original model minimizes the time and has the largest anticipated evacuation risk. Considering the average evacuation time of the ENP model, the EPWP models that minimize evacuation time, risk, and risk & time add approximately 10-, 20- and 30-minute delays in the average evacuation time, respectively.

On the other hand, Figure 29.a shows the difference in the number of vehicles leaving each exit node depending on the model employed. Typically, the number of vehicles leaving each exit node is slightly different when using the EPWP model with the pool of paths that minimize time, risk, and time. Figure 29.b and c. show that the average evacuation rate and cumulative are ordered as ENP, EPWP (t), EPWP (r), and EPWP (r*t), respectively. This behavior increases the clearance time, the total evacuation time, and the average evacuation time of vehicles. Time and risk are inversely proportional because evacuation time increases when minimizing the anticipated risk, and vice versa. Therefore, planners must determine which objective is best for evacuation. For example, a reduction of approximately 50% in risk implies an increase in clearance time of around 20 to 40 minutes, while the average evacuation time increases by 10 to 20 minutes.

Additionally, Figure 30 shows the use of the arcs in the road network regarding flows during the evacuation process, revealing different behaviors among the various models and objectives. The ENP model utilizes most of the arcs of the road network, while the EPWP models change their patterns depending on the objectives. In this context, the authors identified a measure of significance for each arc (a) on the road network in Eq.30, based on the average flows (Eq. 39) and their standard deviation (Eq.40), across the flows obtained in the three scenarios used in the EPWP model: i) time, ii) risk, and iii) time & risk.

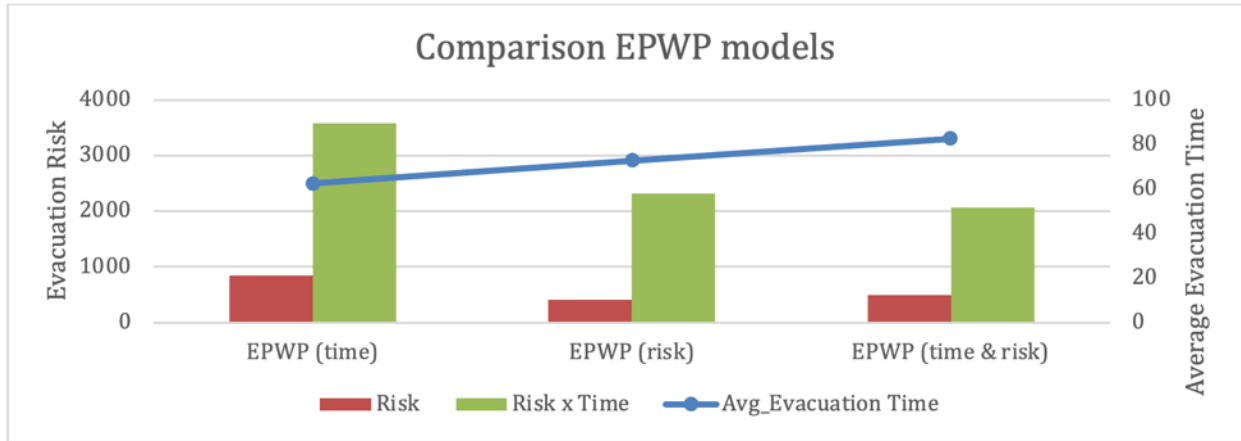


Figure 28. Risk, risk and time, clearance time of EPWP models with different pools of paths.

$$\bar{F}_a = avg(F_a(EPWP(time)), F_a(EPWP(risk)), F_a(EPWP(time\&risk))) \quad \text{Eq.39}$$

$$sd(F_a) = sd(F_a(EPWP(time)), F_a(EPWP(risk)), F_a(EPWP(time\&risk))) \quad \text{Eq.40}$$

$$Importance_a = \bar{F}_a / sd(F_a) \quad \text{Eq.41}$$

The importance $Importance_a$ is greater if the arc has a large average flow and a low standard deviation, meaning that the arc is mostly used independently of the evacuation scenario, with low variability among those scenarios. Figure 30 shows the importance map, highlighting corridors crucial during evacuation processes, regardless of the situation under consideration.

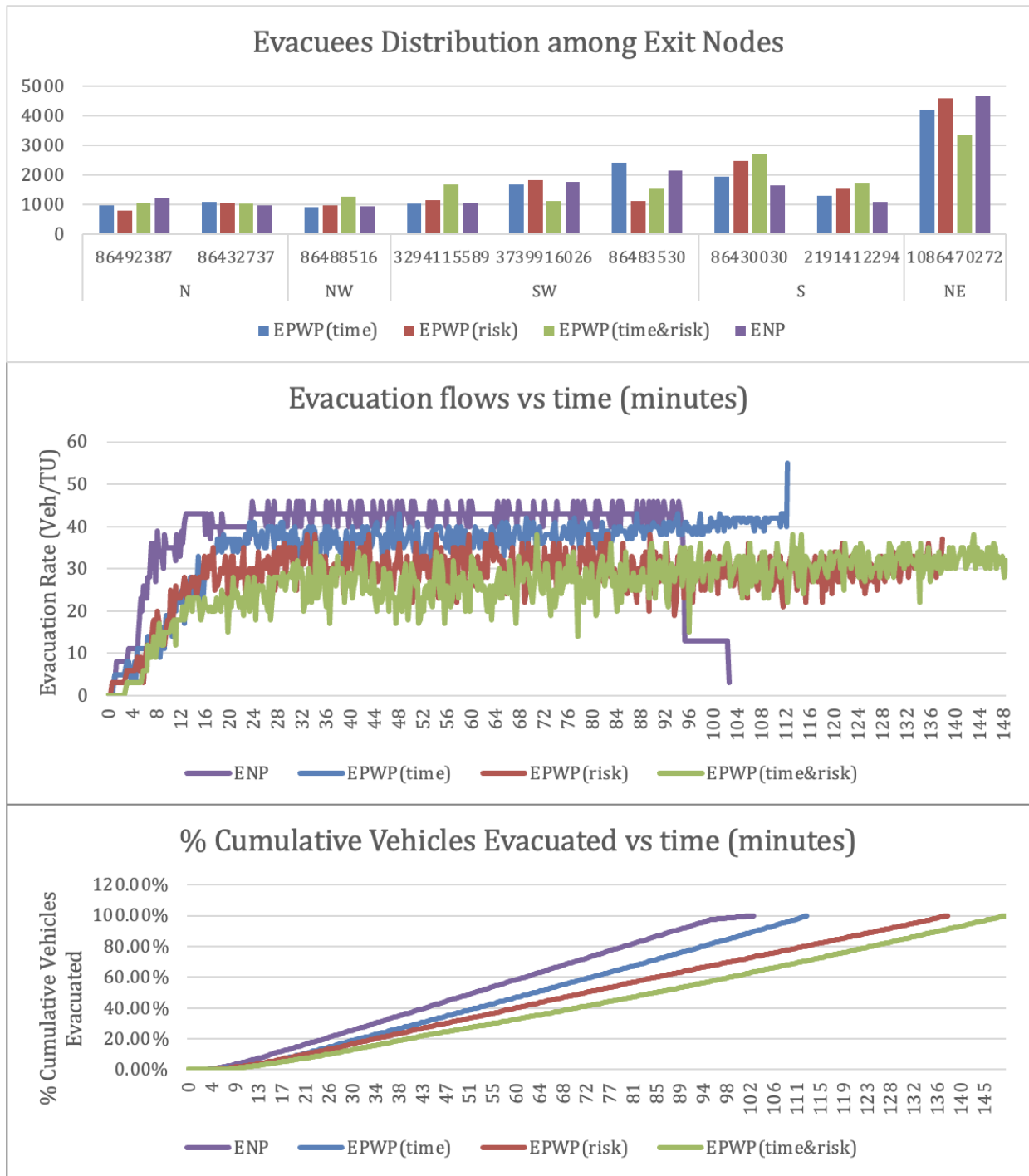
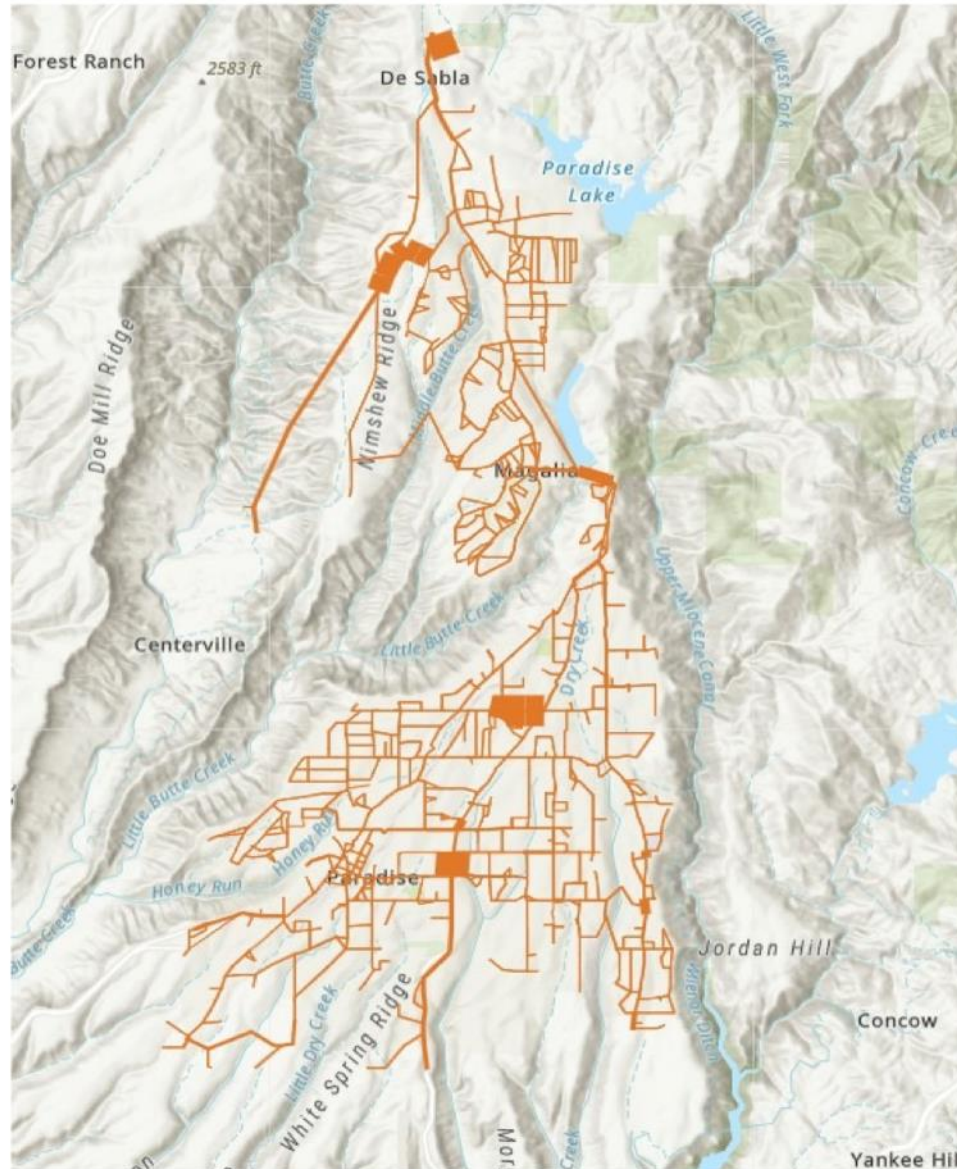


Figure 29. a) distribution of evacuation by exit nodes, b) evacuation flow, and c) cumulative flow of the four models ENP, EPWP (time), EPWP (risk), and EPWP (time & risk)

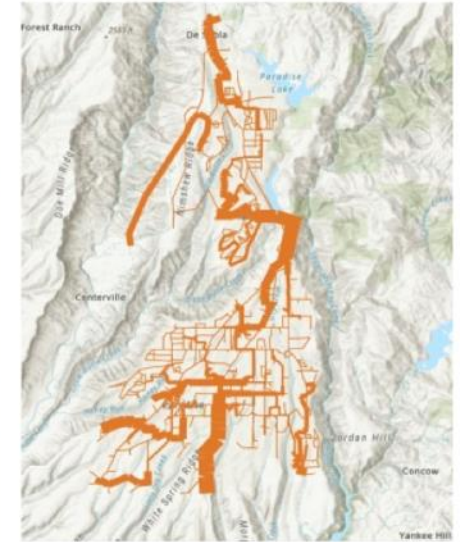
ENP



Importance



EPWP (Risk)



EPWP (Time)



EPWP (Time & Risk)

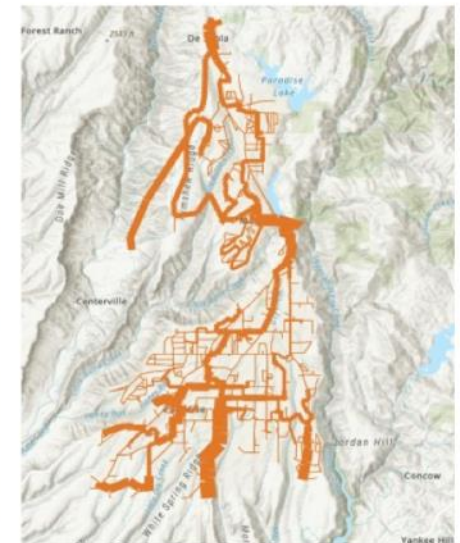


Figure 30. Corridor importance of different EPWP objectives

Impact of exit node availability on evacuation performance

Let us assume that the route leading to the exit node is blocked, and no vehicles can reach a safe destination through this node. Figure 31 and Table 3 show the clearance and average evacuation times when each exit node is closed (independently) using the ENP model. For instance, when node '1086470272' in the NE is closed, the clearance time (CT) increases to 162.5 minutes and the average evacuation time to 72 minutes, compared to the base scenario (102.5 and 52.1 minutes, respectively). This represents a 60% and 38% increase, respectively. In other cases, closing different exit nodes results in evacuation times ranging from 3% to 23% above the base case, while the average evacuation time is 2% to 15% above the base case.

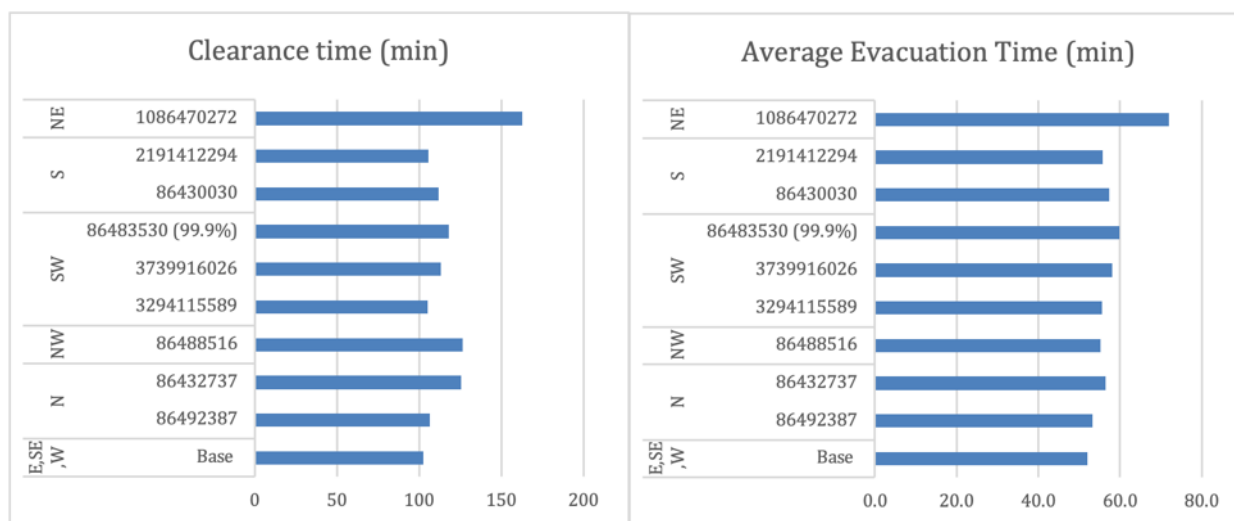


Figure 31. Clearance Time and Average Evacuation Time when closing each exit node

Table 3. Clearance Time, Total Evacuation Time, and Average Evacuation Time when closing each exit node.

Closing scenario		PC Time (mins)	Clearance Time		Total Evacuation Time (ET)		Average ET minutes
			UT	minutes	UT	minutes	
E, SE, W	Base	60	410	102.5	3'248,413	812,103.25	52.1
N	86492387	52	425	106.25	3'318,996	829,749.00	53.2
	86432737	53	501	125.25	3'523,871	880,967.75	56.5
NW	86488516	65	506	126.5	3'443,404	860,851.00	55.2
SW	3294115589	55	421	105.25	3'462,615	865,653.75	55.5
	3739916026	51	452	113	3'625,379	906,344.75	58.1
	86483530 (99.9%)	345	472	118	3'738,000	934,500.00	59.9
S	86430030	55	447	111.75	3'576,064	894,016.00	57.3
	2191412294	71	422	105.5	3'473,506	868,376.50	55.7
NE	1086470272	90	650	162.5	4'494,163	1'123,540.75	72.0

Table 4 provides information about the probability of occurrence of a natural hazard under the eight different directions: d=N, S, W, E, NE, SE, NW, SW. To determine the probability of affecting any of the eight directions: d=N, S, W, E, NE, SE, NW, SW due to the wildfire. The authors use the $\psi_r^{z=wfir}$, this is the *RNP* risk at the regional level $r=\{0, 10, 20, \dots, 340, 350\}$ depicted in Figure 27.f. The eight directions are subsets of the region; for instance, if r is equal to 0, 10, 20, 340, and 350, those values represent the East (E), and if r is equal to 30, 40, 50, 60, then North-East (NE) and so on. The authors utilize Eq.42 and Eq.43 to estimate the probability of each region (r) and direction (d). Moreover, Eq.44 allows us to estimate the expected clearance time (CT), total evacuation time (TET), and average evacuation time (avg_ET) of each direction.

$$p(x = r) = \frac{\psi_r^{z=wfir}}{\sum_r \psi_r^{z=wfir}} \quad \text{Eq.42}$$

$$p(x = r | y = d) = \frac{\psi_r^{z=wfir}}{\sum_{r \in d} \psi_r^{z=wfir}} \quad \text{Eq.43}$$

$$E[Var_d] = \sum_{r \in d} p(x = r | y = d) * Var_r \quad \text{Eq.44}$$

Eq.44 is the sum of the multiplication between the variable's value (CT, TET, avg_ET) when the natural hazard blocks the exit in the region r times the probability of this hazard in the region r belonging to the directions d . For example, note that in the NE direction, the exit node '1086470272' is located in the region 50°. The consequence of closing this exit node is a clearance time of 650 Units of Time (U.T.) (2 hours and 42 minutes). In contrast, if the wildfire affects other regions (r) like 30°, 40°, or 60° in this direction (d), there is no node affected, and the CT is the same as the *base case*, which is 410 U.T. (1 hour and 42 minutes). Therefore, the expected clearance time if a wildfire threatens the northeast side of the road network is around 486 U.T. (around 2 hours) (see Eq.45 and Eq.46).

$$E[CT_{NE}] = p(x = 50 | y = NE) * CT_{50} + (1 - p(x = 50 | y = NE)) * CT_{base} \quad \text{Eq.45}$$

$$E[CT_{NE}] = 0.32 * 650 + (0.68) * 410 = 486 \quad \text{Eq.46}$$

Table 5 provides the steps to estimate the expected CT, TET, and avg_ET for the eight directions. The expected CT under wildfire threat on all cardinal directions independently is 442 UT (110 minutes or 1 hour and 50 minutes), TET is 3'438,858 UT (or 859,714 minutes), and avg_ET is 55.1 minutes.

Table 4. Estimation of the probability of each grade and direction of the road network

Region (r)	ψ_r	Direction (d)	P(r)	P(r)/P(d)
340	0.0008	E	0.02085	0.10754
350	0.0015		0.03871	0.19960
0	0.0024		0.06067	0.31286
10	0.0020		0.05253	0.27087
20	0.0008		0.02116	0.10912
30	0.0017	NE	0.04370	0.14666
40	0.0028		0.07182	0.24103
50	0.0037		0.09467	0.31771
60	0.0034		0.08779	0.29460
70	0.0019	N	0.04829	0.28457
80	0.0018		0.04728	0.27860
90	0.0019		0.04976	0.29319
100	0.0005		0.01217	0.07171
110	0.0005		0.01221	0.07193
120	0.0003	NW	0.00721	0.80668
130	0.0000		0.00000	0.00000
140	0.0001		0.00173	0.19332
150	0.0000		0.00000	0.00000
160	0.0000	W	0.00000	0.00000
170	0.0000		0.00000	0.00000
180	0.0000		0.00000	0.00000
190	0.0002		0.00482	0.37482
200	0.0003		0.00804	0.62518
210	0.0004	SW	0.00909	0.08440
220	0.0005		0.01327	0.12321
230	0.0012		0.03216	0.29853
240	0.0021		0.05320	0.49386
250	0.0012	S	0.03157	0.24428
260	0.0010		0.02473	0.19139
270	0.0017		0.04369	0.33811
280	0.0005		0.01261	0.09759
290	0.0006		0.01662	0.12863
300	0.0005	SE	0.01273	0.15984
310	0.0005		0.01307	0.16412
320	0.0014		0.03544	0.44503
330	0.0007		0.01840	0.23101

Table 5. Estimates the expected clearance time, total evacuation time, and average evacuation time.

Dir	ψ_d	P(Dir)	E[CT]		E[TET]		E[avg ET]	
N	0.0013	0.1510	420.9234	63.5773	3288860.1248	496757.7001	52.7095	7.9614
NE	0.0029	0.3315	486.2513	161.1986	3644204.6465	1208101.2978	58.4045	19.3618
E	0.0015	0.1726	410.0000	70.7605	3248413.0000	560632.1727	52.0612	8.9851
SE	0.0008	0.0886	410.0000	36.3288	3248413.0000	287831.9254	52.0612	4.6130
S	0.0010	0.1150	418.6249	48.1472	3340075.2002	384151.0371	53.5303	6.1567
SW	0.0010	0.1199	449.0779	53.8220	3600591.4995	431531.2897	57.7055	6.9160
W	0.0001	0.0114	410.0000	4.6915	3248413.0000	37170.8505	52.0612	0.5957
NW	0.0001	0.0099	428.5586	4.2622	3286108.3901	32681.8940	52.6654	0.5238
			$\overline{E[CT]}$	442.7882	$\overline{E[TET]}$	3438858.167	$\overline{E[avg ET]}$	55.1134
			Minutes	110.6970531	Minutes	859714.5418		

Evaluate how well-aligned safety elements of emerging plans are to previous evacuations.

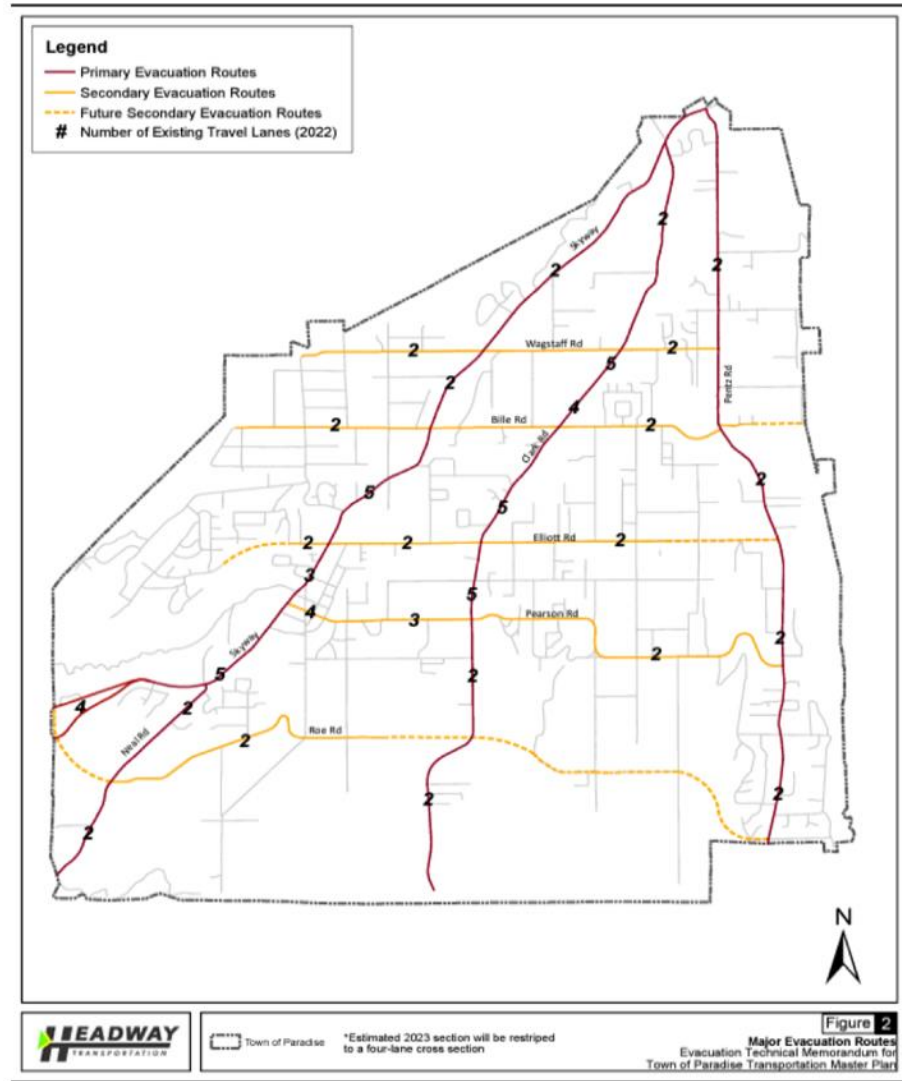
This task examines how well the evacuation route compares to case studies of previous evacuation events, particularly the 2018 Camp Fire in Paradise, California. For this reason, the team used the results of the Evacuation Technical Memorandum from the Paradise Transportation Master Plan [115]. Figure 32 provides an overview of how the evacuation routes of the EPWP models align with the primary and secondary evacuation routes described in the plan [115] for Paradise. Note that the width of the figures in the EPWP models reflects the flow across each arc; the wider the arc, the higher the flow or usage. It is evident that flows become wider on the primary roads, particularly at the endpoints of segments.

Additionally, secondary roads are highlighted in the figures; however, their usage varies depending on the model's objective. Figure 33 illustrates the proposed investments in Paradise for evacuation processes [115], and it includes the map that highlights the importance of the arcs based on their usage, independent of the evacuation scenario objectives. Most of the Paradise administration's recommendations align with the importance analysis. However, the analysis also identifies other segments, specifically the road network, with potential benefits for improvement, given their significant usage and low variability across different scenarios. Specifically, the road leading to SB 191 and some residential streets play an important role in evacuation.

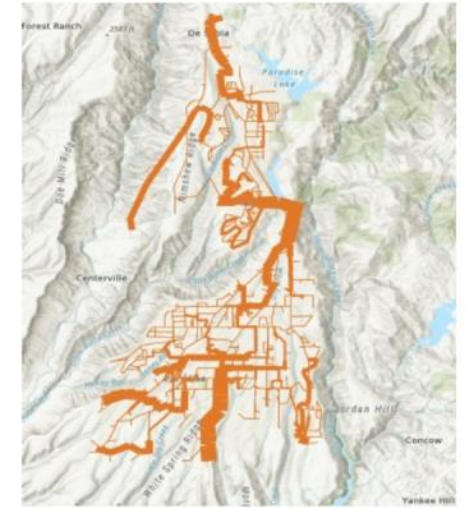
ENP



Evacuation Routes



EPWP (Risk)



EPWP (Time)



EPWP (Time & Risk)

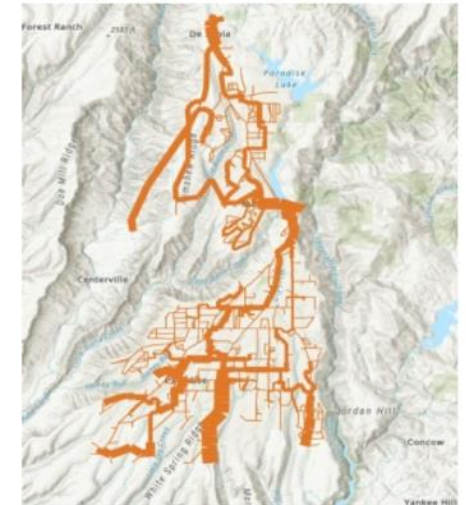


Figure 32. Comparison Evacuation Routes with the routes based on the different models

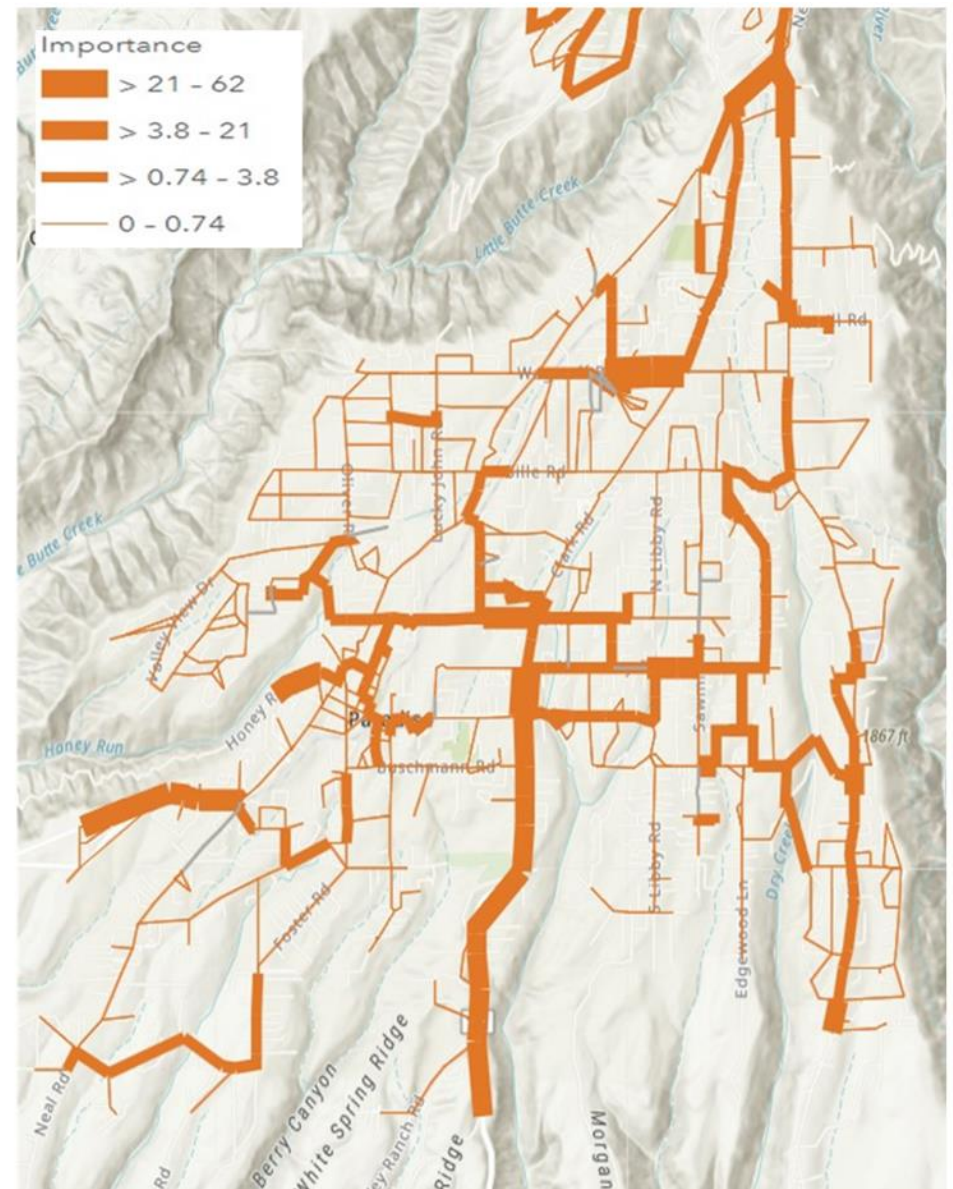
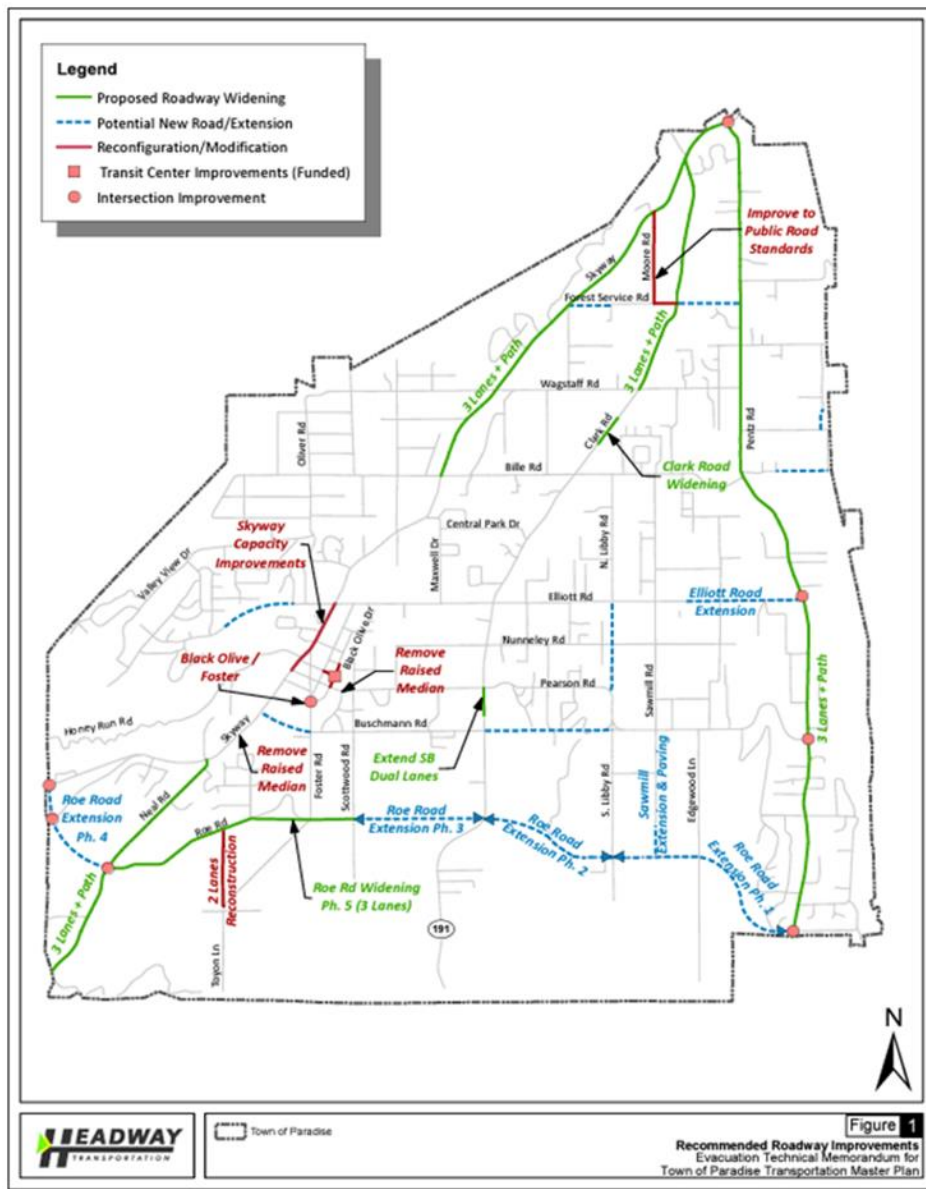


Figure 33. Recommendation Improvement compared with importance measurement of case analysis

Evaluation of the Public Transit Network During Evacuations

The results in Paradise-Magalia show that some stations overlap with high traffic congestion, but there's a strong question as to whether buses would run during an evacuation setting. Operating with the assumption that the routes and stops would be active, the composite vulnerability index provides a more complete view of community vulnerability and accessibility. Understanding the individual empirical contributions and weighting accordingly is beyond this project's scope. This combined index and mapping comparison provides alignment and direction for future work between modeled results and transit routes. This analysis can be repeated in additional regions with the aggregated data provided.

As the CalEnviroScreen score measures pollution burden (average of exposures and environmental effects) multiplied by the population characteristics (average of sensitive populations and socioeconomic factors), a higher value shows a burdened community. We observe (Figure 34) that the more burdened regions in this community are to the southwest, lower to the northwest, and southeast, slightly lower to the north.

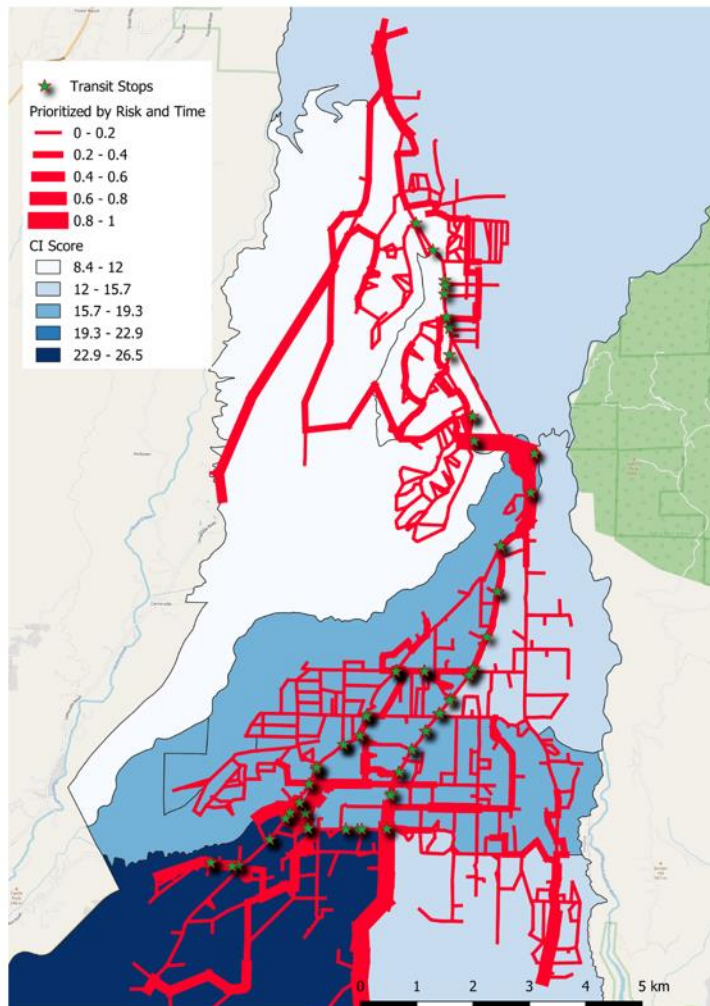


Figure 34. Prioritized risk and time with transit stop and CI Score.

Compared with the FEMA NRI hazard score (Figure 35), it shows an increased trend in the north and northwest but follows the same pattern as the CalEnviroScreen score in the south and southeast. This is likely primarily an indication of the wildfire risk in those directions.

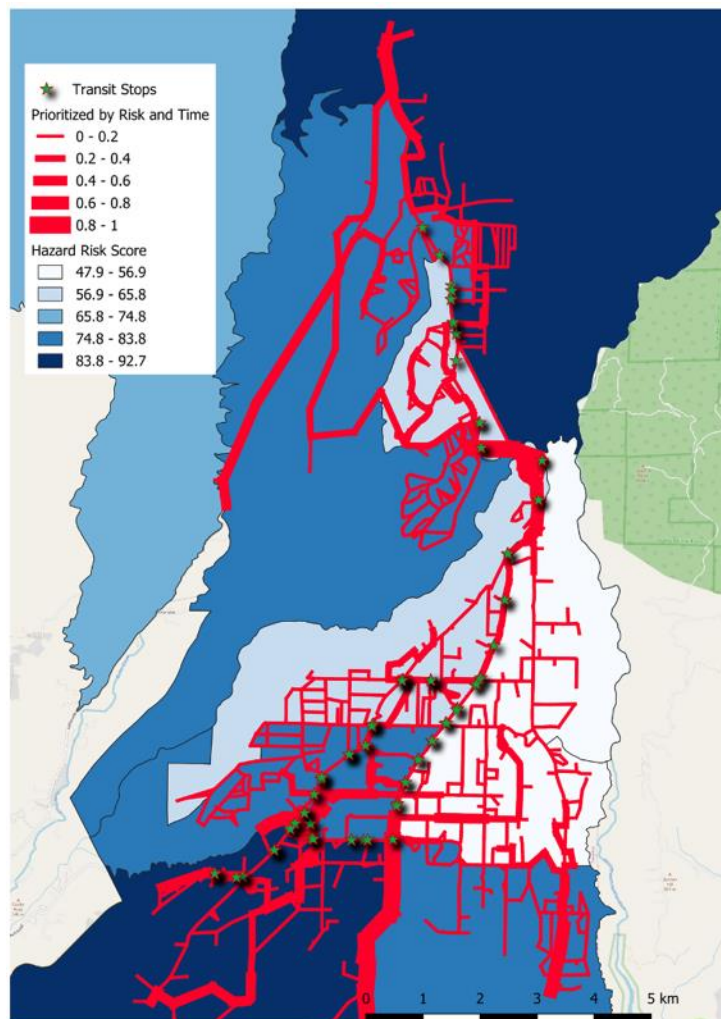


Figure 35. Prioritized risk and time with transit stop and NRI.

The transit stops per 1,000 residents (see Figure 36 left) have a high value in the central Paradise region, where a concentration of transit stops exist. We observe that the route does have some significant alignment with the prioritized evacuation route (risk and time model) and likely reflects the primary structure of the road network through that location.

The combined vulnerability index (see Figure 36 right) shows some of the same trends with the highs to the southwest and north; however, the high in the central region from the CalEnviroScreen Score is offset by the concentration of per capita transit stops.

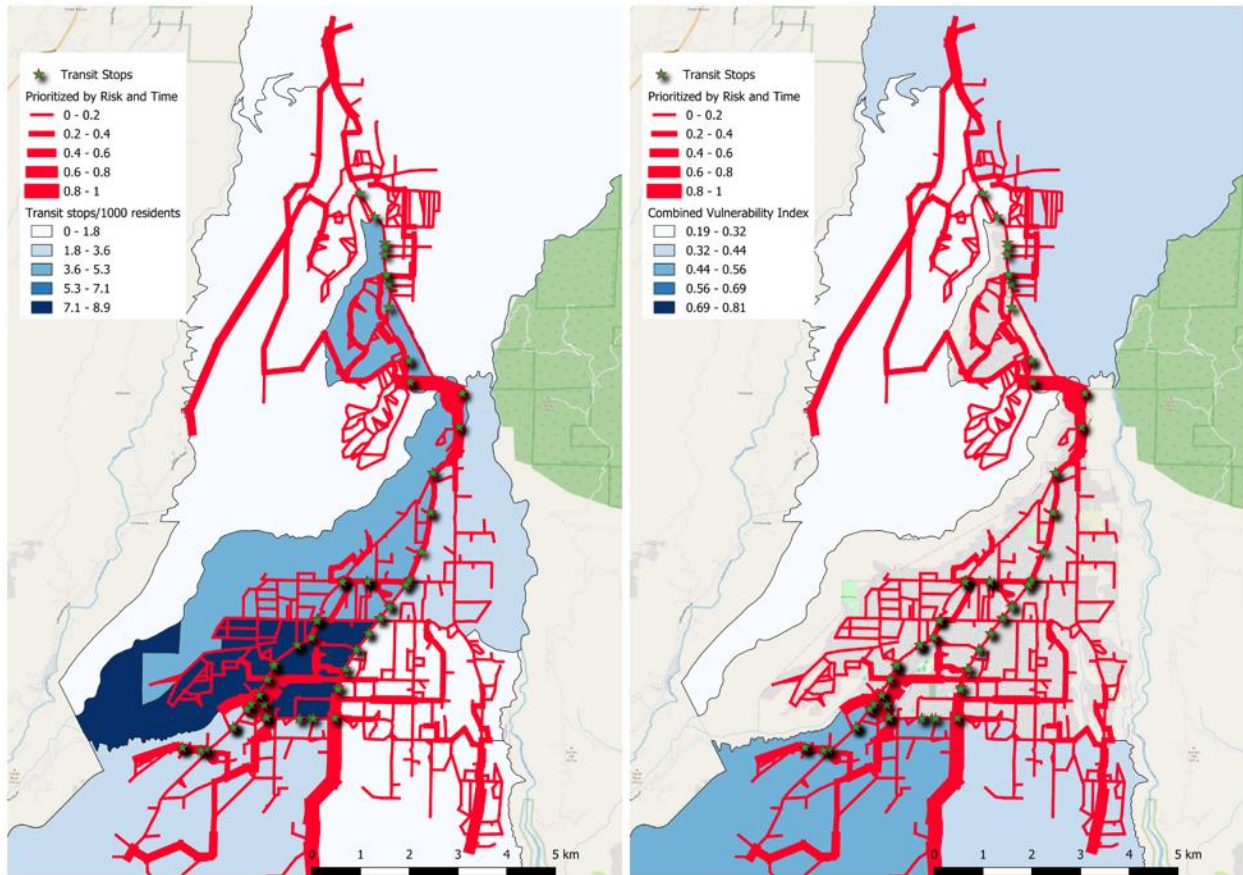


Figure 36. Prioritized risk and time with transit stop and (left) Transit Stops/1000 residents; and (right) Combined Vulnerability Index.

Discussion

This section briefly discusses the results obtained in tasks 2, 3, and 4, which describe the *road network performance risk* and *evacuation performance*. This project's outcomes, methodology, and analyses allow the assessment of the interaction between various factors, including natural hazard risk and road network performance at the topological level. The findings demonstrate that the natural hazard risk can be effectively enhanced or reduced based on the topological characteristics of the road network. The results provide insights and guide future research activities, such as analyzing broader areas like Statistical Metropolitan Areas (SMA) instead of individual cities. Furthermore, there is potential to extend the analysis to the street level (arcs or edges) to identify prioritization in cases such as evacuations. However, it is essential to observe certain limitations in this research, such as using the National Risk Index (NRI) obtained initially at the census tract level and subsequently downscaled to a census block and node level.

Despite some of these limitations, the analysis shows that the proposed approach, using the road network from OpenStreetMaps and the risk from the NRI database, allows planners to measure, quantify, and identify the potential hazard risks associated with each city and the pattern of such risks in a standardized way for a set of multiple urban areas. Knowledge of the risk patterns provides a better understanding of the different issues in diverse geographical areas. The proposed methodology provides additional information for decision-makers to plan against natural hazards. For instance, identifying the locations with the highest risk of being affected by natural hazards and how this risk is distributed within each location provides insights into which localities should be prioritized for future investments under a limited budget. However, identifying specific priority locations or investment opportunities requires a deeper analysis of each selected city. The team focused on two case studies derived from Task 2 to explore these opportunities. In Tasks 3 and 4, the team concentrated on the case of Paradise for evacuation purposes, identifying the most critical corridors within the road network under a set of scenarios. The results showed similarities with the priorities or investment opportunities identified by the local government of Paradise. However, our analysis also highlights opportunities to enhance the capacity or performance of an extended set of corridors based on their importance. Additionally, our case study demonstrated the need to develop alternative strategies to support and alleviate the usage of road network capacities and avoid large-scale calamities in the event of a no-notice wildfire when the city's current road network capacity does not allow demand to evacuate effectively.

The methodology developed in this project helps to close the gap related to the lack of methods that can provide a standardized spatial analysis that permits the comparison between a relatively large set of road networks and includes the latent risks of natural hazards in each location. This method contributes to the literature because it is an understudied use of the RNP concepts, such as spatial analysis. Additionally, this method is applied to a case study with a relatively large set of localities in California, including a wide variety of natural hazard risks. A discussion of the results on the two areas of RNP risk and Evacuation Performance is described below:

Road network performance Risk

On task 2, the team introduced a method to address an underexplored aspect of RNP risk that combines historical data on past natural hazards and the socioeconomic characteristics, e.g., community vulnerability and resilience, given by θ_i^Z , with the topological characteristics of the road network given by BC_i and A_i . Given the different scales of each factor (θ_i^Z , BC_i and A_i) included in the estimation of the RNP_{risk} at the local or node level. This study recommends normalizing these factors to balance their expected influence on the RNP_{risk} at the local level. This normalization will also impact the RNP_{risk} at regional and global levels. The standardized distribution of the contributions of each factor is essential for effective planning. For example, while natural hazard risks are not controllable, other elements, such as topological features, can be improved to enhance the resilience of the road network. These enhancements can inform the population at each location of the expected risk.

Additionally, the results from task 2 offer insights into adapting Boeing's [15] orientation methodology for spatially standardizing natural hazard risk in road networks. This facilitates comparing various locations and natural hazards in a standardized manner, thereby enhancing prioritization in the planning and decision-making process for mitigation, preparedness, and disaster response strategies. Below are the key insights derived from this study:

- The RNP_{risk} at the regional level depicted on the polar histogram of the Risk (ψ_r^Z) works as a tool to identify the pattern of risk inside each city, and its use also depends on the type of natural hazard and the topological characteristics of the city's road network. The polar histogram of the Risk (ψ_r^Z) standardizes the patterns of the natural hazard risks spatially with each city's road network characteristics and allows the comparison of multiple natural hazards and road networks.
- The knowledge of the different patterns of risk that depend on the natural hazard and the topological characteristics of the road network is beneficial for disaster operation managers because such prior knowledge allows for the planning of disaster management operations. For instance, when analyzing natural hazards that require evacuation, like wildfires, hurricanes, tsunamis, or floods, the evacuation routes should consider the city's expected risk direction. In other words, this polar histogram of the risk makes clear where not to try to direct the population in such cases. Another case is for the location of hubs or warehouses with prepositioned inventory. For instance, if the risk of hurricanes or tsunamis in one city is in the North, while the risk of other natural hazards like floods or wildfires is on the West side of the city, it means that the possible location of such hubs or warehouses should be at other locations in the city with a lower risk, like the South, East, or even outside the city when it is clear that the whole city is at risk of being affected by a natural hazard. The selection of this lowest risk direction depends on analyzing the risk of all the common natural hazards in the location.
- $SSRI^Z$ provides information about how the concentration of the risk is distributed across a city's road network. The analysis showed $SSRI^Z$ is affected positively and significantly by θ_i^Z , A_i and BC_i . The share of each factor is particularly interesting because despite the shape of the polar histogram of Risk ($\psi_r^Z(v_i^Z)$) looks similar to the

shape of the Risk ($\psi_r^z(\theta_i^z)$), the $\psi_r^z(A_i)$ and $\psi_r^z(BC_i)$ act as a mediator to increase or decrease the risk in specific directions of the road network, receiving relatively high importance based on the statistical correlation analysis.

- Note also that none of the RNP measurements described in the literature review adequately capture the distribution of risk within a city because they depend only on the topological characteristics of the road network and do not incorporate historical data on natural hazard risks.
- The analysis performed in this study allowed us to identify the areas and directions with the highest risk concentration within a road network to prioritize mitigation, preparedness, and disaster response planning.

Task 2 also introduced a methodology that provides a standardized method for comparing spatially divergent locations, and it effectively enhanced our understanding of the risk by comparing around 475 municipalities in our case study in California. The results provide insights that are relevant to decision-makers, as summarized below:

- The clustering analysis provides a sense of prioritization for a large set of cities. It is important to note that the priority ranks of the cities vary depending on the natural hazards considered. The analysis's variety of natural risk measurements allows disaster managers to design different strategies depending on which natural hazards are most critical to each city. Additionally, thresholds in the cluster analysis are adjustable, depending on the decision-maker's or planner's interests.
- Planners can identify at least two types of cities with high risk among the cluster: those where the risk is concentrated in specific directions and those where the risk affects the entire population or a larger share of it. The strategies to address the risk in these groups of locations may differ. For example, when considering evacuation strategies, areas where the risk affects the entire population will require plans to evacuate the whole population. In contrast, those where the risk is concentrated in specific directions may be able to explore alternatives to evacuation, such as sheltering in place or finding safe zones within the city boundaries. However, specific alternatives should be analyzed individually.
- When aggregating the $SSRI^z$ into regions, it was evident that different areas are more likely to be affected by different natural hazards. Additionally, the authors noted similar risk distributions between cities that are close to each other. This illustrates a spatial correlation between cities based on their distance. The primary evidence of such behavior is found in the cities of the *South Coast* and the *Inland Desert*, where component cities are close. The opposite behavior was found in the *Northern* region of California, where cities are further apart from each other, and their road networks are less complex than those in the rest of the state.

Evacuation Performance

Regarding evacuation performance, Task 3 provided a methodology to identify evacuation plans for no-notice wildfire events. The team used the American Community Survey, OpenStreetMap, NRI datasets, and the RNP risk at different levels of the road network [102]. In Task 3, the authors estimated the minimum clearance time, a pool of paths between each OD pair, the minimum number of paths that could be used to evacuate the population in the minimum time, the RNP risk at the node and arc level, and regional. The authors also analyzed the sensitivity of the evacuation performance based on different objective functions and closures of exit routes. The authors also evaluated how the evacuation plans performed during a simulated wildfire event in Paradise, California. Despite differences in area and vehicle demand, the mathematical programming models showed comparable clearance times (~1 hour, 50 minutes) between the two case studies, the Camp Fire and the Thomas Fire. This was attributed to variations in exit routes and road network capacity. The Thomas Fire area has more exit routes than the Camp Fire area. Additionally, the road network capacity in the Thomas Fire area is greater than that of the Camp Fire area, providing insights into the reasons for this difference in performance.

The travel time from origin to destination for each path is the primary factor guiding the scheduling of vehicle departures and arrivals. However, on Task 4, with the inclusion of an evacuation plan risk assessment that considers the inclusion of a different pool of paths that minimize the total risk between each origin-destination (OD) pair and those that minimize time, it became possible to identify the minimum number of corridors vital for evacuation planning. Additionally, it is possible to identify the most critical exit routes, directions with higher risk, and the expected evacuation time under wildfire risk.

We conducted a second analysis of the road network for the Paradise/Magalia network using Omniscape. Omniscape uses electrical circuit theory to measure the level of connectivity to a central grid cell from a set of cells within a given buffer distance. The central grid cell moves across the entire spatial domain to create a view of the connectivity strength among all cells, in this case, the pixels in the transportation network. We used several buffer distances and found that a more restrictive buffer size permitted the identification of localized or neighborhood-scale bottlenecks, where traffic would be slowed if all the people (from the census) within the buffer were trying to leave at once on the road network. A larger buffer distance identified bottleneck areas that were very similar in location to those identified using the RNP model. No similar studies use Omniscape because this model is primarily a conservation planning tool. However, it has previously been applied to map open space within cities [95]. We found this tool promising because it requires only parameterizing two variables. However, the road network requires both local spatial estimates of the existing population and travel speed on a per-arc basis. However, the Omniscape model was particularly useful in our study because its results converged with the spatial results from the other modeling, for example, with expected high levels of congestion at the point that connects the road network of Paradise in the south and Magalia in the north.

Limitations and Assumptions

This project analyzes the performance of evacuation plans through optimization models, considering factors such as wildfire risk, evacuation time, vehicle demand, and road network capacities. The methodology offers a generalized approach that can be applied to various locations. However, the following limitations and assumptions should be noted:

Limitations

1. Data Resolution and Downscaling:

- The wildfire risk data is derived from the National Risk Index (NRI), originally available at the census tract level. The data was downscaled to the census block and node levels for finer analysis, introducing potential inaccuracies in the risk estimation at these granular levels.

2. Behavioral Dynamics:

- While this study considers the socioeconomic characteristics of the population for evacuation risk estimation, behavioral elements such as individual decision-making, compliance rates, and route choices during evacuations are not explicitly modeled. This limits the real-world applicability of the evacuation performance analysis in highly dynamic and unpredictable settings.

3. Assumptions of Road Network Integrity:

- The analysis uses road network data from OpenStreetMaps. This approach assumes the network accurately represents real-world conditions, including connectivity and capacities. However, it may not account for temporary road closures, maintenance, or other disruptions.

4. Simplified Traffic Congestion Dynamics:

- Traffic congestion estimates rely on aggregated vehicle demand and assumed network capacities. The model does not fully capture micro-level traffic dynamics, such as driver behavior, vehicle breakdowns, or other localized disruptions.

5. Transit Accessibility:

- In areas like Paradise-Magalia, bus stops, and transit routes are assumed to remain active during an evacuation. However, the feasibility of operating public transportation during such events remains uncertain, and the analysis does not account for potential interruptions in service.

Assumptions

1. Evacuation Scheduling:

- Clearing time (when the last individual exits the area) and total evacuation time (the cumulative time for all individuals to evacuate) are key performance indicators. The model assumes vehicles can evacuate uninterrupted to designated safe areas unless explicitly stated otherwise.

2. **Path Diversity:**

- The shortest path between nodes is calculated using the Generalized Path Problem (GPP) model, which generates a more diverse set of evacuation paths than some alternative methods. This assumption enhances route diversity but may deviate from real-world driver preferences.

3. **Blocked Route Scenario:**

- It is assumed that if a route leading to an exit node is blocked, no vehicles can reach a safe destination through that node. This scenario tests the network's resilience under adverse conditions.

4. **Congestion Dynamics in Paradise-Magalia:**

- The analysis emphasizes internal congestion within the combined metro region of Paradise-Magalia and identifies choke points, such as the connector route between the two cities. The model assumes external interventions do not redirect traffic flows.

5. **Vulnerability Index:**

- The composite vulnerability index incorporates assumptions about the availability of evacuation routes, public transit, and community accessibility to provide a comprehensive view of vulnerability.

Despite these limitations and assumptions, the proposed methodology demonstrates utility in quantifying and standardizing city risk patterns. It provides actionable insights for planners, enabling a more informed approach to evacuation planning and disaster risk management.

Tool Limitations

While mathematical programming and Omniscape offer valuable insights for evacuation modeling, several limitations need to be considered for further refinement and future applications:

Mathematical Programming Limitations:

1. **Simplified Assumptions on Behavior and Decision-Making:** Mathematical programming models often utilize simplified assumptions, such as fixed evacuation paths or predetermined vehicle demand. These assumptions are not based on dynamic changes in evacuee behavior, such as deviations from optimal evacuation routes, congestion avoidance, or uncertainty in demand based on real-time information. To address this limitation, future models could incorporate adaptive decision-making mechanisms or machine learning techniques to rapidly adjust to real-time conditions. However, the models used in this project are expected to be used as a planning tool, not an operational tool.
2. **Computational Complexity and Scalability:** As evacuation scenarios grow in complexity, especially when considering large-scale urban areas with numerous nodes and evacuation routes, the computational complexity of mathematical models increases significantly. This can lead to longer solution times, making implementing the models to real-time decision-making difficult. Future research could explore heuristic or metaheuristic approaches, such

as genetic algorithms or simulated annealing, to provide faster and more efficient solutions without sacrificing model accuracy.

3. **Lack of Behavioral Data:** Mathematical models in evacuation planning often exclude behavioral elements that can significantly affect evacuation efficiency. While behavioral factors are outside the scope of this study, future work could incorporate these elements through agent-based modeling or data-driven approaches, improving model realism and predictive accuracy.
4. **Parametrization of the mathematical model:** The minimum travel time on all arcs determines the models' complexity when constructing and loading the road network. Therefore, it is crucial to identify the best tolerance to use when simplifying the network without losing its structure. The ENP model does not provide a plan for the evacuation process. However, it is possible to obtain an evacuation plan when combined with the GPP model and integrated into the EPWP model.

Omniscope Limitations:

Limited Real-Time Adaptability: Like mathematical programming, Omniscope does not account for real-time fluctuations in traffic or emergency response strategies. This limits its applicability for real-time evacuation decision-making. Future developments could incorporate real-time data streams from traffic monitoring systems or integrate Omniscope with real-time optimization models to enhance its adaptability during an ongoing evacuation event.

Future Directions:

Future research should explore:

- Integrating mathematical programming and Omniscope with real-time data for a more dynamic and adaptable evacuation.
- Implementing behavioral insights and traffic simulation models enhances realism and granularity in evacuation scenarios.
- Investigating hybrid approaches that combine the strengths of both methods while mitigating their limitations, such as integrating optimization models with traffic flow simulations and real-time adjustment capabilities.

Future evacuation models can provide more accurate, responsive, and actionable recommendations by addressing these challenges improving emergency preparedness and response strategies.

Conclusion and Key Takeaways

The project focused on enhancing road network performance (RNP) analysis to understand better and mitigate California's natural hazards from the evacuation perspective. Specifically, it introduced a new approach to assessing the risks posed to road networks by natural hazards while incorporating factors such as community vulnerability, resilience, and the topological features of road networks. The study aims to prioritize mitigation efforts, preparedness, and disaster response in areas with the highest level of risk concentration.

Key Takeaways:

- **Methodology Innovation:** The study introduces a new method to assess RNP risk by combining historical natural hazard data and socio-economic factors (e.g., community vulnerability) with the road network's topological features (e.g., betweenness centrality and accessibility). A critical insight is that these factors operate at different levels, necessitating normalization to balance their impact on risk assessments at both local and regional levels. This normalization is crucial for fair planning, allowing decision-makers to improve road networks' resilience by addressing controllable elements, such as road design and connectivity, even if the natural hazards cannot be changed. The methodology allows cities to be compared based on their natural hazards, facilitating the prioritization of disaster preparedness investments.
 - We also found the Omniscape, a spatial tool used for conservation corridor planning, could identify congestion points within city networks, which were also found using the more computationally intensive RNP approach. However, the Omniscape approach did not provide as many highly detailed results.
- **Spatial Standardization:** The study uses a standardization approach to mapping the risk of natural hazards in road networks. This standardization allows for comparisons among different cities and hazards, enabling a strategic prioritization for disaster response. For instance, when planning evacuation routes, decision-makers can use this method to avoid high-risk areas and direct populations to safer areas.
- **Risk Patterns and Decision-Making:** The polar histogram of risk allows disaster managers to visualize how risk is distributed across a city. This tool informs decisions, such as where to locate evacuation routes or pre-position inventory hubs, based on the direction of the highest risk. Alternatively, if certain hazards are predominantly threatening the north or west sides of a city, resources can be strategically located in lower-risk areas to optimize disaster preparedness.
- **Evacuation Insights:** The project provides a framework for evaluating evacuation strategies during no-notice events such as wildfires, including assessing the minimum clearance times, the number of evacuation paths, and critical road corridors. Using a wildfire event in Paradise, California, highlighted the importance of optimizing evacuation routes and ensuring sufficient road capacity to handle emergencies. The project highlights the importance of developing alternative evacuation strategies for

cities with insufficient road network capacity, particularly during no-notice events like wildfires.

- **California Preparedness:** The findings indicate that California has a relatively complex road network, and preparedness levels vary across regions, revealing that California's readiness is uneven. Cities in the South Coast and Inland Desert regions have similarities in risk due to their geographical and network proximity and exhibit a higher spatial correlation of risk due to their proximity and similar network characteristics. Conversely, cities in Northern California face challenges due to isolation and less complex road networks, facing challenges in managing risk effectively. Some high-risk areas are inadequately prepared for evacuation during no-notice events like wildfires. Cities with denser, more connected road networks have a significant advantage in mitigating risk, while more isolated areas may struggle with road capacity during emergencies. Overall, the study emphasizes that preparedness in California is fragmented, with significant improvements needed in infrastructure resilience, especially in regions with higher risk concentrations. One of the next steps is to enhance the granularity of risk data, possibly through downscaling national datasets more precisely, which would allow for more accurate local risk assessments and inform targeted infrastructure investments.

Finally, decision-makers can use the project's results to determine which cities or regions require immediate investment to increase resilience. This could include upgrading road networks in high-risk areas, adjusting land use planning to account for hazard-prone areas, and refining evacuation protocols based on the specific vulnerabilities of each area.

References

- [1] M. Do and H. Jung, "Enhancing road network resilience by considering the performance loss and asset value," *Sustainability*, vol. 11, no. 4188, 2018.
- [2] N. Menon, B. Staes and R. Bertini, "Measuring Transportation Network Performance During Emergency Evacuations: A Case Study of Hurricane Irma and Woolsey Fire.," Arlington TX, 2020.
- [3] DHS, "Department Homeland Security," 05 2022. [Online]. Available: <https://www.dhs.gov/natural-disasters>.
- [4] R. Blanchi, J. Whittaker, K. Haynes, J. Leonard and K. Opie, "Surviving bushfire: the role of shelters and sheltering practices during the Black Saturday bushfires," *Environmental Science & Policy*, vol. 81, pp. 86-94, 2018.
- [5] Climate, "climate.org," 2021. [Online]. Available: <https://www.climate.gov/news-features/blogs/beyond-data/2021-us-billion-dollar-weather-and-climate-disasters-historical>.
- [6] S. Wong, J. Broader and S. Shaheen, "Review of California wildfire evacuations from 2017 to 2019," UCITS, 2020.
- [7] statista, "statista," [Online]. Available: <https://www.statista.com/search/?q=Largest+wildfires+in+California&Search=&p=1>. [Accessed 22 7 2024].
- [8] T. Cova, D. Theobald, J. Norman and L. Siebeneck, "Mapping wildfire evacuation vulnerability in the western US: The limits of infrastructure," *GeoJournal*, vol. 78, p. 273–285, 2013.
- [9] M. Meyer, E. Rowan, M. Savonis and A. Choate, "Integrating extreme weather risk into transportation asset management," *American Association of State Highway and Transportation Officials*, 2012.
- [10] D. Rivera-Royero, G. Galindo, M. Jaller and J. Reyes, "Road network performance: a review on relevant concepts," *Computers & Industrial Engineering*, p. 107927, 2022.
- [11] M. Jaller, C. González-Calderón, W. Yushimito and I. Sánchez-Díaz, "An investigation of the effects of critical infrastructure on urban mobility in the city of Medellín," *International Journal of Critical Infrastructures*, vol. 11, no. 3, pp. 213-232, 2015.
- [12] V. Cantillo, L. Macea and M. Jaller, "Assessing vulnerability of transportation networks for disaster response operations," *Networks and Spatial Economics*, vol. 19, no. 1, pp. 243-273, 2019.
- [13] S. Derrible and C. Kennedy, "Applications of graph theory and network science to transit network design," *Transport reviews*, vol. 31, no. 4, pp. 495-519, 2011.
- [14] E. Jenelius, "Network structure and travel patterns: explaining the geographical disparities of road network vulnerability," *Journal of Transport Geography*, vol. 17, no. 3, pp. 234-244, 2009.
- [15] G. Boeing, "Urban spatial order: Street network orientation, configuration, and entropy," *Applied Network Science*, vol. 4, no. 1, pp. 1-19, 2019.

- [16] R. Faturechi and E. Miller-Hooks, "Measuring the performance of transportation infrastructure systems in disasters: a comprehensive review," *Journal of infrastructure systems*, vol. 21, no. 1, 2014.
- [17] Y. Zhou, J. Sheu and J. Wang, "Robustness assessment of urban road network with consideration of multiple hazard events.," *Risk Analysis*, vol. 37, no. 8, pp. 1477-1494, 2017.
- [18] A. Nelson, S. Lindbergh, L. Stephenson, J. Halpern, F. Arroyo, X. Espinet and M. González, "Coupling natural hazard estimates with road network analysis to assess vulnerability and risk: case study of Freetown (Sierra Leone)," *Transportation research record*, vol. 2673, no. 8, pp. 11-24, 2019.
- [19] T. Grubestic, T. Matisziw, A. Murray and D. Snediker, "Comparative approaches for assessing network vulnerability," *International regional science review*, vol. 31, no. 1, pp. 88-112., 2008.
- [20] M. Taylor, S. Sekhar and G. D'Este, "Application of accessibility based methods for vulnerability analysis of strategic road networks," *Networks and Spatial Economics*, vol. 6, no. 3, pp. 267-291, 2006.
- [21] Y. Casali and H. Heinimann, "A topological analysis of growth in the Zurich road network," *Computers, Environment and Urban Systems*, vol. 75, pp. 244-253, 2019.
- [22] X. Zhang, E. Miller-Hooks and K. Denny, "Assessing the role of network topology in transportation network resilience," *Journal of Transport Geography*, vol. 46, pp. 35-45, 2015.
- [23] W. Ip and D. Wang, "Resilience evaluation approach of transportation networks," in *In 2009 International Joint Conference on Computational Sciences and Optimization*, 2009.
- [24] Y. Casali and H. Heinimann, "A topological characterization of flooding impacts on the Zurich road network," *PLoS one*, vol. 14, no. 7, p. e0220338, 2019.
- [25] N. Zhang and A. Alipour, "Integrated framework for risk and resilience assessment of the road network under inland flooding," *Transportation research record*, vol. 2673, no. 12, pp. 182-190, 2019.
- [26] N. Altay and W. Green, "Or/ms research in disaster operations management," *European Journal of Operation Research*, vol. 175, no. 1, pp. 475-93, 2006.
- [27] E. Maspero and H. Ittmann, "Rise of humanitarian logistics," 2008.
- [28] C. Rawls and M. Turnquist, "Pre-positioning of emergency supplies for disaster response," *Transportation research part B: Methodological*, vol. 44, no. 4, pp. 521-534, 2010.
- [29] G. Galindo and R. Batta, "Review of recent developments in or/ms research in disaster operations management," *European Journal of Operation Research*, vol. 230, no. 2, pp. 201-11, 2013.
- [30] G. Galindo and R. Batta, "Prepositioning of supplies in preparation for a hurricane under potential destruction of prepositioned supplies," *Socio-Economic Planning Sciences*, vol. 47, no. 1, pp. 20-37, 2013.

- [31] D. Rivera-Royero, G. Galindo and R. Yie-Pinedo, "A dynamic model for disaster response considering prioritized demand points," *Socio-economic planning sciences*, vol. 55, pp. 59-75, 2016.
- [32] D. Rivera-Royero, G. Galindo and R. Yie-Pinedo, "Planning the delivery of relief supplies upon the occurrence of a natural disaster while considering the assembly process of the relief kits," *Socio-Economic Planning Sciences*, vol. 69, p. 100682, 2020.
- [33] T. Cova, P. Dennison and F. Drews, "Modeling evacuate versus shelter-in-place decisions in wildfires.," *Sustainability*, vol. 3, no. 10, pp. 1662-1687, 2011.
- [34] S. Grajdura, X. Qian and D. Niemeier, "Awareness, departure, and preparation time in no-notice wildfire evacuations," *Safety science*, vol. 139, p. 105258, 2021.
- [35] H. Irsyad and N. Hitoshi, "Flood disaster evacuation route choice in Indonesian urban riverbank kampong: Exploring the role of individual characteristics, path risk elements, and path network configuration," *International Journal of Disaster Risk Reduction*, vol. 81, p. 103275, 2022.
- [36] V. Bayram, "Optimization models for large scale network evacuation planning and management: A literature review," *Surveys in Operations Research and Management Science*, vol. 21, no. 2, pp. 63-84, 2016.
- [37] P. Murray-Tuite and B. Wolshon, "Evacuation transportation modeling: An overview of research, development, and practice," *Transportation Research Part C: Emerging Technologies*, vol. 27, pp. 25-45, 2013.
- [38] B. Zhao and S. Wong, "Developing transportation response strategies for wildfire evacuations via an empirically supported traffic simulation of Berkeley, California.," *Transportation research record*, vol. 2675, no. 12, pp. 557-582, 2021.
- [39] C. Xie, D. Lin and S. Waller, "A dynamic evacuation network optimization problem with lane reversal and crossing elimination strategies," *Transportation research part E: logistics and transportation review*, vol. 46, no. 3, pp. 295-316, 2010.
- [40] N. Nassir, M. Hickman, H. Zheng and Y. Chiu, "Network flow solution method for optimal evacuation traffic routing and signal control with nonuniform threat," *Transportation Research Record*, vol. 2459, no. 1, pp. 54-62, 2014.
- [41] S. Shahparvari, P. Chhetri, A. Abareshi and B. Abbasi, "Multi-objective decision analytics for short-notice bushfire evacuation: an Australian case study," *Australasian Journal of Information Systems*, 2015.
- [42] B. Liang, C. van der Wal, K. Xie, Y. Chen, F. Brazier, M. Dulebenets and Z. Liu, "Mapping the knowledge domain of soft computing applications for emergency evacuation studies: A scientometric analysis and critical review.," *Safety science*, vol. 158, no. 105955, 2023.
- [43] S. Khan, I. Shafi, W. Butt, I. Diez, M. Flores, J. Galán and I. Ashraf, "A systematic review of disaster management systems: approaches, challenges, and future directions.," *Land*, vol. 12, no. 8, p. 1514, 2023.
- [44] A. Albahri, Y. Khaleel, M. Habeeb, R. Ismael, Q. Hameed, M. Deveci and L. Alzubaidi, "A systematic review of trustworthy artificial intelligence applications in natural disasters," *Computers and Electrical Engineering*, vol. 118, p. 109409, 2024.

- [45] R. Damaševičius, N. Bacanin and S. Misra, "From sensors to safety: Internet of Emergency Services (IoES) for emergency response and disaster management," *Journal of Sensor and Actuator Networks*, vol. 12, no. 3, p. 41, 2023.
- [46] Q. Lu, B. George and S. Shekhar, "Capacity constrained routing algorithms for evacuation planning: A summary of results," in *International symposium on spatial and temporal databases*, Berlin, Heidelberg, 2005.
- [47] M. Osman and B. Ram, "Evacuation route scheduling using discrete time-based capacity-constrained model," in *IEEE International Conference on Industrial Engineering and Engineering Management*, 2011.
- [48] M. Rungta, G. Lim and M. Baharnemati, "Optimal egress time calculation and path generation for large evacuation networks," *Annals of Operations Research*, vol. 201, no. 1, pp. 403-421, 2012.
- [49] H. Zheng, Y. Chiu, P. Mirchandani and M. Hickman, "Modeling of evacuation and background traffic for optimal zone-based vehicle evacuation strategy," *Transportation Research Record*, vol. 2196, no. 1, pp. 65-74, 2010.
- [50] M. Siam, H. Wang, M. Lindell, C. Chen, E. Vlahogianni and K. Axhausen, "An interdisciplinary agent-based multimodal wildfire evacuation model: Critical decisions and life safety," *Transportation research part D: transport and environment*, vol. 103, p. 103147, 2022.
- [51] G. Lim, S. Zangeneh, M. Baharnemati and T. Assavapokee, "A capacitated network flow optimization approach for short notice evacuation planning," *European Journal of Operational Research*, vol. 223, no. 1, pp. 234-245, 2012.
- [52] Y. Sheffi, H. Mahmassani and W. Powell, "A transportation network evacuation model," *Transportation research part A: general*, 16(3), 209-218., 1982.
- [53] S. Tweedie, J. Rowland, S. Walsh, R. Rhoten and P. Hagle, "A methodology for estimating emergency evacuation times," *The Social Science Journal*, vol. 23, no. 2, pp. 189-204, 1986.
- [54] E. Stern and Z. Sinuany-Stern, "A behavioural-based simulation model for urban evacuation," in *Papers of the regional science association*, 1989.
- [55] H. Sherali, T. Carter and A. Hobeika, "A location-allocation model and algorithm for evacuation planning under hurricane/flood conditions," *Transportation Research Part B: Methodological*, Vols. , 25(6), , pp. 439-452, 1991.
- [56] R. Church and T. Cova, "Mapping evacuation risk on transportation networks using a spatial optimization model," *Transportation Research Part C: Emerging Technologies*, vol. 8, no. 1-6, pp. 321-336, 2000.
- [57] T. Cova and J. Johnson, "Microsimulation of neighborhood evacuations in the urban-wildland interface," *Environment and Planning A*, vol. 34, no. 12, pp. 2211-2229, 2002.
- [58] S. Kongsomsaksakul, C. Yang and A. Chen, "Shelter location-allocation model for flood evacuation planning," *Journal of the eastern Asia society for transportation studies*, vol. 6, pp. 4237-4252, 2005.

- [59] H. Sbayti and H. Mahmassani, "Optimal scheduling of evacuation operations," *Transportation Research Record*, vol. 1964, no. 1, pp. 238-246, 2006.
- [60] L. Han, F. Yuan, S. Chin and H. Hwang, "Global optimization of emergency evacuation assignments," *Interfaces*, vol. 36, no. 6, pp. 502-513, 2006.
- [61] B. Wolshon and E. Marchive III, "Emergency planning in the urban-wildland interface: Subdivision-level analysis of wildfire evacuations," *Journal of Urban Planning and Development*, vol. 133, no. 1, pp. 73-81, 2007.
- [62] Y. Chiu, H. Zheng, J. Villalobos and B. Gautam, "Modeling no-notice mass evacuation using a dynamic traffic flow optimization model," *Transactions*, vol. 39, no. 1, pp. 83-94, 2007.
- [63] Y. Chiu and H. Zheng, "Real-time mobilization decisions for multi-priority emergency response resources and evacuation groups: model formulation and solution," *Transportation Research Part E: Logistics and Transportation Review*, vol. 43, no. 6, pp. 710-736, 2007.
- [64] E. Miller-Hooks and G. Sorrel, "Maximal dynamic expected flows problem for emergency evacuation planning," *Transportation research record*, vol. 2089, no. 1, pp. 26-34, 2008.
- [65] M. Lindell, "EMBLEM2: An empirically based large scale evacuation time estimate model," *Transportation research part A: policy and practice*, vol. 42, no. 1, pp. 140-154, 2008.
- [66] S. Opananon and E. Miller-Hooks, "The safest escape problem," *Journal of the Operational Research Society*, vol. 60, no. 12, pp. 1749-1758, 2009.
- [67] A. Stepanov and J. Smith, "Multi-objective evacuation routing in transportation networks," *European Journal of Operational Research*, vol. 198, no. 2, pp. 435-446, 2009.
- [68] H. Noh, Y. Chiu, H. Zheng, M. Hickman and P. Mirchandani, "Approach to modeling demand and supply for a short-notice evacuation," *Transportation Research Record*, vol. 2091, no. 1, pp. 91-99, 2009.
- [69] L. Alçada-Almeida, L. Tralhão, L. Santos and J. Coutinho-Rodrigues, "A multiobjective approach to locate emergency shelters and identify evacuation routes in urban areas," *Geographical analysis*, vol. 41, no. 1, pp. 9-29, 2009.
- [70] H. Abdelgawad, B. Abdulhai and M. Wahba, "Multiobjective optimization for multimodal evacuation," *Transportation Research Record*, vol. 2196, no. 1, pp. 21-33, 2010.
- [71] A. Yazici and K. Ozbay, "Evacuation network modeling via dynamic traffic assignment with probabilistic demand and capacity constraints," *Transportation Research Record*, vol. 2196, no. 1, pp. 11-20, 2010.
- [72] M. Ng, J. Park and S. Waller, "A hybrid bilevel model for the optimal shelter assignment in emergency evacuations," *Computer-Aided Civil and Infrastructure Engineering*, vol. 25, no. 8, pp. 547-556, 2010.
- [73] M. Ng and S. Waller, "Reliable evacuation planning via demand inflation and supply deflation," *Transportation Research Part E: Logistics and Transportation Review*, vol. 46, no. 6, pp. 1086-1094, 2010.

- [74] G. Lämmel, D. Grether and K. Nagel, "The representation and implementation of time-dependent inundation in large-scale microscopic evacuation simulations," *Transportation Research Part C: Emerging Technologies*, vol. 18, no. 1, pp. 84-98, 2010.
- [75] K. Ozbay, M. Yazici, S. Iyer, J. Li, E. Ozguven and J. Carnegie, "Use of regional transportation planning tool for modeling emergency evacuation: Case study of northern New Jersey," *Transportation research record*, vol. 2312, no. 1, pp. 89-97, 2012.
- [76] A. Li, L. Nozick, N. Xu and R. Davidson, "Shelter location and transportation planning under hurricane conditions," *Transportation Research Part E: Logistics and Transportation Review*, vol. 48, no. 4, pp. 715-729, 2012.
- [77] J. Coutinho-Rodrigues, L. Tralhão and L. Alçada-Almeida, "Solving a location-routing problem with a multiobjective approach: the design of urban evacuation plans," *Journal of Transport Geography*, vol. 22, pp. 206-218, 2012.
- [78] X. Chen and F. Zhan, "Agent-based modeling and simulation of urban evacuation: relative effectiveness of simultaneous and staged evacuation strategies," in *Agent-based modeling and simulation*, Palgrave Macmillan, London., 2014, pp. 78-96.
- [79] G. Lim, M. Rungta and M. Baharnemati, "Reliability analysis of evacuation routes under capacity uncertainty of road links," *lie Transactions*, vol. 47, no. 1, pp. 50-63, 2015.
- [80] H. Tuydes-Yaman and A. Ziliaskopoulos, "Modeling demand management strategies for evacuations," *Annals of Operations Research*, vol. 217, no. 1, pp. 491-512, 2014.
- [81] V. Bayram, B. Tansel and H. Yaman, "Compromising system and user interests in shelter location and evacuation planning," *Transportation research part B: methodological*, vol. 72, pp. 146-163, 2015.
- [82] S. Shahparvari, P. Chhetri, A. Abareshi and B. Abbasi, "Multi-objective decision analytics for short-notice bushfire evacuation: An Australian case study," *Australasian Journal of Information Systems*, vol. 19, 2015.
- [83] H. Gan, K. Richter, M. Shi and S. Winter, "Integration of simulation and optimization for evacuation planning," *Simulation Modelling Practice and Theory*, vol. 67, pp. 59-73, 2016.
- [84] A. Beloglazov, M. Almashor, E. Abebe, J. Richter and K. Steer, "Simulation of wildfire evacuation with dynamic factors and model composition," *Simulation Modelling Practice and Theory*, vol. 60, pp. 144-159, 2016.
- [85] K. Steer, E. Abebe, M. Almashor, A. Beloglazov and X. Zhong, "On the utility of shelters in wildfire evacuations," *Fire safety journal*, vol. 94, pp. 22-32, 2017.
- [86] K. Shahabi and J. Wilson, "Scalable evacuation routing in a dynamic environment," *Computers, Environment and Urban Systems*, vol. 67, pp. 29-40, 2018.
- [87] S. Shahparvari, B. Abbasi, P. Chhetri and A. Abareshi, "Fleet routing and scheduling in bushfire emergency evacuation: A regional case study of the Black Saturday bushfires in Australia," *Transportation Research Part D: Transport and Environment*, 2019.
- [88] S. Grajdura, S. Borjigin and D. Niemeier, "Fast-moving dire wildfire evacuation simulation," *Transportation research part D: transport and environment*, vol. 104., p. 103190, 2022.

- [89] B. Mcrae, K. Hall, K. Popper, Unnasch, B, A. Jones, J. Platt, M. Schindel and S. Buttrick, Conserving Nature's Stage: Mapping Omnidirectional Connectivity for Resilient Terrestrial Landscapes in the Pacific Northwest the Nature, <http://nature.org/resilienceNW>, 2016.
- [90] B. Mcrae, V. Shah and T. Mohapatra, Circuitscape 4 User Guide, (The Nature Conservancy) <https://circuitscape.org/>, 2013.
- [91] A. Keeley, D. Ackerly, D. Cameron, N. Heller, S. C. J. Thorne and A. Merenlender, "A M 2018 New concepts, models, assessments of climate-wise connectivity," Environ. Res. Lett. 13 073002.
- [92] C. C. Schloss, B. T. D. McRae and A. Jones, "No-regrets" pathways for navigating climate change: planning for connectivity with land use, topography, and climate., " Ecological Applications 32(1), vol. 32, no. 1, p. e02468, 2022.
- [93] C. Littlefield, C. Carroll, B. McRae, J. Michalak and J. Lawler, "Connecting today's climates to future climate analogs to facilitate movement of species under climate change," Conservation Biology, vol. 31, p. 1397–1408., 2017.
- [94] C. Littlefield, M. Krosby, J. Michalak and L. J. , "Connectivity for species on the move: supporting climate-driven range shifts," Frontiers in Ecology and the Environment, vol. 17, p. 270–278, 2019.
- [95] J. Thorne, H. Choe, R. Boynton and D. Lee, "Open space networks can guide urban renewal strategies in a megacity," Environmental Research Letters, vol. 15:094080. , no. <https://iopscience.iop.org/article/10.1088/1748-9326/ab9fad> , 2020.
- [96] California State Geoportal, "gis.data.ca.gov/search?collection=Dataset," 2 2022. [Online]. Available: <https://gis.data.ca.gov/search?collection=Dataset>.
- [97] FEMA, "National Risk Index Map," 2023. [Online]. Available: <https://hazards.fema.gov/nri/map>.
- [98] G. Boeing, "OSMnx: New Methods for Acquiring, Constructing, Analyzing, and Visualizing Complex Street Networks," Computers, Environment and Urban Systems, vol. 65, pp. 126-139, 2017.
- [99] OpenStreetMap contributors, "Planet dump retrieved from <https://planet.osm.org>," <https://www.openstreetmap.org> , 2023.
- [100] M. Bründl, H. Romang, N. Bischof and C. Rheinberger, "The risk concept and its application in natural hazard risk management in Switzerland," Natural Hazards and Earth System Sciences, vol. 9, no. 3, pp. 801-813, 2009.
- [101] Federal Emergency Management Agency , "National Risk Index (Technical Documentation) v 1.19," FEMA, 2023.
- [102] U.S. Census Bureau, "American Community Survey 3-year Public Use," U.S. Census Bureau, 2020.
- [103] CDC/ATSDR, "CDC/ATSDR SVI Data and Documentation Download," 2023. [Online]. Available: https://www.atsdr.cdc.gov/placeandhealth/svi/data_documentation_download.html.

- [104] A. Hagberg, D. Schult and P. Swart, "Exploring network structure, dynamics, and function using NetworkX," in in Proceedings of the 7th Python in Science Conference (SciPy2008), Gael Varoquaux, Travis Vaught, and Jarrod Millman (Eds), Pasadena, CA, USA, 2008.
- [105] S. Handy and D. Niemeier, "Measuring accessibility: an exploration of issues and alternatives," *Environment and planning A*, vol. 29, no. 7, pp. 1175-1194, 1997.
- [106] M. Zilske, A. Neumann and K. Nagel, "OpenStreetMap for traffic simulation," 2011.
- [107] D. Rivera-Royero and M. Jaller, "A Methodology for Assessing the Road Network Risk Performance Employing a Standardized Spatial Risk Analysis," 2024.
- [108] WPR, "worldpopulationreview," 2020. [Online]. Available: <https://worldpopulationreview.com/states/cities/california>.
- [109] Chapman university, "chapman.edu," [Online]. Available: <https://libguides.law.chapman.edu/calmunicipalcodes>.
- [110] G. McDonald, "Ridge regression," *Wiley Interdisciplinary Reviews: Computational Statistics*, vol. 1, no. 1, pp. 93-100, 2009.
- [111] J. Ranstam and J. Cook, "LASSO regression," *Journal of British Surgery*, vol. 105, no. 10, pp. 1348-1348, 2018.
- [112] T. Hastie, *Generalized additive models in Statistical models in S*, Routledge, 2017, pp. 249-307.
- [113] W. Garrison and D. Marble, "A prolegomenon to the forecasting of transportation development.," *NORTHWESTERN UNIV EVANSTON IL*, 1965.
- [114] J. Rodrigue, *The geography of transport systems*. Routledge., Routledge, 2020.
- [115] Mark Thomas, "EVACUATION TECHNICAL MEMORANDUM PARADISE TRANSPORTATION MASTER PLAN," *Headway Transportation, LLC, Paradise, California*, 2022.
- [116] T. Lam and H. Schuler, "Connectivity index for systemwide transit route and schedule performance," *Transportation Research Record*, p. 854, 1982.
- [117] D. Scott, D. Novak, L. Aultman-Hall and F. Guo, "Network robustness index: A new method for identifying critical links and evaluating the performance of transportation networks," *Journal of Transport Geography*, vol. 14, no. 3, pp. 215-227, 2006.
- [118] N. Aydin, H. Duzgun, F. Wenzel and H. Heinimann, "Integration of stress testing with graph theory to assess the resilience of urban road networks under seismic hazards," *Natural Hazards*, vol. 91, no. 1, pp. 37-68, 2018.
- [119] V. Latora and M. Marchiori, "Efficient behavior of small-world networks," *Physical review letters*, vol. 87, no. 19, p. 198701, 2001.
- [120] L. Mattsson and E. Jenelius, "Vulnerability and resilience of transport systems—A discussion of recent research," *Transportation research part A: policy and practice*, vol. 81, pp. 16-34, 2015.
- [121] M. Dehghani, G. Flintsch and S. McNeil, "Impact of road conditions and disruption uncertainties on network vulnerability," *Journal of Infrastructure Systems*, vol. 20, no. 3, p. 04014015, 2014.

- [122] M. Bell, "A game theory approach to measuring the performance reliability of transport networks," *Transportation Research Part B: Methodological*, vol. 34, no. 6, pp. 533-545, 2000.
- [123] S. Wang, L. Zheng and D. Yu, "The improved degree of urban road traffic network: A case study of xiamen, china," *Physica A: Statistical Mechanics and its Applications*, vol. 469, p. 256-264, 2017.
- [124] M. Snelder, H. Van Zuylen and L. Immers, "A framework for robustness analysis of road networks for short term variations in supply," *Transportation Research Part A: Policy and Practice*, vol. 46, no. 5, p. 828-842, 2012.
- [125] M. Akbarzadeh, S. Memarmontazerin, S. Derrible and S. Reihani, "The role of travel demand and network centrality on the connectivity and resilience of an urban street system," *Transportation*, p. 1-15, 2017.
- [126] A. Kermanshah and S. Derrible, "Robustness of road systems to extreme flooding: using elements of gis, travel demand, and network science," *Natural hazards*, vol. 86, no. 1, p. 151-164, 2017.
- [127] S. Chang and N. Nojima, "Measuring post-disaster transportation system performance: the 1995 kobe earthquake in comparative perspective," *Transportation Research Part A: Policy and Practice*, vol. 35, no. 6, p. 475-494, 2001.
- [128] M. Taylor, "Critical transport infrastructure in urban areas: Impacts of traffic incidents assessed using accessibility-based network vulnerability analysis," *Growth and Change*, , vol. 39, no. 4, p. 593-616. , 2008.
- [129] W. Hansen, "How accessibility shapes land use," *Journal of the American Institute of planners*, vol. 25, no. 2, pp. 73-76, 1959.
- [130] J. Sohn, "Evaluating the significance of highway network links under the flood damage: An accessibility approach," *Transportation research part A: policy and practice*, vol. 40, no. 6, p. 491-506, 2006.
- [131] A. Paez, D. Scott and C. Morency, "Measuring accessibility: positive and normative implementations of various accessibility indicators," *Journal of Transport Geography*, vol. 25, p. 141-153, 2012.
- [132] K. Berdica, "An introduction to road vulnerability: what has been done, is done and should be done," *Transport Policy*, vol. 9, no. 2, p. 117-127, 2002.
- [133] P. Luathep, A. Sumalee, H. Ho and F. Kurauchi, "Large-scale road network vulnerability analysis: a sensitivity analysis based approach," *Transportation*, vol. 38, no. 5, p. 799-817, 2011.
- [134] J. Sullivan, D. Novak, L. Aultman-Hall and D. Scott, " Identifying critical road segments and measuring system-wide robustness in transportation networks with isolating links: a link-based capacity-reduction approach," *Transportation Research Part A: Policy and Practice*, vol. 44, no. 5, p. 323-336, 2010.
- [135] E. de Oliveira, L. da Silva Portugal and W. Junior, "Indicators of reliability and vulnerability: Similarities and differences in ranking links of a complex road system," *Transportation Research Part A: Policy and Practice*, vol. 88, p. 195-208, 2016.

- [136] R. Vodak, M. Bil and J. Sedonik, "Network robustness and random processes," *Physica A: Statistical Mechanics and its Applications*, vol. 428, p. 368–382, 2015.
- [137] O. Cats, "The robustness value of public transport development plans," *Journal of Transport Geography*, vol. 51, p. 236–246, 2016.
- [138] H. Sakakibara, Y. Kajitani and N. Okada, "Road network robustness for avoiding functional isolation in disasters," *Journal of transportation Engineering*, vol. 130, no. 5, p. 560–567, 2004.
- [139] W. Ip and D. Wang, "Resilience evaluation approach of transportation networks.," in *International joint conference in Computational sciences and optimization*, 2009.
- [140] M. Sharov and A. Mikhailov, "Urban transport system reliability indicators," *Transportation Research Procedia*, vol. 20, p. 591–595, 2017.
- [141] J. Van Lint, H. Van Zuylen and H. Tu, "Travel time unreliability on freeways: Why measures based on variance tell only half the story," *Transportation Research Part A: Policy and Practice*, vol. 42, no. 1, p. 258–277, 2008.
- [142] A. Shariat-Mohaymany and M. Babaei, "An approximate reliability evaluation method for improving transportation network performance," *Transport*, vol. 25, no. 2, p. 193–202, 2010.
- [143] A. Chen, H. Yang, H. Lo and W. Tang, "A capacity related reliability for transportation networks," *Journal of advanced transportation*, vol. 33, no. 2, p. 183–200, 1999.
- [144] E. Jenelius, T. Petersen and L. Mattsson, "Importance and exposure in road network vulnerability analysis," *Transportation Research Part A: Policy and Practice*, vol. 40, no. 7, p. 537–560, 2006.
- [145] N. Khademi, B. Balaei, M. Shahri, M. Mirzaei, B. Sarrafi, M. Zahabiun and A. Mohaymany, "Transportation network vulnerability analysis for the case of a catastrophic earthquake," *International journal of disaster risk reduction*, vol. 12, p. 234–254, 2015.

Data Summary

Products of Research

The project used the following public datasets:

- Open Street Map. The team collected the road network arcs and nodes of the selected localities and will make the graph used for each public locality.
- National Risk Index (NRI): The team used the NRI obtained publicly from FEMA at the census tract level
- American Community Survey (ACS): The team used ACS data to estimate the Social Vulnerability Index at the census block level.

Data Format and Content

The team processed the raw data and created several datasets:

- Geo-located risk data. The team processes the methodology developed by the authors to obtain the risk at the node level of the road network. The data generated is made available in the Comma-delimited format. The data is useful for risk and spatial analyses.

Data Access and Sharing

The algorithms in Python and Excel and file reports are made available through Dryad.

Reuse and Redistribution

Data generated from this research have been transferred to a publicly accessible data archive, available at <https://doi.org/10.5061/dryad.w9ghx3g0j>. The resulting analysis incorporating these will be published as part of reports and peer-reviewed journal articles archived for public access.

Appendix A. Summary of RNP Metrics and Models

Table A.1. Overview of Mathematical formulation for the 11 RNPs (connectivity, redundancy, accessibility, reliability, resilience, robustness, flexibility, and vulnerability)

RNP	Name Measurement	Mathematical Formulation	Reference	Traffic Data?	Global(G)/Regional (R)/Local (L)
Connectivity	Cyclomatic Number	$\mu = e - v + g$ $v = \text{No. vertices}$ $e = \text{No. Edges}$ $g = \text{No. Subgraphs}$	[108, 19, 13, 109, 22]	N	G
	Maximum Network Circuits (No planar)	$\mu_{\max} = (1/2)v(v-1) - (v-1) = \text{No. vertices}$	[19, 13]	N	G
	Maximum Number Edges (No planar)	$e_{\max} = \frac{1}{2}v(v-1)$ $v = \text{No. vertices}$	[19, 13]	N	G
	Beta Index	$\beta = e/v$ $e = \text{No. edges}$ $v = \text{No. vertices}$	[19, 13, 109, 22, 14, 21]	N	G
	Alpha Index	$\alpha = \left(\frac{e - v + 1}{e_{\max} - (v - 1)} \right)$ $e_{\max} = \frac{1}{2}v(v-1)$ $e = \text{No. edges}$ $v = \text{No. vertices}$	[19, 13]	N	G
	Gamma Index	$\gamma = \left(\frac{e}{v(v-1)/2} \right) * 100$ $e = \text{No. edges}$ $v = \text{No. vertices}$	[19, 13]	N	G
	Maximum Number Edges Planar	$e_{\max} = 3(v-2)$ $v = \text{No. vertices}$	[13, 109, 22]	N	G
	Maximum Network Circuits (Planar)	$\mu_{\max} = 2v - 5$ $v = \text{No. vertices}$	[13, 109, 22, 21]	N	G
	Alpha Index (Planar)	$\alpha = \frac{\mu}{2v-5}$ $\mu = \text{cyclomatic number}$ $v = \text{No. vertices}$	[14, 13, 109, 22, 21]	N	G
	Gamma Index (Planar)	$\gamma = \frac{e}{3(v-2)}$ $v = \text{No. vertices}$ $e = \text{No. Edges}$	[108, 13, 109, 22, 21, 111, 112]	N	G
	Lambda	$\lambda = \frac{1}{v(v-1)} \sum_{i,j \in E_{i \neq j}} d_{ij}$ $d_{ij} = \text{SP distance between } i \text{ and } j$ $v = \text{No. vertices}$	[108, 19, 113, 114, 115]	N	G*
	Efficiency	$E = \frac{1}{v(v-1)} \sum_{i,j \in E_{i \neq j}} \frac{1}{d_{ij}}$ $E = \text{average efficiency intact road network}$ $d_{ij} = \text{SP distance between } i \text{ and } j$ $v = \text{No. vertices}$	[114, 115, 116]	N	G*
	Degree Node	$c_i = \sum_{j=1}^N c_{ij}, c_{ij} = \begin{cases} 1, & \text{if } i \text{ is adjacent to } j \\ 0, & \text{otherwise} \end{cases}$	[19]	N	L
	Average Degree	$\bar{d} = \frac{\sum_i \delta_i}{v}$ $v = \text{No. vertices}$	[22]	N	G
	Average Node Degree	$\langle k \rangle = \frac{2e}{v}$ $v = \text{No. vertices}$ $e = \text{No. edges}$	[21]	N	G

RNP	Name Measurement	Mathematical Formulation	Reference	Traffic Data?	Global(G)/ Regional (R)/Local (L)
	Matrix Of Network Accessibility	$T = c + c^2 + c^3 + \dots + c^n = \sum_{k=1}^n C^k$ $T_i = \sum_{i \neq j} T_{ij}$	[19]	N	G*
	Number Of Paths	$P_{ij} = \text{complete enumeration}$ $P_i = \sum_{i \neq j} P_{ij}$	[19]	N	L
	Eta (Average Edge Length)	$\eta = \frac{R}{e}$ $R = \text{total route length}$ $e = \text{number of edges}$	[13, 109]	N	G
	Pi	$\pi = \frac{R}{d}$ $R = \text{total route length}$ $d = \text{network diameter}$	[13, 109]	N	G*
	Theta (Average Traffic)	$\theta = \frac{T}{v}$ $T = \text{Total traffic flow}$ $v = \text{number of vertices}$	[13, 109]	Y	G
	Iota	$l = \frac{R}{\omega}$ $R = \text{Total length}$ $\omega = \text{observed number of vertices eighted by their function.}$	[13]	N	G*
	Iota	$l = \frac{R}{T}$ $R = \text{Total length}$ $T = \text{total traffic flow}$	[13]	Y	G
	Lower Bound Network Connectivity	$LC = \frac{n}{m(n-m)} \sum_{e \in \partial(S)} W_e$ $n = V , m = S , W_e \in w$ $\partial(S) \equiv \{(u, v) \in E : u \in S, v \in V - S\}, \text{ boundary of } S$ $V = \text{set of nodes}, S = \text{subnetwork}, e = \text{edge}$	[117]	N	G*
	Degree of K of a Node	$k = k^{in} + k^{out}$ $\langle k \rangle = \sum_{i=1}^N \frac{k_i}{N}$ $P(k) = \frac{n_k}{N},$ $n_k = \text{number of nodes with degree } k$	[118]	N	G
	Normalized Reciprocal Harmonic Mean	$R_t = \frac{\bar{T}}{\bar{t}} = \frac{\frac{1}{\left(\frac{1}{n}\right) * \sum_{i=1}^n \left(\frac{1}{T_i}\right)}}{\frac{1}{\left(\frac{1}{n}\right) * \sum_{i=1}^n \left(\frac{1}{t_i}\right)}}$	[111, 13]	Y	Dynamic
Redundancy	*Clustering	$C_i = \frac{e_i}{e_i^{\max}} = \frac{2e_i}{k_i(k_i - 1)}$ $C = \frac{1}{v} \sum_i C_i$ $e_i = \text{No. Edges in cluster } i$ $k_i = \text{No. vertices sharing edge } i$ $v = \text{Total No vertices}$	[13]	N	R
	Alternative Routes	$Altroutes_a = \frac{cap_a}{\sum_{aa \in A_a} (cap_{aa} * \zeta_1^{dist_{a,aa}})}$ $= \frac{cap_a}{\sum_{aa \in A_a} (cap_{aa} * e^{\zeta_2 dist_{a,aa}})}$ $\zeta_2 = \ln(\zeta_1)$ $a = \text{link where disturbance occurs}$ $aa = \text{link from the collection } A_a \text{ alternative to link } a$ $cap = \text{link capacity}$ $\zeta_1 \text{ and } \zeta_2 \text{ importance of the distance from alternative routes}$ $dista, aa = \text{shortest distance between } a \text{ and } aa$	[119]	N	L(arcs)

RNP	Name Measurement	Mathematical Formulation	Reference	Traffic Data?	Global(G)/ Regional (R)/Local (L)
	Alternative Routes 2a	$Altroutes2_a = \frac{v_a}{\sum_{aa \in A_a} (rc_{aa} * e^{\zeta_2 * dist_{a,aa}})}$ $= \frac{cap_a}{\sum_{aa \in A_a} (cap_{aa} * e^{\zeta_2 * dist_{a,aa}})}$ $\zeta_2 = \ln(\zeta_1)$ $v_a = \text{flow}$ <p>ζ_1 and ζ_2 importance of the distance from alternative routes $dist_{a,aa}$ = shortest distance between a and aa rc_{aa} = spare capacity on link aa</p>	[119]	N	L (arcs)
Accessibility	Diameter	$D = \max(SP_{i,j})$ $SP = \text{Shortest path between } i \text{ and } j$	[109, 22, 21]	N	G*
	Shimbel Index	$D(V) = \sum_{i=1}^n \sum_{j=1}^n d_{ij}$ $d_{ij} = \text{shortest path between } i, j$	[19]	N	G*
	Average Shimbel Index	$A_i = \frac{\sum_{j=1}^n d_{ij}}{v-1}$ $d_{ij} = \text{shortest path between } i, j$	[22]	N	L
	Betweenness	$CB_k = \sum_i \sum_j \frac{m_{ijk}}{\sum_k m_{ijk}} \quad i \neq j \neq k$ $m_{ijk} = \text{number of shortest path linking } i \text{ and } j \text{ involving node } k$	[19, 22, 113, 21, 120, 121]	N	L
	Normalized Betweenness	$BC(i) = \frac{1}{(v-2)(v-1)} \sum_{s \neq i \neq j} \frac{\sigma_{st}(i)}{\sigma_{st}}$ $\sigma_{st} = \text{shortest paths from } s \text{ to } j$ $\sigma_{st}(i) = \text{shortest paths from } s \text{ to } j \text{ that pass through } i$ $v = \text{No. vertices}$	[21]	N	L
	Normalized Closeness Centrality	$CC(i) = \frac{v-1}{l_{ij}}$ $l_{ij} = \text{shortest path length between } i \text{ and } j$	[21]	N	L
	Detour Index (circuitry)	$DI = \frac{D(S)}{D(T)}$ $D(S) = \text{straight distance}$ $D(T) = \text{real distance}$	[109]	N	G
	Efficiency	$E_{rel} = \frac{DI - DI^{MST}}{DI^{GT} - DI^{MST}}$ $MST = \text{minimum spanning tree}$ $GT = \text{greedy triangulation}$ $Cost = \sum_{ij} a_{ij} l_{ij}$	[109]	N	G*
	Network Density	$NS = \frac{R}{S}$ $R = \text{total route length}$ $S = \text{Surface area}$	[109]	N	G
	Length Of Network Open	$L(t) = \frac{x(t)}{\bar{x}}$ $\bar{x} = \text{pre-earthquake open}$ $x(t) = \text{open at time } t$	[122]	N	G (dynamic)
	Total Distance-Base Accessibility	$D(t) = \frac{f - A(t)}{f - 1}$ $A(t) = \frac{\sum_i \sum_j d_{ij}(t)}{\sum_i \sum_j \bar{d}_{ij}}, \quad 1 \leq A \leq f$ $f = \text{effective distance multiplier for link closure}$ $A = \text{total network accessibility ratio}$ $d_{ij} \text{ and } \bar{d}_{ij} = \text{minimum travel distance between } i \text{ and } j \text{ on damaged network and intact network}$	[122]	N	G (dynamic)

RNP	Name Measurement	Mathematical Formulation	Reference	Traffic Data?	Global(G)/ Regional (R)/Local (L)
	Areal Distance-Base Accessibility	$D_s(t) = \frac{f - A_s(t)}{f - 1}$, accessibility performance for area s $A_s(t) = \frac{1}{n_s} \sum_{i \in N_s} A_i(t)$, transport accessibility ratio area s. $A_i(t) = \frac{\sum_{j \neq i} w_{ij} d_{ij}(t)}{\sum_{j \neq i} w_{ij} \bar{d}_{ij}}, w_{ij} = \frac{1}{n_r - \delta_r} \cdot \frac{v_{sr}}{\sum_p v_{sp}} \quad i \in N_s, j \in N_r$ n_s =number of nodes on area s, N_s = set of nodes on area s, w_{ij} = destination weight for node j for commuter originated from i, v_{sr} =commuter traffic flow subarea s to subarea r	[122]	Y	G (Dynamic)
	ARIA (Access/Remoteness Index of Australia)	$v_{rs} = \sum_i \sum_j d_{ij} v_{ijrs}$ v_{ijrs} = change in generalized cost of travel from i to j if network link e_{rs} fails. e_{rs} link connecting r and s) d_{ij} =demand movement from i to j.	[20]	Y	G
	Aria L	$ARIA_{iL} = \sum_L \min \left\{ 3, \frac{x_{iL}}{\bar{x}_L} \right\}$ L= category A, B, C, D, E. \bar{x}_L = mean road distance to the nearest category L service	[20]	N	G*
	Hansen Integral Accessibility Index	$A_i = \sum_j B_j f(c_{ij}) \sim \frac{\sum_j B_j f(c_{ij})}{\sum_j B_j}$ B_j = attractiveness of location j (pop) $f(c_{ij}) = \frac{1}{x_{ij}}$, impedance function x_{ij} = cost for travel between i to j	[123, 20, 124]	N	L
	Accessibility Score	$A_i = 4 \left[\alpha \frac{P_i}{\sum_{k=1}^{24} P_k} \sum_{j=1}^{23} \left(\frac{P_j}{\sum_{k=1}^{24} P_k} \frac{d_{ij}^{-\beta}}{\sum_{k=1}^{24} d_{ik}^{-\beta}} \right) + (1 - \alpha) \frac{P_i}{\sum_{k=1}^{24} P_k} \sum_{j=1}^{23} \left(\frac{P_j}{\sum_{k=1}^{24} P_k} \frac{t_{ij}}{\sum_{k=1}^{24} t_{ik}} \right) \right] \quad (i \neq j)$ A_i = accessibility county i, α =weighting factor (0-1), $P_i(j)$ = Population in County i(j) d_{ij} = shortest road distance between i and j under a scenario d_{ij}^* = initial shortest road distance between i and j $t_{ij} = \sum_{m=1}^n \frac{AADT_m d_m}{d_{ij}}$, average traffic between i and j on the sp $AADT_m$ = annual average daily traffic on link m d_m = distance on link segment m	[125]	Y	L
	Origin Standpoint	$A_{ik}^p = \sum_j g(W_{jk}) f(c_{ij}^p) = \sum_{j \in R_i^p} g(W_{jk})$ i= location, k=opportunity, p=individual, R_i^p =region defined for individual p based at location i	[126]	N	L
	Destination Standpoint	$M_{kj}^p = \sum_i g(P_{ik}^p) f(c_{ij}^p)$ j= location, k=opportunity, p=individual, P=size p of population segment p at i. c_{ij}^p = cost of traveling between i and j as perceived by members of population segment p	[126]	N	L
	Accessibility	$A = \text{mean}(\text{Travel time})$ A=Percentage of objectives reachable within a specified time	[127]	Y	G

RNP	Name Measurement	Mathematical Formulation	Reference	Traffic Data?	Global(G)/Regional (R)/Local (L)
	Accessibility Index	$AI^w = \frac{1}{\text{Average path travel cost}^w}$ $= \frac{1}{\sum_{k \in H^w} f_k^w c_k^w}, \forall w \in W$ $AI = \frac{\sum_{w \in W} q^w \cdot AI^w}{\sum_{w \in W} q^w}, \forall w \in W$ <p>q^w = travel demand of OD movement w c^w = travel cost of paths connecting OD movement w</p>	[128]	Y	G
Robustness	Normalized Giant Connected Component	$\text{Normalized GCC} = \frac{N_{GCC,after}}{N_{GCC,before}}$ <p>GCC=Giant connected component</p>	[113]	N	G*
	Network Robustness Index	$NRI_a = q_a = c_a - c$ $c_a = \sum_i t_i x_i \delta_i$ $\delta_i = \begin{cases} 1 & \text{if link } i \text{ is not removed} \\ 0 & \text{otherwise} \end{cases}$ $c = \sum_a t_a x_a, t_a = t_a(x_a)$ <p>= travel time (flow)</p>	[112, 129]	Y	G
	Modified NRI	$NRI_{a(mod)} = q_a = c_a - c$ $c_a = \sum_i t_i x_i \delta_i$ <p>p_i =percentage of capacity reduction on link i {99, 95, 90, 85, 80, 75, 70, 65, 60, 55, 50, 45, 40, 35, 30}.</p> $c = \sum_a t_a x_a, t_a = t_a(x_a)$ <p>= travel time (flow)</p>	[129, 130]	Y	G
	Network Trip Robustness	$NTR_n = \frac{\sum_{a \in I} NRI_a}{D_n}$ <p>D_n =Total demand between all origins and all destinations in network n.</p>	[129]	Y	G
	R1	$R_1(n) = \frac{anl(n)}{m}, R_1(n) \in (0, +\infty)$ <p>n= number of components to decompose the network m= number of nodes in the network $anl(n)$ = average number of nodes to remove from the network to disintegrate it in n parts.</p>	[131]	N	G*
	R2	$R_2(n) = \frac{1}{k} \sum_{i=1}^k \frac{comp(G_i) - 1}{link(G_i)}, R_2 \in (0, 1),$ $k = \sum_j \binom{l}{j}$ <p>K = number of combinations of links that can be removed from the network $comp(G_i)$ = number of components after removal of the i^{th} link, $link(G_i)$ = number of links in the i^{th} combination of links removed from network. G_i = Network after removal of i^{th} combination of links</p>	[131]	N	G*
	Robustness Network Design Alternative	$r_n^{\max} = \max_{e \in E} (\Delta y(n e))$ $r_n = E[\Delta y(n e)] = \sum_{e \in E} [p_e \Delta y(n e)]$ <p>$\Delta y(e n) = y(n, e) - y(n_0, e)$ $y(n, e)$=disturbance occurs on link e $y(n_0, e)$=disturbance occurs on link e on base case network p_e = probability link e fail</p>	[132]	N	G*
	Topological Index	$TI(G) = \sum_{k=0}^m \llbracket P(G, k) \rrbracket, m = \begin{cases} \frac{n}{2}, & \text{if even} \\ \frac{n-1}{2}, & \text{if odd} \end{cases}$	[133]	N	G*

RNP	Name Measurement	Mathematical Formulation	Reference	Traffic Data?	Global(G)/ Regional (R)/Local (L)
Resilience	*Node Resilience	$r_i = \sum_{j=1, j \neq i}^n v_j \sum_{\forall k \text{ link}(i,j)} \sum_{l \in L_k(i,j)} q_l$ $v_j = \frac{u_i}{(\sum_j^n [u_j - u_i])}$ $v_j = \text{self-exhausted weight}$ $u_j = \text{population on node } i$	[134]	N	L
	Resilience	$R(G) = \sum_{i=1}^n w_i \sum_{j=1, j \neq i}^n v_j \sum_{\forall k \text{ link}(i,j)} \sum_{l \in L_k(i,j)} q_l$ $w_i = \frac{u_i}{\sum_j^n u_j}$ $w_j = \text{weight}$ $u_j = \text{population on node } i$	[134]	N	G*
	Adaptive Capacity	$A = \frac{\sum_i^n m_i(k)}{m_i}$ $m_i = C-F \text{ (Capacity- Flow)}$ $m_i = \text{margin of node } i$ $m_i(k) = \text{margin of node } i \text{ after node } k \text{ is removed.}$	[20]	Y	G
	Resilience Metric	$Res_{s1,eff} = \frac{\int_{p_0}^{p_{0.95}} \lambda_{\text{hypothetical}} - \int_{p_0}^{p_{0.95}} \lambda_{\text{network}}}{\int_{p_0}^{p_{0.95}} \lambda_{\text{hypothetical}}} * 100$ $Res_{s1,GCC} = \frac{\int_{p_0}^{p_{0.95}} N_{GCC, \text{hypothetical}} - \int_{p_0}^{p_{0.95}} N_{GCC, \text{network}}}{\int_{p_0}^{p_{0.95}} N_{GCC, \text{hypothetical}}} * 100$ $Diff_x = BC_{x, \text{before}} - \frac{1}{s} BC_{x, \text{after}}$	[113]	Y	G
	Travel Time Resilience	$T_{r,b} = \frac{tt^{r-1}}{tt^{o-1}} = \frac{< x^0, t^0 >}{< x^r, t^r >}$ $tt^{r-1} = \text{reciprocal ttt achieved in reaching a PUE at the end of the response stage}$ $tt^{o-1} = \text{reciprocal ttt achieved in reaching a UE in pre-event}$	[16]	Y	G
Reliability	Travel Time Index	$TTI = \frac{T_{PP}}{T_{FF}}$ $T_{PP} = \text{time passing peak period}$ $T_{FF} = \text{time passing free flow}$	[135]	Y	G
	Herman-Prigogine	$T = T_r + T_s$ $T = \text{trip time per unit distance}$ $T_r = \text{running time "per unit distance"}$ $T_s = \text{stop time per unit distance.}$	[135]	Y	G
	Buffer Time	$T_b = T_{90\%(95\%)} + \bar{T}$ $T_{90\%(95\%)} = 90 \text{ or } 95 \text{ percentile of trip duration}$ $\bar{T} = \text{average trip duration}$ $I_b = \frac{T_b}{\bar{T}} * 100\%$	[135]	Y	G
	Coefficient Of Variation	$CV = \frac{\sigma}{\bar{t}} = \beta \beta_{tod} \beta_{speed} L^\alpha t^{\gamma-1} \left(\frac{\bar{t}}{\bar{T}} - 1 \right)^\omega$ $\sigma = \text{standard deviation travel time, } \bar{t} = \text{mean travel time,}$ $T = \text{travel time under free flow, } L = \text{length link}$ $\beta_{tod}, \beta_{speed} = \text{dummy variable for the time of day and speed,}$ $\omega, \alpha, \gamma, \beta = \text{estimated parameters}$	[130, 136]	Y	G
	Statistical Range	$\sigma = \sqrt{\frac{1}{N-1} \sum_N (TT_i - \bar{t})^2}$	[136]	Y	G
	Buffer Time	$BI = \frac{TT_{90} - \bar{t}}{\bar{t}}$	[136]	Y	G
	Tardy Trip	$MI = \frac{MI_{TT_i > TT_{80}} - \bar{t}}{\bar{t}}$			
	Probabilistic	$P(\alpha) = P(TT_i \geq \alpha TT_{50})$ $\text{e.g., } \alpha = 1.2$			

RNP	Name Measurement	Mathematical Formulation	Reference	Traffic Data?	Global(G)/ Regional (R)/Local (L)
	Skewness	$G = \frac{N \sum_N (TT_i - \bar{T})^3}{3\sigma^3(N-1)(N-2)}$			
	Lambda Skew	$\lambda^{skew} = \frac{TT_{90} - TT_{50}}{TT_{50} - TT_{10}}$			
	Lambda Width	$\lambda^{var} = \frac{TT_{90} - TT_{10}}{TT_{50}}$			
	Unreliability	$UI_r = \begin{cases} \frac{\lambda^{var} \ln(\lambda^{skew})}{L_r}, & \text{if } \lambda^{skew} > 1 \\ \frac{\lambda^{var}}{L_r}, & \text{otherwise} \end{cases}$ $L_r = \text{length route}$			
	Arc Performance Reliability	$R_i = P(C_i \geq v_i) = \{ \blacksquare (a, v_i \geq c_{min} \wedge i @ 0, c_{max} \wedge i < v_i) \}$ $a = \int_{-(v_i) \wedge (C_{max} \wedge i)}^{\infty} f_i(x) p(x) dx$ $= \int_{-(v_i) \wedge (C_{max} \wedge i)}^{\infty} f_i(x) + (1 - \int_{-(c_{min} \wedge i) \wedge (C_{max} \wedge i)}^{\infty} f_i(c) dc) / (c_{max} \wedge i - c_{min} \wedge i) dx$ $v_i = \text{flow volume}, C_i = \text{random capacity}$ $R_i = P(C_i \geq v_i / \alpha_i)$ $= \{ \left(\frac{v_i}{\alpha_i} \int_{c_i}^{c_i^{(max)}} f_i^p(c) dc =, \frac{v_i}{\alpha_i} c \geq \min_i c, \max_i c < \frac{v_i}{\alpha_i} \right.$	[137]	Y	
	Capacity Reliability	$\begin{aligned} & \text{Max } \mu \\ & \text{s.t. } v_a(\mu q) \leq, \forall a \in A \\ & v_a(\mu q) \text{ user equilibrium flow on a link } a \\ & \text{with the demands of all OD pairs} \end{aligned}$	[138]	Y	G
Vulnerability	Objectives	$\text{Max}((\text{Min}(\text{trip cost}))$	[117]	Y	G
	Link Failure Vulnerability	$v_{rs} = \sum_i \sum_j d_{ij} v_{ijrs}$ $d_{ij} = \text{demand for movement } i \text{ to } j$ $v_{ijrs} = \text{change in generalised cost of travel from } i \text{ to } j \text{ if link } rs \text{ fails}$ $v_{ijrs} = s[ij, G(N, E)] - s[ij, G(N, E - e_{rs})]$ $s[] \text{ path from } i \text{ to } j$	[123]	Y	G
	Vulnerability Index	$v_{ijrs} = s[ij, G(N, W)] - s[ij, G(N, E - e_{rs})]$ $s[ij, G(N, E)] = \text{cost of the least cost from } i \text{ to } j$	[123]	N	L (arc)
	*Structural Vulnerability	$V_t = \frac{E - E_t}{E}, E = \frac{1}{v(v-1)} \sum_{i,j \in E, i \neq j} \frac{1}{d_{ij}}$ $E = \text{average efficiency intact road network}$ $E_t = \text{average efficiency intersection or section } t \text{ interrupted road network}$ $d_{ij} = \text{SP distance between } i \text{ and } j$ $v = \text{No. vertices}$	[114]	N	G (dynamic)
	Importance	$\text{importance}_{net}(k) = \frac{\sum_i \sum_{j \neq i} w_{ij} \Delta c_{ij}^{(k)}}{\sum_i \sum_{j \neq i} w_{ij}}, k \in E^{nc}$ $u_{ij}^{(e)} = \begin{cases} x_{ij} & \text{if } c_{ij}^{(e)} = \infty \\ 0 & \text{if } c_{ij}^{(e)} < \infty \end{cases}, \Delta c_{ij}^{(e)} = c_{ij}^{(e)} - c_{ij}^{(0)}$ $c_{ij}^{(e)} = \text{cost of travel } i \text{ to } j \text{ link } e \text{ failed}, c_{ij}^{(0)} = \text{cost of undamaged network}, x_{ij} = \text{travel demand } i \text{ to } j, E = E^C \cup E^{NC}, w_{ij} = \{\text{equal } \text{ xij}\}$	[139]	Y	G
	Exposure	$\text{exposure}_{rand}(m) = \frac{\sum_{k \in E^{nc}} \sum_{i \in V_m^d} \sum_{j \neq i} w_{ij} \Delta c_{ij}^{(k)}}{L^{nc} \sum_{i \in V_m^d} \sum_{j \neq i} w_{ij}}$ $L^{nc} = \text{number of noncut links}$			G

RNP	Name Measurement	Mathematical Formulation	Reference	Traffic Data?	Global(G)/ Regional (R)/Local (L)
		$V_m^d = \text{set of demand nodes located in municipality } m$ $exposure_{\max(m)} = \max_{k \in K^{nc}} \frac{\sum_{i \in V_m^d} \sum_{j \neq i} w_{ij} \Delta c_{ij}^{(k)}}{\sum_{i \in V_m^d} \sum_{j \neq i} w_{ij}}$			
	Expected User Exposure	$UE_r = \frac{\sum_k w_k \sum_{i \in r} \sum_{j \neq i} \Delta c_{ij}^{(k)}}{\sum_{i \in r} \sum_{j \neq i} x_{ij} \tau}$ $\tau = \text{time from the closure to fully functional}$ $\Delta c_{ij}^{(k)} = \text{total increase in travel time between } i \text{ and } j$ $x_{ij} = \text{average travel demand per unit of time}$ $r = \text{region}, l_k = \text{length link } k, w_k = \frac{l_k}{\sum_k l_k}$ $\text{Closure probability link } k.$	[14]	Y	G
	Total Exposure	$TE_r = \sum_k w_k \sum_{i \in r} \sum_{j \neq i} \Delta c_{ij}^{(k)}$ $\Delta c_{ij}^{(k)} = \text{total increase in travel time between } i \text{ and } j$ $r = \text{region}, l_k = \text{length link } k, w_k = \frac{l_k}{\sum_k l_k}$ $\text{Closure probability link } k.$	[14]	N	R
	*Regional Importance	$I_r = \sum_k v_k \sum_{i \in r} \sum_{j \neq i} \Delta c_{ij}^{(k)}$ $\Delta c_{ij}^{(k)} = \text{total increase in travel time between } i \text{ and } j$ $r = \text{region}, l_k = \text{length link } k, v_k = \frac{l_k}{\sum_{k \in r} l_k} \text{ Closure probability link}$ $k. \Delta c_{ij}^{(k)} = \begin{cases} \frac{x_{ij} \tau^2}{2} & \text{if } \Delta c_{ij}^k \geq \tau \\ x_{ij} \Delta c_{ij}^k \left(\tau - \frac{\Delta c_{ij}^k}{2} \right) & \text{if } \Delta c_{ij}^k < \tau \end{cases}$	[14]	N	R
	Vulnerability	$E[r(s)] = \sum_{a \in A} p(a) r(a)$ $V_r(s) = \frac{ E[r(s_0)] - r^0 }{r^0}$	[116]	Y	G
	Isolation Index	$I(s, t) = (r^{s, \gamma}(s, t))^{-1} \times e^{(\alpha \times \bar{d}(s, t))}$ $r^{s, \gamma}(s, t) = \text{redundancy index } s \text{ to } t$ $e^{(\alpha \times \bar{d}(s, t))} = \text{exp. function of avg. length of redundant paths}$	[140]	N	L (dynamic)
	Trip Type Isolation Index	$I_i = \sum_{t_i} \sum_{s_i} (r^{s_i, \gamma}(s_i, t_i))^{-1} \times e^{(\alpha \times \bar{d}(s_i, t_i))}$ $r^{s_i, \gamma}(r, t) = \text{redundancy index } s \text{ to } t$ $e^{(\alpha \times \bar{d}(s, t))} = \text{exp. function of avg. length of redundant paths}$	[133]	N	L (dynamic)

Appendix B. SSRI and NRI for Multiple Hazards

This appendix shows the cluster of each Natural Hazards analyzed by setting the cluster on 0.9 on SSRI and 0.5 on NRI. The captions of the figures identify the natural hazard into consideration.

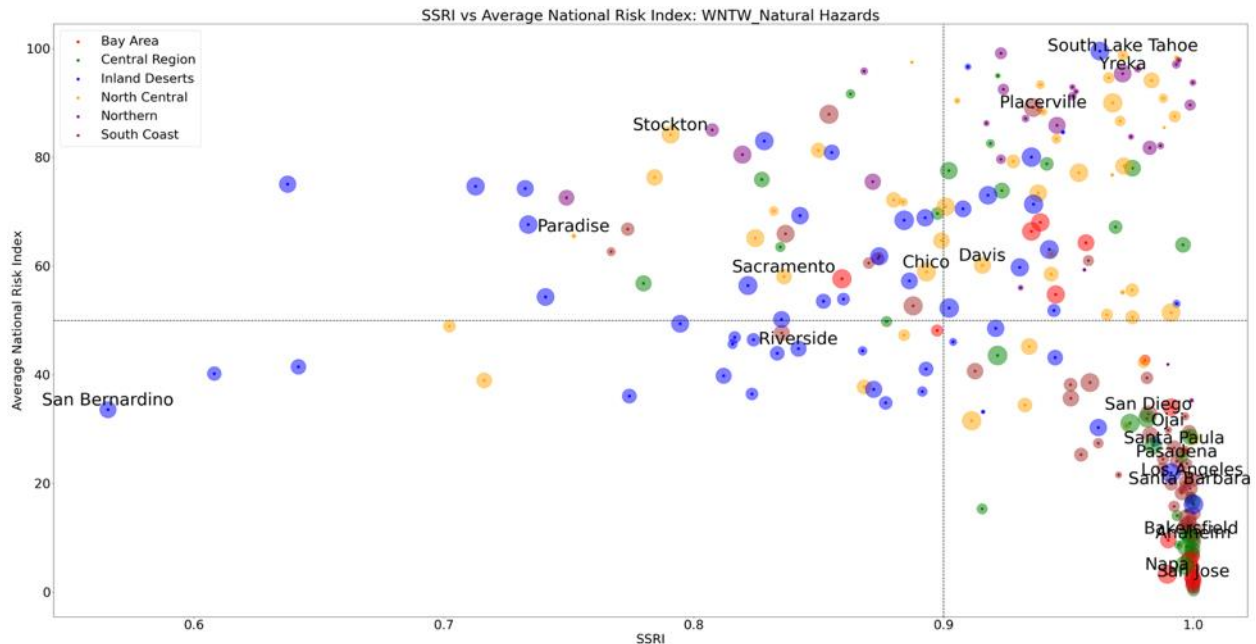


Figure B.1. Winter Weather (WNTW)

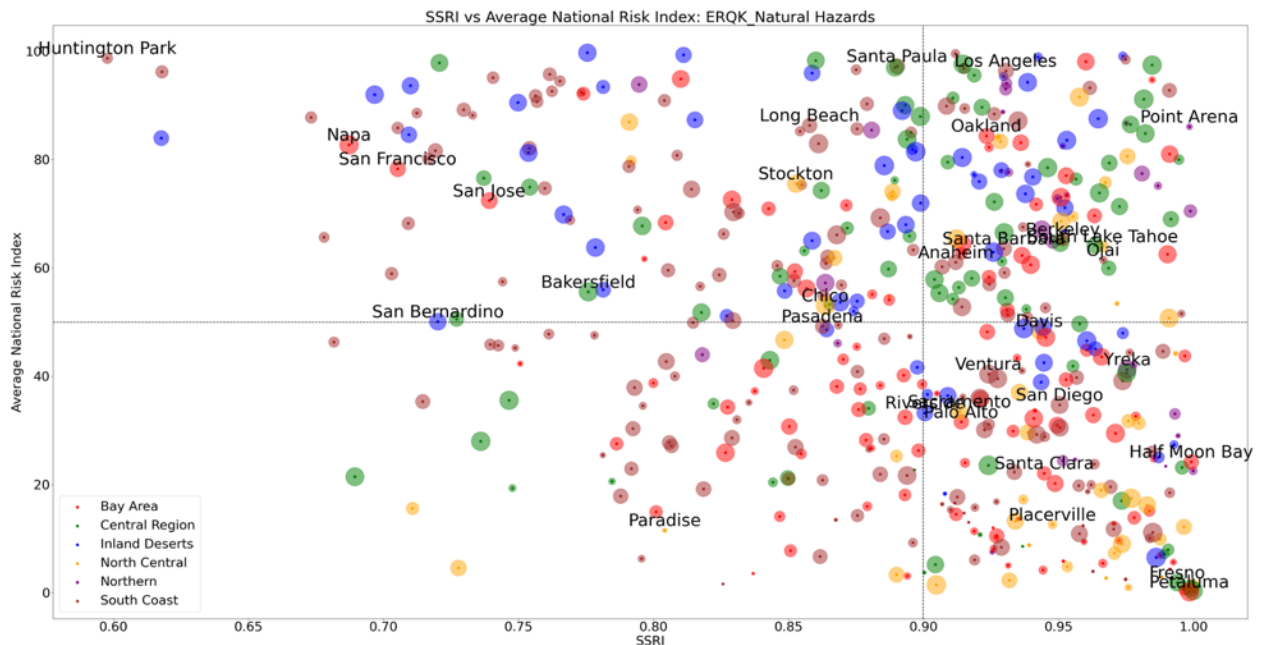


Figure B.2. Earthquake (ERQK)

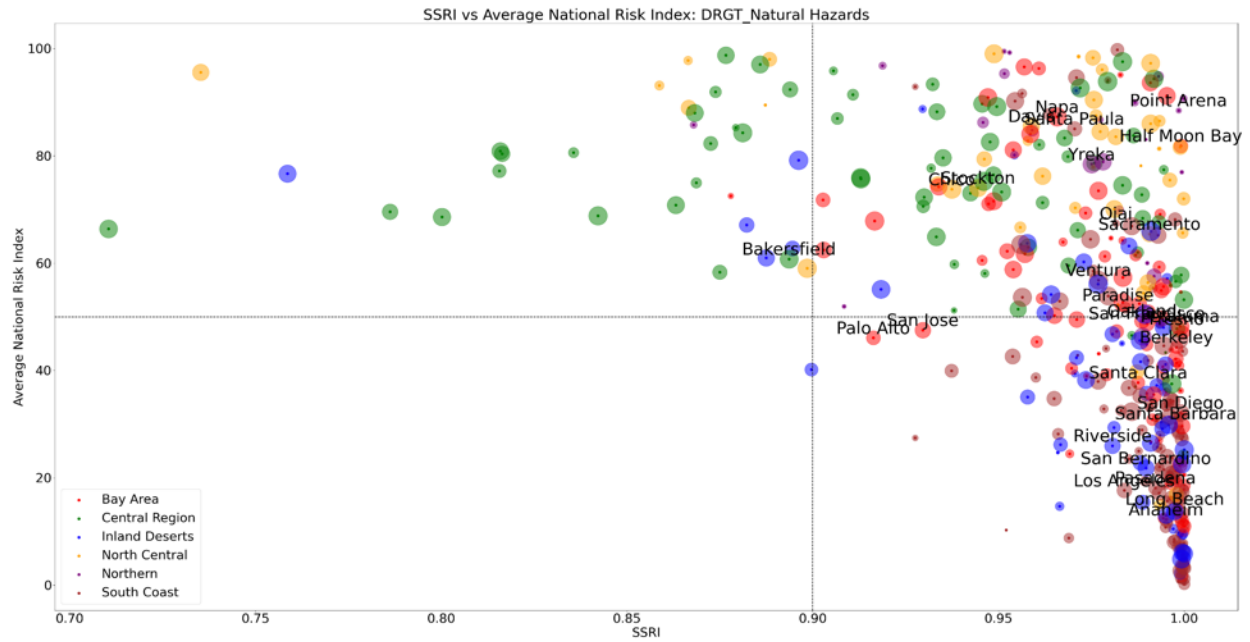


Figure B.3. Drought (DRGT)

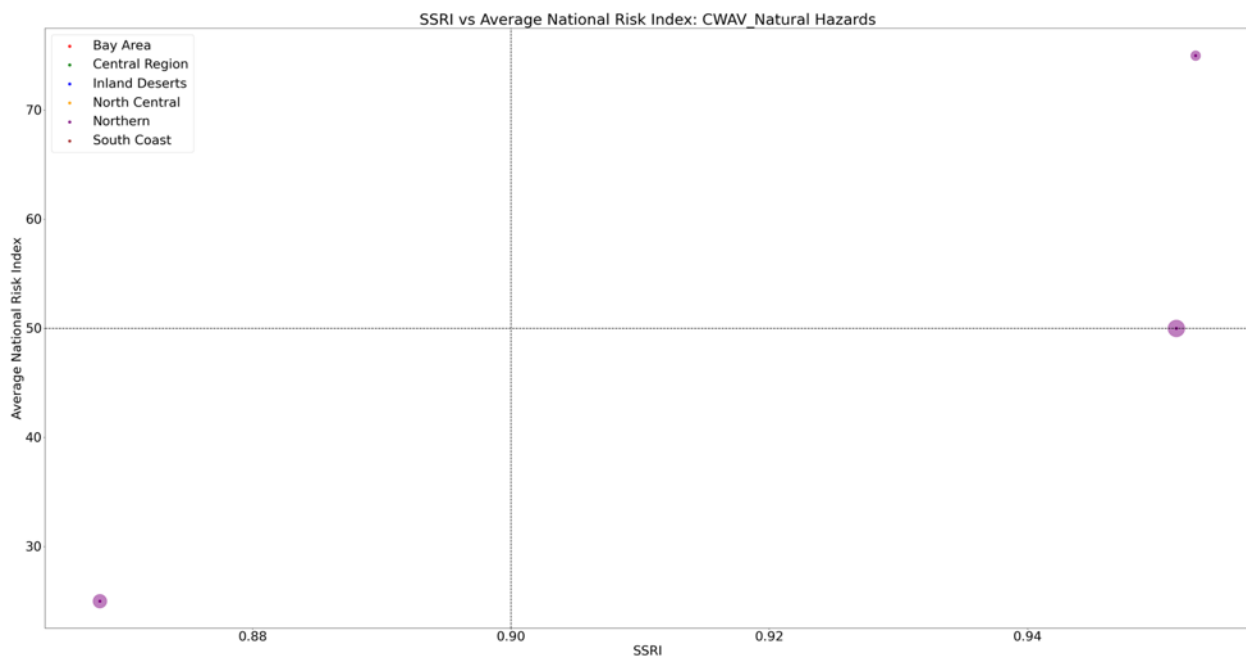


Figure B.4. Cold Wave (CWAV)



Figure B.5. Coastal Flooding (CFLD)

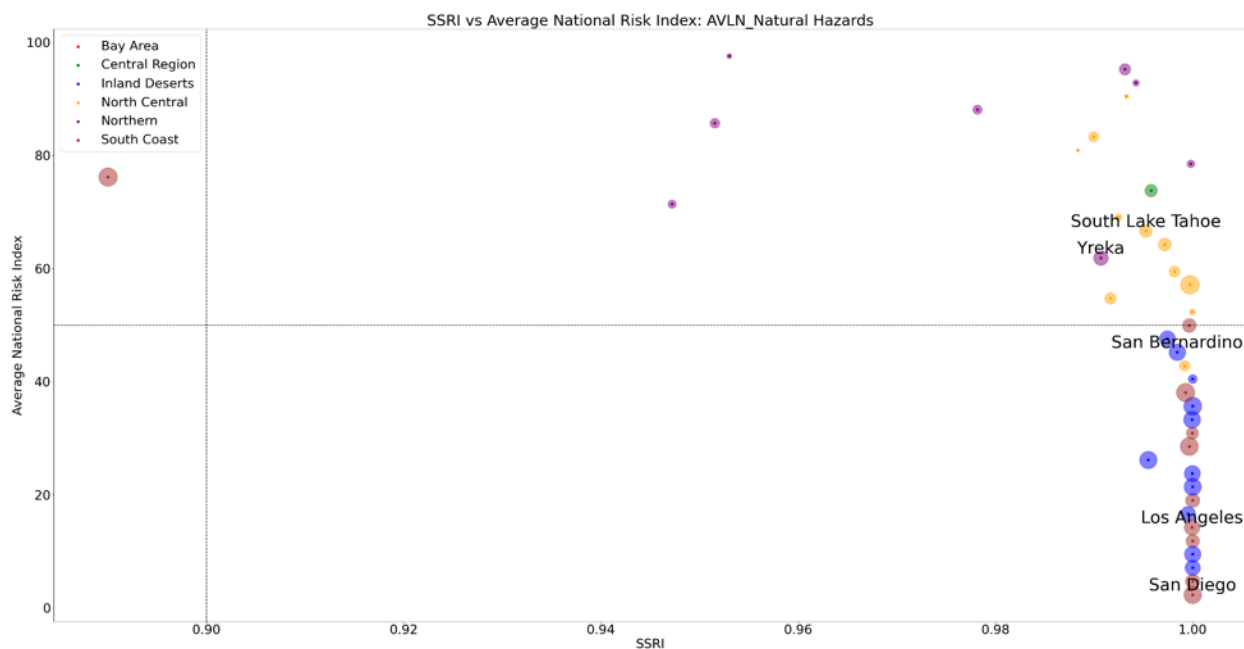


Figure B.6. Avalanche (AVLN)

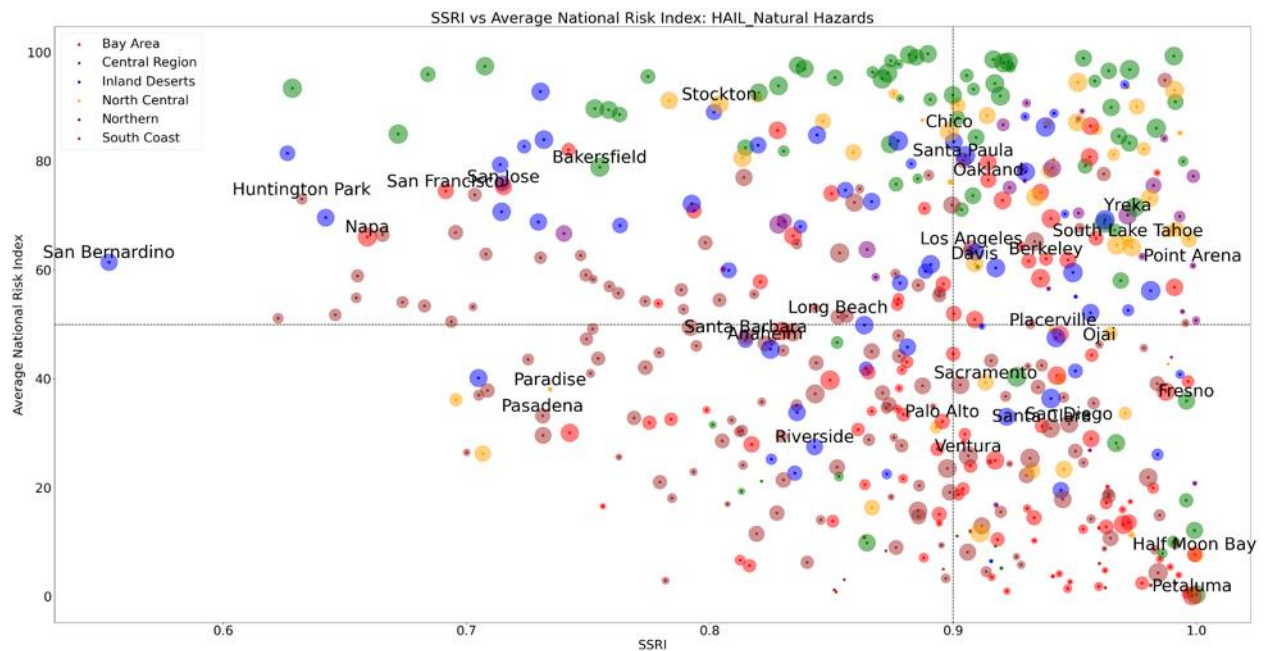


Figure B.7. Hail (HAIL)

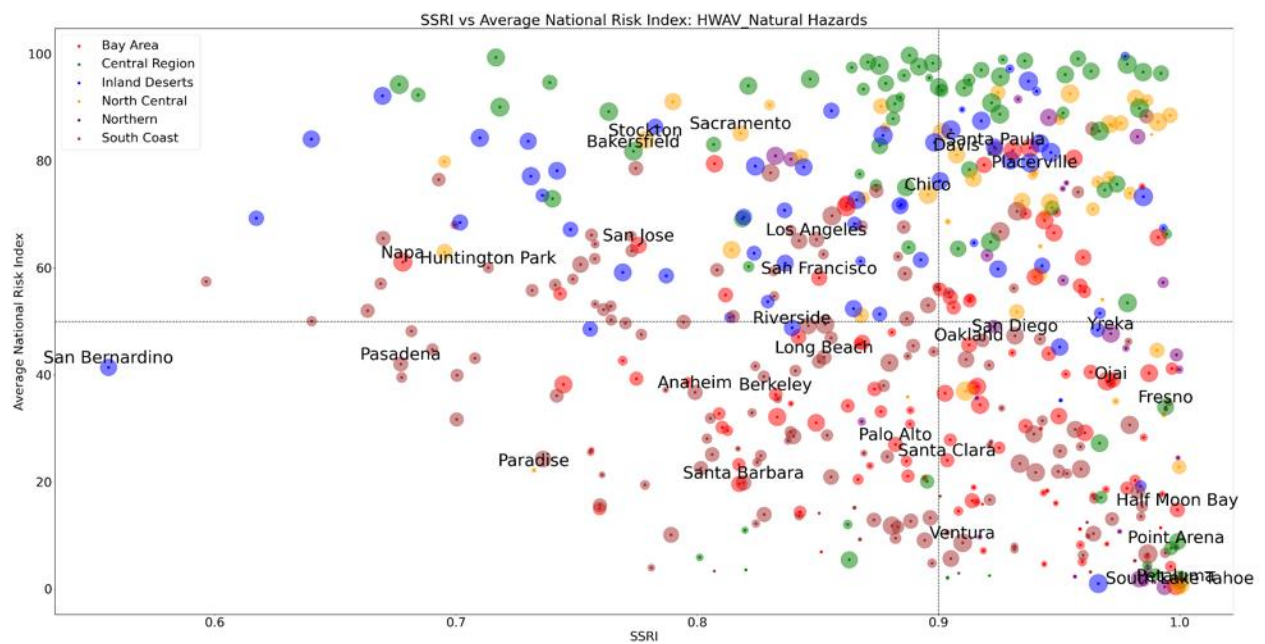


Figure B.8. Hot Wave (HWAV)

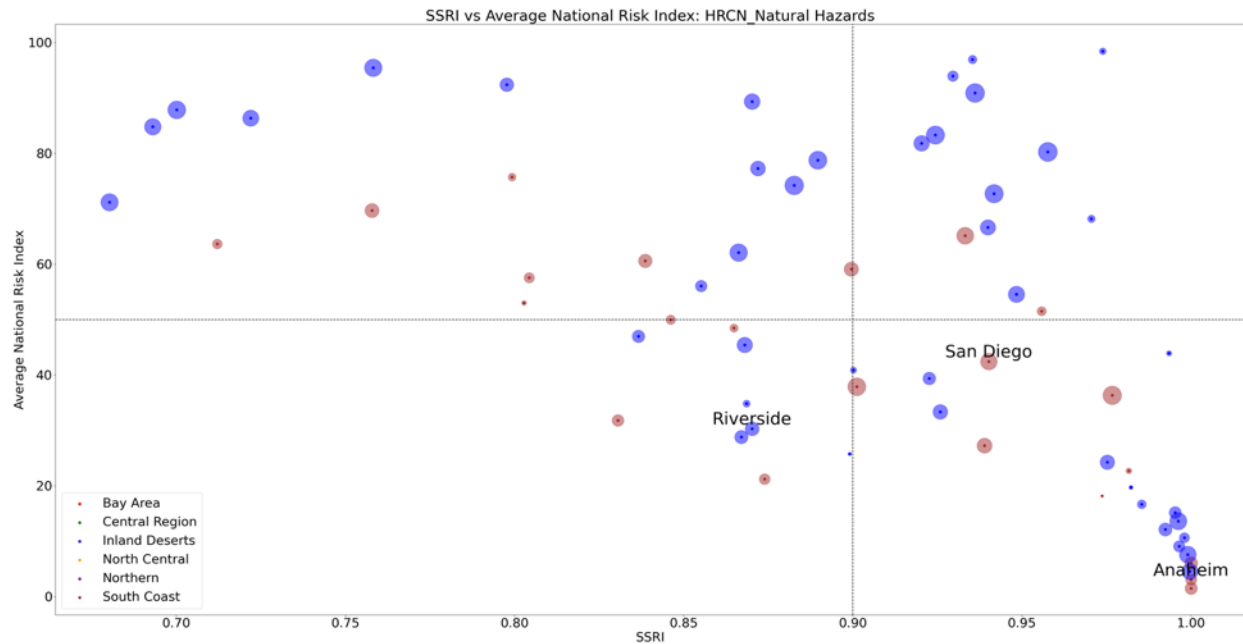


Figure B.9. Hurricane (HRCN)



Figure B.10. Landslide (LNDS)

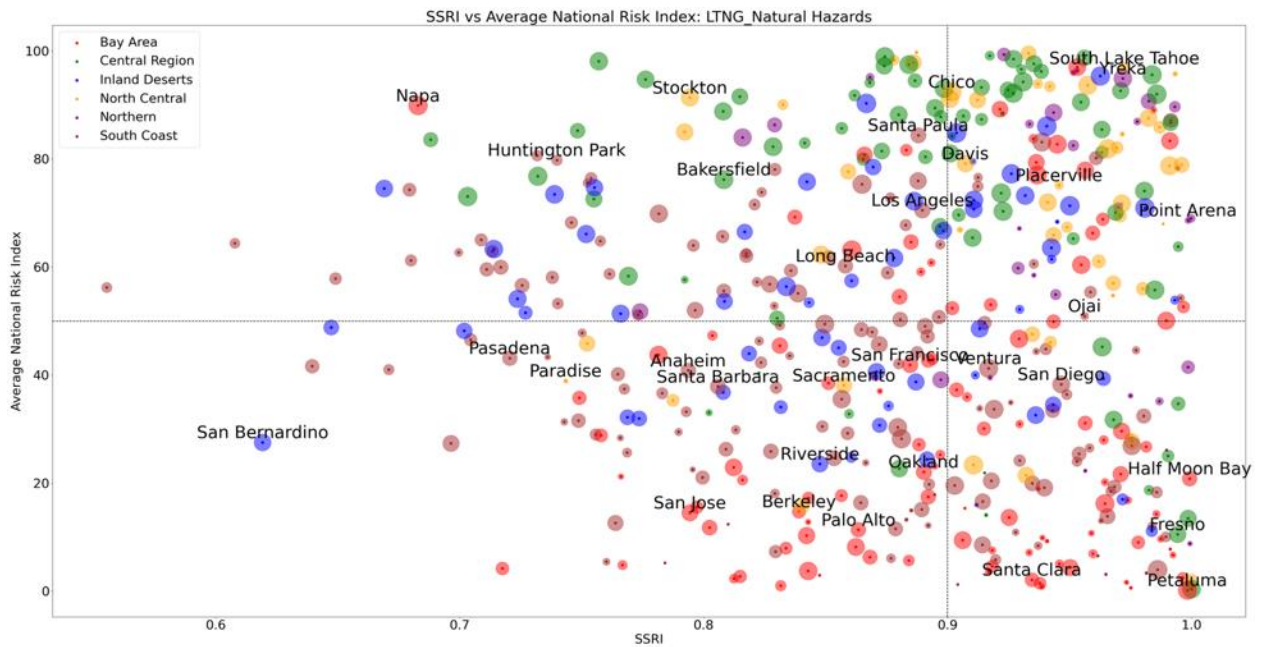


Figure B.11. Lighting (LTNG)

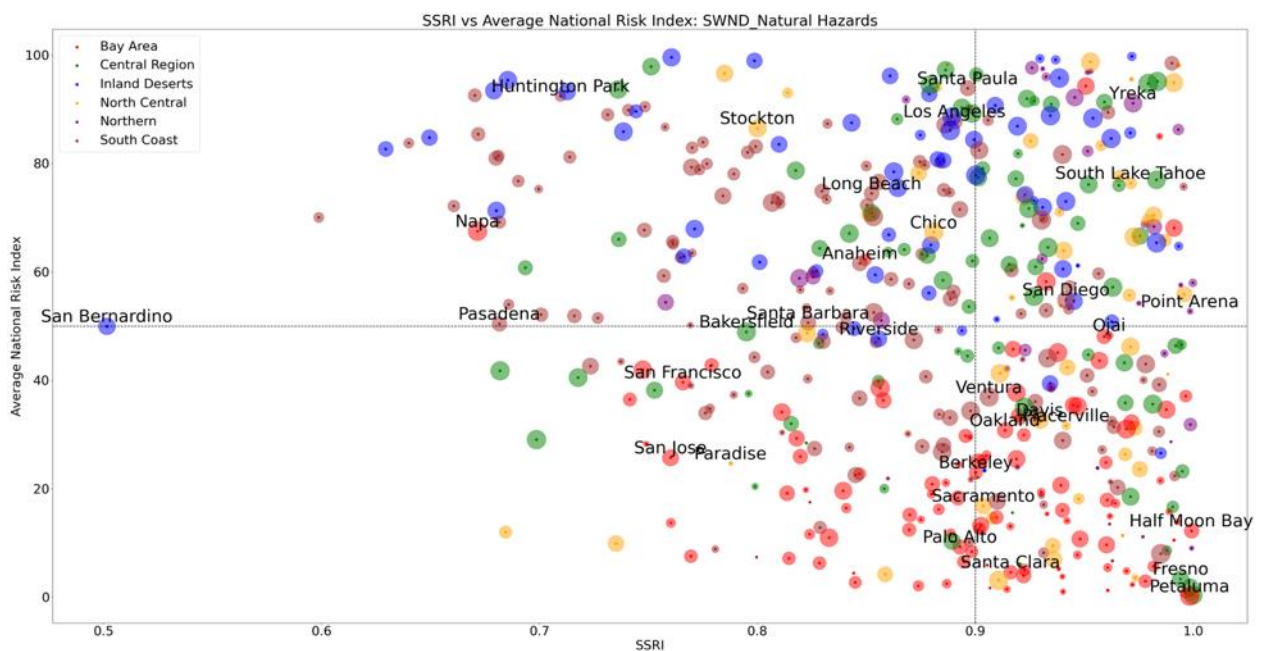


Figure B.12. Strong Wind (SWND)

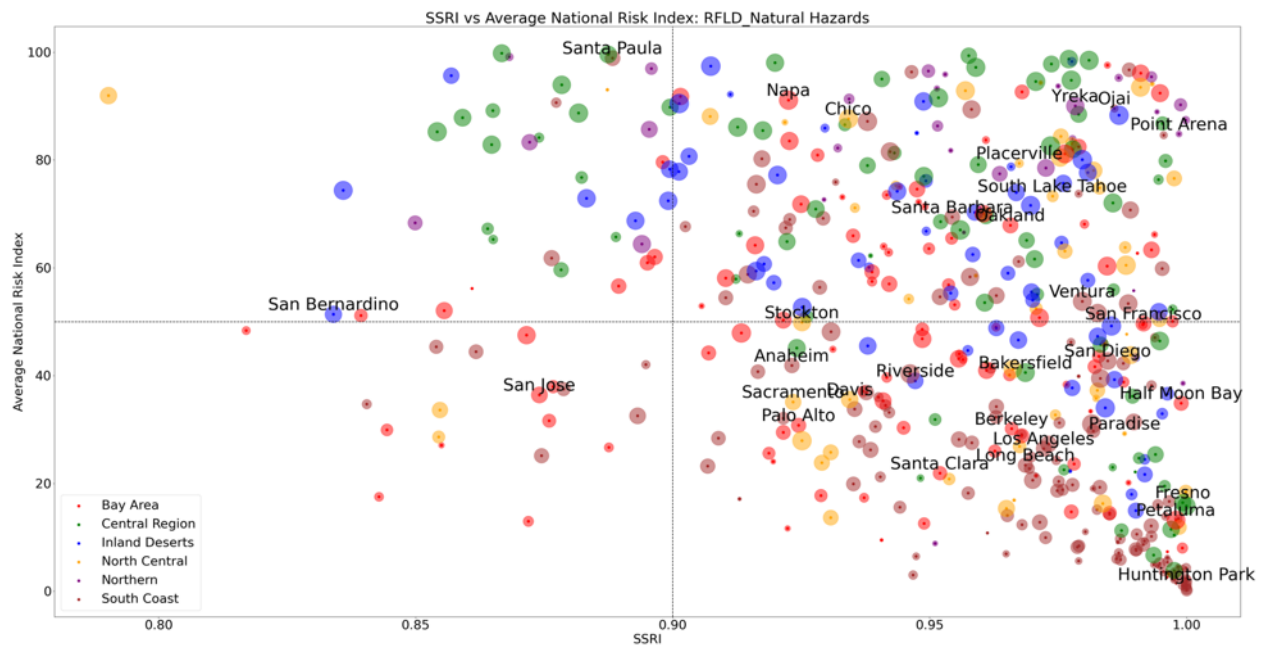


Figure B.13. Rapid Flood (RFLD)

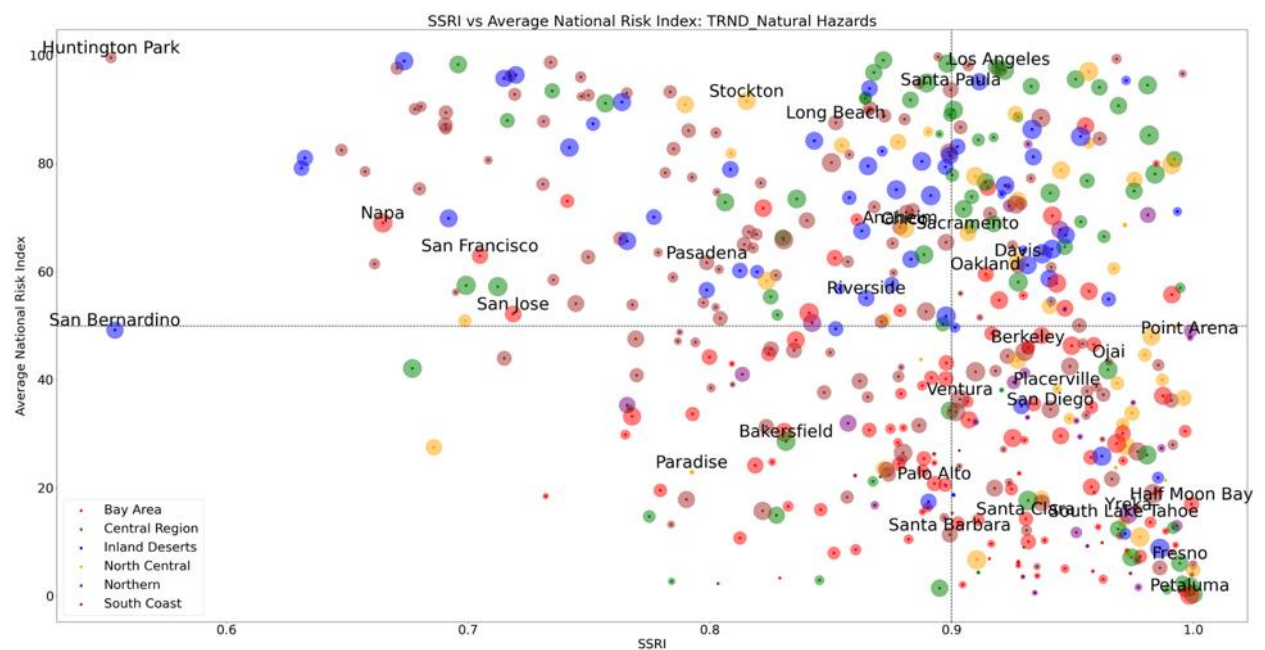


Figure B.14. Tornado (TRND)

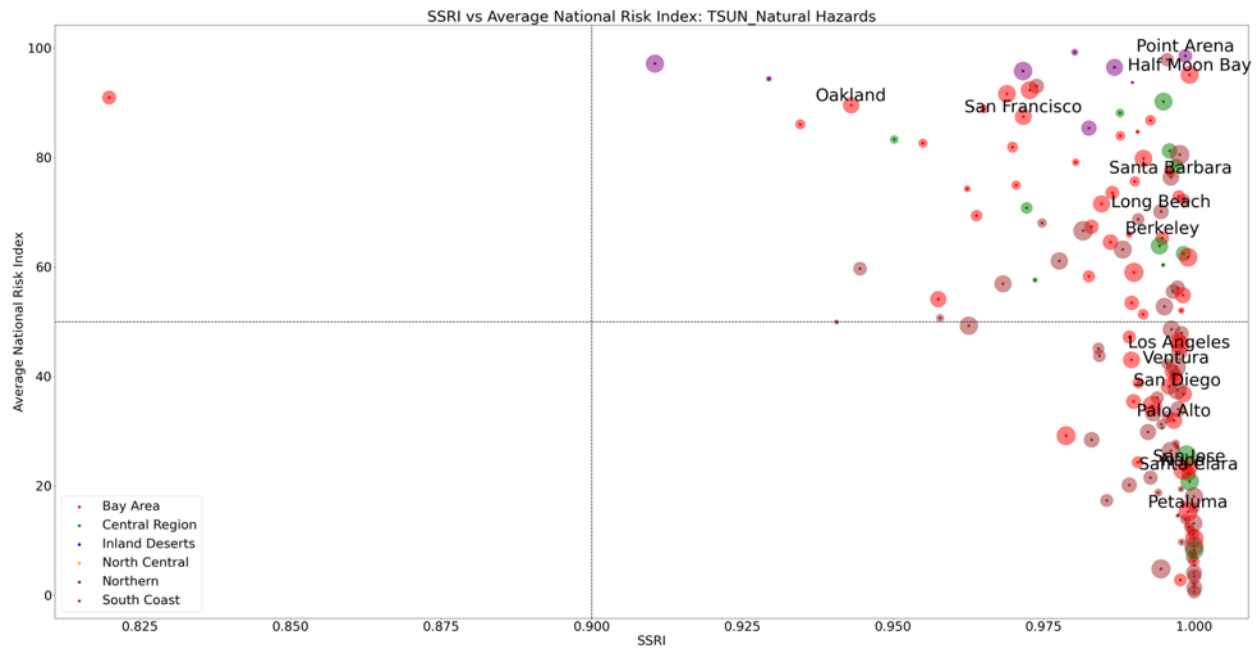


Figure B.15. Tsunami (TSUN)

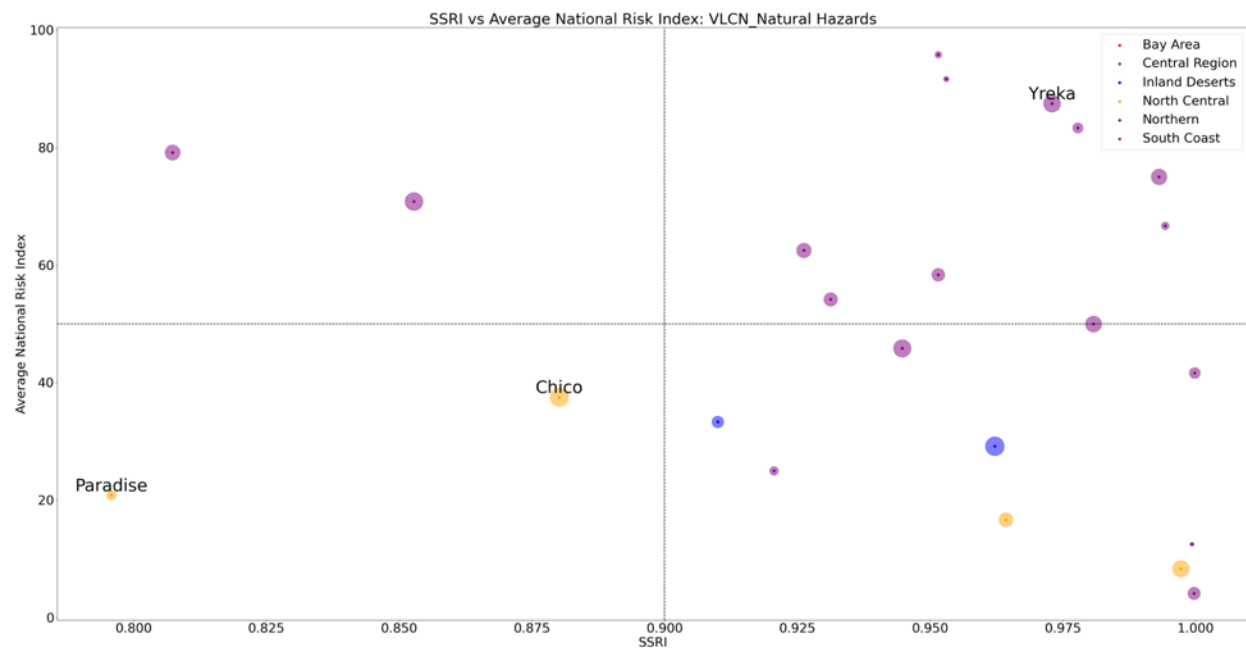


Figure B.16. Volcano (VLCN)



Figure B.17. Wildfire (WFIR)

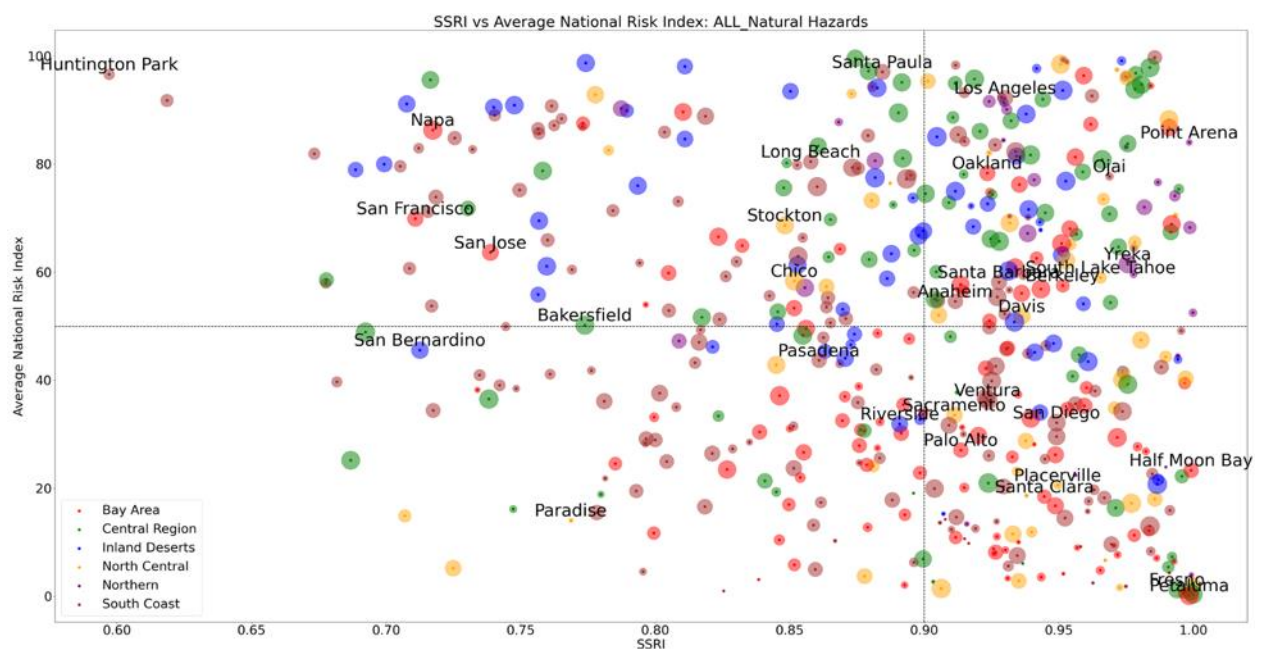


Figure B.18. All hazards (ALL)

Appendix C. Thomas Fire Case Study

Like the case study described in the Results section, this appendix summarizes the results of the Thomas Fire affecting the cities of Ventura, Ojai, Santa Paula, Meiners Oaks, Mira Monte, and Oak View. The team used their data or reports regarding the previous evacuations to evaluate how well aligned the safety elements of the emerging plans are relative to previous evacuation routes. The team conducted the same modeling and quantitative assessments.

Data Management

Generally, this project uses data from three main sources. Open Street Maps (OSM), the American Community Survey (ACS), and the National Risk Index (NRI) from FEMA. To estimate the social Vulnerability Index (SOVI), the team collected the following variables from the American Community Survey [98]:

Table C.1. Theme and variables used for the Social Vulnerability Index from American Community Survey.

Theme	Variable
Theme 1: Socioeconomic Status	POV150: Proportion of population under 150% poverty level.
	UNEMP: Proportion of population unemployed.
	HBURD: Proportion of population cost-burdened.
	NOHSDP: Proportion of the population with no high school diploma.
	UNINSUR: Proportion of the population with no insurance.
Theme 2: Household characteristics	AGE65: Proportion of the population with 65 or more years.
	AGE17: Proportion of population with 17 or less years.
	DISABL: Proportion of population with disability.
	SNGPNT: A proportion of the population is considered to be single parents.
	LIMENG: Proportion of population with English limitations.
Theme 3: Minority	MINRTY: The proportion of the population considered to be a minority.
Theme 4: housing type & transportation	MUNIT: Proportion of structures with 10 or more units.
	MOBILE: Proportion of the population living in mobile homes.
	CROWD: Proportion of structures with more inhabitants than rooms.
	NOVEH: Proportion of the population with no vehicle.
	GROUPQ: Proportion of population living in group quarters.

Tables C.2 through C.8 summarize the key characteristics of the study region based on the variables across the four themes.

Table C.2. Summary of the population percentage with each of the characteristics required to estimate the Social Vulnerability Index at the census block group in Ventura, Santa Paula, and Ojai.

Census block group:	THEME 1: Socio Economic Status					THEME 2: Household characteristics					THEME 3: Racial & Ethnic Minority Status		THEME 4: Housing Type & Transportation				
	POV150	UNEMP	HBURD	NOHSDP	UNINSUR	AGE65	AGE17	DISABL	SNGPNT	LIMENG	MINRTY		MUNIT	MOBILE	CROWD	NOVEH	GRQ
61110004001	29%	7%	37%	21%	14%	10%	8%	11%	1%	22%	49%		0%	4%	1%	4%	7%
61110004002	29%	0%	37%	9%	14%	26%	21%	11%	0%	22%	40%		0%	4%	0%	0%	7%
61110004003	29%	7%	37%	36%	14%	20%	22%	11%	4%	22%	83%		0%	4%	14%	0%	7%
61110004004	29%	1%	37%	48%	14%	8%	37%	11%	8%	22%	100%		0%	4%	18%	0%	7%
61110005001	22%	3%	34%	28%	8%	32%	24%	23%	7%	14%	52%		0%	48%	7%	6%	0%
61110006001	34%	14%	51%	36%	9%	6%	32%	16%	10%	27%	87%		0%	0%	5%	24%	0%
61110006002	34%	6%	51%	42%	9%	16%	48%	16%	14%	27%	91%		42%	0%	0%	16%	0%
61110006003	34%	4%	51%	66%	9%	1%	22%	16%	5%	27%	99%		10%	0%	8%	6%	0%
61110006004	34%	7%	51%	51%	9%	15%	33%	16%	0%	27%	94%		17%	0%	21%	15%	0%
61110006005	34%	5%	51%	29%	9%	3%	26%	16%	14%	27%	89%		2%	0%	7%	11%	0%
61110007011	30%	8%	41%	25%	16%	8%	31%	10%	5%	19%	91%		7%	13%	18%	1%	1%
61110007012	30%	10%	41%	45%	16%	8%	40%	10%	19%	19%	93%		22%	13%	18%	4%	1%
61110007013	30%	1%	41%	54%	16%	8%	23%	10%	9%	19%	97%		0%	13%	24%	2%	1%
61110007014	30%	7%	41%	51%	16%	3%	30%	10%	12%	19%	93%		16%	13%	20%	6%	1%
61110007021	13%	7%	33%	27%	7%	6%	24%	15%	1%	12%	90%		0%	0%	8%	8%	0%
61110007022	13%	8%	33%	15%	7%	26%	18%	15%	4%	12%	78%		0%	0%	1%	1%	0%
61110008001	17%	8%	29%	16%	8%	8%	44%	8%	8%	12%	96%		0%	8%	0%	0%	0%
61110008002	17%	6%	29%	26%	8%	10%	33%	8%	11%	12%	68%		0%	8%	7%	1%	0%
61110008003	17%	3%	29%	24%	8%	17%	15%	8%	0%	12%	79%		2%	8%	6%	2%	0%
61110008004	17%	5%	29%	13%	8%	33%	22%	8%	4%	12%	74%		0%	8%	2%	2%	0%
61110009011	11%	2%	32%	5%	6%	40%	11%	11%	5%	1%	12%		11%	0%	6%	7%	3%
61110009012	11%	10%	32%	7%	6%	30%	3%	11%	0%	1%	17%		0%	0%	0%	13%	3%
61110009021	27%	2%	33%	2%	10%	27%	16%	11%	2%	4%	11%		5%	1%	3%	0%	1%
61110009022	27%	2%	33%	13%	10%	19%	24%	11%	1%	4%	34%		11%	1%	5%	6%	1%
61110009031	8%	5%	29%	23%	6%	29%	9%	11%	6%	5%	42%		0%	8%	0%	0%	6%
61110009032	8%	0%	29%	5%	6%	28%	7%	11%	0%	5%	32%		10%	8%	0%	10%	6%
61110009033	8%	0%	29%	0%	6%	14%	30%	11%	4%	5%	18%		0%	8%	0%	0%	6%
61110009034	8%	10%	29%	4%	6%	42%	11%	11%	3%	5%	14%		12%	8%	4%	20%	6%
61110009035	8%	17%	29%	7%	6%	25%	19%	11%	8%	5%	25%		0%	8%	0%	0%	6%
61110010021	15%	8%	21%	8%	4%	46%	15%	15%	0%	3%	21%		0%	25%	1%	0%	1%
61110010022	15%	12%	21%	8%	4%	34%	16%	15%	0%	3%	15%		0%	25%	2%	11%	1%
61110010023	15%	9%	21%	10%	4%	21%	22%	15%	5%	3%	39%		0%	25%	0%	0%	1%
61110010024	15%	1%	21%	5%	4%	16%	13%	15%	9%	3%	25%		7%	25%	0%	4%	1%
61110011011	7%	1%	26%	11%	7%	18%	12%	16%	3%	4%	38%		0%	12%	2%	5%	0%
61110011012	7%	7%	26%	17%	7%	11%	17%	16%	2%	4%	37%		0%	12%	2%	2%	0%
61110011021	15%	6%	22%	2%	7%	28%	13%	9%	2%	3%	16%		1%	3%	6%	1%	0%
61110011022	15%	0%	22%	11%	7%	17%	24%	9%	1%	3%	23%		0%	3%	7%	0%	0%
61110012011	14%	2%	42%	16%	4%	5%	30%	13%	16%	4%	72%		30%	9%	10%	9%	0%
61110012012	14%	5%	42%	8%	4%	26%	16%	13%	7%	4%	43%		48%	9%	1%	19%	0%
61110012013	14%	16%	42%	18%	4%	35%	15%	13%	3%	4%	62%		0%	9%	11%	13%	0%
61110012021	5%	4%	9%	2%	5%	12%	22%	8%	0%	0%	42%		0%	0%	2%	0%	0%

Census block group:	THEME 1: Socio Economic Status					THEME 2: Household characteristics					THEME 3: Racial & Ethnic Minority Status	THEME 4: Housing Type & Transportation				
	POV150	UNEMP	HBURD	NOHSDP	UNINSUR	AGE65	AGE17	DISABL	SNGPNT	LIMENG	MINRTY	MUNIT	MOBILE	CROWD	NOVEH	GRQ
61110012022	5%	4%	9%	4%	5%	16%	19%	8%	1%	0%	35%	6%	0%	0%	1%	0%
61110012023	5%	4%	9%	1%	5%	30%	18%	8%	2%	0%	33%	0%	0%	0%	0%	0%
61110012041	17%	3%	28%	21%	12%	10%	22%	9%	13%	8%	58%	0%	28%	4%	2%	3%
61110013021	21%	1%	23%	25%	4%	31%	22%	25%	1%	14%	75%	9%	33%	11%	9%	0%
61110013031	11%	1%	28%	19%	5%	8%	29%	12%	0%	9%	61%	0%	0%	0%	0%	0%
61110013032	11%	6%	28%	10%	5%	19%	18%	12%	6%	9%	55%	28%	0%	15%	4%	0%
61110013041	13%	0%	33%	23%	1%	33%	6%	11%	0%	2%	50%	2%	3%	0%	2%	0%
61110013042	13%	4%	33%	12%	1%	5%	21%	11%	9%	2%	54%	7%	3%	5%	5%	0%
61110014011	9%	7%	21%	1%	8%	23%	21%	10%	17%	4%	46%	0%	0%	2%	5%	1%
61110014012	9%	6%	21%	7%	8%	18%	23%	10%	7%	4%	31%	6%	0%	5%	3%	1%
61110014021	10%	11%	22%	7%	5%	8%	24%	10%	3%	2%	53%	0%	0%	4%	0%	0%
61110014022	10%	2%	22%	2%	5%	31%	10%	10%	1%	2%	21%	47%	0%	1%	13%	0%
61110014023	10%	4%	22%	3%	5%	22%	17%	10%	0%	2%	45%	0%	0%	0%	3%	0%
61110015061	9%	3%	24%	6%	4%	20%	16%	13%	2%	5%	52%	1%	2%	0%	11%	0%
61110015062	9%	2%	24%	14%	4%	20%	22%	13%	1%	5%	54%	0%	2%	6%	0%	0%
61110015063	9%	3%	24%	5%	4%	25%	15%	13%	3%	5%	38%	0%	2%	2%	2%	0%
61110015071	15%	8%	31%	8%	6%	10%	27%	10%	0%	2%	41%	0%	1%	0%	11%	1%
61110015072	15%	0%	31%	7%	6%	21%	23%	10%	4%	2%	45%	17%	1%	1%	5%	1%
61110015073	15%	5%	31%	22%	6%	9%	25%	10%	9%	2%	64%	14%	1%	10%	3%	1%
61110015081	18%	4%	26%	9%	4%	16%	24%	15%	8%	5%	50%	8%	17%	4%	6%	0%
61110015091	25%	15%	57%	25%	6%	15%	29%	15%	16%	8%	73%	13%	7%	5%	9%	4%
61110015092	25%	6%	57%	9%	6%	21%	21%	15%	6%	8%	51%	35%	7%	7%	18%	4%
61110015101	22%	10%	34%	3%	3%	23%	15%	17%	3%	2%	44%	15%	24%	4%	12%	27%
61110015111	27%	0%	42%	11%	4%	7%	25%	11%	5%	15%	59%	26%	0%	3%	11%	0%
61110015112	27%	0%	42%	4%	4%	9%	21%	11%	0%	15%	77%	64%	0%	6%	0%	0%
61110016021	15%	2%	28%	8%	2%	28%	16%	16%	3%	1%	36%	10%	12%	2%	4%	1%
61110016022	15%	1%	28%	2%	2%	20%	30%	16%	2%	1%	31%	0%	12%	2%	0%	1%
61110018011	13%	10%	12%	3%	5%	27%	18%	13%	2%	0%	32%	2%	1%	0%	3%	2%
61110018012	13%	2%	12%	2%	5%	16%	28%	13%	4%	0%	24%	0%	1%	5%	3%	2%
61110018013	13%	5%	12%	3%	5%	18%	32%	13%	2%	0%	35%	0%	1%	8%	2%	2%
61110019011	24%	7%	34%	2%	5%	22%	22%	11%	2%	1%	18%	0%	0%	2%	2%	2%
61110019012	24%	5%	34%	9%	5%	20%	24%	11%	18%	1%	51%	5%	0%	3%	0%	2%
61110020001	7%	2%	27%	0%	6%	20%	18%	13%	7%	1%	22%	0%	0%	0%	0%	1%
61110020002	7%	7%	27%	0%	6%	26%	17%	13%	2%	1%	18%	0%	0%	6%	0%	1%
61110020003	7%	15%	27%	1%	6%	34%	18%	13%	6%	1%	16%	12%	0%	0%	1%	1%
61110021021	14%	5%	41%	4%	1%	10%	15%	22%	2%	2%	30%	52%	0%	3%	15%	0%
61110021022	14%	2%	41%	0%	1%	17%	8%	22%	0%	2%	26%	40%	0%	4%	1%	0%
61110022001	29%	7%	42%	34%	14%	5%	32%	12%	3%	8%	88%	10%	1%	26%	15%	1%
61110022002	29%	4%	42%	10%	14%	13%	29%	12%	8%	8%	63%	12%	1%	5%	0%	1%
61110022003	29%	1%	42%	11%	14%	5%	33%	12%	22%	8%	82%	10%	1%	8%	13%	1%
61110022004	29%	15%	42%	17%	14%	22%	16%	12%	16%	8%	48%	14%	1%	7%	13%	1%
61110023011	33%	3%	58%	35%	29%	5%	35%	12%	29%	24%	84%	16%	6%	0%	5%	4%
61110023012	33%	18%	58%	42%	29%	6%	9%	12%	0%	24%	68%	23%	6%	0%	8%	4%
61110023021	43%	11%	61%	50%	10%	2%	41%	23%	27%	15%	89%	0%	1%	2%	0%	0%

Census block group:	THEME 1: Socio Economic Status					THEME 2: Household characteristics					THEME 3: Racial & Ethnic Minority Status	THEME 4: Housing Type & Transportation				
	POV150	UNEMP	HBURD	NOHSDP	UNINSUR	AGE65	AGE17	DISABL	SNGPNT	LIMENG	MINRTY	MUNIT	MOBILE	CROWD	NOVEH	GRQ
61110023022	43%	0%	61%	3%	10%	2%	30%	23%	0%	15%	52%	0%	1%	0%	0%	0%
61110023023	43%	0%	61%	44%	10%	14%	22%	23%	0%	15%	88%	5%	1%	6%	26%	0%
61110024001	39%	5%	47%	14%	10%	24%	11%	26%	0%	4%	40%	87%	2%	4%	22%	4%
61110024002	39%	7%	47%	4%	10%	13%	13%	26%	11%	4%	30%	37%	2%	7%	19%	4%
61110025001	14%	0%	29%	2%	4%	19%	9%	11%	0%	0%	22%	0%	18%	5%	0%	0%
61110025002	14%	11%	29%	2%	4%	15%	24%	11%	3%	0%	56%	17%	18%	13%	0%	0%
61110025003	14%	0%	29%	0%	4%	73%	0%	11%	0%	0%	8%	0%	18%	0%	0%	0%
61110025004	14%	0%	29%	3%	4%	30%	12%	11%	5%	0%	17%	3%	18%	1%	2%	0%
61110026001	11%	4%	23%	5%	7%	18%	8%	13%	2%	1%	38%	4%	0%	0%	3%	2%
61110026002	11%	4%	23%	3%	7%	19%	14%	13%	8%	1%	24%	9%	0%	2%	3%	2%
61110026003	11%	7%	23%	7%	7%	15%	16%	13%	3%	1%	41%	0%	0%	0%	6%	2%
61110027001	15%	2%	32%	5%	7%	8%	15%	18%	7%	5%	46%	27%	0%	0%	12%	2%
61110027002	15%	1%	32%	7%	7%	25%	19%	18%	7%	5%	40%	28%	0%	0%	24%	2%
61110028001	22%	15%	26%	14%	7%	17%	20%	13%	1%	3%	51%	43%	1%	13%	11%	2%
61110028002	22%	0%	26%	1%	7%	12%	16%	13%	0%	3%	34%	0%	1%	0%	3%	2%
61110028003	22%	5%	26%	0%	7%	11%	21%	13%	4%	3%	36%	0%	1%	0%	2%	2%
61110028004	22%	3%	26%	10%	7%	10%	32%	13%	7%	3%	32%	1%	1%	0%	5%	2%
61110028005	22%	0%	26%	20%	7%	0%	21%	13%	0%	3%	37%	0%	1%	0%	0%	2%
61110050041	11%	1%	29%	13%	5%	7%	23%	7%	9%	8%	73%	45%	0%	4%	3%	1%
61110050062	21%	7%	44%	50%	15%	14%	14%	11%	0%	26%	91%	0%	0%	6%	2%	0%
61110052041	5%	4%	12%	2%	2%	31%	11%	16%	2%	2%	21%	1%	0%	0%	0%	0%
61110052051	6%	7%	17%	2%	2%	45%	10%	11%	1%	1%	31%	0%	5%	0%	0%	0%
61110092002	12%	0%	34%	20%	9%	8%	26%	11%	5%	11%	95%	15%	0%	12%	0%	0%
61110093002	12%	3%	20%	17%	7%	22%	18%	12%	2%	6%	57%	0%	6%	5%	0%	4%
61110094001	10%	0%	33%	2%	5%	8%	35%	6%	6%	3%	42%	0%	0%	0%	1%	0%
61110094002	10%	10%	33%	6%	5%	13%	23%	6%	2%	3%	45%	45%	0%	11%	4%	0%
61110095001	16%	24%	26%	3%	5%	27%	16%	15%	9%	1%	27%	0%	13%	0%	0%	1%
61110095002	16%	0%	26%	5%	5%	21%	17%	15%	1%	1%	19%	0%	13%	4%	4%	1%
61110095003	16%	0%	26%	14%	5%	15%	28%	15%	0%	1%	26%	0%	13%	0%	6%	1%
61110095004	16%	0%	26%	8%	5%	40%	11%	15%	2%	1%	37%	0%	13%	0%	2%	1%
61110096001	4%	3%	10%	0%	11%	24%	23%	14%	0%	1%	19%	0%	0%	0%	0%	1%
61110096002	4%	11%	10%	5%	11%	36%	15%	14%	0%	1%	24%	2%	0%	0%	1%	1%
61110097003	18%	21%	32%	3%	10%	22%	8%	14%	0%	15%	8%	0%	8%	3%	7%	0%

Table C.3. Spatial distribution of the variables required to estimate Theme 1: Socio-economic status: poverty, unemployment, house burdened, high school diploma, and health insurance (Thomas Fire Cities).

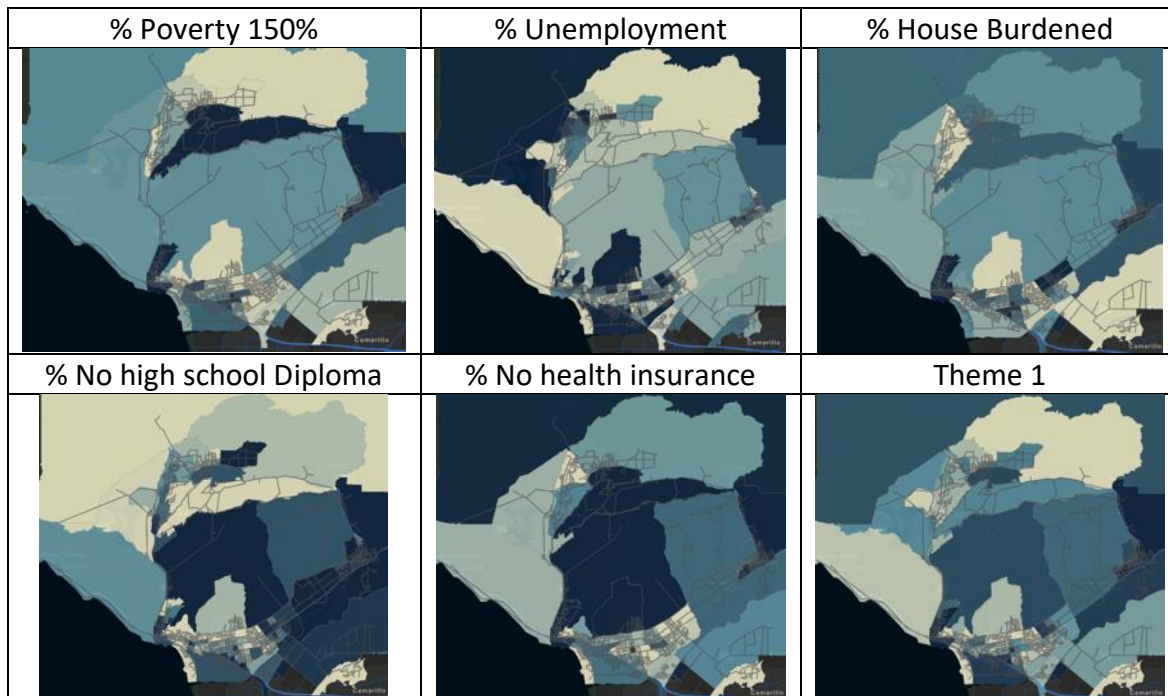


Table C.4. Spatial distribution of the variables required to estimate Theme 2: Household characteristics: Age 65 or older, age 17 and younger, civilian with a disability, single-parent households, English language proficiency (Thomas Fire Cities).

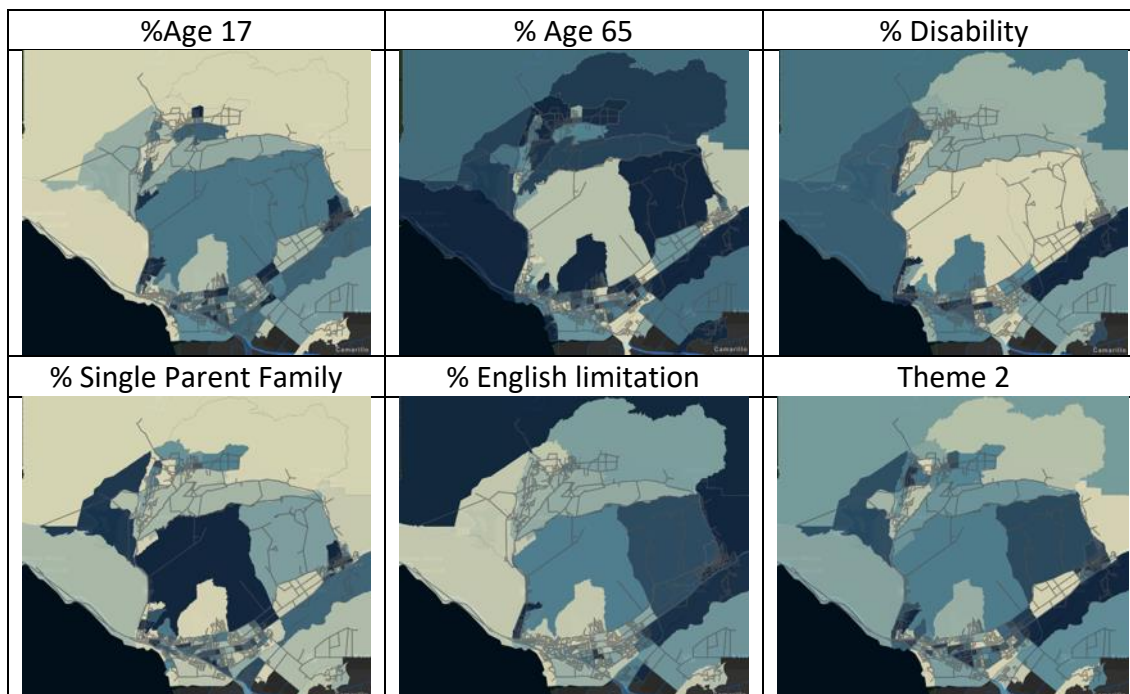


Table C.5. Spatial distribution of the variables required to estimate Theme 3: Racial & Ethnic: Minority status: belongs to a minority group (Thomas Fire Cities).

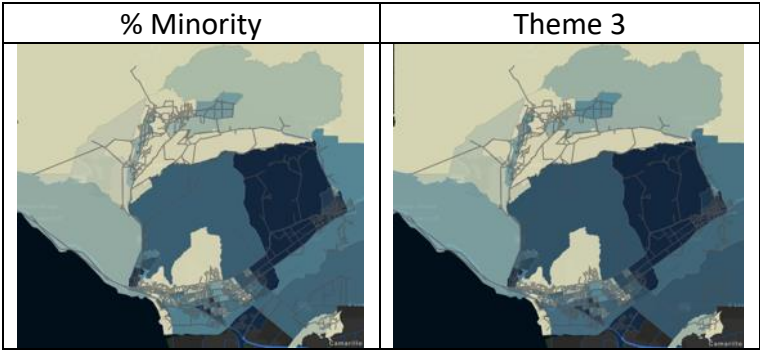


Table C.6. Spatial distribution of the variables required to estimate Theme 4: Housing type and Transportation: Multi-unit structure, mobile home, crowding, no vehicle, group quarter (Thomas Fire Cities).

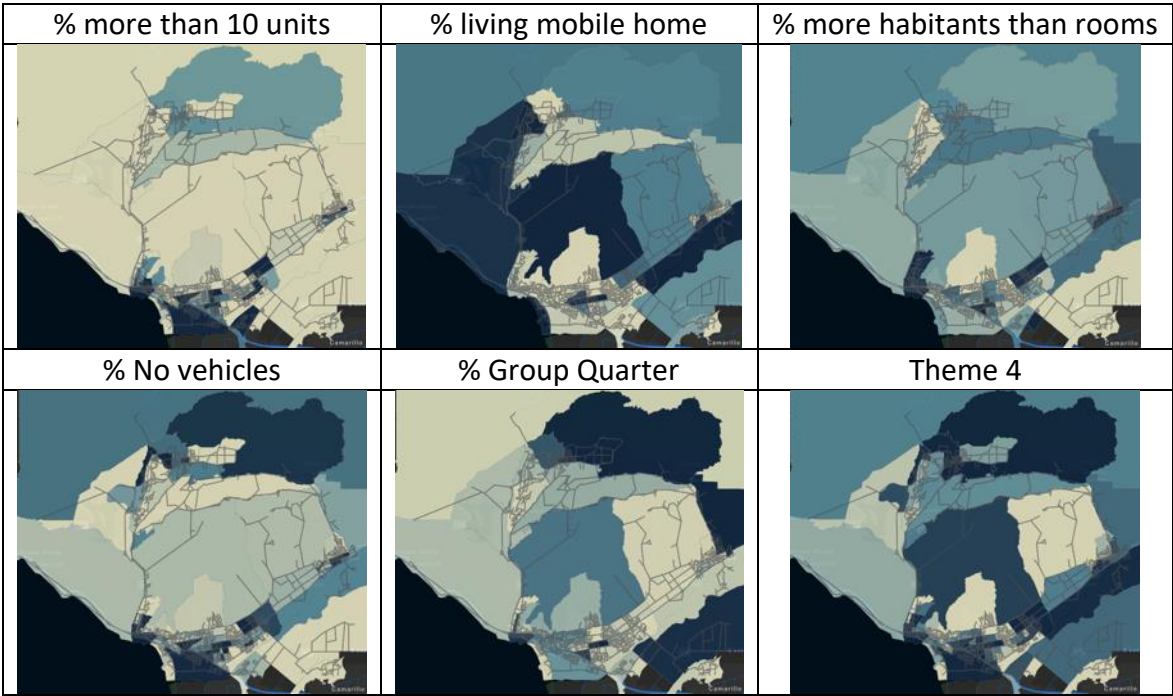


Table C.7. Spatial distribution of the four themes and the Social Vulnerability index at the census block level.






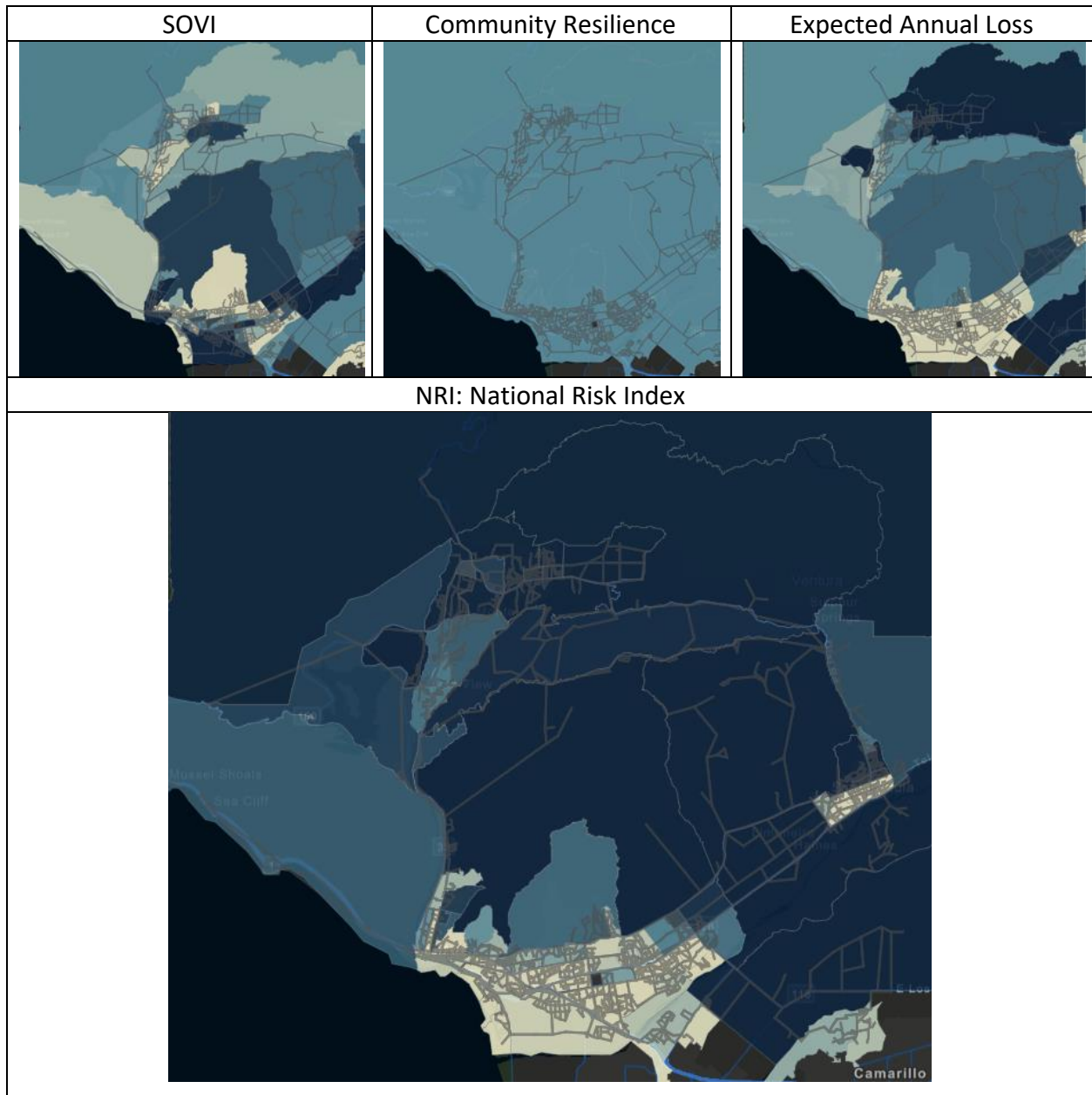
Theme 1: Socio-economic status	Theme 2: Household characteristics	Theme 3: Minority
		
Theme 4: Housing and transportation	SOVI: Social Vulnerability Index	
		

Figure C.1 shows the Ventura, Ojai, Santa Paula, Mira Monte, and Oaks map. Each origin node has assigned a vehicle demand obtained from the American Community Survey at the Census Block group level. Additionally, Figure C.2 summarizes the most important parameters of the 4,787 arcs of the road network of Ventura, Santa Paula, Ojai, Meiners Oaks, Mira Monte, and Oak View. In this study, the authors used a congestion factor obtained from [101] to reduce the speed as an approximation of congestion speed in each arc of the road network to obtain the travel time for each arc. Note that the minimum travel time is a crucial parameter in the ENP model because it is the foundation for transforming (expanding) the road network for mathematical modeling.

Table C.8. Spatial distribution of each Social Vulnerability index, Community Resilience, Expected Annual Loss, and the National Risk Index (NRI) at the census block level.



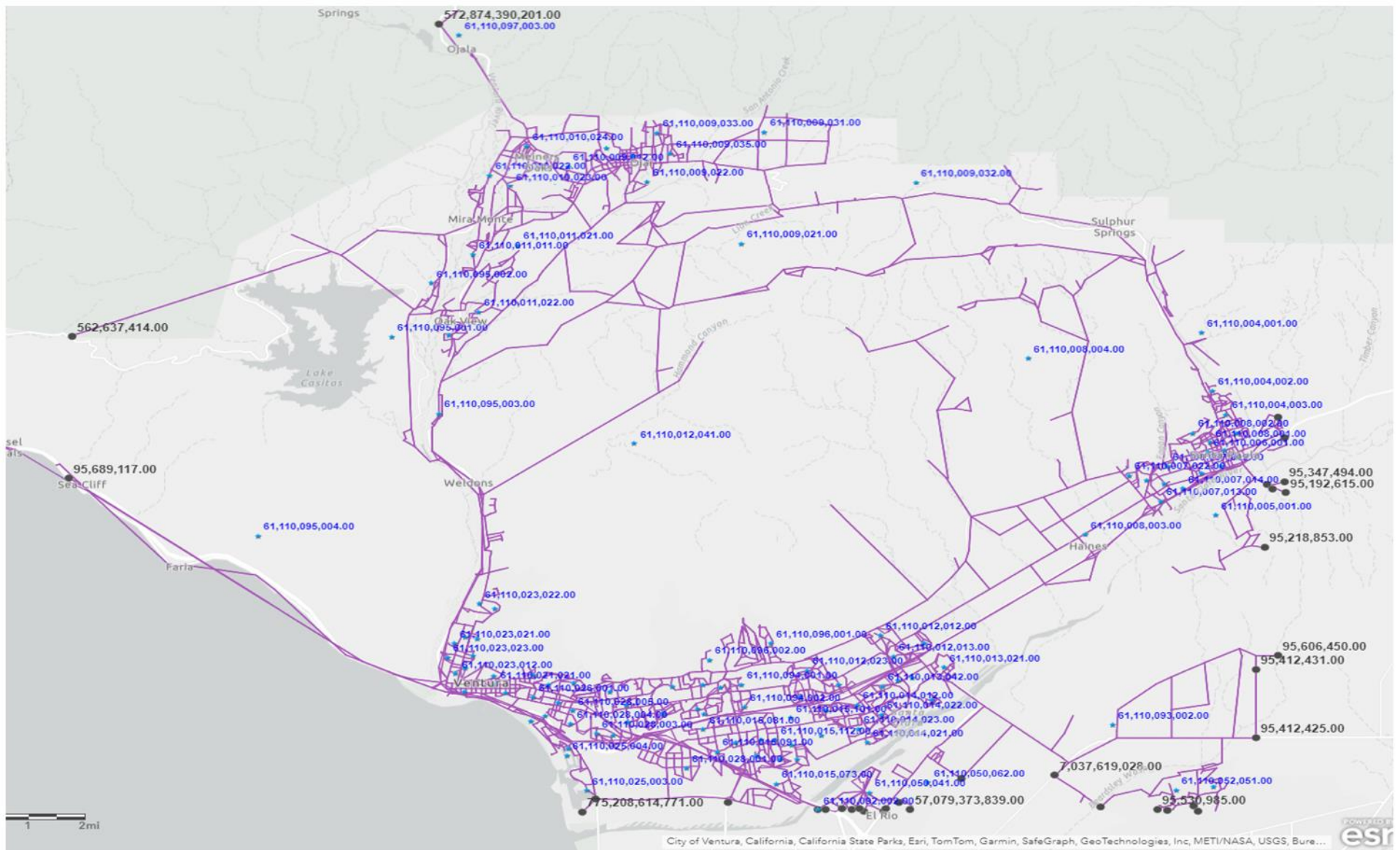
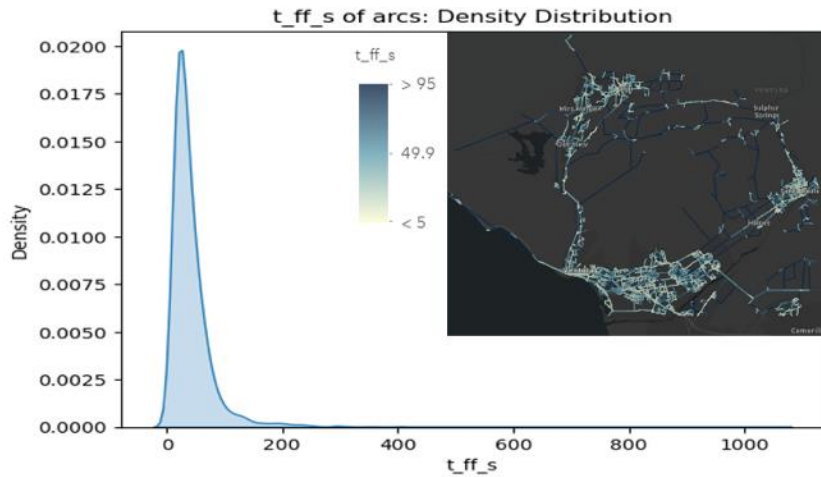


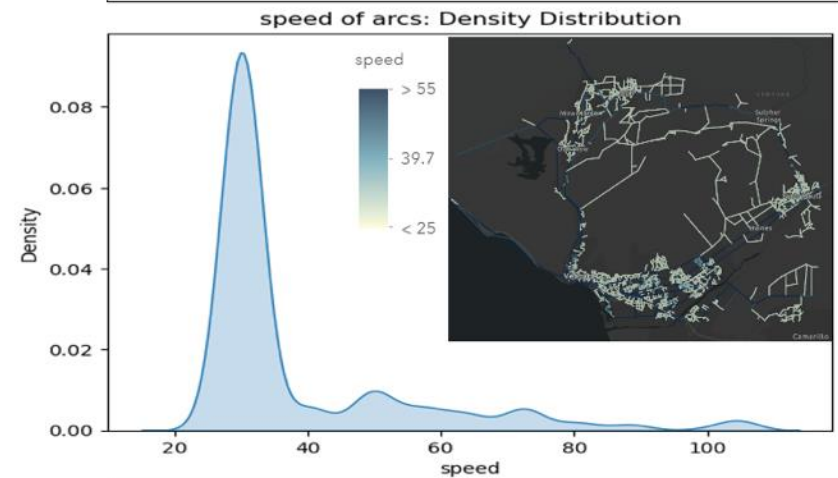
Figure C.1. Ventura, Ojai, Santa Paula with the labels of the source and sink nodes demand and sink capacity

Parameter (units) (min. max. mean)

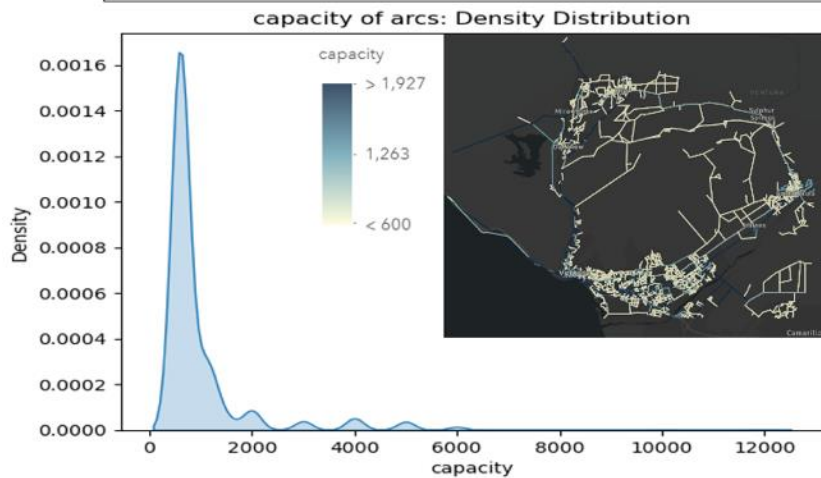
Travel time (s) (6.28. 1053. 43.6)



Speed (km/h) (24. 104.6. 38.6)



Capacity (veh/h) (600. 12000. 974.4)



Length (m) (99.88. 14626.1. 437.9)

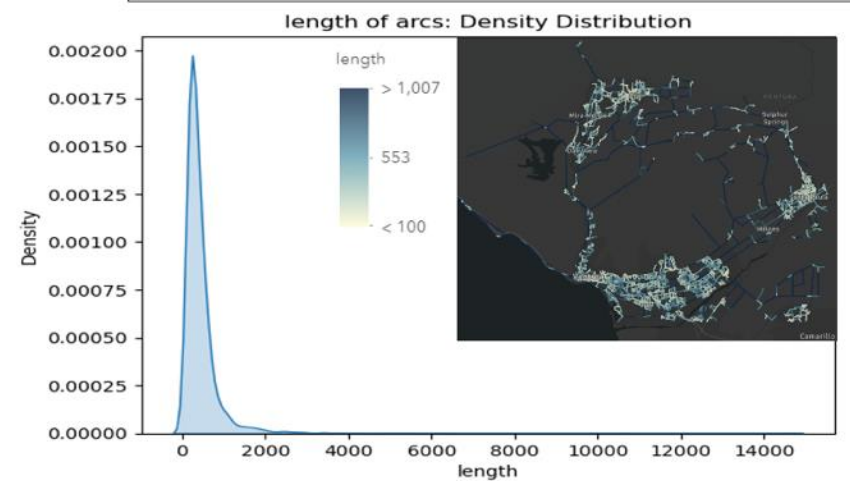


Figure C.2. Density distribution of the arcs of the road network, including length, capacity, speed, and travel time Thomas Fire

Ventura, Santa Paula, Ojai, Meiners Oaks, Mira Monte, and Oak View: The arc's length ranges from 99.8 to 14626.1 meters, and most arcs are shorter than 2 km (2000 m). Furthermore, the arc's capacity ranges from 600 to 12000 vehicles/hour, and most arcs have a capacity of 6000 vehicles/hour or less. The speed information not available in OSM was completed with the information given by [101], resulting in speeds ranging from 24 to 104.6 km/h. In the case of Ventura, Santa Paula, Ojai, Meiners Oaks, Mira Monte, and Oak View, the minimum travel time, including the congestion factor, is 6.28 seconds. In comparison, the maximum is 1053 seconds, determined by the speeds, arc lengths, and congestion factors.

When comparing the characteristics of the road network of both sets of cities, we note that the road network of the cities in the Thomas Fire case has higher capacities than the ones in the Camp Fire cities. Importantly, the number of exit nodes is more than three times higher in the case of the Thomas Fire cities than in the case of the Camp Fire. The ENP model requires expanding the road network, resulting in a time-expanded network with 53509 nodes and 56780 arcs for Thomas Fire Cities. The authors initiated the modeling with a large value of T . The authors used 1500 time units for the Thomas Fire, where each TU represents 6.28 seconds. The objective of the ENP model is to maximize the number of vehicles reaching the SN at the minimum time. In the case of the Thomas Fire, the last time window is 1074 TU (6749 seconds, 112 minutes, 1 hour and 51 minutes). Figure C.3 shows the evacuation rate and % of evacuated vehicles by time in minutes during their respective planning period.

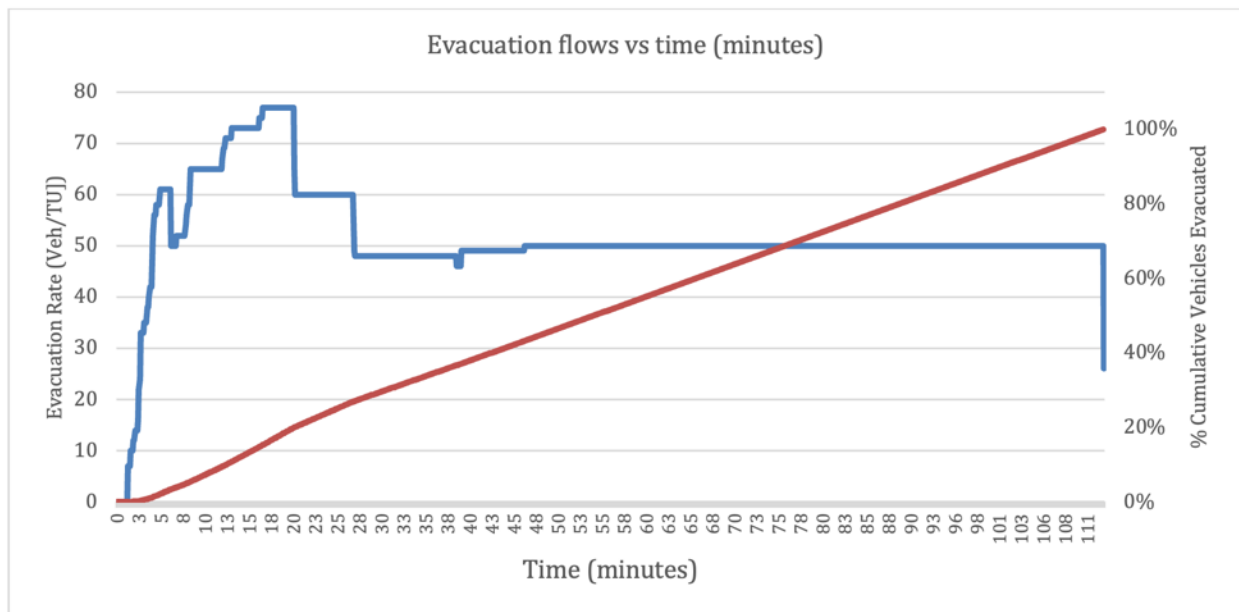


Figure C.3. Evacuation percentage with time in minutes in 2018 Thomas Fire Cities

Evacuation Plan Risk Assessment

The authors followed the methodology in [86], described in Task 2, to obtain the values of the natural hazard risk at the node level v_j for each node of the road network. Figure C.4 provides an overview of the density distribution of the factors affecting the RNP risk at the local level, particularly for all the road network nodes. The Hansen Accessibility Index (b) displays an almost symmetric distribution, while the Betweenness Centrality (d) among the nodes is skewed to the right. The NRI (c) shows a distribution with three modes. When analyzing the RNP at the local or node level v_j , it has a right-skewed distribution, indicating that some nodes have higher RNP risk than others. The RNP risk at the regional level shows that the RNP risk is higher in the northwest direction; however, there are some smaller peaks of risk in the north, east, west, and southwest of the cities affected by the Thomas Fire. In this stage, we identify the expected impact of a wildfire on the evacuation by affecting the exit routes in different directions of the road network, such as N, S, W, E, NE, NW, SE, and SW. The RNP risk at the regional level allows for the identification of the probability of wildfire and the estimation of the expected evacuation time under risk conditions.

Additionally, Table C.9, Table C.10, and Table C.11 show the results of the clearance time, total evacuation time, average evacuation time, the probability of risk in each region and direction, and the expected value of each of the mentioned performance measures. Additionally, Figure C.5 provides a picture of the performance measures when closing the exit nodes in each region and direction.

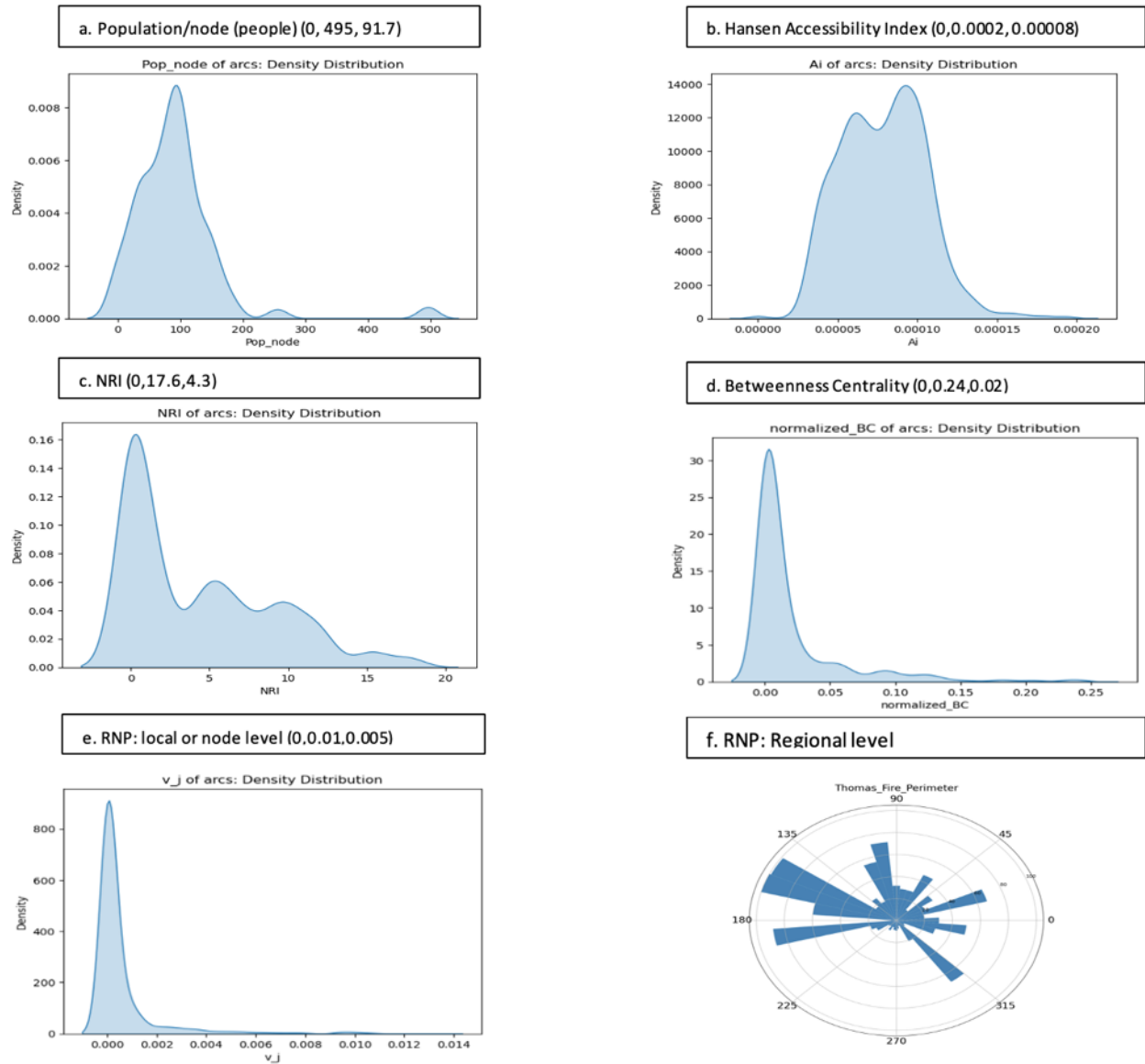


Figure C.4. Density probability factors of the v_j parameter (units) (min, max, mean) in Thomas Fire Cities

Table C.9. Clearance Time, Total Evacuation Time, and Average Evacuation Time when closing each exit node.

DIRECTION	exit nodes	ET		Total ET		Average ET
		UT	minutes	UT	minutes	minutes
E	[102425678718, 483579341244]	1306	136.7942	35349905	3702651.11	65.75009962
NW	[572874390201]	1166	122.1302	31650479	3315162.55	58.869243
W	[562637414]	1133	118.6737	30237384	3167150.9	56.24091523
	[95689117]	1288	134.9088	34466398	3610110.036	64.10679469
SW	[410553504009, 775208614771]	1166	122.1302	31645668	3314658.632	58.86029464
S	[432216758]	1119	117.2073	30437032	3188062.608	56.61225642
	[233843828790, 95390273, 562903250678, 853783080, 62411927331, 853782913]	1122	117.5215	32176577	3370267.574	59.84777451
	[365903020800, 918451694332, 95558731, 57079373839]	1074	112.4939	29333196	3072443.638	54.55914406
SE	[10566765649]	1074	112.4939	29231902	3061833.812	54.37073929
	[7037619028, 95408984]	1075	112.5986	29311868	3070209.682	54.51947441
	[95431819, 95431833, 95476934, 95530985]	1074	112.4939	29397862	3079216.942	54.67942149
	[95412425]	1074	112.4939	29248798	3063603.548	54.4021655
E	[95412431, 95606450]	1074	112.4939	29234841	3062141.652	54.37620577
	[95218853]	1084	113.5413	29648654	3105485.62	55.14588948
	[962823779392, 95260763, 95192615, 95347494]	1109	116.1599	30384490	3182559.207	56.51452937
NE, N	Base	1074	112.4939	29223662	3060970.731	54.35541306

Table C.10. Estimation of the probability of each grade and direction of the road network

Region (r)	ψ_r	Direction (d)	P(r)	P(r)/P(d)
340	0.000643	E	0.02724	0.14593
350	0.001126		0.04770	0.25559
0	0.000683		0.02891	0.15489
10	0.000453		0.01920	0.10289
20	0.001502		0.06359	0.34071
30	0.000502	NE	0.02128	0.20105
40	0.000709		0.03004	0.28385
50	0.000265		0.01122	0.10599
60	0.001022		0.04330	0.40910
70	0.000637	N	0.02699	0.13219
80	0.000643		0.02723	0.13336
90	0.000708		0.02996	0.14674
100	0.0016		0.06776	0.33183
110	0.001234		0.05225	0.25587
120	0.000426	NW	0.01803	0.11835
130	0.000553		0.02343	0.15384
140	0.000404		0.01712	0.11239
150	0.002214		0.09375	0.61542
160	0.00224	W	0.09487	0.36873
170	0.001342		0.05683	0.22088
180	8.64E-05		0.00366	0.01423
190	0.001979		0.08380	0.32570
200	0.000428		0.01813	0.07046
210	0.000352	SW	0.01489	0.40777
220	0.000152		0.00642	0.17580
230	0.000138		0.00585	0.16015
240	0.000221		0.00936	0.25628
250	0.000146	S	0.00618	0.17631
260	0.000193		0.00818	0.23314
270	0.000208		0.00881	0.25117
280	0.000167		0.00709	0.20227
290	0.000114		0.00481	0.13710
300	0.000462	SE	0.01957	0.20169
310	0.001527		0.06466	0.66636
320	0.000164		0.00695	0.07161
330	0.000138		0.00586	0.06034

Table C.11. Estimation of the expected clearance time, total evacuation time, and average evacuation time.

Dir	PSI_DIR	P(direction)	E[ET]		E[TET]		E[avg_ET]	
N	0.0010	0.1741	1074.00	186.98	29223662.00	5087649.44	54.36	9.46
NE	0.0006	0.1128	1074.00	121.15	29223662.00	3296496.59	54.36	6.13
E	0.0009	0.1591	1105.85	175.98	30144049.62	4796940.01	56.07	8.92
SE	0.0006	0.1034	1074.67	111.14	29298092.46	3029999.85	54.49	5.64
S	0.0002	0.0299	1094.20	32.71	30118858.78	900484.48	56.02	1.67
SW	0.0002	0.0389	1097.58	42.73	29844375.46	1161753.73	55.51	2.16
W	0.0012	0.2194	1143.02	250.75	30755469.07	6746878.33	57.20	12.55
NW	0.0009	0.1624	1084.89	176.14	29510882.83	4791215.46	54.89	8.91
6.284573229			$\overline{E}[CT]$	1097.57	$\overline{E}[TET]$	29811417.88	$\overline{E}[avg ET]$	55.45
			Minutes	114.96	Minutes	3122533.98		

When comparing the expected total evacuation time, the Camp Fire area involves 859,714.54 minutes, while the Thomas Fire involves 3,122,533 minutes, given the total evacuation demand. However, the average evacuation time in the case of the Thomas Fire is around 55.44 minutes, which is close to that expected in Paradise (55.11 minutes), despite the Thomas Fire region having a larger area and a higher demand for vehicles compared to the Camp Fire region. One reason for this performance is that the Thomas Fire area has more exit routes, unlike Paradise. Additionally, the road network capacity in the Thomas Fire region is larger than in Paradise, providing insights into the reasons for this performance.

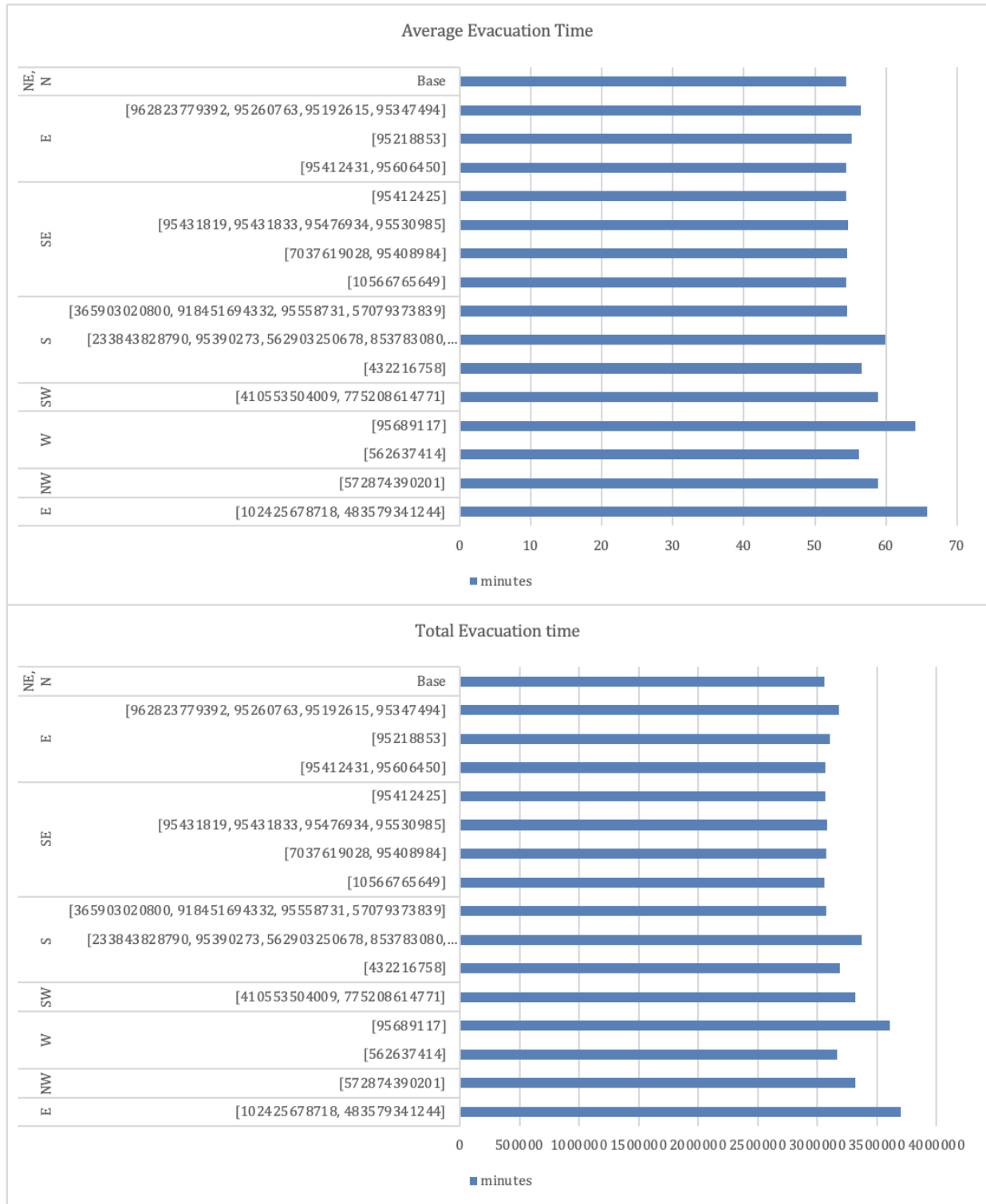


Figure C.5. Clearance Time and Average Evacuation Time when closing each exit node

Appendix D. Sociodemographic Characteristics of Paradise and Magalia

This appendix summarizes the data used to estimate the SOVI for the Camp Fire case study.

Table D.1. Spatial distribution of the variables required to estimate Theme 1: Socio-economic status: poverty, unemployment, house burdened, high school diploma, and health insurance.

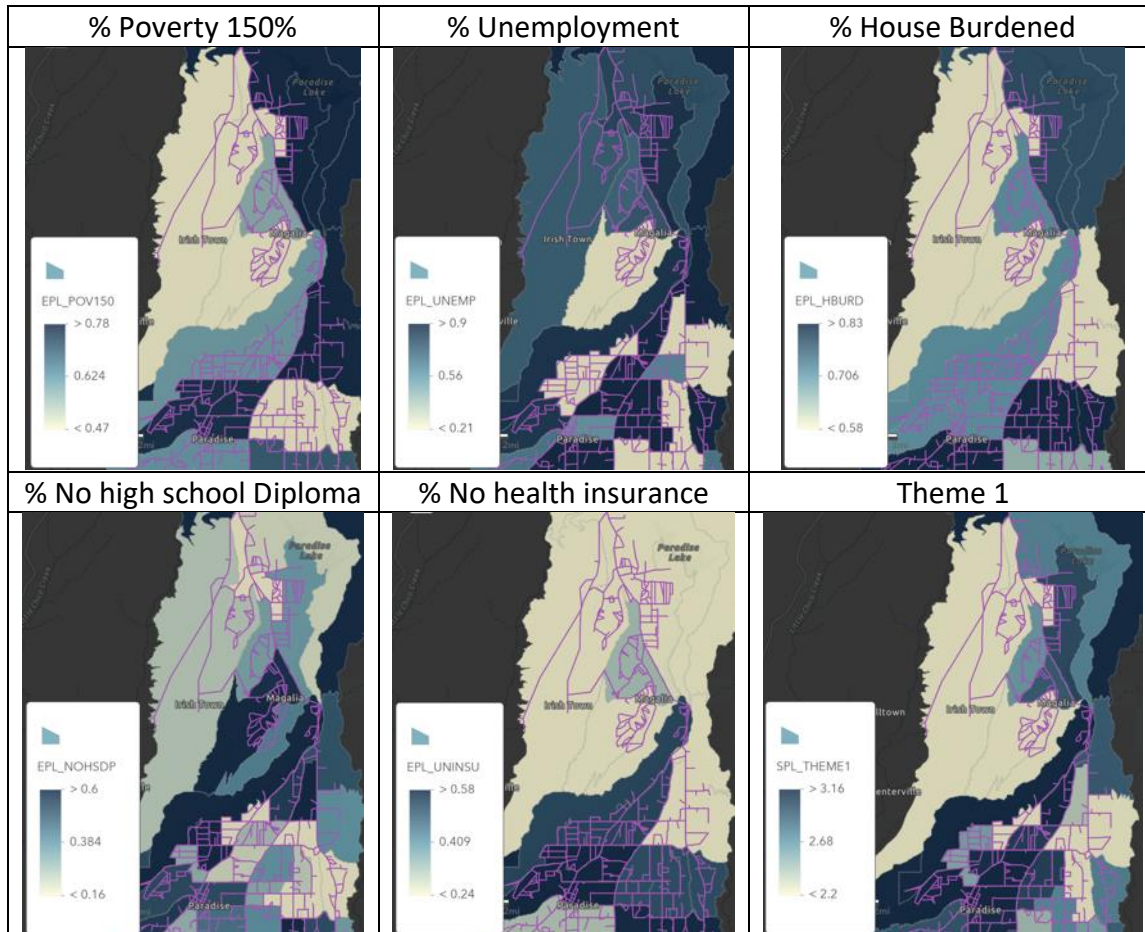


Table D.2. Spatial distribution of the variables required to estimate Theme 2 Household characteristics

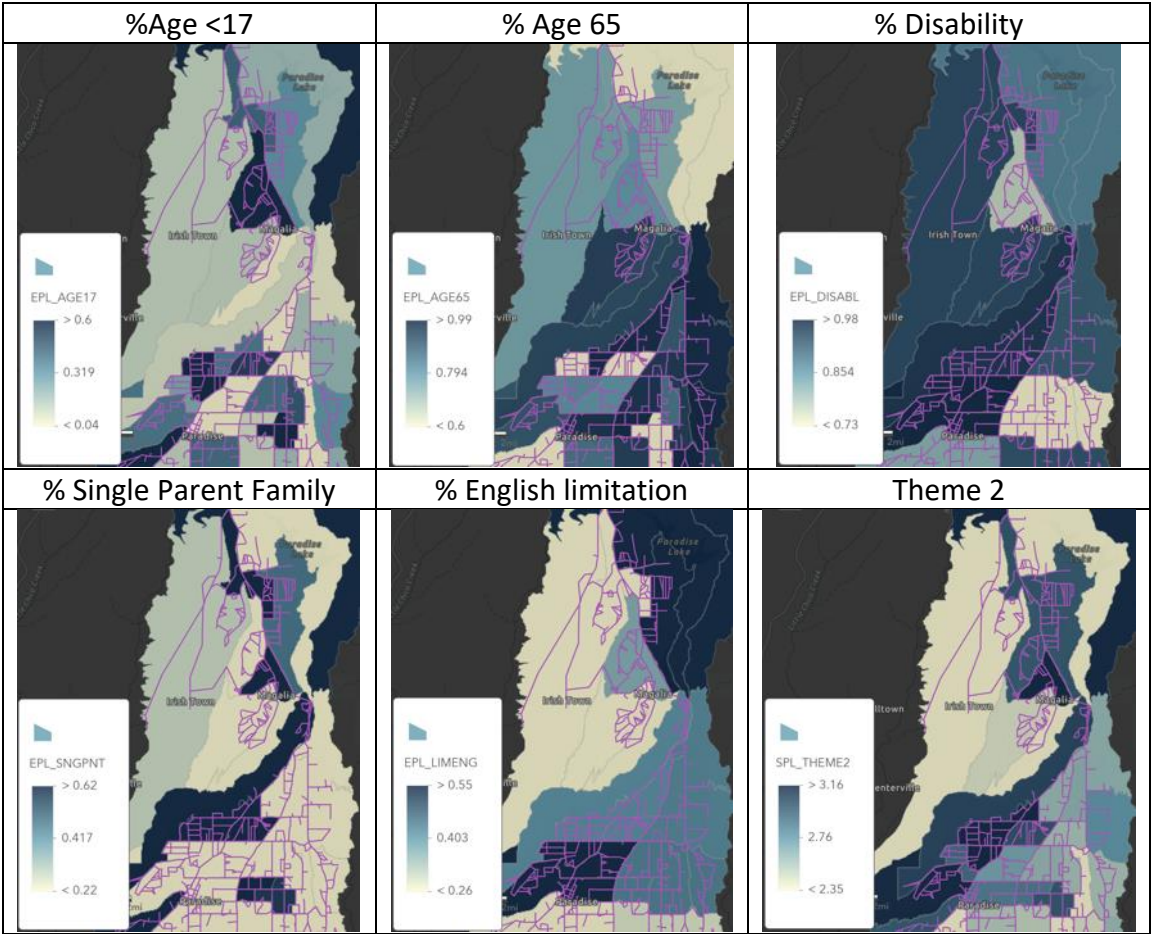


Table D.3. Spatial distribution of the variables required to estimate Theme 3: Racial & Ethnic

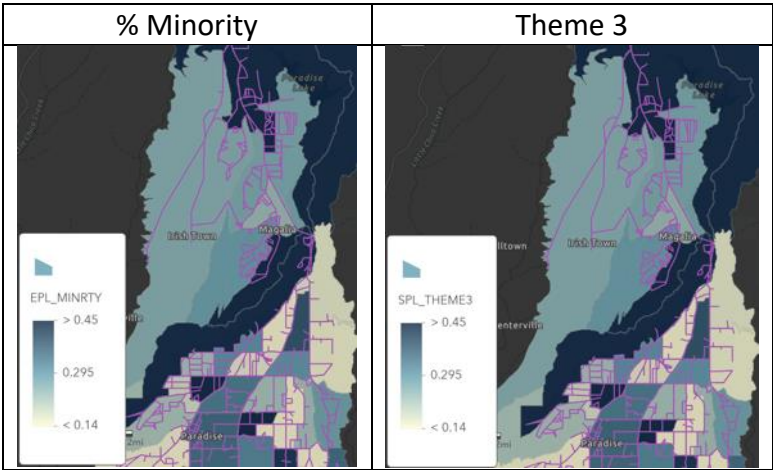


Table D.4. Spatial distribution of the variables required to estimate Theme 4: Housing type and Transportation: Multi-unit structure, mobile home, crowding, no vehicle, group quarter.

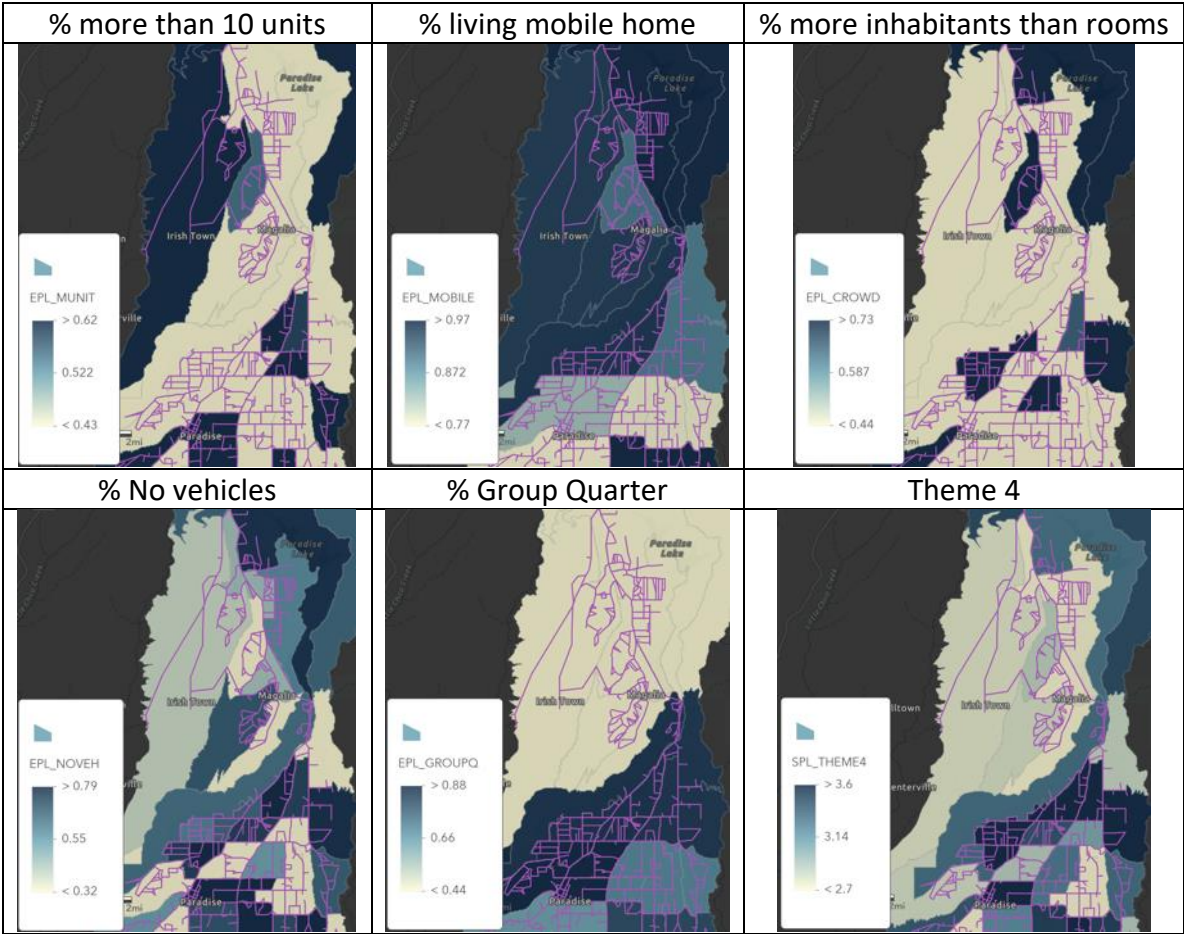


Table D.5. Spatial distribution of the four themes and the Social Vulnerability index at the census block level.

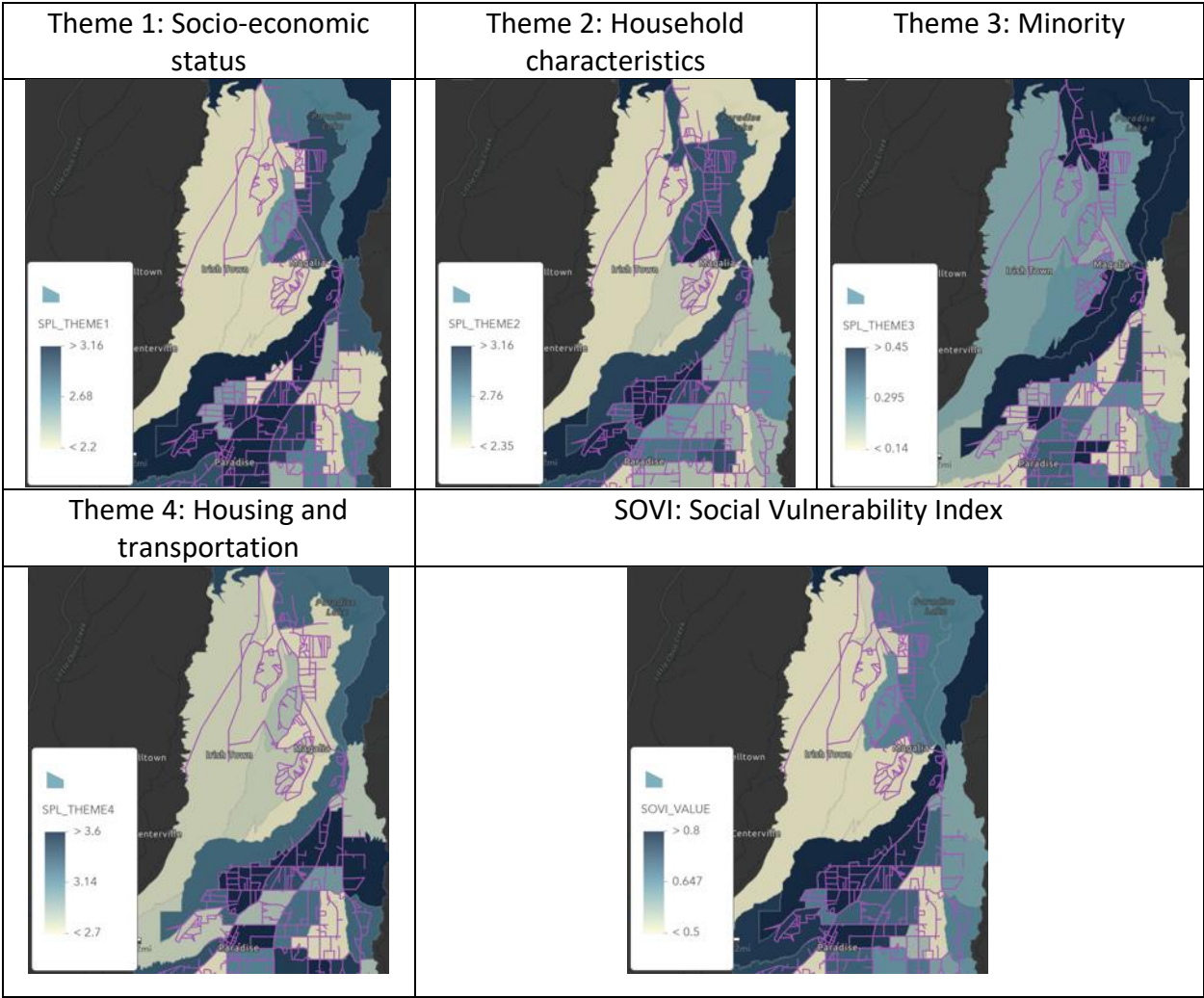


Table D.6. Spatial distribution of each Social Vulnerability index, Community Resilience, Expected Annual Loss, and the National Risk Index (NRI) at the census block level.

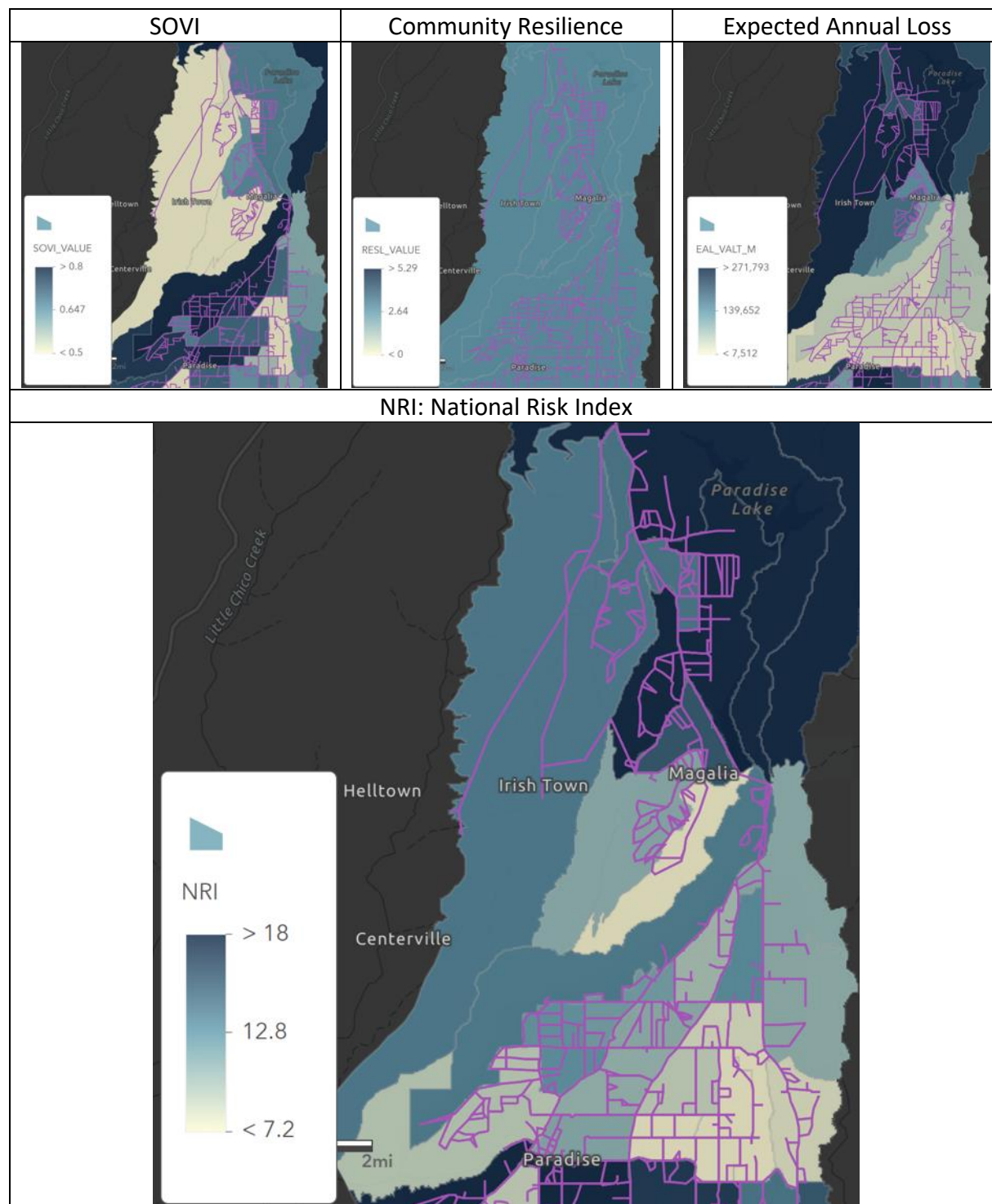


Table D.7. Summary of the population percentage with each characteristic required for the SOVI at the census block group.

Census block group:	THEME 1: Socioeconomic Status					THEME 2: Household characteristics					THEME 3: Racial & Ethnic	THEME 4: Housing Type & Transportation				
	POV150	UNEMP	HBURD	NOHSDP	UNINSUR	AGE65	AGE17	DISABL	SNGPNT	LIMENG	MINRTY	MUNIT	MOBILE	CROWD	NOVEH	GRQ
60070017021	17%	0%	26%	6%	3%	34%	0%	24%	0%	0%	33%	0%	29%	0%	0%	0%
60070017022	17%	0%	26%	15%	3%	37%	11%	24%	0%	0%	13%	0%	29%	0%	8%	0%
60070017023	17%	7%	26%	3%	3%	23%	11%	24%	1%	0%	11%	9%	29%	0%	2%	0%
60070017024	17%	9%	26%	0%	3%	22%	20%	24%	7%	0%	26%	0%	29%	0%	3%	0%
60070017031	22%	8%	33%	10%	4%	24%	25%	17%	7%	1%	10%	0%	20%	0%	3%	0%
60070017032	22%	7%	33%	5%	4%	24%	30%	17%	0%	1%	11%	2%	20%	10%	0%	0%
60070017041	34%	18%	37%	13%	3%	16%	28%	21%	8%	2%	36%	6%	42%	8%	7%	0%
60070017042	34%	8%	37%	2%	3%	14%	13%	21%	0%	2%	42%	0%	42%	7%	12%	0%
60070017043	34%	11%	37%	5%	3%	22%	17%	21%	4%	2%	11%	0%	42%	0%	5%	0%
60070018001	23%	11%	33%	18%	7%	35%	9%	26%	7%	1%	24%	0%	31%	0%	7%	3%
60070018002	23%	0%	33%	2%	7%	53%	19%	26%	22%	1%	14%	0%	31%	8%	7%	3%
60070018003	23%	13%	33%	10%	7%	48%	3%	26%	0%	1%	3%	13%	31%	0%	15%	3%
60070018004	23%	19%	33%	4%	7%	7%	22%	26%	20%	1%	6%	0%	31%	0%	10%	3%
60070018005	23%	0%	33%	11%	7%	13%	32%	26%	20%	1%	9%	0%	31%	17%	6%	3%
60070019001	37%	18%	25%	9%	2%	69%	6%	23%	0%	1%	6%	0%	19%	0%	0%	3%
60070019002	37%	0%	25%	6%	2%	50%	14%	23%	0%	1%	6%	0%	19%	6%	12%	3%
60070019003	37%	5%	25%	0%	2%	39%	3%	23%	0%	1%	13%	5%	19%	0%	0%	3%
60070019004	37%	0%	25%	18%	2%	31%	13%	23%	0%	1%	20%	3%	19%	2%	10%	3%
60070020001	15%	17%	43%	0%	7%	65%	17%	14%	0%	1%	12%	12%	9%	0%	8%	1%
60070020002	15%	0%	43%	0%	7%	38%	0%	14%	0%	1%	9%	0%	9%	0%	0%	1%
60070020003	15%	0%	43%	3%	7%	27%	21%	14%	0%	1%	5%	0%	9%	0%	0%	1%
60070020004	15%	14%	43%	0%	7%	14%	35%	14%	6%	1%	1%	0%	9%	0%	0%	1%
60070020005	15%	13%	43%	6%	7%	42%	19%	14%	0%	1%	9%	0%	9%	7%	4%	1%
60070020006	15%	16%	43%	4%	7%	55%	9%	14%	10%	1%	27%	0%	9%	0%	26%	1%
60070021001	32%	22%	32%	3%	9%	24%	3%	29%	0%	3%	16%	0%	12%	0%	1%	4%
60070021002	32%	1%	32%	19%	9%	25%	38%	29%	0%	3%	51%	0%	12%	13%	28%	4%
60070021003	32%	0%	32%	4%	9%	24%	15%	29%	0%	3%	7%	0%	12%	0%	10%	4%
60070021004	32%	11%	32%	9%	9%	31%	19%	29%	0%	3%	9%	0%	12%	0%	0%	4%
60070021005	32%	4%	32%	9%	9%	43%	0%	29%	0%	3%	17%	8%	12%	0%	16%	4%
60070022001	24%	16%	40%	7%	4%	27%	19%	19%	0%	0%	17%	13%	3%	0%	8%	1%
60070022002	24%	0%	40%	1%	4%	42%	15%	19%	3%	0%	21%	0%	3%	0%	6%	1%
60070022003	24%	14%	40%	4%	4%	17%	10%	19%	0%	0%	1%	0%	3%	0%	0%	1%
60070022004	24%	6%	40%	10%	4%	15%	27%	19%	9%	0%	5%	10%	3%	7%	4%	1%
60070023001	28%	6%	30%	5%	8%	38%	14%	23%	0%	0%	17%	0%	41%	0%	0%	2%
60070023002	28%	0%	30%	9%	8%	60%	0%	23%	0%	0%	2%	0%	41%	0%	17%	2%
60070023003	28%	0%	30%	13%	8%	17%	13%	23%	0%	0%	23%	9%	41%	0%	9%	2%
60070023004	28%	0%	30%	6%	8%	37%	10%	23%	0%	0%	15%	0%	41%	0%	17%	2%